# Curved Sandwich Panel

A study on the feasibility of transparent sandwich facade panels

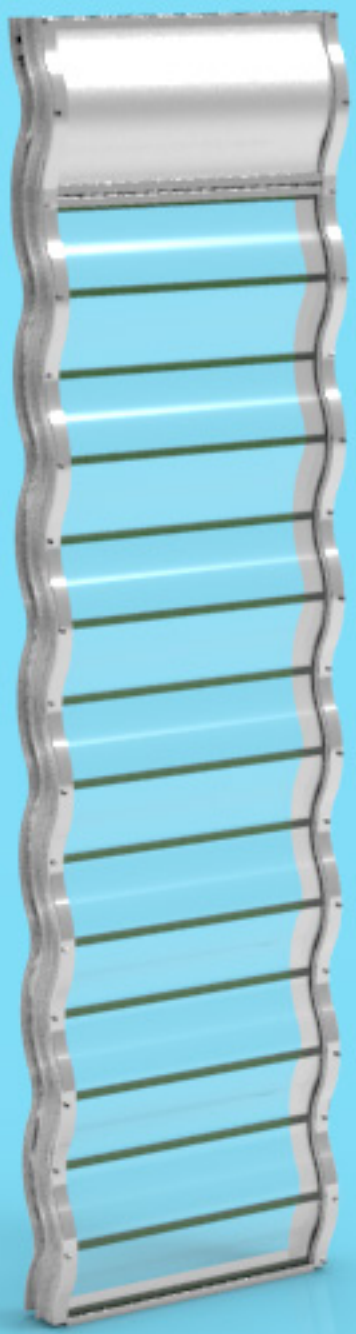

Msc Thesis | Ahmed Ahmed | 4084292 | Faculty of Architecture and the Built environment
TU Delft technology | 25 January 2018

***Research question:***

*How can a curved façade element be made of thin glass and GFRP profiles and what could be the implementations in utility buildings?*

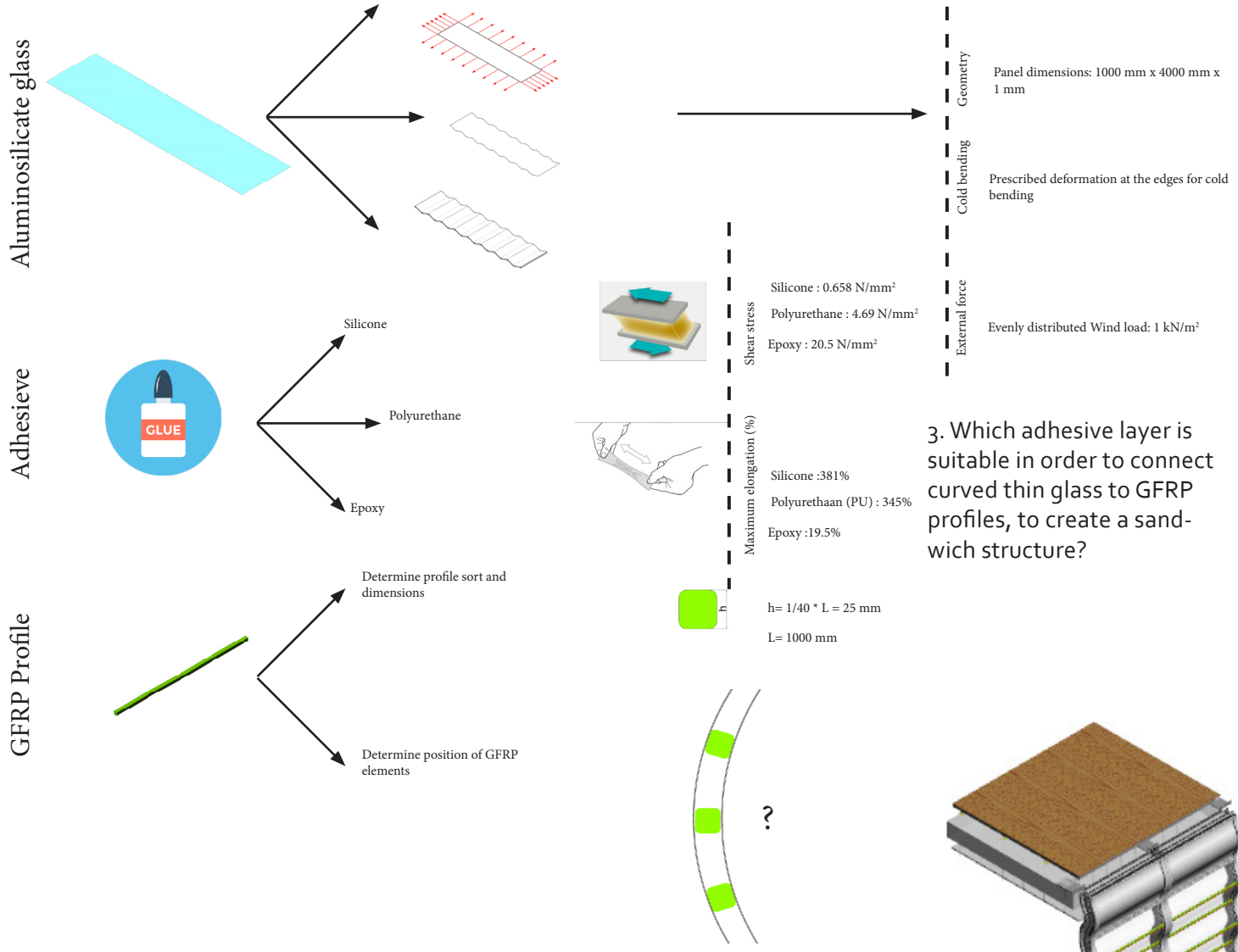


3. Which adhesive layer is suitable in order to connect curved thin glass to GFRP profiles, to create a sandwich structure?

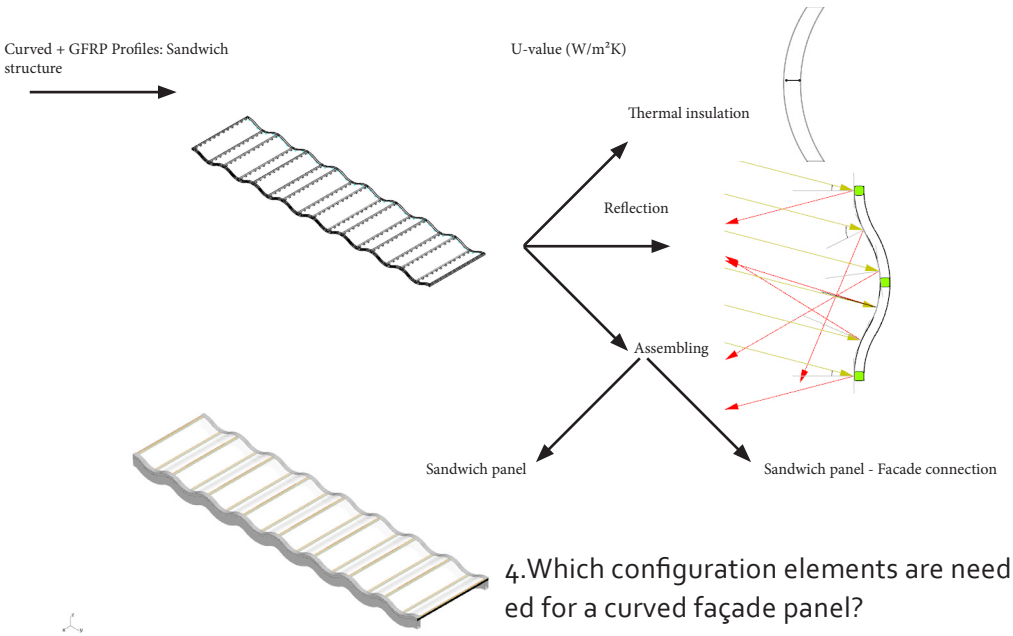


4.Which configuration elements are needed for a curved façade panel?

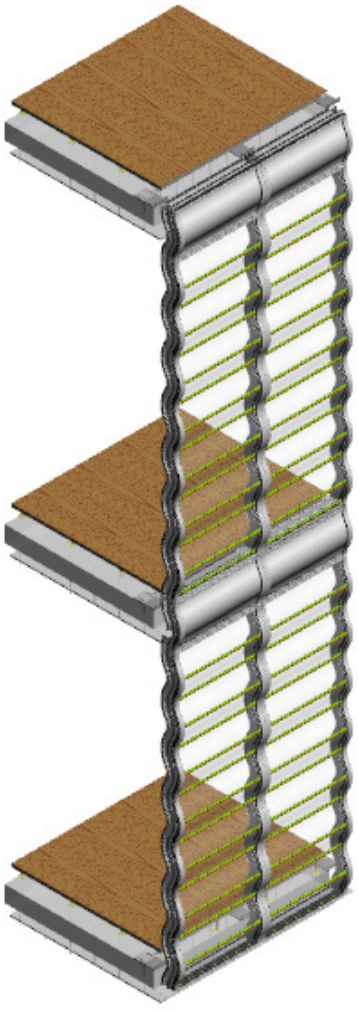

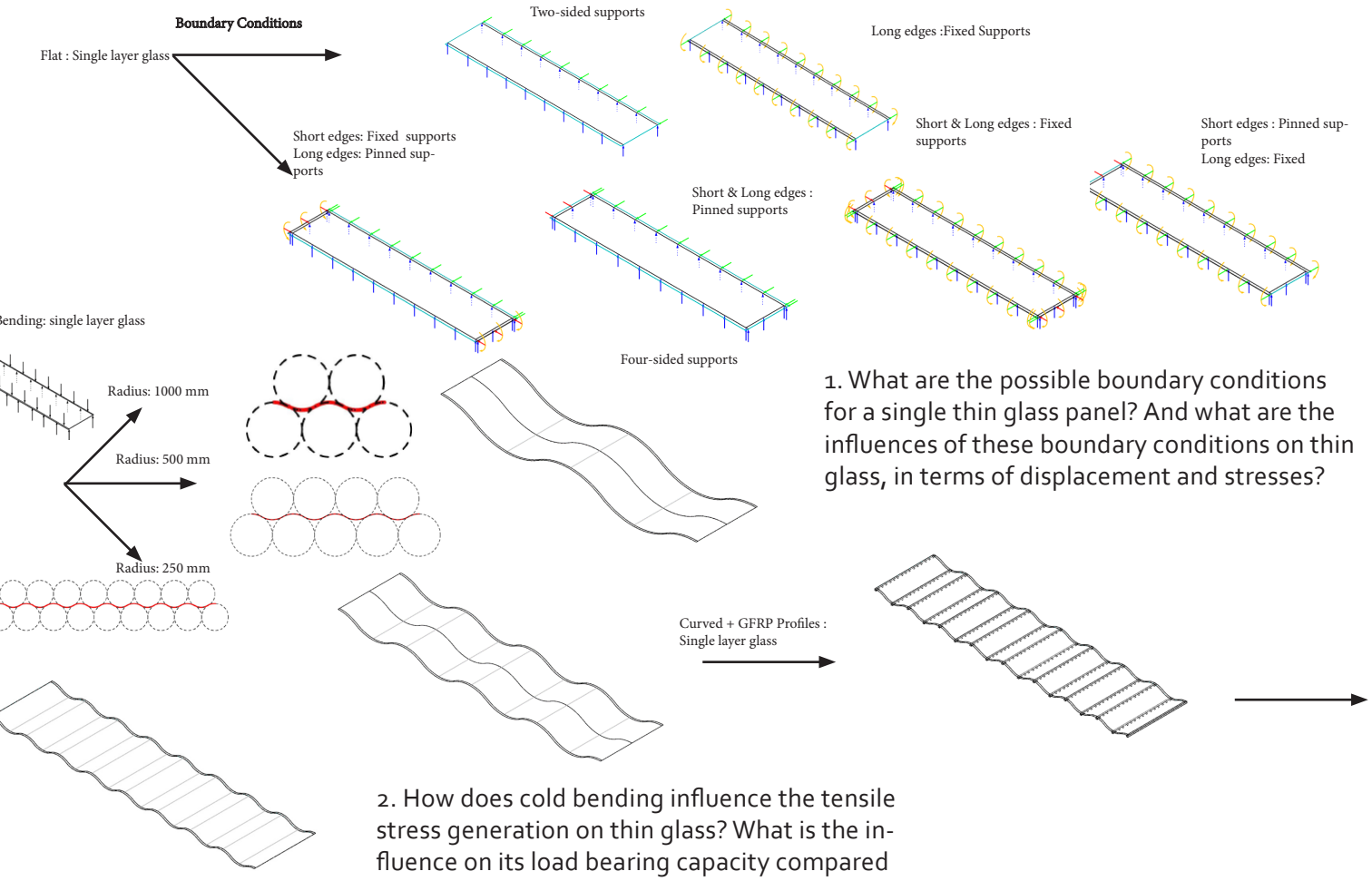


1. What are the possible boundary conditions for a single thin glass panel? And what are the influences of these boundary conditions on thin glass, in terms of displacement and stresses?

2. How does cold bending influence the tensile stress generation on thin glass? What is the influence on its load bearing capacity compared to a flat panel?

## Table of Content


ARCHITECTURE IS LIKE WRITING
YOU HAVE TO EDIT IT OVER AND OVER
SO IT LOOKS EFFORTLESS
- ZAHA HADID

# 1. Introduction

Since the invention of glass, the demand to implement transparency in the built environment has been increased. Glass is known as a transparent strong material with a very brittle property. Glass can break at a certain point and this causes safety problems.

Ensuring safety is a major challenge to consider before implementing glass into the built environment. Scientific studies suggest that glass should be reinforced to provide load-bearing capacity. This will give glass a huge potential to be implemented as a transparent load-bearing  element in the built environment.

Since the raise of technology a few decades ago, glass and its reinforcing elements have been developed. Nowadays, glass is used for many applications, such as stairs, roof beams and façade elements. The common glass is usually stiffened by lamination, but recent researches indicates that glass could also be reinforced with other materials, such as metal and fiber reinforced polymers (FRP).

The common glass designs for architecture purposes are faced with challenges related to its mechanical and physical properties. To ensure the stiffness and safety of glass, it is necessary to laminate two or more layers of glass which results in an increase of the dead load of glass (2500 kg/m3). In addition, bending glass to achieve complex geometry is a big challenge.

Hot bending glass is costly due to high energy demand and cold bending of glass is limited to a large radius range. Recent technological developments in glass production are transforming those limitations and challenges of glass into potential by using (ultra) thin glass. Therefore, ultra-thin glass can substitute common glass.

(Ultra) thin glass is a relatively new material. It is mainly used as a protection layer on mobile electronics screens for impacts and scratches. The mobile electronic industry is constantly developing (ultra) thin glass to achieve a thinner, lighter and more impact and scratch resistant material.

The main advantages of using (ultra) thin glass above common glass in the architecture field are its light weight and flexibility. (Ultra) thin glass reduces the total dead load of a glass panel and can therefore reduce the amount of structure material as well. Due to its flexibility, (ultra) thin glass is able to bend and can achieve curved shapes without the need of hot bending.

Like common glass, ultra-thin glass needs to be reinforced to gain stiffness by implementing reinforcing elements, like lamination. The reinforcement is mainly relevant to allow it to handle high stress and prevent it from deforming due to its flexibility.

Glass fiber reinforced polymer, hereafter GFRP, has been researched as a reinforcement for glass beams. The main aim was to use glass as a load bearing structure. These studies show that GFRP provides glass extra strength and stiffness in order to behave as a load bearing structure. GFRP is also used as a façade element for sandwich panels due to its light weight, corrosion resistance and high strength.

Therefore, combining (ultra) thin glass with GFRP reinforcement can be an innovative façade element in the built environment. Light weight and high strength are the main properties of these materials. In order to take advantages of and optimize these properties, it is necessary to study their employments in the build environment.

This thesis project focuses on designing and building a façade sandwich panel with reinforced (ultra) thin glass with GFRP. Hereby, the potentials of combining these materials will be explored as a façade panel.

# 2. Problem analysis

## 2.1 Problem description

Glass is a brittle material. Although it's properties are strong and stiff, glass is still susceptible to tensile bending stress. A float glass has a tensile bending strength 10 to 20 times lower than the compression bending strength. Moreover, the theoretical value of tensile bending strength of glass is not fully guaranteed, due to fallibility of the glass surface. That can happen during the transport, assembly of the pane or the production.

In addition, safety for users cannot be fully guaranteed when glass breaks. In case of fracture, the strength and stiffness of a glass element decrease immediately and lead to unsafe situations for the users.

Applying reinforcements to glass brings more stiffness to the whole pane and partly solve the safety problem of glass. There are multiple ways to apply reinforcements to glass pane. It is essential to apply the reinforcements to the tension part of the glass pane (fig. 2.1.1).

In case of fracture of the glass pane due to high tensile forces, t the reinforcements bears the loads and prevents the panel from totally failing. That will prevent large damage to the whole pane and save the glass from falling apart.

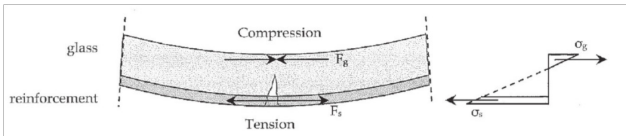

Figure 2.1.1 Force distribution after glass failure (Louter, 2007).

(Ultra) thin glass has higher tensile and compressive bending strength compared to common glass. This makes it able to handle more compressive and tensile forces. However, (ultra) thin glass needs to be reinforced for building applications, in order to prevent too much deformation and sudden failure.

GFRP is a usual reinforcement, even for concrete, due to its high tensile strength. In addition, its light weight brings more potential to use it in a façade panel. Therefore, it will be applied as a reinforcement to the (ultra) thin glass pane.

However, talking about reinforcement in glass is simple, but it is still undefined how and to what extent this reinforcement should be applied in ultra-thin glass to gain optimal results. What should be the best bonding system to combine these materials? And how will the interaction between these materials be? Those are just a few questions regarding the reinforcement of (ultra) thin glass with GFRP. It is obvious that a lot of research is required to gain a deep insight about the behavior of these materials.

## 2.2 Objective

The main objective of this thesis project is to design a curved sandwich façade panel consisting of thin glass and GFRP reinforcement, especially designed for applications in the built environment. By researching the constraints and benefits of thin glass reinforced with GFRP a preliminary design will be defined. The shape of the curved sandwich facade panel will be based on the minimum curvature radius of thin glass with GFRP reinforcement to improve their strength and stiffness.

## Sub objective

To increase the knowledge and benefits of using thin glass reinforced or supported with GFRP in the built environment, especially on façade design.

## 2.3 Research question

The main research question for this thesis project is described as the following:

*How can a curved façade element be made of thin glass and GFRP profiles and what could be the implementations in utility buildings?*

### Sub questions:

1. What are the possible boundary conditions for a single thin glass panel? And what are the influences of these boundary conditions on thin glass, in terms of displacement and stresses?

2. How does cold bending influence the tensile stress generation on thin glass? What is the influence on its load bearing capacity compared to a flat panel?

3. Which adhesive layer is suitable in order to connect curved thin glass to GFRP profiles, to create a sandwich structure?

4.Which configuration elements are needed for a curved façade panel?

## 2.4 Approach and Methodology

This research will start with an interpretation of what would be a suitable application for reinforced thin glass with GFRP in the built environment and how that should substitute common glass.

The first step is to identify the characteristics and properties of thin glass and of GFRP as a material and reinforcement based on literature studies.

The next step is to focus on the adhesive bonding. The research will mainly focus on the current used adhesives for common glass reinforced with GFRP. Based on that and the research on the two materials a preliminary design will be defined. This design will consist of two layers of curved thin glass with GFRP reinforcements to create a sandwich panel. It will substitute a conventional curtain wall panel in order to take advantage of its light weight compared to the common curtain wall panel.

It is essential to know the benefits and the constraints of the current curtain wall system in order to define an innovative design of curved thin glass reinforced with GFRP. The innovative design should have at least the same strength, stiffness and insulation values as a conventional curtain wall panel.

The analysis of the advantages and disadvantages of the design will determine the development of the research. The aim is to transform a flat single layer of thin glass panel into a curved sandwich panel, by taking advantage of the flexibility of thin glass.

The third step is to design several numerical models of a single layer of thin glass with different boundary conditions. That will lead to the most suitable boundary conditions which provide the panel with the minimum stresses and displacement. In addition, it will determine the influence of boundary conditions on the behavior of thin glass.

The fourth step is to repeat the third step, but with bending the thin glass into different radii and to study its mechanical behavior. Furthermore, after analyzing the outcomes of a bended single layer of thin glass, GFRP elements will be added to study the influence of reinforcing curved thin glass.

The fifth step is to design numerical models to implement several adhesive bonding. That will determine the most suitable adhesive to connect thin glass to GFRP reinforcements.

The results of the numerical model will determine the final shape of the curved sandwich panel made of GFRP reinforced thin glass.

This is followed by a specific case study from the utility buildings in order to implement the curved sandwich façade panel.

Once a specific building is selected, the research will explore and explain how to attach the curved sandwich panel to the building.

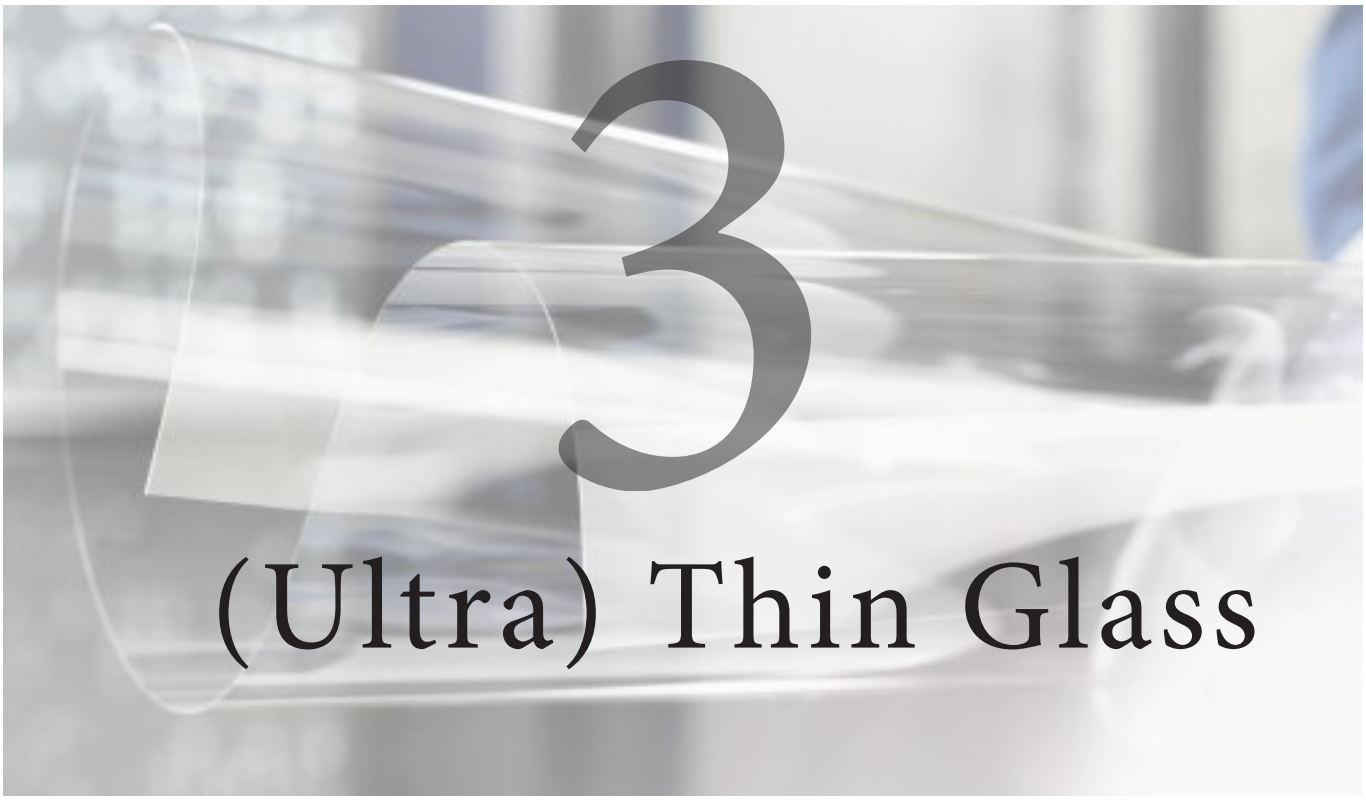

# 3 (Ultra) Thin Glass

## 3.1 Introduction

Thin glass and ultra thin glass are relatively new terms in the built environment. Thin glass is defined as a glass sheet with a thickness under 2 mm. Ultra thin glass has been characterized by a thickness of 0.1 mm (AGC, 2011). The minimum thickness of ultra thin glass that has been achieved till now is 0.025 mm. This material is developed by the glass industries for special purposes. The main function is to protect mobile electronic screens, due to its high impact and scratch resistance. It has been proved that glass can be light weight with high strength and stiffness despite of its thinness. Therefore, glass industries are still improving this material in order to get thinner and harder products with higher impact and scratch resistance.

## 3.2 Material properties

The properties of thin glass depend on its composition. The glass types used for manufacturing thin glass are aluminosilicate glass, borosilicate glass and soda lime glass (where float glass is made of) (Albus & Robanus, 2015).

Each of these three glass types has special characteristics. Soda lime glass, is the main glass type for float glass. It is a solid but very brittle material with heat capturing possibilities. Borosilicate glass has outstanding thermal resistance and chemical durability. Aluminosilicate glass has a relatively high chemical durability, fracture toughness, Young's modulus, lower coefficient of thermal expansion and low electrical conductivity (Ces Edupack, 2015).

Aluminosilicate glass has an excellent capacity to resist mechanical influences. Therefore, aluminosilicate glass is the primarily glass type that is implemented in technical glass, as a protection layer for screens of electronics devices or as an underlying layer in bio-technology and laboratories for example (Albus & Robanus, 2015).

The most noticeable characteristic of this material is its ability for deformation.

Thin glass has an excellent surface quality due to the manufacturing process. As a result of no contact with solid objects during its production, it has an almost flawless surface. Thin glass has a withstanding capacity against bending stresses, because of the combination of high strength and high surface quality. This allows thin glass to bend to a smaller radius. The thickness of this material is the parameter to how much it can bend. So the thinner the glass sheet, the smaller the curvature radius without fracture.

Table 1 gives an overview of the properties of aluminosilicate glass and soda lime glass. Considering these properties, it is obvious that aluminosilicate glass is much stronger than soda lime glass. The most remarkable differences are that Young's modulus, which defines the elasticity of the material, is around 20*10^3 N/mm2 higher, the hardness of the material, is about 5 times higher and the thermal expansion of the material is about half the thermal expansion of the soda lime glass.

Table 3.2.1 : A comparison of properties: Aluminosilcate and Soda lime glass (Ces Edupack, 2015).

| Properties | | Soda lime glass | Aluminosilicate glass |
|---|---|---|---|
| Density | Kg/m3 | 2.47e3 – 2.52e3 | 2.49e3-2.5e3 |
| Young's Modulus | GPa | 68-72 | 84.8-89.1 |
| Tensile Strength | MPa | 30.3-32.2 | 39.9-43.9 |
| Shear Modulus | GPa | 27.9-29.6 | 33.9-35.6 |
| Poisson's ratio | | 0.21-0.22 | 0.23-0.22 |
| Compressive Strength | MPa | 303-322 | 376-414 |
| Flexural Strength | MPa | 39.4-41.9 | 48.9-53.8 |
| Fracture Toughness MPa*m^0.5 | | 0.63-0.65 | 0.7-0.72 |
| Fatigue Strength | Mpa | 28.2-31.2 | 35.6-39.4 |
| Shape Factor | | 15 | 15 |
| Thermal Expansion coefficient | μ strain/ºC | 8.92-9.28 | 4.5-4.69 |
| Hardness – Vickers | HV | 89-98.4 | 477-525 |
| Elongation | %strain | 0.04-0.05 | 0.04-0.05 |

Moreover, thin glass (made of aluminosilicate glass) has a higher optical quality due to deficiency of iron in the glass sheet. The edges of thin glass do not contain green tint like the edges of common soda lime glass, which is caused by presence of iron in the composition.

## 3.3 Production technique

Thin glass can be produced by different manufacturing techniques: float technique, overflow fusion technique or down-draw technique (Albus & Robanus, 2015). Soda lime glass is mainly manufactured by float technique as it has been explained in chapter 1. Therefore, the manufacturing techniques of overflow process and down draw process will be explored and explained in this section.

In 1964, Corning was the first company to introduce overflow fusion technique to innovative material science. It was first meant for the automobile windshield industry. At that time, there was very little interest and market for that kind of production techniques for the product. But a remarkable change happened during the 1980s. There was an increase in the need for thin and flat glass because of the growth in demand for LCD screens. This set off development of this production technique (Corning museum of glass, 2011).

And till this day, the overflow fusion production technique has the same base principles as in 1964. The manufacturing process starts by mixing and melting the raw materials into molten glass under a temperature of less than 1000 oC. This molten glass is then poured into an inverse triangle shaped bath. Next, this composition flows evenly out of the bath through the edges. These two even overflows of the molten glass meet and join each other at the bottom of the bath. This fusion is caused by the shape of bath and by gravity which allows the overflowed molten glass to flow down vertically. Then, the thin glass sheet cools down directly after the fusion and gets from liquid to a thin, flexible solid material, without contact to any surface. Finally, the sheet is cut by a cutting machine and stored.

During the 1970s, the down draw manufacturing technique was invented and patented. In the beginning, this manufacturing technique faced the same fate as the overflow fusion technique: a lack of need in the market for this kind of product and manufacturing technique. However, this technique has since developed.

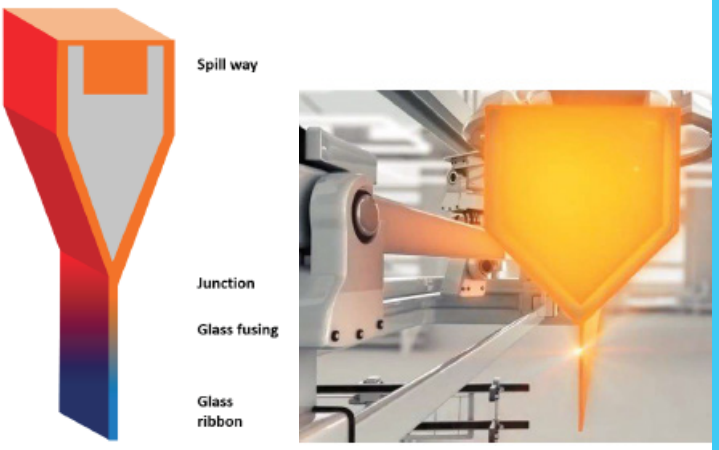


Figure 3.3.1 : Over flow fusion (Neugebauer, 2015).

The down draw technique is similar to the overflow technique (fig. 3.3.2). The first difference is that the molten glass flows down from the bath through an orifice (Albus & Robanus, 2015). The second difference is that the molten glass goes through rollers and a cooling channel to cool down. At the end, when it is stiff enough, the glass sheet is cut.

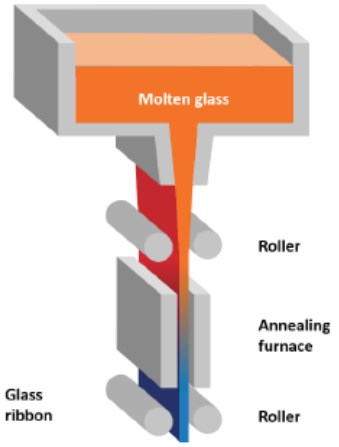


Figure 3.3.2 : Down flow process (Neugebauer, 2014)

## 3.4 Chemical strengthening

Thin glass compared to common float glass, is toughened by a relatively new tempering technique. This toughening process is called chemical strengthening. Chemical strengthening is meant for pre-stressing thin glass in order to improve the strength property of thin glass. In this section chemical strengthening process will be explored and explained.

Chemical strengthening process can be applied to glass sheets with thickness above 2 mm. However, the utilization of this tempering process is more suitable for glass sheets thinner than 2 mm. According to the article "Ion exchange for glass strengthening", it is very difficult to apply and to provide reinforcement to glass with a thickness smaller than 2mm with a conventional industrial thermal tempering installation. Therefore a new toughening technique had to be invented, namely the chemical strengthening process.

The purpose of using chemical strengthening process is to improve and to increase the compression strength of the thin glass surface. Due to this process, a compression zone will be formed in the outer surfaces of the glass sheet and tension zone in the glass itself (figure 4). This principle is used for hardening common float glass by either a toughened or heat strengthening process.
The compressive and tensional stresses in glass due to different types of toughening processes, are illustrated in figure 3.4.1. The distributed stresses are illustrated in the cross section of the glass according to its strengthening process. It is remarkable that the compressive and tensional stresses of chemically strengthened glass are much thinner and evenly distributed than that of heat or toughened strengthened glass.

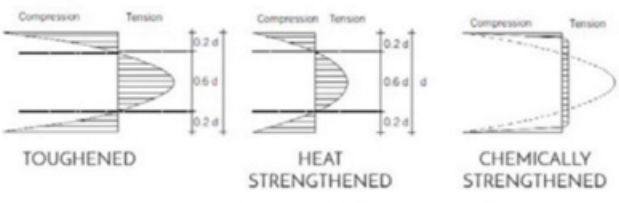


Figure 3.4.1: Stress distribution (Wurm, 2007)

The chemical strengthening process has its own characteristic. Tempering thin glass through chemical treatment depends on an ion changing process instead of thermal treatment (which is used for float glass). This kind of tempering thin glass panes take place in a chemical salt bath. The purpose is to replace the smaller Na+ ions from thin glass panes by bigger K+ ions from the chemical bath. This causes pre-stressed surfaces of the thin glass pane with a high compressive strength. This process is achieved by temperatures around 400 oC, which is 200 oC lower than thermal toughening process.

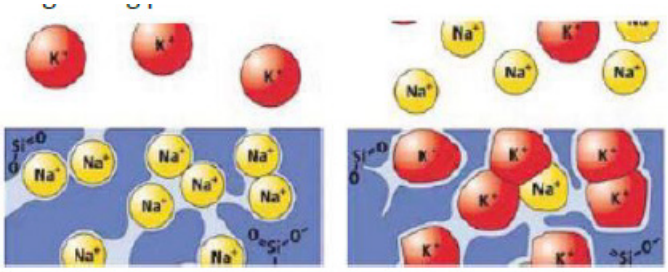

Figure 3.4.2: Chemical strengthening process (Hundevad, 2014)

This process enables the creation of strengthened flexible thin glass in order to achieve a material that can deform into complex shapes without fracture. The thin glass dimensions are dependent on the size of the chemical salt bath. In other words, the maximum size of thin glass panes is limited by the size of the chemical salt bath (Weller, et al, 2009).

The minimum achieved compressive strength on thin glass surface due to chemical strengthening process is 230 N/mm2 (Lu & Overend). This compressive strength is about 12 times higher than that of annealed glass (20 N/mm2), 6 times than heat strengthened (40 N/mm2) and 2.5 times than toughened strengthened (90 N/mm2) (Schittich, et al, 2007).

Currently, there are three main companies for manufacturing and producing (ultra) thin glass available in the market. Those companies are AGC (Asahi Glass corporation), Corning and SCHOTT. All three produce (ultra) thin glass sheet according to the chemical strengthening process. Each company has its specific name to their (ultra) thin glass.

For example, AGC named its thin glass "Leoflex", Corning called it "Gorilla glass" and SCHOTT titled it as "Xensation". The attached appendix 1 gives an indication about the specifications of each of these (ultra) thin glass types. According to these specifications a compressive strength of >600 N/mm2 (Leoflex), >800 N/mm2 (Gorilla glass) and >900 N/mm2 (SCHOTT) can be achieved.

## 3.5 Breakage behavior

Although the breakage behavior of (ultra) thin glass is still under investigation, some facts can be described. Even a strong chemical strengthened thin glass sheet has its limits to handle stresses. The breakage behavior starts when stresses reach the fracture point of (ultra) thin glass.

According to the book "Fracture Mechanics of Ceramics" the fragmentation in ion exchanged glass is observed to be a multiple crack branching process that cause smaller fragments further from fracture origin, when its maximum stress has been exceeded. In general, when tensile stress increases, a higher fragmentation density with uniform fragment size is obtained.
The breakage behavior of thin glass is influenced by its thickness. When ion exchanged glass breaks, there is no such fine dicing of glass, except for when the glass is very thin; with a thickness of the order of few hundreds of microns (Bouyne & Gaume, 2002). On the other hand, when chemically toughened thin glass is broken, it is remarkable that it breaks into tiny fragments, to an almost powder like state. (Hundevad, 2014)

Because (ultra) thin chemically strengthened glass is still a developing technology, further investigation in the breakage behavior is needed to define the exact safety factor in order to prevent damages and injuries. To avoid these safety problems, I suggest that thin glass should be laminated. This so that when it breaks, the fragments remain in place without falling down. In addition, it can behave like a protection layer for the inner thin glass pane.

## 3.6 Bending radius

The most remarkable characteristics of thin glass are its flexibility and high compressive strength. The relation between the bending curvature of thin glass and its generated stress is depended on the thickness of the glass pane. In chart 3.6.1, this relationship is expressed and explained by an equation. In general, glass has an average breaking stress around 100-200 N/mm2. However, the breaking stress can be degraded by an edge condition (Murata, et al). Due to safety approaches the breaking stress will be assumed by 50 N/mm2. So for example, a 0.05 mm glass pane with limited breaking stress of 50 N/mm2 has a minimum curvature bending of 40 mm. Furthermore, according to the graph, the thinner the glass pane is, the more it can bend.

This property of (ultra) thin chemically strengthened glass has to be further investigated, like the breakage behavior. One of the improvements is to apply the four-point bend test instead of a three-point bend test in order to achieve more accurate results regarding this relation between the bending curvature of thin glass and its generated stress. These thin chemically strengthened glass panes are tested by a three-point bend test, which is less accurate than the four-point bend test to define the weakest spot of a thin glass pane. That is because the three-point bend test focuses the forces on one point of the glass sheet until it breaks. The four-point bend test, however, focuses its forces on two points in order to define the weakest spot of the thin glass between these forces points.

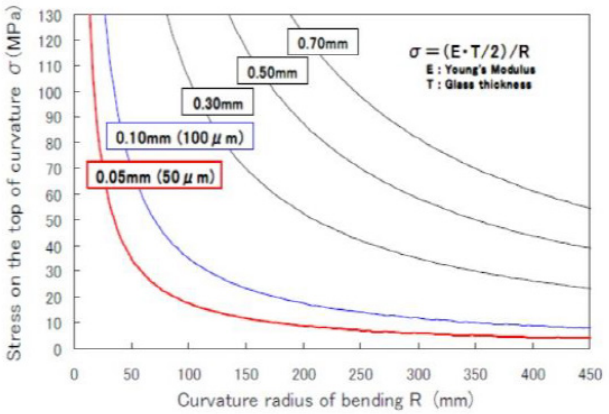


Chart 3.6.1: Bending radius thin sheet (Murata, et al).

## 3.7 Conclusion

Thin glass is defined as a glass sheet with a thickness under 2 mm. Ultra thin glass has been characterized by a thickness of 0.1 mm and the minimum thickness of ultra thin glass that has been achieved till now is 0.025 mm. The glass types used for manufacturing thin glass are aluminosilicate glass, borosilicate glass and soda lime glass with each type with different characteristics. Soda lime glass, is the main glass type for float glass and it is a solid but very brittle material with heat capturing possibilities. Borosilicate glass has outstanding thermal resistance and chemical durability. Aluminosilicate glass has a relatively high chemical durability, fracture toughness, Young's modulus, lower coefficient of thermal expansion and low electrical conductivity. Aluminosilicate glass has an excellent capacity to resist mechanical influences and therefore, aluminosilicate glass is the primarily glass type that is implemented in technical glass.

The production techniques of thin glass are: float technique, overflow fusion technique or down-draw technique. The manufacturing process of overflow fusion technique starts by mixing and melting the raw materials into molten glass under a temperature of less than 1000 oC and is then poured into an inverse triangle shaped bath. Then, this composition flows evenly out of the bath through the edges. These two even overflows of the molten glass meet and join each other at the bottom of the bath. Then, the thin glass sheet cools down directly after the fusion and gets from liquid to a thin, flexible solid material, without contact to any surface. The down draw technique is similar to the overflow technique with the next differences: the molten glass flows down from the bath through an orifice and that the molten glass goes through rollers and a cooling channel to cool down and when it is stiff enough the glass sheet is cut.

In order to improve and to increase the compression strength of the thin glass surface chemical strengthening process is used.

Due to this process a compression zone will be formed in the outer surfaces of the glass sheet and tension zone in the glass itself. This process is used for hardening common float glass by either a toughened or heat strengthening process.

Tempering thin glass through chemical treatment depends on an ion changing process instead of thermal treatment, this kind of tempering thin glass panes take place in a chemical salt bath. The purpose is to replace the smaller Na+ ions from thin glass panes by bigger K+ ions from the chemical bath. This causes pre-stressed surfaces of the thin glass pane with a high compressive strength. This process is achieved by temperatures around 400 oC, which is 200 oC lower than thermal toughening process.

The minimum achieved compressive strength on thin glass surface due to chemical strengthening process is 230 N/mm2. This compressive strength is about 12 times higher than that of annealed glass (20 N/mm2), 6 times than heat strengthened (40 N/mm2) and 2.5 times than toughened strengthened (90 N/mm2).

In order to avoid safety problems of the breakage behaviour of thin glass, I suggest that it should be laminated. In this way the fragments remain in place and it can be a protection layer for the inner thin glass pane.

# 4

# Glass Fiber Reinforced Polymer

## 4.1 Introduction

Fiber reinforced polymer (FRP) has been used in many applications during the last decades in the built environment, from façade elements to reinforcement and structural elements. FRP is a lightweight material with outstanding strength and stiffness. Considering these characteristics, FRP composites have been used in the improvement of structural elements. For example, FRP is used as a reinforcement in concrete, modular structural elements and bridge decks.

The main ingredients of FRP composite are fibers and resin. The key role of fibers is to provide strength and stiffness to the FRP composite and to carry the tension of the composite while the resin acts as a matrix in order to distribute the stress consistently among the fibers. In addition, the resin is responsible for protecting the fibers from external influences and keeping the composite in proper shape. The most commonly used fibers are glass, carbon and aramid, while epoxy, polyester and vinyl ester are the most common resin for built environment applications.

In this report, a special form of FRP, glass fiber reinforced polymer (GFRP) will be explored. The aim is to understand the mechanical and physical properties of this material and how it acts as a reinforcement for thin glass. The first section will describe GFRP regarding its composition and its characteristics.

Subsequently, the variety of manufacturing techniques of GFRP composites will be explored and explained. At the end, the current use of GFRP as a reinforcement for building elements will be analyzed in order to define its constraints and potentials as an element that can be used to reinforce thin glass.

4.2 What is GFRP?

Glass fiber reinforced polymer (GFRP) is a composite material consisting of reinforced polymer matrix by fine glass fibers. Glass fiber is light weight, robust and strong and can be used for many products. Compared to carbon fiber, glass fiber is less stiff but much cheaper, because of its source raw materials are much less expensive.

In addition, the combination of its bulk strength and its light weight compares very favorablyto metals. Due to molding processes, GFRP can easily be produced as curved forms. The most common applications for GFRP are automobiles, airplanes, roofing, cladding, pipes and bridge decks.
Glass fiber is formed from thin strands of glass that has been extruded into extremely thin fibers. It was invented by Russell Games Slayter in 1938, for insulation and electrical purposes. Glass fiber is subdivided into eight different types each with different purposes:

- Alkali glass fiber (A-glass);
- Electrical grade glass fiber (E-glass);
- Electrical grade glass fiber with acid corrosion resistance (E-CR glass);
- Chemical resistant glass fiber (C-glass);
- Borosilicate glass fiber (D-glass) mainly used for electrical purposes;
- Alkali glass fiber (AR-glass), mainly used as substrate for cement and concrete;
- Acid corrosion resistance glass fiber with high strength (R-glass);
- High strength glass fiber for reinforcement with high stiffness (S-2 glass);

Currently, E-glass and S-2 glass are the most commonly used types of glass fiber and hence will be the focus of this chapter. (Hartman, et al, 1998). The physical properties of this types of glass are illustrated in Table 4.2.1. It is remarkable that S-2 glass fiber has higher tensile strength and a higher young's modulus value compared to the other types of glass fiber under temperature of 23 oC.

In addition, S-2 glass fiber has the highest elongation value, which allows more deformation before it breaks. S-2 glass can even reach a shear modulus of 38000 N/mm2 (MPa) .

Considering the properties of all the competing types of glass fiber noted above, S-2 glass fiber is the most suitable fiber for reinforcement purposes, due to its relatively high tensile strength and elasticity. However, in terms of cost, S-2 glass fiber is very expensive compared to other glass fiber types. E- glass fiber could be an alternative for S 2- glass, due to the fact that E-glass is 10 times cheaper than S-2 glass fiber and yet it still provides a good combination of high tensile strength and a high value of the young's modulus.

However, it is important to note thatS-2 glass fiber is still about 40% stronger. and may be difficult to replace in more demanding applications. In this chapter, due to their relative advantages over other GFRP products for the built environment, we will focus only on S-2 and E-glass fiber types.

| PHYSICAL PROPERTIES | | | | | | | | |
|---|---|---|---|---|---|---|---|---|
| | A-GLASS | C-GLASS | D-GLASS | E-GLASS | ECRGLAS® | AR-GLASS | R-GLASS | S-2 GLASS® |
| Density, gm/cc | 2.44 | 2.52 | 2.11 | 2.58 | 2.72 | 2.70 | 2.54 | 2.46 |
| Refractive index | 1.538 | 1.533 | 1.465 | 1.558 | 1.579 | 1.562 | 1.546 | 1.521 |
| Softening Point, C (F) | 705 (1300) | 750 (1382) | 771 (1420) | 846 (1555) | 882 (1619) | 773 (1424) | 952 (1745) | 1056 (1932) |
| Annealing Point, C (F) | | 588 (1090) | 521 (970) | 657 (1215) | | | | 816 (1500) |
| Strain Point, C (F) | | 522 (1025) | 477 (890) | 615 (1140) | | | | 766 (1410) |
| Tensile Strength, MPa | | | | | | | | |
| -196°C | | 5380 | | 5310 | 5310 | | | 8275 |
| 23°C | 3310 | 3310 | 2415 | 3445 | 3445 | 3241 | 4135 | 4890 |
| 371°C | | | | 2620 | 2165 | | 2930 | 4445 |
| 538°C | | | | 1725 | 1725 | | 2140 | 2415 |
| Young's Modulus, GPa | | | | | | | | |
| 23°C | 68.9 | 68.9 | 51.7 | 72.3 | 72.3 | 73.1 | 85.5 | 86.9 |
| 538°C | | | | 81.3 | 81.3 | | | 88.9 |
| Elongation % | 4.8 | 4.8 | 4.6 | 4.8 | 4.8 | 4.4 | 4.8 | 5.7 |

Table 4.2.1: Physical properties types of glass fibers (Hartman, et al, 1998).

The most commonly used resin for GFRP composite is epoxy. Epoxy resin is a member of the thermosets. Thermoset is a term for a specific category of polymer matrix. Thermosets are characterized by high mechanical and physical strength. The most commonly used thermosets are polyesters, vinyl esters, phenol and epoxies. Due to the high yield crosslink structure of epoxy polymer matrix, it performs much better compared to other thermosets. In table 4.2.2, a comparison of the physical and mechanical properties of these thermosets is illustrated. It is remarkable that epoxy poly matrix has relatively high strength, chemical resistance and impact resistance (Campbell, 2010).

| | | Polyester | vinyl ester | Epoxy | Phenol |
|---|---|---|---|---|---|
| Strength | Mpa | 40-85 | 50-80 | 60-80 | 28-50 |
| Young's modulus | Gpa | 2,4-4,5 | 3-3,5 | 3,5 | 2,8-5 |
| Mass per length | kg/m3 | 1200-1500 | 1100-1400 | 1100-1400 | 1240-1320 |
| material cost | EUR/kg | 1,72-1,89 | medium | 2,47-2,72 | 1,24-1,4 |
| processing difficulty | | low | low | medium | high |
| Colour | | divers | divers | subdued | only dark |
| UV-resistance | relative | good | good | fair | good |
| chemical resistance | relative | acceptable | acceptable-good | good | good |
| impact strength | relative | low | medium | high | medium |
| Contraction | % | 6-8 | 5-7 | <2 | high |
| Thermal expansion | mm/mK | 140 e-3 | | 100 e-3 | 122 e-3 |
| Glass temperature | °C | 150-210 | | 67-167 | 170-270 |
| Maximum service temp | | 112-128 | | 122-138 | 142-157 |

Table 4.2.2: Comparison of the physical and mechanical properties of thermosets (Campbell, 2010).

## 4.3 Material properties

The amount of glass fibers in a GFRP composite pane determine the mechanical strength of the composite. while the resin is responsible for the chemical and thermal behavior of the composite. In addition, the resin is also responsible to keep the composite in a certain shape.

GFRP composite is strong and stiff along its axis in both compression and tension, however it is weak in shear, across its axis. In other words, during manufacturing the glass fibers should be positioned in the same direction as the exerted forces, in order to prevent buckling.

In general, GFRP composite has high corrosion resistance and low moisture absorption, which makes it very favorable for external applications in the built environment, like roofing and cladding.

In addition, the combination of light weight and high strength makes GFRP an excellent reinforcement element, that is resistant to high tensile stresses and does not add much weight to the reinforced element for example: a thin glass sandwich façade panel. Considering these properties, the weight of the load bearing structure will be decreased and as consequence much material will be saved. Chart 4.3.1 shows the ratio between the length of an E-glass fiber and its tensile strength (Bagherpour, 2012).

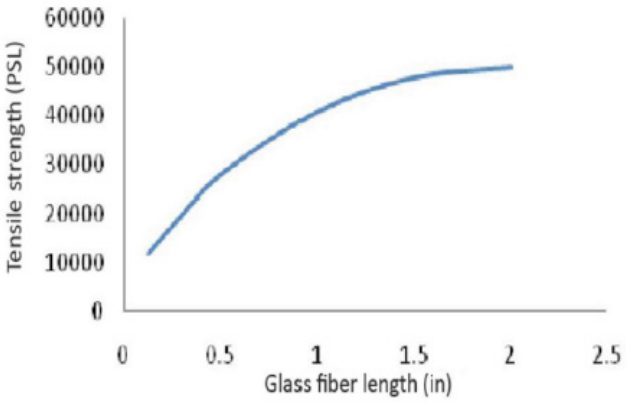


Chart 4.3.1: Relation between Glass fiber length and tensile strength (Bagherpour, 2012).

According to the graph, increasing the length of the glass fibers causes an increase of tensile strength in the composite. The angle between the fibers and stress is significant for determining the tensile strength of the composite. In order to obtain the maximum tensile strength of the GFRP composite, the glass fibers have to be orientated in the same direction of the applied forces.Chart 4.3.2 shows the relationship of the angle of glass fibers and its tensile stress.

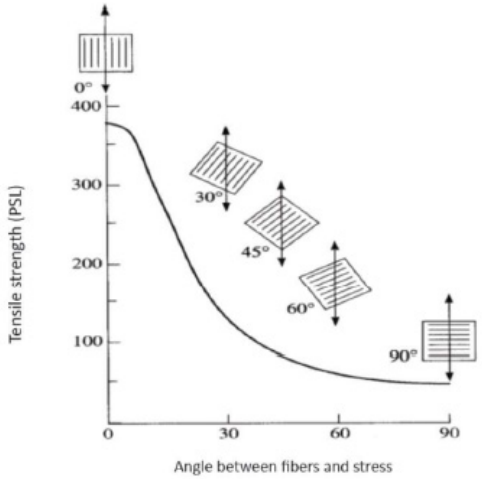


Chart 4.3.2: Relation between angle of fibers and tensile strength (Bagherpour, 2012).

## 4.4 Manufacturing techniques

In general, GFRP composites can be manufactured by many techniques. The selection of the proper manufacturing technique depends on the size, shape and application of the final product.

In this section, two manufacturing techniques of GFRP for linear and curved reinforcement will be explained. These manufacturing techniques are pultrusion (for linear products) and vacuum infusion process (for curved products). Both techniques are suitable for applications in the built environment, such as beams, window frames and reinforcement elements.

The pultrusion process in figure 4.4.1 is one of the most used manufacturing techniques for GFRP linear products. This production method starts by pulling continuously the resin saturated glass fibers through a heated die, which cures and defines the form of the composite. The curing occurs under high temperature and takes a few minutes. At the end, the pultruded and shaped profile is cut in the predetermined length. In this technique, the glass fibers are set parallel to the longitudinal direction of the profile. This technique is suitable for production of I-beams, pipes and solid rods.

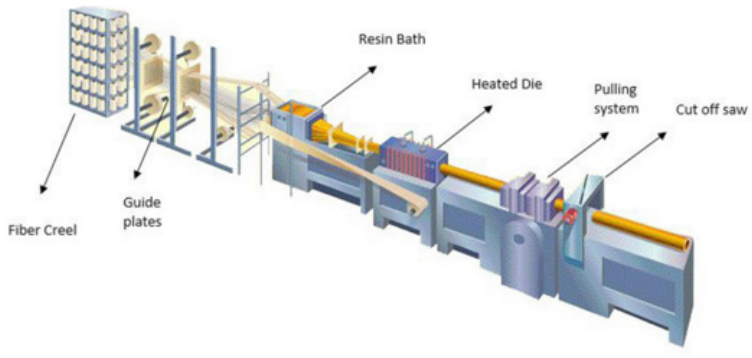


Figure 4.4.1: Pultrusion process (http://www.libertypultrusions. com/pultrusion-process/).

The vacuum infusion process (VIP) in figure 4.4.2 is one of the most commonly used techniques to produce curved shaped GFRP elements. VIP is a closed molding, which starts by positioning the glass fibers as a sheet or as single filaments in the mold, including a layer of the laminate. Then a perforated peel ply is placed over the reinforcement. After that, a layer of infusion mesh is positioned, and a perforated tubing is positioned in order to distribute the resin across the laminate. Next, a vacuum bag is placed and sealed at the edges of the mold. The vacuum bag is connected to a vacuum pump, which pulls out the air between these layers.

Meanwhile, on the other side a resin container is connected by a tube, which allows the resin to flow into the mold during the vacuum process. The resin will be uniformly distributed among the glass fibers.

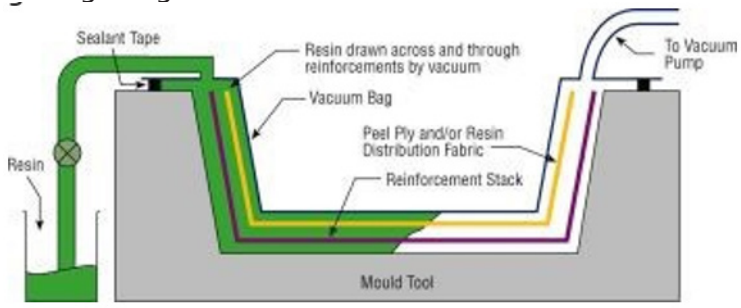


Figure 4.4.2: Vacuum infusion process. (http://www.composites.ugent.be/home_made_composites/ organizing_your_composite_workshop.html)

## 4.5 Conclusion

Glass fiber reinforced polymer (GFRP) is a composite material consisting of reinforced polymer matrix by fine glass fibers. The combination of its bulk strength and its light weight compares very favourably to metals. Due to molding processes, GFRP can easily be produced as curved forms. Glass fiber is formed from thin strands of glass that has been extruded into extremely thin fibers. Glass fiber is subdivided into eight different types with different purposes. E-glass and S-2 glass are the most commonly used types of glass fiber and therefor will be the focus.

S-2 glass fiber is the most suitable fiber for reinforcement purposes, due to its relatively high tensile strength and elasticity. However, S-2 glass fiber is very expensive compared to other glass fiber types and therefor E- glass fiber could be an alternative for S 2- glass, due to the fact that E-glass is 10 times cheaper than S-2 glass fiber with good combination of high tensile strength and a high value of the young's modulus. However, S-2 glass fiber is still about 40% stronger.
The most commonly used resin for GFRP composite is epoxy. The epoxy poly matrix has relatively high strength, chemical resistance and impact resistance as a resin.

GFRP composite is strong and stiff along its axis in both compression and tension, however it is weak in shear, across its axis. Therefore, during manufacturing the glass fibers should be positioned in the same direction as the exerted forces, in order to prevent buckling.

The combination of light weight and high strength makes GFRP an excellent reinforcement element, that is resistant to high tensile stresses and does not add much weight to the reinforced element. However In order to obtain the maximum tensile strength of the GFRP composite, the glass fibers have to be orientated in the same direction of the applied forces.

The 2 manufacturing techniques of GFRP are pultrusion (for linear products) and vacuum infusion process (for curved products). The pultrusion method starts by pulling continuously the resin saturated glass fibers through a heated die, which cures and defines the form of the composite. This curing occurs under high temperature and takes a few minutes. The pultruded and shaped profile is cut in the predetermined length. In this technique, the glass fibers are set parallel to the longitudinal direction of the profile.

The vacuum infusion process is a closed molding, which starts by positioning the glass fibers as a sheet or as single filaments in the mold, including a layer of the laminate. Next a perforated peel ply is placed over the reinforcement and a layer of infusion mesh is positioned, a perforated tubing is positioned in order to distribute the resin across the laminate. A vacuum bag is placed and sealed at the edges of the mold.

The vacuum bag is connected to a vacuum pump, which pulls out the air between these layers. Meanwhile, on the other side a resin container is connected by a tube, which allows the resin to flow into the mold during the vacuum process. The resin will be uniformly distributed among the glass fibers.

# 5 Adhesive bonding

## 5.1 Introduction

In this section different adhesives will be explained. The adhesives are distinguished in 3 types: Liquid, film or tapes and interlayer.

Most of these adhesives are usually used for insulated glass units. This chapter will explore them by comparing their mechanical and physical properties.

## 5.2 Epoxy

An epoxy is known as a thermoset product that consists of a mixture of resin and hardener. It is essential to mix these two components in the right quantities to ensure that the chemical reaction is completed, providing the final product with proper properties.

This precise measuring could be seen as a disadvantage of epoxies, where a mistake can cause an incorrect chemical reaction. Therefore, it is recommended to use a helix nozzle to ensure good mixing of the aforementioned components (fig. 5.2.1).

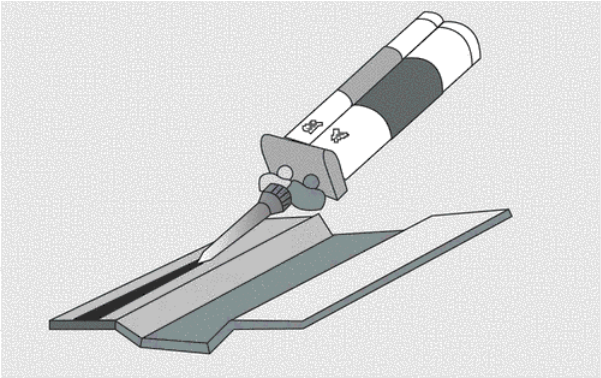

Figure 5.2.1: Helix nozzle (Goss, 2010).

In general, epoxies have an excellent bonding property to ceramics, metals and glass and have rather poor adhesion to elastomers, polyolefin plastics and fluoropolymers (Goss, 2010). Especially on most thermoplastics, epoxies outperform cyanoacrylates. Epoxy adhesives provide a good bonding to thermoset plastics and are widely used for bonding sheet moulding compound door and body panels in the transportation industries. Furthermore, epoxies are excellent adhesives regarding to thermal and environmental resistance.

The advantages of using epoxies include the high bond strength, which is suitable for bonding various materials and its ability to resist water. Epoxies are able to fill large gaps, which is a specific property compared to cyanoacrylate. Epoxies are relatively less expensive than cyanoacrylates and are often the toughest and most durable adhesive of the adhesive technologies (Goss, 2010).

However, epoxies have disadvantages in the curing process, which is relatively slow compared to the most adhesives because of carefully mixing the two components. Moreover, some hardeners are toxic which pose a threat to health and safety at the workplace. The main disadvantage of epoxies is that they have the lowest elongation compared to polyurethane, cyanoacrylate and silicone adhesives, mainly due its high Young's Modulus.

## 5.3 Polyurethane

Polyurethane have different types of adhesives. There is a distinction between physically curing and chemical curing. Physical curing includes solvent-based adhesives, dispersion adhesives or contact adhesives. Chemical curing comprises of one or two components adhesives. Chemical curing is mainly used for structural applications (Bels, et al.).

Like Epoxies, Polyurethane adhesives strongly depend on the exact proportions of the two components. By adjusting the ratio of constituents, the desired elasticity, curing velocity, strength, adhesion, etc. are achieved. The strengths of the different polyurethane adhesives vary enormously. Values of 1 to 15 N/mm2 can be achieved (these values are not including the safety factor). The strength and the stiffness of polyurethane are in general lower compared to acrylates and epoxies (Bels, et al.). However, it is still higher compared to typical silicone adhesives. In addition, an advantage of using polyurethane adhesives is that they can resist dynamic loads. Therefore, it has a good resistance can be obtained against differential thermal expansion.

The main disadvantage of using conventional polyurethane adhesions for glass-metal bonding is its limit of UV resistance. This can be remedied by adding UV-blocking primers to the mixture, although that in turn limits the durability of the connection.

Polyurethane adhesives are widely used in the automotive industries, where it is necessary to ensure structural bonding between glass windshield and the chassis (fig. 5.3.1). For such an application, where the adhesive is exposed to sunlight, an UV-protecting coated is required.

Figure 5.3.1: Gluing a glass windshield to the chassis with Polyurethane adhesive (Bels, et al.)

Polyurethane is also regularly applied in the architecture industry, but mainly for applications where polyurethane does not have to be exposed directly to sunlight, such as bonding façade panels and outdoor insulation systems. For double glazing systems, polyurethane is regularly applied if the adhesive is fully covered and protected against sunlight.

## 5.4 Silicone

In general, silicones are characterized by a relatively low tensile strength compared to the aforementioned liquid adhesives (table 5.5.1) and has an insignificant stiffness. Silicones are distinguished into two types, namely one component and two components systems. The one component type cures by air, where a reaction arises with the moisture in the air. The two component type cures by adding an extra chemical constituent. One component silicones are generally slightly stiffer and stronger than the two components variants due to more hardening.

The low stiffness of silicone causes the adhesive to resist differential thermal expansion allowing the adhesive to incorporate tolerance. Silicones are applied in a linear seam of at least a thickness of 6 mm. In addition, they can be applied to a considerable interval of temperatures compared to the other liquid adhesives. Moreover, silicones have an excellent ability to resist UV radiation, moisture and environmental influences.

The main disadvantages of the one component silicones are its slow curing velocity, its compatibility problems with certain types of coatings and adhesive interlayer, such as Polyvinyl butyral (PVB), which can cause possibilities of corrosion (Bels, et al.). In addition, the relatively low strength of silicones forms a disadvantage in structural applications in the building industry.

Recently, an adhesive film based on silicone has been developed. This product is called TSSA and it stands for "Transparent Structural Silicone Adhesive". It is a fully transparent adhesive that cures in a high temperature furnace. It achieves a relatively higher strength in comparison with the traditional silicones. TSSA-film is not developed for linear seams, in contrast with silicones, but is meant for point by point applications.

Silicones are mainly used for structural silicone glazing (SSG) applications (Bels, et al.). Silicones are also used for non-structural applications, for instance as a weather sealant. Just like with sealing double glazing, it is preferred to use polyurethane for its durability. Traditional silicones play an insignificant role in applications where high structural performance is required and the adhesive bonding is responsible for transferring the mechanical stresses.

## 5.5 Interlayers

Adhesive interlayers or laminates are developed mainly to create a glass on glass connection for laminated glass. In practice, several attempts have been made to use interlayer for glass-metal connections for innovative applications.

The main purpose for interlayers is to produce a safer product. When several thin glass panels are incorporate by an adhesive interlayer, it increases the chance that the integrity of the entire element is not affected by impact or scratches. In addition, laminated glass ensures better post fraction behavior, because all glass splinters remain attached to the adhesive interlayer in case of breakage. Adhesive interlayers were originally developed for automotive industries, where impact resistance is required more than high stiffness.

The most used interlayer nowadays is polyvinyl butyral foil (PVB) of which there are numerous variants depending on the final application. For instance, flexible PVB's are used for acoustic and vibration damping purposes and stiffer PVB's for constructive objectives. The interlayers that are based on PVB will provide several materials with good performance on bonding with, amongst others, metals and glass.

Another important interlayer type is SentryGlass (GS). SentryGlass is stiffer than PVB and it has great potential for use in glass to metal bonding (fig. 5.5.1). SG is an adhesive interlayer which is based on ionomer bonding (Bouwen met glas en adhesieven). Due to this ionomer bonding, SG is stiffer compared to traditional PVB foil (Bels, et al.) .This interlayer is used by architectural application where a stiffer laminated glass panel is required, to improve the post fraction behavior.

Interlayer adhesives are characterized by curing according to a lamination process where high pressure and temperature is applied in an autoclave. The interlayer becomes liquid and develops a sufficient bonding with the glass surface through a chemical reaction. When the entire composed panel cools down, the interlayer turns back to a solid condition and accomplishes its cohesive strength.

The strength of adhesive bonding of traditional PVB is lower compared to SG. However, SG becomes sensitive to a differential thermal expansion (Bels, et al.). Both interlayers have a disadvantage when it comes to moisture and temperature sensitivity. Both interlayers are mainly manufactured and applied to laminated glass. A glass to metal bonding barely uses interlayer adhesives. Since SG is a relatively new product where it has not fully been experimented with in the field of glass to metal bonding, further research is necessary.

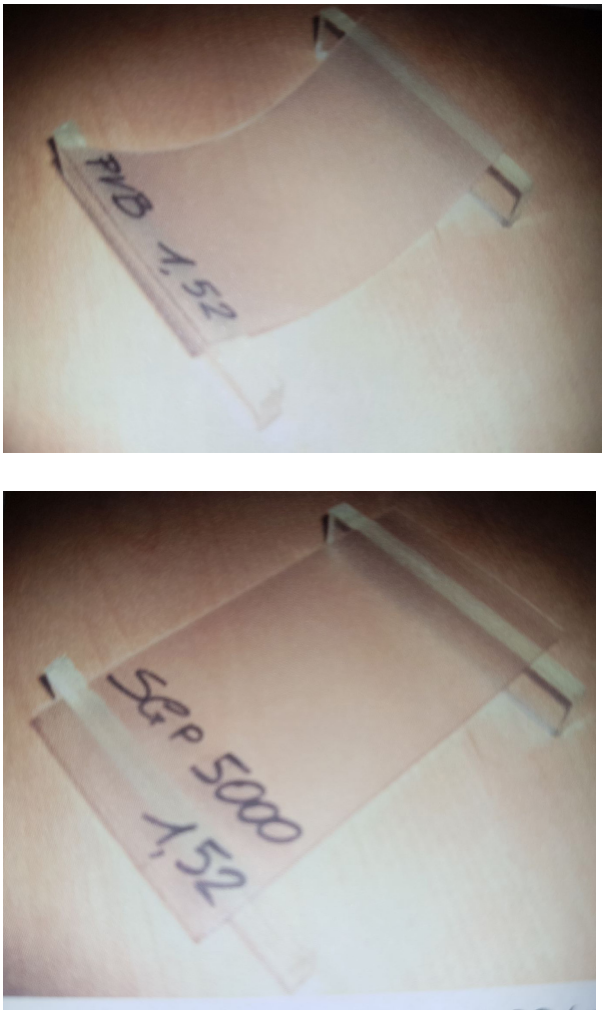


Figure 5.5.1: Comparsion between the stiffness of PVB and SG (Bels, et al.)

Table 5.5.1 gives an overview of the mechanical and physical properties of the mentioned adhesive types. These properties are obtained from an online database 'Matweb' of several materials including thermosets and thermoplastics adhesive types, that are been used to structural purposes. According to table 5.5.1 epoxy is the stiffest adhesive compared to the mentioned liquid adhesives. Later in section 9.4, two adhesives, namely Epoxy and polyurethane will be analysed to mention their influence on bonding thin glass with GFRP profiles. Therefore, these values of table 5.5.1 will be used to simulate the adhesives.

| | | Liquid | | | | Film/tape | | Interlayer | |
|---|---|---|---|---|---|---|---|---|---|
| | Properties/ Adhesive | Epoxy | Polyurethrane | Acrylic /Cyanoacrylate | Silicones | TSSA Dow corning (1mm thickness) | 3M VHB Tape | Sentry Glass (SG) | Polyvinyl butyral (PVB) |
| Mechanical properties | Density (kg/m3) | 1530 | 1210 | 1110 | 1290 | - | 980 | 950 | 1070 |
| | Ultimate Tensile strength N/mm2 | 50.3 | 9.8 | 25.7 | 6.78 | 8.5 | 0.690 | 34.5 | 20.8 |
| | Young's modulus N/mm2 | 6490 | 33.1 | 1360 | 249 | 9 | (0.45) | 300 | 18 |
| | Shear strength N/mm2 | 20.5 | 4.69 | 20.3 | 0.658 | 5.7 | 0.552 | - | - |
| | Elongation at break % | 19.5 | 345 | 104 | 381 | 250 | (high) | 400 | 250 |
| Physical properties | UV-light resistance | Good | Low | Low | Excellent | Good | Excellent | Excellent | Excellent |
| | Chemical resistance | Excellent | Medium | Low | Low | Good | Excellent | Good | Medium |
| | Temperature resistance | High, 160 °C – 177 °C | High, 100 °C – 200 °C | Low 80°C | Excellent > 300 °C | High, >150 °C | Medium (40 °C - 150 °C) | Low (82 °C) | Excellent (150-275°C) |
| | Optical performance (Transparent) | Good (87.3 %) | Excellent (90 %) | Good (80.2%) | Good (87.3%) | Excellent (crystal clear) | Medium (<80%) | Excellent(90%) | Excellent (90%) |

5.5.1 Table: Comparison of adhesive types according to their Mechanical and Physical properties.

## 5.6 Conclusion

The adhesives are distinguished in 3 types: Liquid, film or tapes and interlayer.

An epoxy is a thermoset product that consists of a mixture of resin and hardener. It is essential to mix these two components in the right quantities to ensure that the chemical reaction is completed. A disadvantage of epoxies is the precise measuring, where a mistake can cause an incorrect chemical reaction and also a slow curing process. The main disadvantage of epoxies is that they have the lowest elongation compared to polyurethane, cyanoacrylate and silicone adhesives, mainly due its high Young's Modulus.

Advantages of epoxies are however numerous: an excellent bonding property to ceramics, metals and glass and have rather poor adhesion to elastomers, polyolefin plastics and fluoropolymers, a good bonding to thermoset plastics and are widely used for bonding sheet moulding compound door and body panels in the transportation industries, excellent adhesives regarding to thermal and environmental resistance, able to fill large gaps, are relatively less expensive than cyanoacrylates and are often the toughest and most durable adhesive of the adhesive technologies.

One of the Disadvantages of Polyurethane adhesives is that it strongly depends on the exact proportions of the two components. The main disadvantage of using conventional polyurethane adhesions for glass-metal bonding is its limit of UV resistance. However, this can be remedied by adding UV-blocking primers to the mixture, although that in turn limits the durability of the connection. Advantage of using polyurethane adhesives is that it can resist dynamic loads.

Silicones are distinguished into two types, namely one component and two components systems. The one component type cures by air, where a reaction arises with the moisture in the air. The two component type cures by adding an extra chemical constituent.

Advantages of silicone is that they can be applied to a considerable interval of temperatures compared to the other liquid adhesives. Besides, silicones have an excellent ability to resist UV radiation, moisture and environmental influences. However, the main disadvantages of the one component silicones are its slow curing velocity, its compatibility problems with certain types of coatings and adhesive interlayer, such as Polyvinyl butyral (PVB), which can cause possibilities of corrosion. The relatively low strength of silicones forms also a disadvantage in structural applications in the building industry.

Interlayers or laminates are developed mainly to create a glass on glass connection for laminated glass. By incorporation of several thin glass panels the adhesive interlayer increases the chance that the integrity of the entire element is not affected by impact or scratches. In addition, laminated glass ensures better post fraction behaviour, because all glass splinters remain attached to the adhesive interlayer in case of breakage.

The two most used interlayer types are the polyvinyl butyral foil (most used type) and the Sentry Glass. SentryGlass is stiffer than the first and it has great potential for use in glass to metal bonding. The strength of adhesive bonding of traditional PVB is lower compared to SG. However, SG becomes sensitive to a differential thermal expansion. Both interlayers have a disadvantage when it comes to moisture and temperature sensitivity. Both interlayers are mainly manufactured and applied to laminated glass. A glass to metal bonding barely uses interlayer adhesives.

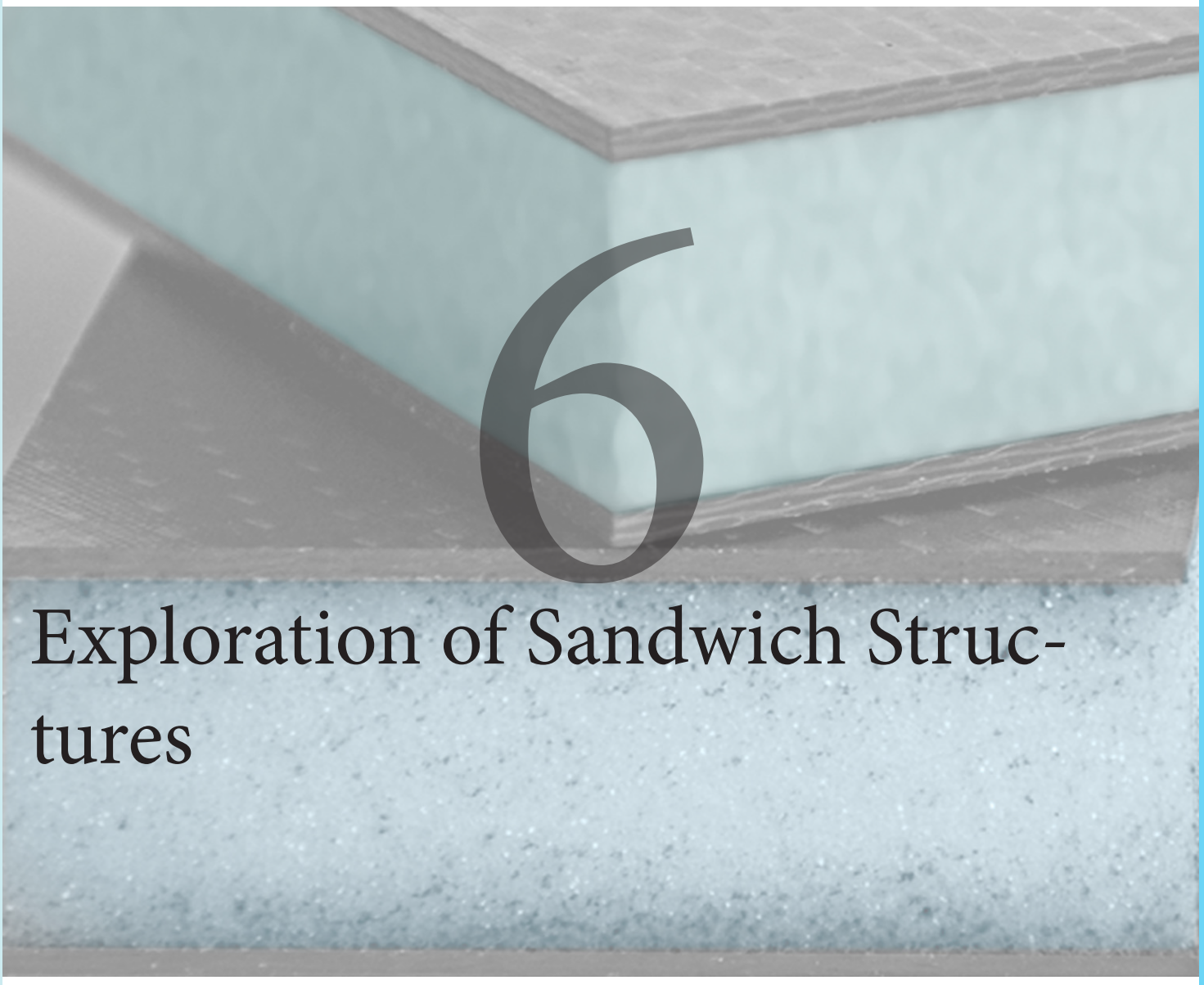

# 6 Exploration of Sandwich Structures

## 6.1 Introduction

In this section, the definition of a sandwich panel will be explained. This is necessary to understand the configuration of a sandwich panel. This will lead to the essential facts of how to make a sandwich façade panel.

## 6.2 What is a sandwich panel?

The first description of a sandwich wall was in a 1924 patent (von Karmen et al.,2014). At that time, sandwich structures were made from natural materials. Ten years later, S.E. Mautner started experimenting with a sandwich structure of plywood facings and a cork core. He fabricated this sandwich structure in the airplane plants of Schneider-Creusot in France. Later in 1940, sandwich panels composed of plywood-balsa-plywood were used in the de Havilland Mosiquito aircraft .That sandwich panel type represented the high point of engineering with wood(Prove Kluit, 1997). In 1943, sandwich panels constructed of a glass fiber, reinforced polyester laminate facing and a honeycomb core were used for the first time in the aft fuselage of a training aircraft in the USA. After the Second World War, the polyester resin was replaced by epoxy resins. In 1950s, the use of sandwich structures in the building industry began. They were used for building envelopes as a prefabricated, light weight and opaque sandwich panels (mainly made of aluminum or steel sheets with adhesively bonded reinforced paper honeycomb). They were widely utilized in the American building construction market (Prove Kluit,1997) . Applications of sandwich panels can be found in any industry where a combination of light weight and high strength is crucial.

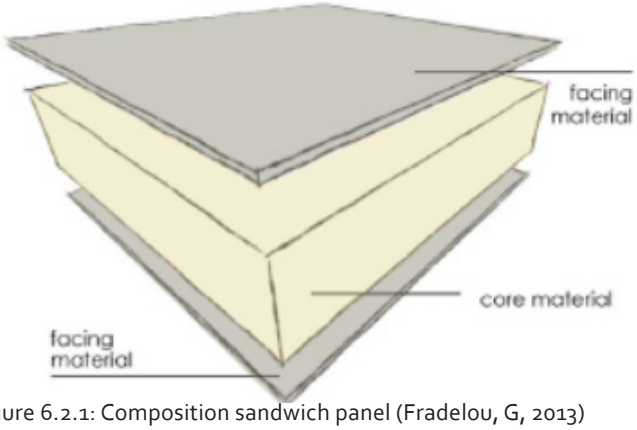


Figure 6.2.1: Composition sandwich panel (Fradelou, G, 2013)

The basic composition of a sandwich panel consists of three main layers: two surface layers, called facings and a core layer (fig. 6.2.1). The facings can be made from aluminum or fiber reinforced polymers. The core layer can be made from foam or a honeycomb structure. The most common sandwich façade panels nowadays are made of glass fiber reinforced polymers facings and foam as a core. This combination highlights the load-bearing potential of such a structure. Moreover, sandwich panels can be composed of different thermoplastic polymers and be used as insulated facade panels in the built environment. These sandwich panels can be made translucent or even transparent with the sacrifice of loadbearing capacity.

The design principle of a sandwich panel is comparable to an I-beam structure (fig. 6.2.2). An I-beam structure is an efficient structural element, because the top and the bottom flanges handle compression and tension stresses when a certain load is applied and also to resist most of the bending movement. These flanges are connected by the web, which is responsible to resist shear stress. An I-beam structure element is very effective for carrying shear and bending loads in the plane of the web. In addition, an I-beam is an economical structure, because its minimal shape reduces the use of raw materials. In the case of a sandwich panel, the flanges of the I-beam are replaced by facings and the I-beam web is replaced by the sandwich panel core. The core differs from the web, because it can be made of different material from the facings and it offers an evenly distributed support for the facings rather than the relatively thin web at the concentrated center.

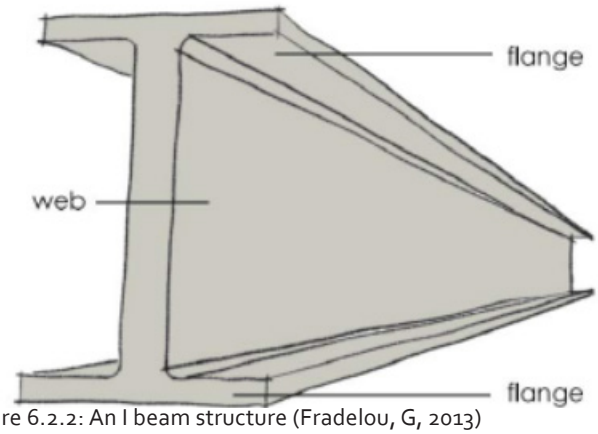


Figure 6.2.2: An I beam structure (Fradelou, G, 2013)

The core materials should have three main functions: load-bearing capacity, thermal insulation and acoustical insulation. These functions largely depend on the thickness and the material of the core. Moreover, the core should have a low density in order to reduce the total weight of the sandwich panel. Beyond the basic functions, the other key properties for the core include:

- Low density
- Shear strength
- Shear modulus
- Stiffness perpendicular to the facings.

The main core materials can be divided in to into four categories. These are (spacer fabrics), foams, honeycomb and balsa wood (fig. 6.2.3). Foams and honeycomb structures are superior for load transfer compared to balsa wood and Fleeces.
In principle, the most critical functions of the core are transferring the shear between the facing plies and providing the sandwich panel with thermal insulation.

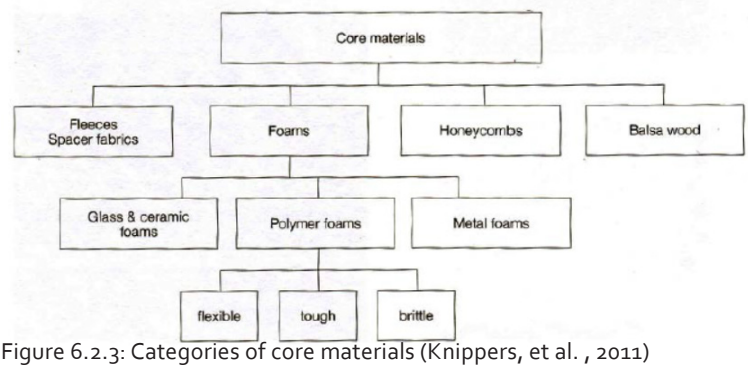


Figure 6.2.3: Categories of core materials (Knippers, et al. , 2011)

Using low weight sandwich elements enables more economical forms of construction and allows for longer spans as well. In addition, when a sandwich element does not have to be translucent or transparent, the first choice for a core would be polymer foams. Polymer foams ensure the best mechanical and physical properties for sandwich elements in the built environment. In the case of a sandwich element that requires transparency, honeycomb as a core would be suitable . While honeycomb hollow structures are more economical, they offer lower thermal insulation than foam cores and are more complex to work with (Knippers, et al. , 2011).

In addition, they are less flexible which limits the freedom of form.

When honeycomb structures are combined with transparent facings to form a sandwich element, they have great ability to diffuse sunlight and hence reduce glare (Knippers, et al. , 2011). Balsa wood is mainly used as a core for thin sandwich structures. The biggest disadvantages of balsa wood are poor load bearing capacity and weak mechanical properties compared to the foams and honeycomb structures. Moreover, balsa wood is sensitive to moisture, which causes problems when implemented as a core for a façade sandwich panel. In this research document, the main focus is sandwich structures which include transparent facings and translucent cores. Potential transulent façade sandwich panels will be explored in the next section.

## 6.3 Translucent sandwich panel

The aim of this section is to compare the various translucent sandwich panels according to their physical and mechanical properties. Two different kinds of translucent sandwich façade panels will be explained: Polycarbonate and Glass Fiber Reinforced Polymer.

### 6.3.1 Polycarbonate façade sandwich panel

In general, these panels are made from polymers consisting of carbonate groups. The polymers are mostly made from a particular group of thermoplastic polymers. Polycarbonates are not usually manufactured in solid sheets but rather as hollow products (fig. 6.3.1.1). Typical polycarbonate façade sandwich panels have between two and six levels of orthogonal voids (Knippers, et al. , 2011). That provides the panel with better load-bearing capacity and stiffness than solid polycarbonate sheets and improves the thermal insulation effect. Panel sheets with x-shaped webs have improved the insulation properties even more (fig. 6.3.1.2).

Figure 6.3.1.1: Typical polycarbonate facade sandwich panels(Knippers, et al. , 2011).

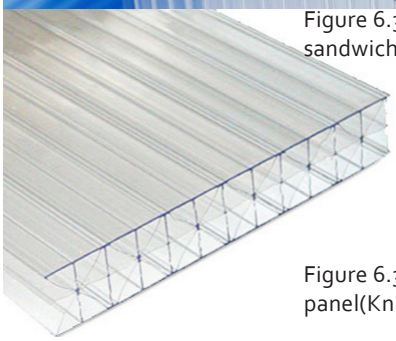

Figure 6.3.1.2: X-shaped polycarbonate panel(Knippers, et al. , 2011).

Polycarbonate façade sandwich panels are mainly manufactured by extrusion technology. The thermoplastic resin in the form of clear or tinted pellets is melted and pushed through a die. After crossing the die, the panel enters a preheated oven to release tension. The panels then travel over rollers in order to cool down and finally be cut in the desired dimensions. This technology allows for the contiguous production of any length of product in a wide variety of profiles that is limited only by transport .

The panels, which are transported by ships, typically have a maximum length of 12 meters due to the standard container length of 12 meters. An exception to this is when the panels are manufactured in Europe where the length of the panel can reach 30 meters. The crucial key to manufacturing polycarbonate sheets is to use advanced and refined dies which set the thickness, the width, the height and the structure in agreement with the particular specifications of design professionals.

In order to create different end products of polycarbonate sheets, co-extrusion technology is applied (fig. 6.3.1.3). The main function of this technology is to add a thin layer containing a mixture of different resin to one or both sides to the extruded polycarbonate panel. The added material can provide the panel with an ultraviolet (UV) light protection layer since UV radiations can degrade unprotected polycarbonate sheets. In addition, the co-extruded resin can provide the panel with a color or to add improved solar heat reduction.

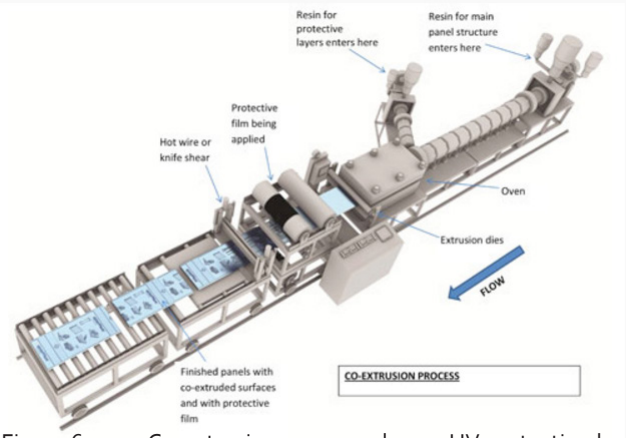


Figure 6.3.1.3: Co-extrusion process where a UV protection layer i added to extruded polycarbonate (Telow, 2012).

Polycarbonates have multi-faceted properties which situates polycarbonates between commodity plastics and engineering plastics. The first use of polycarbonates is for electronics components while the second use is for construction material. As proof of their strength, polycarbonate is in fact used as a main material for airplane windows. Polycarbonate façade sandwich panels offer high resistance against impacts, storm and vandalism.

It's proved by studies that in some applications polycarbonates are impressively unbreakable. In general, polycarbonates are 30 times more impact resistant than an unmodified acrylic with an equivalent thickness and 250 times more than annealed glass.

Polycarbonates are characterized by clarity and good light transmission (fig. 6.3.1.4) . Polycarbonate façade sandwich panels allow more light entering the room than glass fiber reinforced panels (GFRP) but less than glass. Soft light and daylight can be accomplished through opal or frosted polycarbonate panels. Studies have shown the importance of daylight on improving the quality of life and well-being. In addition, daylight is directly linked to increased productivity of office workers including improved learning curves.


Figure 6.3.1.4: Polycarbonate Police shield and Light transmission through polycarbonate facade panels (http://www.iplasticsupply.com/) (http://www.archdaily.com/9218/hq-13-parisian-subway-line-atelier-phileas/) .

In terms of thermal insulation, polycarbonate panels offer significant benefits due to the cavity chambers between the inner and the outer facings. A high level of light transmission in combination with high thermal resistance can be achieved due to the variety of available profiles and resins. A cellular polycarbonate façade sandwich panel of 25 mm thickness has a thermal resistance value of 0.52 and an insulated glass unit with the same thickness has an R-value of 0.37 (table 6.3.1.1). Their U-values are 1.92 and 2.70 respectively. In addition, filling polycarbonate façade sandwich panels with translucent aerogel helps to increase their thermal performance.

This material is derived from a gel which in this case the liquid component of the gel is replaced by a gas. However, we should notice that cellular polycarbonate panels filled with aerogel is relatively new and unproven for long-term field performance.

| PRODUCT | U | R | LT% |
|---|---|---|---|
| 10mm | 0.53 | 1.89 | 81 |
| 16mm | 0.40 | 2.50 | 74 |
| 16mm | 0.37 | 2.70 | 67 |
| 25mm | 0.34 | 2.94 | 72 |
| 25mm | 0.26 | 3.85 | 58 |
| 35mm | 0.21 | 4.76 | 51 |
| 40mm | 0.19 | 5.26 | 51 |
| 45mm | 0.18 | 5.56 | 50 |
| 50mm | 0.17 | 5.88 | 50 |

Table 6.3.1.1: Thermal conductivity, thermal resistance and light transmission of polycarbonate panels with different thicknesses (Telow, 2012).

Moreover, polycarbonate panels are characterized by light weight. In comparison with a standard 25 mm thick insulated glass unit, which weights 30 kg/m2 a polycarbonate façade sandwich panel with the same thickness weighs 3 kg/ m2. This difference in weight has direct influence on the frame and the support systems in the built environment. As a result, these construction systems can be lighter and less expensive. In addition, the light weight of polycarbonate panels offers significant savings in transportation, handling and installation.

Polycarbonate façade sandwich panels have sufficient elasticity to be cold bent (fig.6.3.1.5). They are suitable for applications as curved canopies and barrel vault skylights. They can be curved by cold bending, on site, across their length over their supports which are distanced to determine the curvature radius. It should be mentioned than when the curved panel is removed from its applied shape, it will return to its original form, namely a flat panel. In addition, curved panels have a limitation in bending because of the added spanning stress that occurs when you bend

| | |
|---|---|
| 2610-4 | minimum radius 3.00m |
| 2625-5 | minimum radius 8.00m |
| 2253-2 | minimum radius 2.00m |
| 2250-10-4 | minimum radius 3.00m |

Figure 6.3.1.5: Cold bent polycarbonate sheet with certain radii depending on the thickness (http://www.rodeca.de/?L=1).

Table of Bending Radii

| Thickness | Min. Radius |
|---|---|
| 6mm | 41 in. |
| 8mm | 55 in. |
| 10mm | 69 in. |
| 16mm | 110 in. |
| 25mm | 173 in. |

Table 6.3.1.2: Typical allowable radii for cold bending multiwall polycarbonate sheets (Telow, 2012).

It is remarkable that polycarbonate panels are able to reflect sound more than other panel types which have softer and more textured surfaces. Table 6.3.1.2 shows the sound transmission levels through a polycarbonate façade sandwich panel with different thicknesses.

| Multiwall polycarbonate sheet | |
|---|---|
| 4mm-8mm | 18dB |
| 10mm-16mm | 20dB-21dB |
| 20mm-35mm | 22dB |
| 40mm | 23dB |

Table 6.3.1.2: Sound transmission multiwall polycarbonate sheets (Telow, 2012).

### 6.3.2 GFRP façade sandwich panel

When polymers are unsuitable for the intended applications due to inappropriate mechanical properties then it is possible to combine the polymers with other materials or fibers in order to form a composite. Therefore, the following improvements are achievable:

- Higher load carrying capacity and reduced deformation;
- Better thermal insulation properties;
- Increased surface hardness (higher scratch resistance);
- Wider range of design options.

Combining the polymer with fibers, wood, paper, foam or mineral aggregates usually results in an opaque composite product. Only the combination of glass fibers and a polymer can achieve a translucent composite with a certain desired thickness (fig. 6.3.2.1). It is still not possible to produce a fully transparent composite sheets or panels. The thermosets polymers (resins) create a consistent bond with the fibers, while the glass fibers are used for the reinforcement.

A printed foil can be inserted which then glimmers light through the polymer and remains visible.

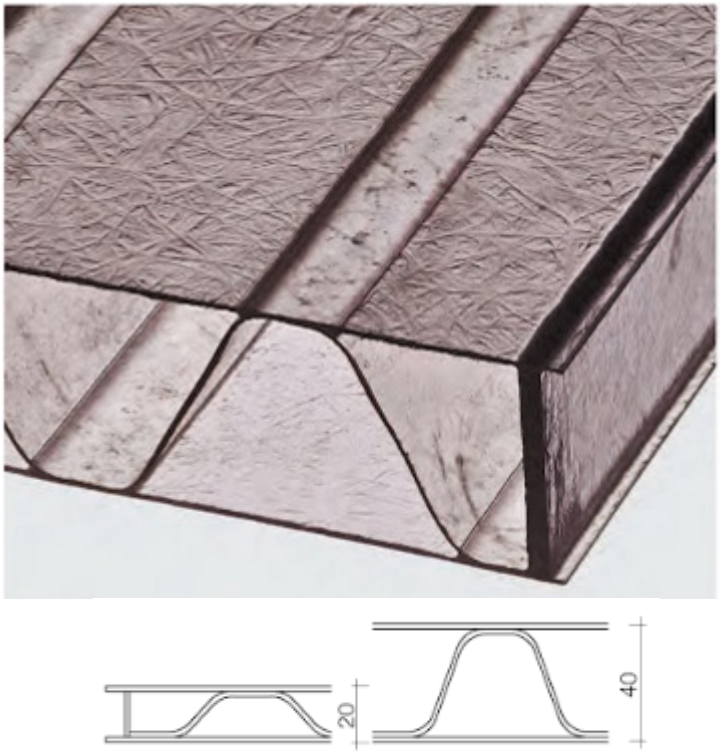


Figure 6.3.2.1: A GFRP sandwich panel with different thicknesses (Knippers, et al. , 2011).

GFRP sandwich panels are used when a planar element requires high stiffness, like shells in compression, long spans or even panels with point loads as in bridge-building. In addition, light weight core layers have a low thermal conductivity. It is also possible to fill hollow GFRP sandwich panels with either translucent thermal insulation materials like aerogel or thermal mass like foams (fig. 6.3.2.2). Either the load-bearing capacity or the thermal insulation can be improved by manufacturing fiber reinforced sheets in the form of a sandwich structure with a light weight core or as planks with strengthening ribs.

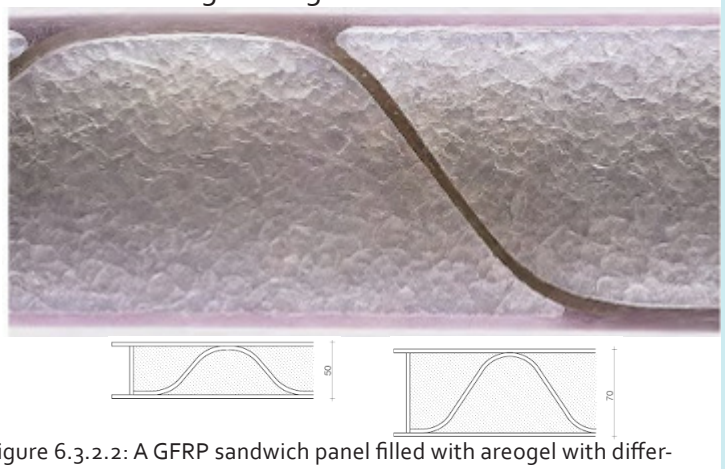

Figure 6.3.2.2: A GFRP sandwich panel filled with areogel with different thicknesses (Knippers, et al. , 2011).

Another type of GFRP planar element is the plank. Planks are planar elements provided with strengthening ribs on one side(fig. 6.3.2.3). The manufacturing technique of planks are much simpler than that of sandwich panels. The main reason is that planks are made from only one material.

Pultrusion is the main manufacturing technique that has been used to make planar products and profiles, so it is possible to produce planks elements as well with the same technique. Moreover, the webs are mostly positioned parallel which makes it easier to use the pultrusion process than other GFRP manufacturing processes. A further development of the plank element is twin-wall transparent planks which has closed voids. However, the web thickness should be at least 2 mm because of the fiber reinforcement. Both elements, planks and twin-wall planks can be used as façade cladding or even for walkway surfacing.

While some polycarbonate façade sandwich panels are manufactured by the extrusion process, in contrast these GFRP planar products are mainly produced by the pultrusion process (see section 4.4) . The main key of this process is the heated section die, which determines the shape of the pultruded element. Sections made from fiber reinforced polymers are primarily suited to load bearing applications (Knippers, et al. , 2011). In particular, the built environment industry prefers to use glass fibers as reinforcement because they are relatively less expensive and durable. Moreover, GFRP are favorable as structures in the building industry when excellent corrosion resistance must be combined with economy. Since the 1990s, GFRP pultruded section structures are increasingly used in bridges, buildings and façades.

The arrangement of the fiber reinforcements in the pultruded sections is primarily in the form of long fibers positioned in the longitudinal direction of the composite. Moreover, textiles and fleeces can be added to integrate in the section of the surfaces of the sections (fig.6.3.2.4).

While the fibers are responsible for the load-carrying capacity in the longitudinal direction, the outer layers improve the shear capacity and the appearance (knippers, et al., 2011). In addition, when in a custom section a high load-bearing capacity in the transverse direction is required, then there may be more textile reinforcement than fibers.

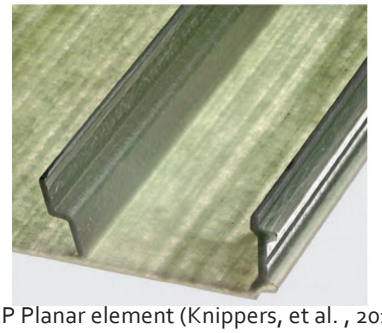

Figure 6.3.2.3: GFRP Planar element (Knippers, et al. , 2011).

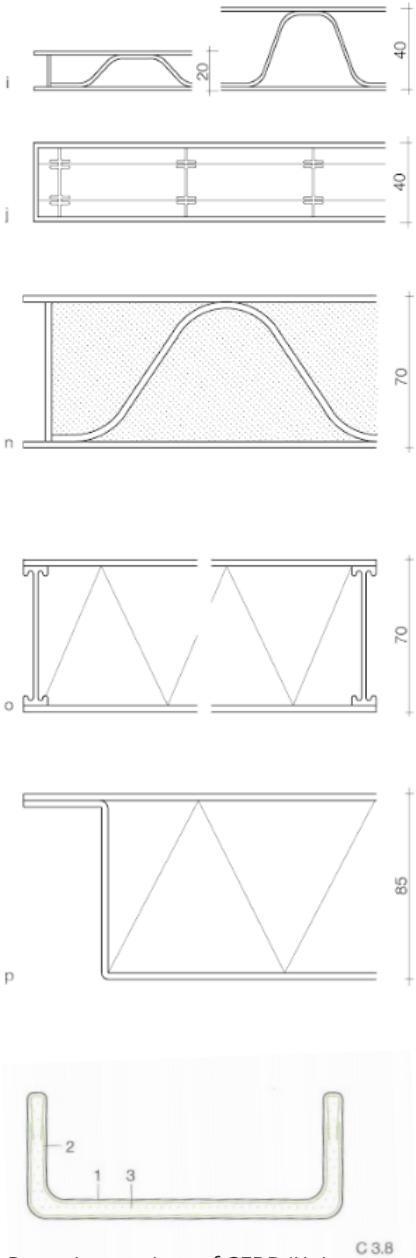


Figure 6.3.2.4: Putrusion sections of GFRP (Knippers, et al. , 2011).

Pultruded sections are always prismatic which serves as a constant cross section over their entire length. Moreover, it is possible to include core materials or longitudinal ribs and cable ducts, but transverse ribs are impossible . Overall dimensions of 1250 x 650 mm of a sandwich panel or a plank as a pultruded section can be achieved, but this depends on the manufacturer (knippers, et al., 2011). In theory, there are no limits to the length of the composite because of the contiguous method of production of sections. However, the sections are generally cuts in lengths of 6 meters. In addition, the internal corners of pultruded sections of GFRP should contain a radius of at least a 5 mm.

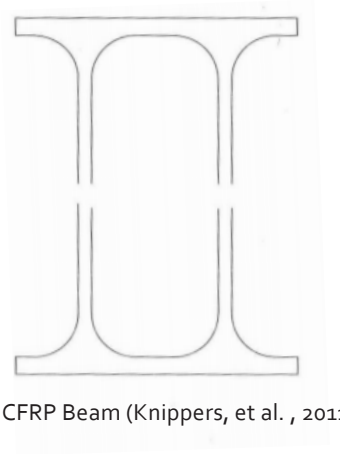

Figure 6.3.2.5: CFRP Beam (Knippers, et al. , 2011).

## Simple cross-sectional geometries

The pultruded sections made from fiber reinforced polymers in figure 6.3.2.6. are very similar to those of structural steelwork. These sections types are marketed by various manufactures. Pultruded beams have a comparable axial force and bending capacity to steel sections. However, the much lower elastic modulus of GFRP results in much larger deformation.  As a consequence, the structures made from these sections leads to stability problems. In particular, the I-beams must be continuously supported to avoid lateral buckling of the compression flange.

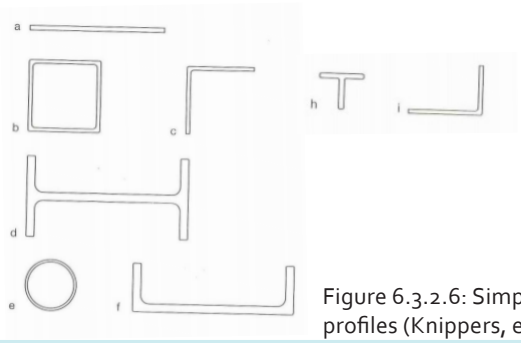

Figure 6.3.2.6: Simple pultruded GFRP profiles (Knippers, et al. , 2011).

The composite beam made of GFRP and carbon fiber reinforced polymer illustrated in figure 6.3.2.5 was developed in order to reduce the deformations of GFRP beams. The flanges consist of unidirectional carbon fibers which are mainly responsible for the bending capacity of the beam. The webs and the textile reinforcement on the surface are made from the relatively less expensive glass fibers. This type of beam reflects the optimized use of materials and results in a higher load-bearing capacity.

## Complex cross-sectional geometries

Sandwich structure designs inspired by the sections used in structural steelwork usually result in a very high consumption of materials and structures that do not make the best use of those materials (knippers, et al., 2011).  In response to this, the improvement of cross sectional geometries have increased in recent years resulting in products that should be more suitable for specific applications requiring optimal material use (fig 6.3.2.7). Accordingly, potential design options can be fully exploited in terms of the form of the cross sections and the combination of materials. Another design point is the thermal insulation which can be increased by sections that have inclusion voids. Furthermore, multi-cellular sections permit a better use of material. In the case of a window frame cross sections, they can have a specific shape that fits to the glass pane. This simplifies the final assembly of a glass unit to the frame. In contrast, with steel are such complex cross-sections forms are impossible to make. This last fact crystallizes the advantages of using fiber reinforced polymers over steel.

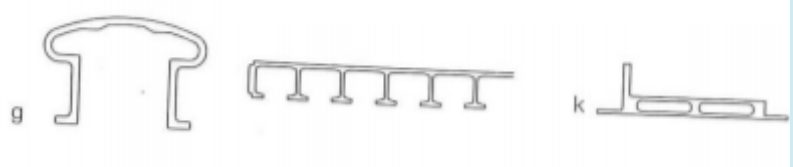

Figure 6.3.2.7: Complex pultruded GFRP profiles (Knippers, et al. , 2011).

A subtype of manufacturing GFRP elements by pultrusion is the modular system. Modular systems are pultruded cross sections in the form of a closed module instead of a structural profile (fig.6.3.2.8 ). The main advantage of the modular system is that it overcomes the limited dimensions that are possible with pultruded cross-sections. The modules can be fitted or glued together in order to construct bridge decks or cladding. In addition, modules can be clipped together in order to accelerate the final assembly.

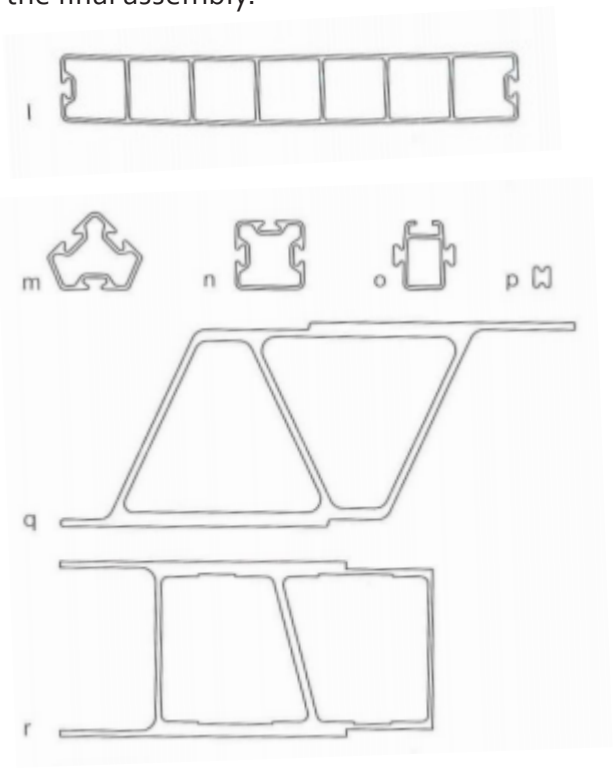


Figure 6.3.2.8: pultruded GFRP closed modules (Knippers, et al. , 2011).

## 6.4 Conclusion

The basic composition of a sandwich panel consists of three main layers: two surface layers, called facings and a core layer. The facings can be made from aluminum or fiber reinforced polymers. The core layer can be made from foam or a honeycomb structure. The core materials should have three main functions: load-bearing capacity, thermal insulation and acoustical insulation. Beside the basic functions, the other key properties for the core include:
- Low density
- Shear strength
- Shear modulus
- Stifness perpendicular to the facings.

The main core materials can be divided into four categories. These are spacer fabrics, foams, honeycomb and balsa wood. The most critical functions of the core are transferring the shear between the facing plies and providing the sandwich panel with thermal insulation.

When a sandwich element does not have to be translucent or transparent, the first choice for a core would be polymer foams. In the case of a sandwich element that requires transparency, honeycomb as a core would be the choice. Balsa wood is mainly used as a core for thin sandwich
structures. The biggest disadvantages of balsa wood are poor load bearing capacity and weak mechanical properties compared to the foams and honeycomb structures. Beside it is sensitive to moisture.

Two different kinds of translucent sandwich façade panels will be explained: Polycarbonate and Glass Fiber Reinforced Polymer.

These panels are made from polymers consisting of carbonate groups. Typical polycarbonate façade sandwich panels have between two and six levels of orthogonal voids, that provides the panel with better load-bearing capacity and stiffness than solid polycarbonate sheets and improves the thermal insulation effect. Polycarbonate façade sandwich

panels are mainly manufactured by extrusion technology.

The thermoplastic resin in the form of clear or tinted pellets is melted and pushed through a die. After crossing the die, the panel enters a preheated oven to release tension. The panels then travel over rollers in order to cool down and finally be cut in the desired dimensions. In order to create different end products of polycarbonate sheets, co-extrusion technology is used. This technology adds a thin layer containing a mixture of different resin to one or both sides to the extruded polycarbonate panel. Polycarbonate Is very strong and offer high resistance against impacts, storm and vandalism. Other advantages of Polycarbonate is clarity and good light transmission and it is characterized by its light weight.

Polycarbonate façade sandwich panels have sufficient elasticity to be cold bent. They can be curved and when the curved panel is removed from its applied shape, it will return to its original form, a flat panel. Polycarbonate panels are
able to reflect sound more than other panel types which have softer and more textured surfaces.

Only the combination of glass fibers and a polymer can achieve a translucent composite with a certain desired thickness. The thermosets polymers (resins) create a consistent bond with the fibers, while the glass fibers are used for the reinforcement. GFRP sandwich panels are used when a planar element requires high stiffness, like shells in compression, long spans or even panels with point loads as in bridge-building.
Another type of GFRP planar element is the plank. Planks are planar elements provided with strengthening ribs on one side. The manufacturing technique of planks are much simpler than that of sandwich panels, because planks are made from only one material

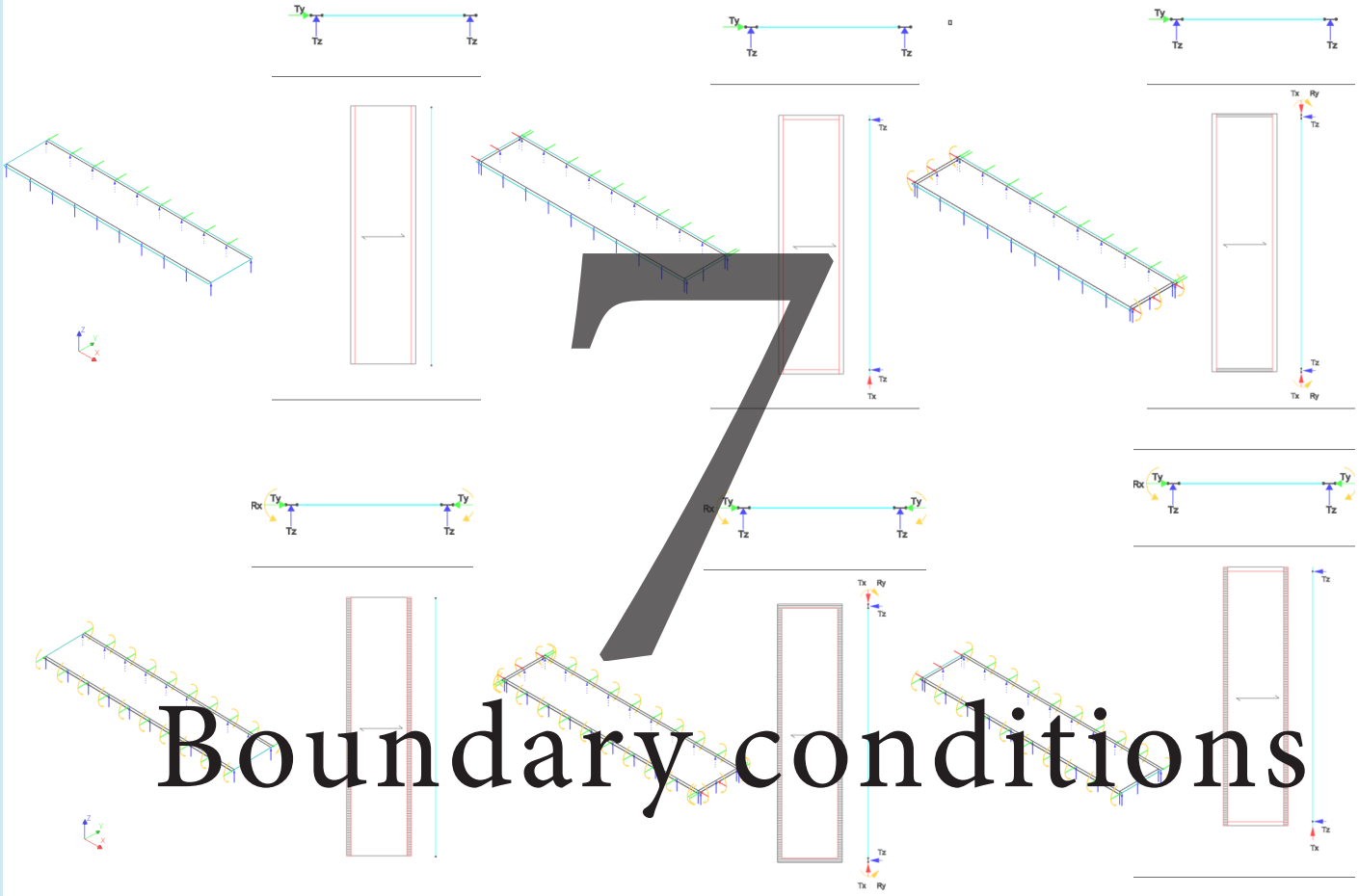


# 7 Boundary conditions

## 7 Introduction

After studying the properties of Glass fiber reinforced polymer and thin glass and analyzing the possible uses of these materials in the building industries, my interest has increased to explore the potential use of combining these material as a façade sandwich panel. It will be done according to the following design steps.

The first phase is defining the required dimensions of a single layer of a glass panel. As mentioned in section 3.4, the maximum dimensions of chemically strengthened glass depends on the maximum size of the chemical salt bath (Weller, et al, 2009). Chemically strengthened glass can be produced and delivered in maximum dimension of 1000 mm x 2000 mm x 19 mm (Wurm, 2007). I have selected a single layer of Aluminosilicate glass panel of 1 mm thickness with a dimension of 1000 mm x 4000 mm. The advantage of this dimension is that it will save time during the manufacturing process and labor time on site compared to the current maximum size. In addition, this dimension will be suitable for façade applications for office buildings, since the height of an office room is considered 4 meters.

After that the maximum bending stress and the maximum displacement of these flat glass panels will be calculated, according to the rules of thumb. This is necessary in order to get an estimate of the behavior of the glass panel when a certain wind load is applied.

Secondly, this glass panel will be modeled in a Finite Element Analysis software, called FEA Diana. The purpose of the analysis is to have an accurate result of the bending stress and the displacement of the glass panel regarding to the influence of wind load.

The way how a single thin glass panel is supported has a significant effect on the bending stress generation and the displacement of that panel.

Moreover, the boundary condition is a crucial factor to define the aesthetical value of the façade design. Therefore, this chapter explores diverse possibilities of boundary condition.

It is important to mention that this chapter is not covering all possible alternatives of supporting thin glass. The aim of this chapter is to apply suitable boundary constrains on thin glass, in order to locate and to define the stress concentrations and the displacement caused by bending in case of applying evenly distributed wind load of 1 kN/m$^2$. Additionally, supporting the edges of thin glass is crucial, since they are the most sensitive and vulnerable areas to bending stress (Murata, et al). The breaking stress of glass is 100-200 MPa, however this can be degraded by the edges (Murata, et al). The manufacturing treatment, like cutting the panel in desired sizes, makes the edges vulnerable to stress concentrations. Point supporters are not suitable for cold bending process of thin glass panel, because these can cause a deviation from the ideal curvature (Herwijnen, 2008). Therefore, all possible alternatives of boundary conditions that do not protect the edges or do not ensure an ideal curvature are excluded.

Finally, a conclusion will be drawn in order to answer the first sub question of this research, which is:

"What are the possible boundary conditions for a single thin glass panel? And what are the influences of these boundary conditions on thin glass, in terms of displacement and stresses?"

## 7.1 Two-sided pinned supported single thin glass layer

The first possible boundary condition is determined by using pinned supports, allowing for rotation. The linear supports are exclusively applied along the longitudinal edges, to create a short span length. The pinned supports consist of a vertical support reaction on one edge (support line A) and vertical and horizontal support reactions on the other edge (support B). Support A prevents the supported area from translation in z-axis direction, allowing translation in Y-axis direction. Support B prevents translation in either Z- and Y-axis directions. These linear supporters are moved 50 mm from the edges of the panel, which creates a span length of 900 mm (fig. 7.1.1). In addition this will allow the edges to move towards the z-direction in case of a displacement caused by evenly distributed wind load of 1 kN/m².

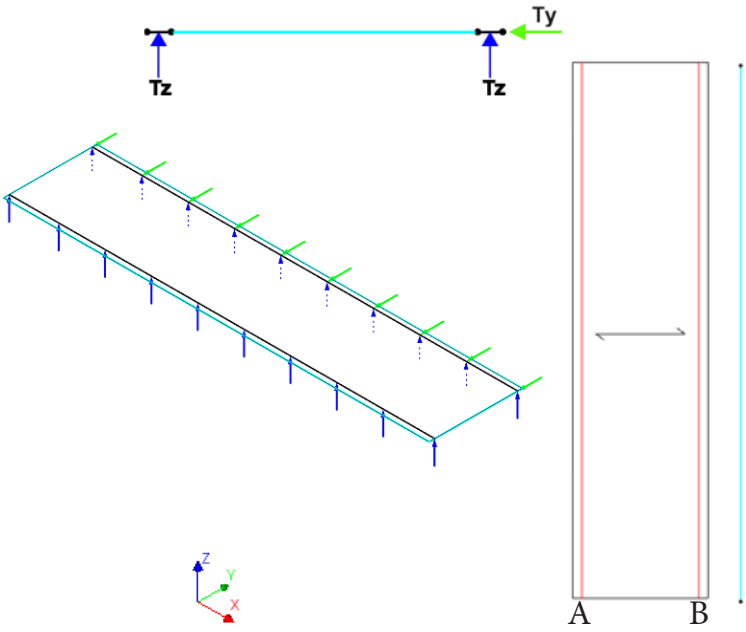


Figure 7.1.1: Two-sided pinned supports configuration.

According to the rules of thumbs, it is expected that the highest stress concentration and displacement will be situated in the middle of the thin glass panel with a value of 68.34 N/mm2 and a deformation of 155.85 mm in the opposite direction of the z-axis (Appendix 2). These values are based on a linear static calculation, where a linear relation is between the applied load and displacement. In practice, linear static analysis is suitable to structural problems where stresses stay in the linear range of the used material. The stiffness matrix of this material remains constant. Therefore, linear static calculation is used to get the first estimation of the behaviour of the thin glass panel in terms of stress concentration and displacement.

In contrast to linear static analysis, a non-linear static analysis has a nonlinear relation between applied load and displacement. Non-linear effects can derive from geometrical nonlinearity's (i.e. large deformation) and material elasticity, which results in an inconstant stiffness matrix during the load application. To obtain more accurate results regarding to the generated stress and displacement, a non-linear analysis will be used in a Finite Element Analysis software "Diana".

To be able to model thin glass panel in Diana the following parameters are used:

| Variant | Variant 1 |
|---|---|
| Geometry | |
| Density kg/m³ | 2480 |
| Length (mm) | 4000 |
| Width (mm) | 1000 |
| Thickness (mm) | 1 |
| Elastic modulus (N/mm²) | 74000 |
| Poisson ratio | 0.23 |
| Boundary conditions | Two sided pinned |
| Wind load (kN/m²) | 1.0 |

Table 7.1.1: Parameters and requirements for simulating thin glass in FEA Diana.

In order to define the exact values of displacement at the bottom, in the middle and on top of thin glass panel during the applied wind load three cross-sections were made. These sections are aligned with the nodes of x-axis respectively x= 0 mm, x= 2000 mm and x= 4000 mm (fig. 7.1.2). The nodes are generated by the mesh properties, which divide the entire glass panel in quadratic element sizes of 10 mm by 10 mm.

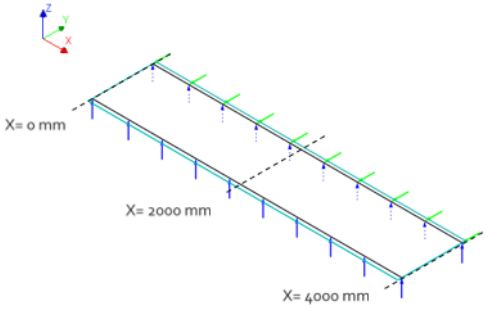


Figure 7.1.2: Three section parallel the Y-axis ( x= 0 mm, x= 2000 mm, x= 4000 mm.

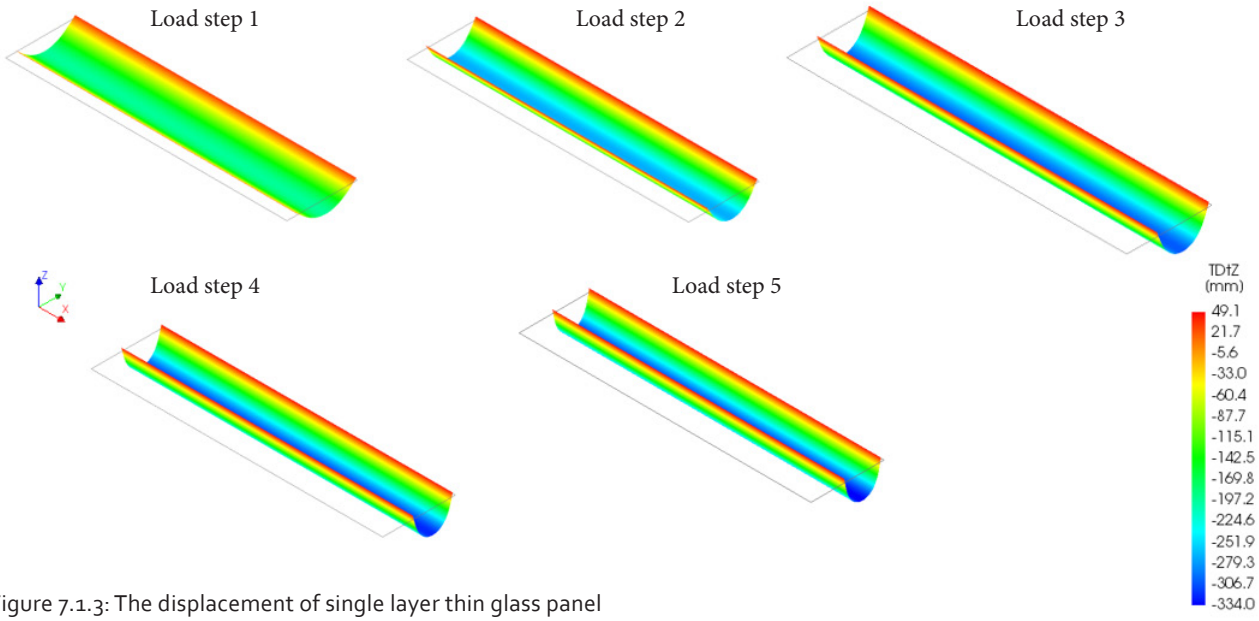


Figure 7.1.3: The displacement of single layer thin glass panel in five steps according to Pinned supports.

To establish the relation between the altitude of displacement and the amount applied wind load, a nonlinear analysis has been made. Figure 7.1.3 shows in five steps the displacement process of thin glass caused by wind load. The first step represents one-fifth of the evenly distributed wind load (1 kN/m²), which is equal to 0.2 kN/m2. Each step adds 0.2 kN/m2 of load to thin glass, till 1.0 kN/m2 is reached.

The analysis of the obtained results show that by applying 0.2 kN/m2 of distributed load, a maximum displacement of 194.4 mm in the opposite direction of Z-axis is reached from its initial state. This value is positioned in the middle of panel. That displacement is increased by 75.5 mm when 0.4 kN/m2 of wind load is applied to get 269.9 mm of displacement. At step 3 the maximum displacement is 303.8 mm, which is 33.9 mm higher than the previous step. In case of using 0.8 kN/m2 of wind load the panel reaches 322.3 mm of maximum displacement. Finally, when a wind load of 1.0 kN/m2 is reached by step 5, causing a maximum total displacement of 334.0 mm.

Chart 7.1.1 implied the cross-sections that emphasize the displacement of the panel at the bottom, in the middle and on the top. A symmetrical geometry is originated relating to similarity of displacement of these cross-sections.

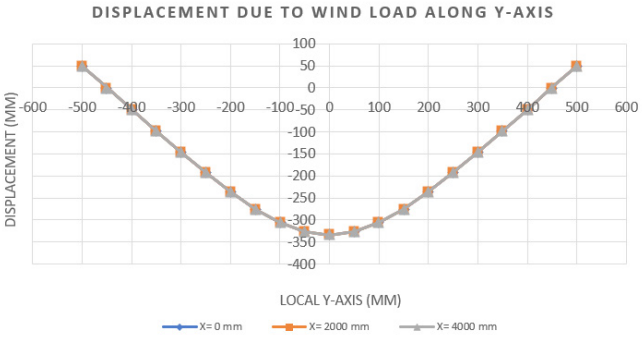


Chart 7.1.1: The displacement due to wind load 1 kN/m² of single layer thin glass panel according to Pinned supports.

In addition, support A has a considerable translation towards the Y-axis with each step. That is caused by allowing the support to have the freedom to move in the horizontal direction during bending thin glass. In case of implementing maximum wind load, the horizontal displacement of support A will be 456.5 mm (fig. 7.1.4).

The unsupported longitudinal edges of thin glass are affected by bending and forcing them to move towards the z-axis with 49.1 mm from its initial state, while support B remains at its initial place.

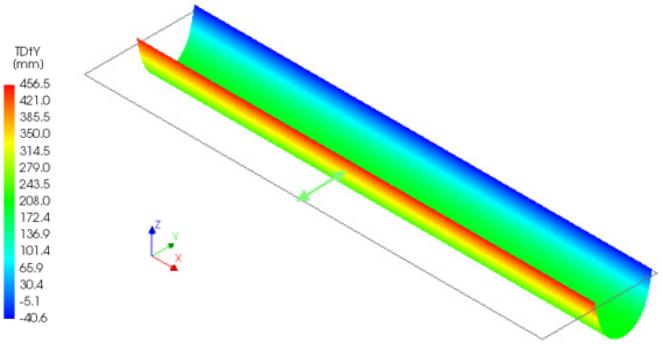


Figure 7.1.4: The horizontal displacementdue to wind load 1 kN/m² of single layer thin according to Pinned supports.

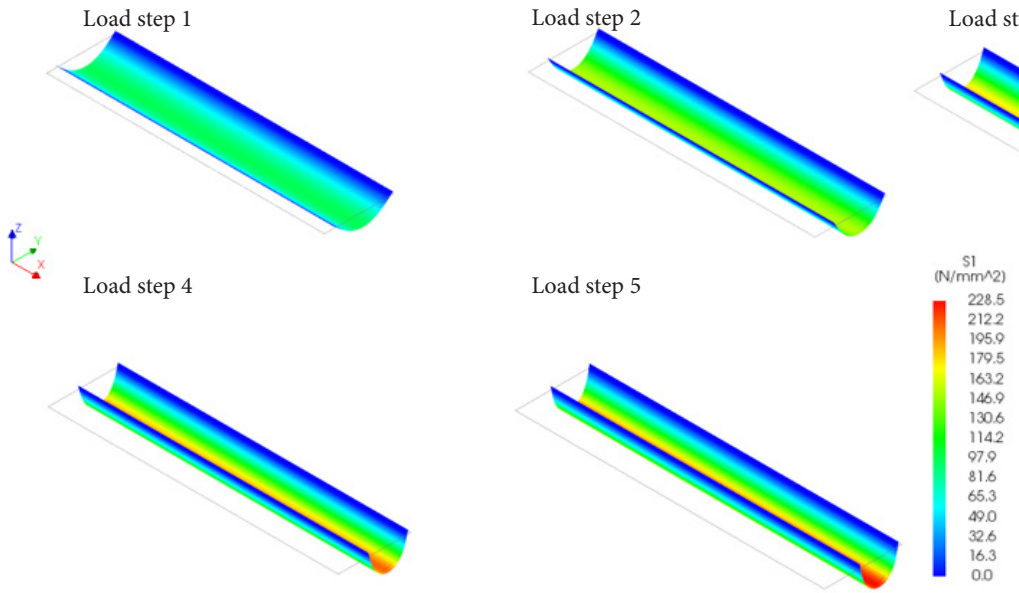


Figure 7.1.5: Principal stress distribution on the top layer due to wind load 1kN/m² of single layer thin glass panel in five steps according to Pinned supports.

After identifying the amount of displacement caused by applying wind load to the panel, it is necessary to analyse the principal stresses related to these displacements.

As with the analysis of displacements, the first approach was to divide the total wind load pressure into 5 load-steps. Secondly, a relation between the amount of displacement and the generated stress is explored. By increasing 0.2 N/mm² of wind load for each load-step the amount of displacement and the generated stresses increased as expected.

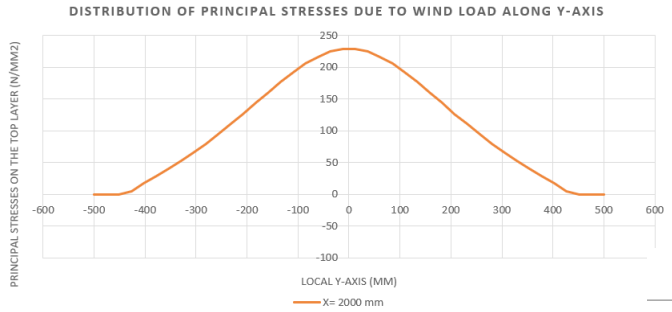


Chart 7.1.2: Principal stress distribution due to wind load 1kN/m² on the top layer of single layer thin glass panel according to Pinned supports.

At load-step 1 the principal stresses reach its maximum in the middle of the panel by a value of 98.6 N/mm2. This value is increased by 53.4 N/mm2 at load-step 2 to get 152 N/mm² of principal stress. The principal stresses keep rising at load-step 3 and load-step 4 to 185.5 N/mm2 and 209.5 N/mm2 respectively. With the final load-step the maximum principal stress is established by a value of 228.5 N/mm² on the top layer of thin glass (figure 7.1.5).

Furthermore, the principal stresses of the supported areas are equal to zero. This is caused by a lack of performance of bending moment at the supported areas, which is directly related to the principal stresses. However, the maximum bending moment is situated in the middle.

The obtained results are visible in table 7.1.2 and chart 7.1.3. It shows a linear pattern between the first and the second load-steps. By doubling the amount of wind load, both displacement and principal stress increase approximately two times. After load-step 2 the linear pattern differs from its path and becomes steeper. However, the amount of added principal stress between load-step 2 and load-step 3 is less than between load-step 1 and load-step 2. In general, both the displacement as the principal stresses seem to increase slightly after load-step 2.

| Load-steps | Wind load (N/mm²) | Displacement (mm) | Principal stress (N/mm²) |
|---|---|---|---|
| 1 | 0.2 | -194.4 | 98.6 |
| 2 | 0.4 | -269.9 | 152 |
| 3 | 0.6 | -303.8 | 185.5 |
| 4 | 0.8 | -322.3 | 209.5 |
| 5 | 1.0 | -344.0 | 228.5 |

Table 7.1.2: Overview of displacement and principal stress of single layer thin glass panel according to Pinned supports.

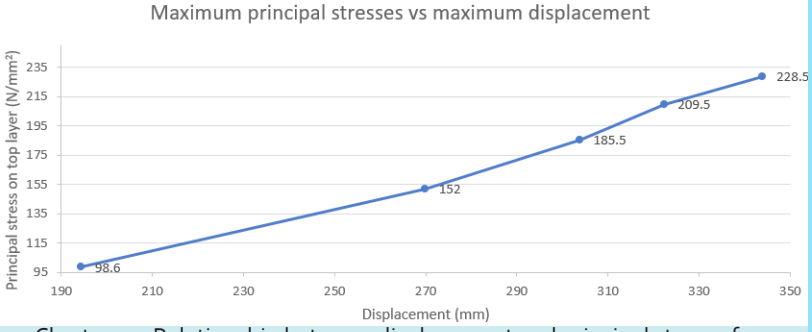


Chart 7.1.3: Relationship between displacement and principal stress of single layer thin glass panel according to Pinned supports.

This is because the flexible flat panel becomes stiffer and therefore the influence of wind load on the panel in terms of increasing the displacement as the principal stress becomes less affective. Thus, by bending thin glass it increases its ability to resist high displacement and principal stresses.

### 7.2 Two-sided fixed supported single thin glass layer

The second possible boundary condition is using fixed supports along the longitudinal edges, preventing rotation. Both supports are avoiding translation in the Y-axis and Z-axis and rotation around the X-axis. Both linear supports are covering a surface of 50 mm on both edges. Therefore, span length is considered as 900 mm (fig. 7.2.1 & 7.2.2) .

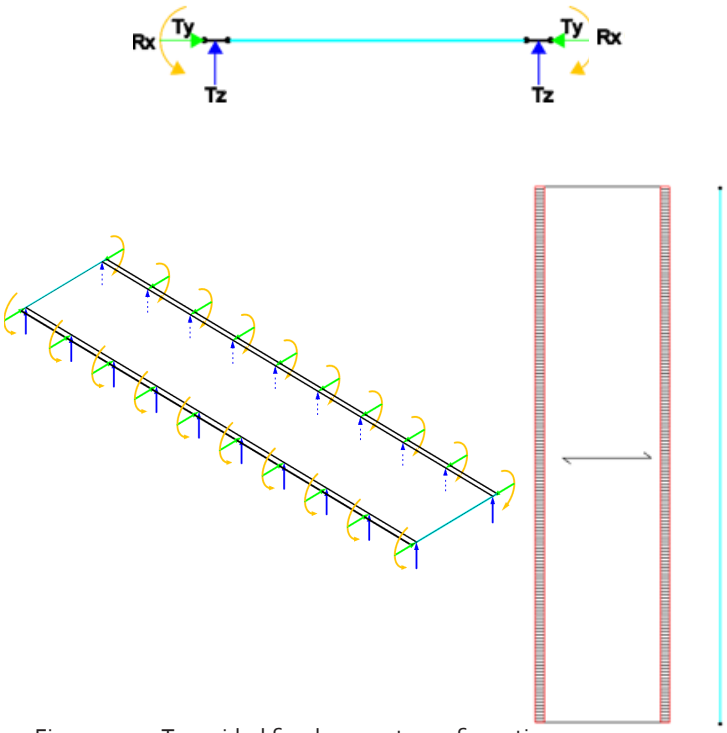


Figure 7.2.1: Two-sided fixed supports configuration.

This type of boundary conditions differs from pinned supports, in terms of generated principal stresses and displacement. It is expected that the supported areas will not have any displacement and will remain at its initial state, because of the applied support reactions. However, the maximum displacement is assumed to be in the middle of the panel. In case of generated principal stresses, it will be more concentrated close to the supported surfaces, because of increasing of bending moment in that area.

To obtain a first estimation of the values of the displacement and the stresses, I made hand calculation according to rules of thumbs (Appendix 3). The displacement is at a maximum in the middle of the panel with a value of 31.2 mm. Moreover, it is obvious that stresses in the middle make up half of the generated stress nearby the edges. The stresses are 22.8 N/mm$^2$ in the middle, while it doubled nearby the edges to 45.6 N/mm$^2$.

After identifying the material properties of thin glass and adding the mentioned boundary conditions with prescribed amount of evenly distributed wind load, a model is created in FEA Diana in able to run a non-linear analysis.

The results are analysed with the same method as for the results of pinned supports. First, the displacement of the panel is analysed in five load-steps. Secondly, the generated principal stresses to point out the relation between these two will be outlined. In addition, three sections were made to identify the values in the middle and at the short edges.

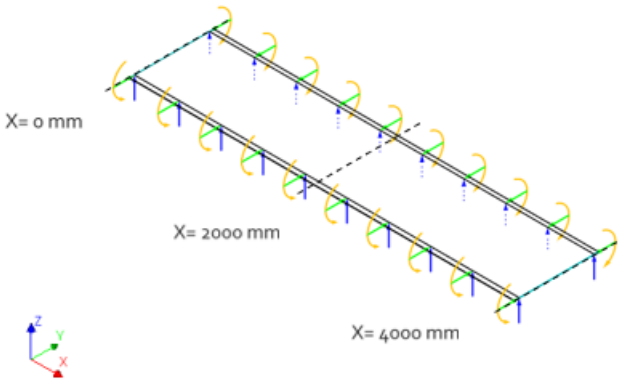


Figure 7.2.2: Three section parallel the Y-axis ( x= 0 mm, x= 2000 mm, x= 4000 mm.

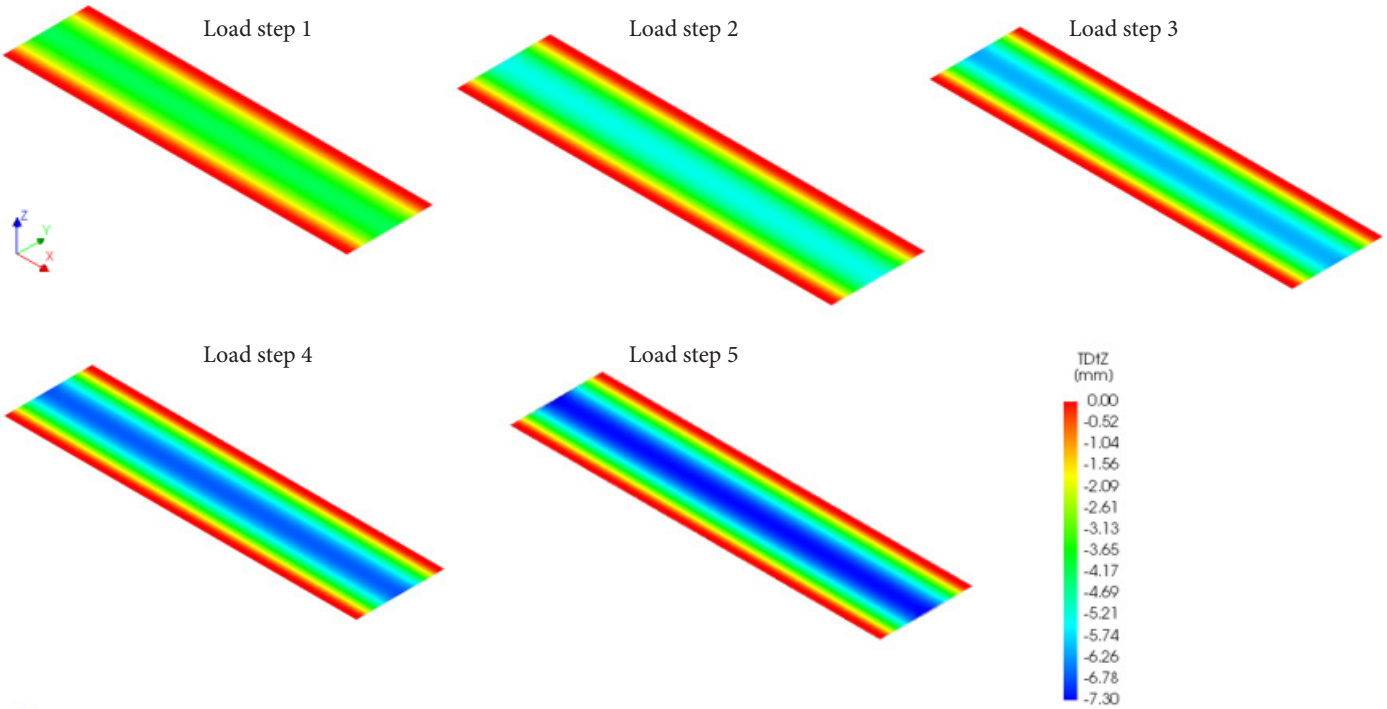


Figure 7.2.3: The displacement of single layer thin glass panel in five steps according to fixed supports.

The results of the displacement are visible in figure 7.2.3. Regarding these obtained results, the first remarkable observation is the magnitude of the displacement, which is much lower than with pinned supports. The displacements are directed in the opposite direction of the Z-axis with magnitude of 4.23, 5.38, 6.18, 6.82 and 7.3 mm respectively. When a full wind load is applied, the middle of the panel will bend by 7.3 mm. This maximum displacement of fixed supports is only 2% of the maximum displacement of pinned supports.

As expected the fixed supports prevent the edges of the panel to move toward the Y-axis or to rotate around the X-axis, forcing the edges to remain in its initial state.

The cross-section indicates and verify the magnitude of the displacement across the entire panel. Chart 7.2.1 shows that the displacement at the bottom, in the middle and on the top is identical and symmetrical.

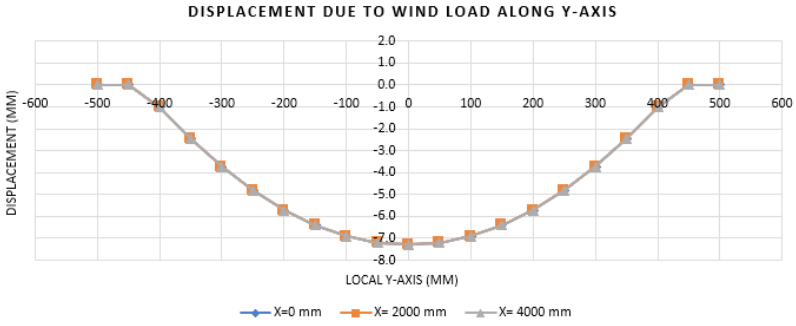


Chart 7.2.1: The displacement due to wind load 1 kN/m² of single layer thin glass panel according to fixed supports.

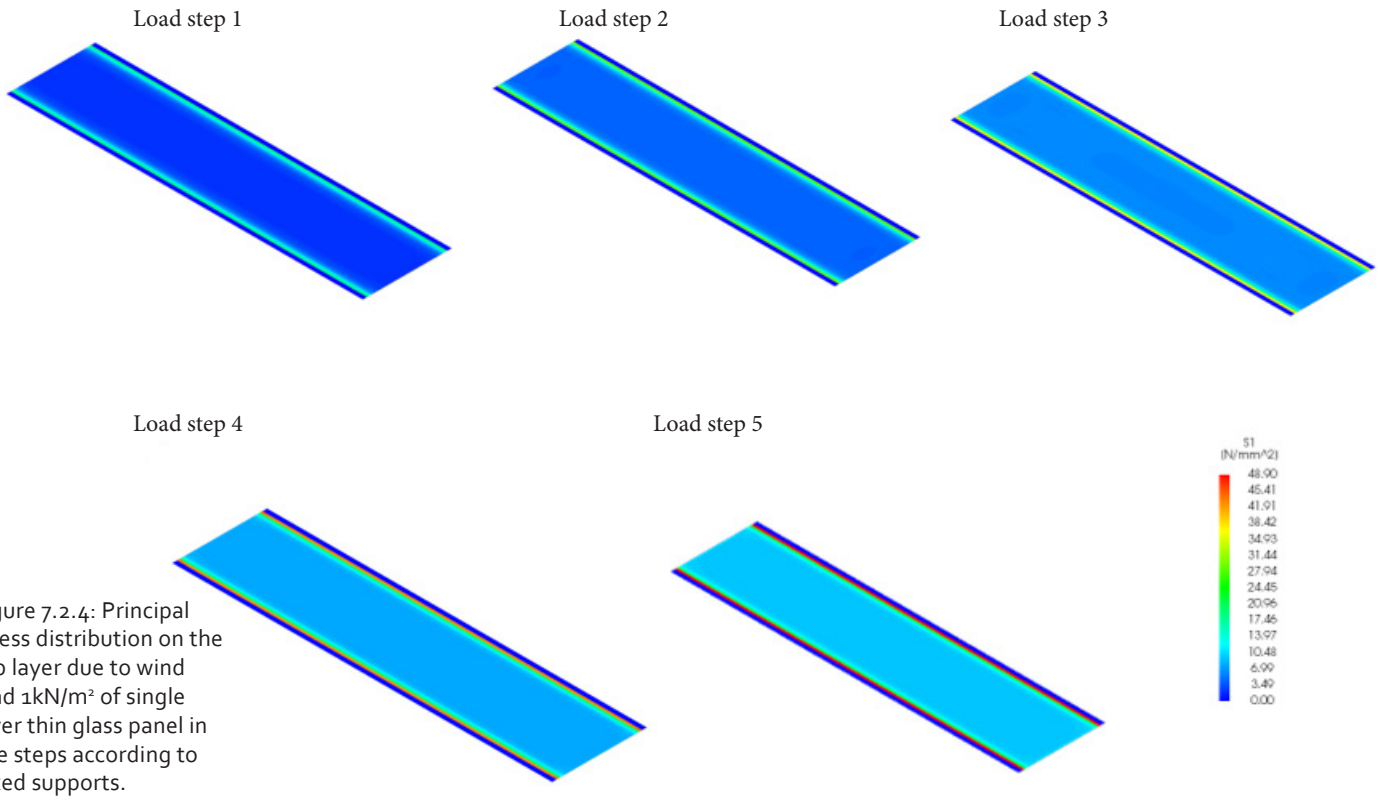


Figure 7.2.4: Principal stress distribution on the top layer due to wind load 1kN/m² of single layer thin glass panel in five steps according to Fixed supports.

Figure 7.2. shows the evaluation in five load-steps of displacement during the increasing of wind load on the panel. Unlike the pinned supports, the principal stresses are here more concentrated nearby the fixed supported surfaces than in the middle of the panel. The maximum principal stress at load-step 5 is 48.90 N/mm2, while in the middle is 10 N/mm² (chart 7.2.2). In other words, the principal stress nearby the supported surfaces is around 5 times higher than in the middle of the panel. The maximum principal stress covers only 6 % of the entire panel.

Even with fixed supports, the related displacements and principal stresses increase as the amount of wind pressure on the panel increases (table 7.2.1). However, both stresses and displacement reduce its magnitude of increasing as the wind load pressure increases. For instance, between load step 1 and load-step 2 the displacement increases by 1.15 mm and the stresses increase by 9.8 N/mm2, whereas between load-step 4 and load-step 5 the displacement increases by 0.48 mm and the stresses increase by 5.8 N/mm² (chart 7.2.3). That has to do with the increasing of the stiffness of the panel by bending.

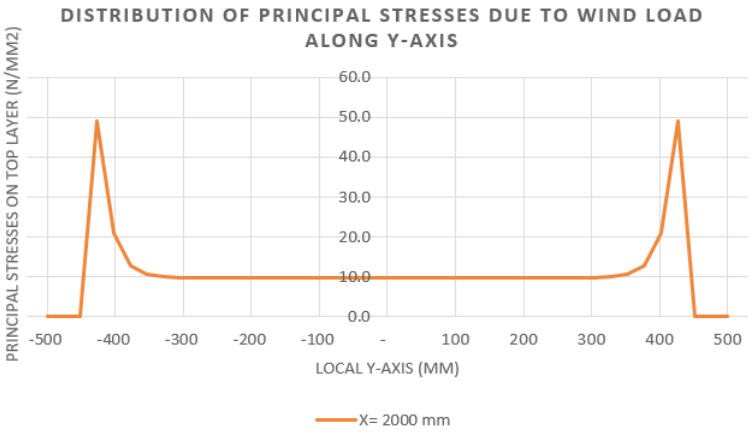


Chart 7.2.2: Principal stress distribution due to wind load 1kN/m² on the top layer of single layer thin glass panel according to fixed supports.

| Load-steps | Wind load (N/mm²) | Displacement (mm) | Principal stress (N/mm²) |
|---|---|---|---|
| 1 | 0.2 | -4.23 | 18.7 |
| 2 | 0.4 | -5.38 | 28.5 |
| 3 | 0.6 | -6.18 | 36.4 |
| 4 | 0.8 | -6.82 | 43.1 |
| 5 | 1.0 | -7.3 | 48.9 |

Table 7.2.1: Òverview of displacement and principal stress of single layer thin glass panel according to fixed supports.

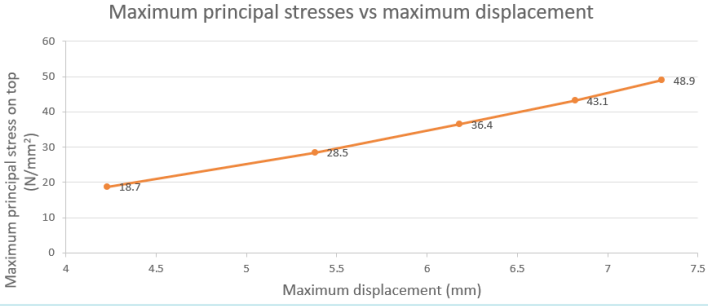


Chart 7.2.3: Relationship between displacement and principal stress of single layer thin glass panel according to Pinned supports.

By comparing pinned and fixed supports in terms of displacement, an enormous difference is concluded. First, the maximum displacement supported by fixed supports is 2% of the maximum displacement supported by pinned supports in the middle. Secondly, pinned supports allow rotation, which gives the edges the ability to rotate during bending. Although, the edges of the fixed supports remain at its initial state (chart 7.2.4).

The generated principal stresses between pinned and fixed supports are also different. Fixed supports are 21% of the total generated principal stress by pinned supports. Although, these principal stresses are more concentrated by the longitudinal edges (chart 7.2.5).

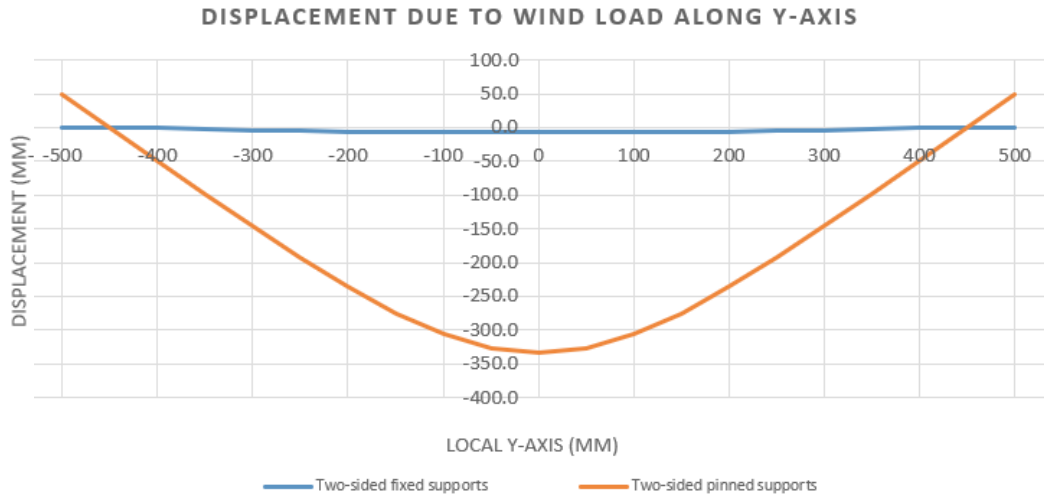


Chart 7.2.4: Comparsion between displacements of Two-sided fixed and Two-sided pinned of single layer thin glass panel.

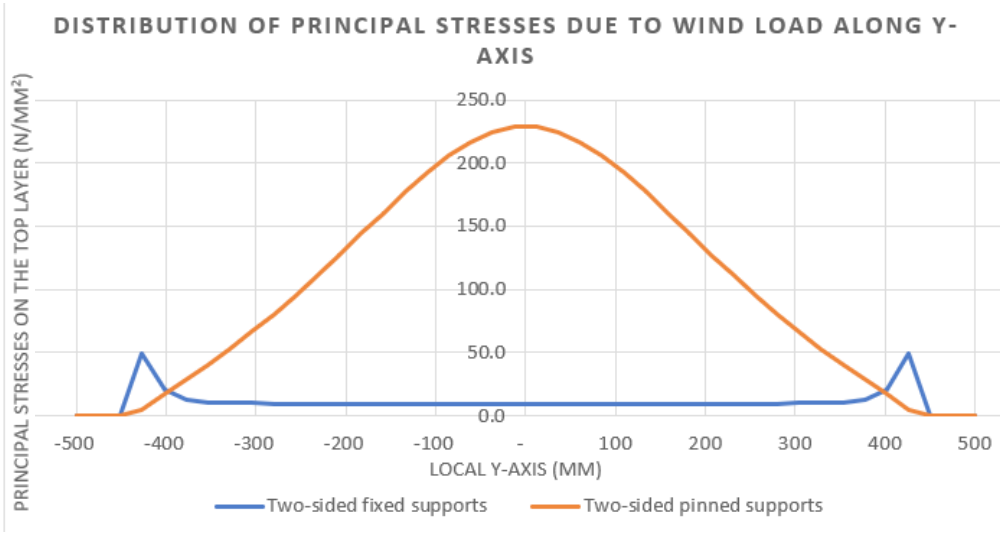


Chart 7.2.5: Comparsion between generated principal stresses on the top layer of Two-sided fixed and Two-sided pinned of single layer thin glass panel.

## 7.3 Four-sided pinned supported single thin glass layer

The previous sections studied the advantages and disadvantages of supporting a flat single layer thin glass on two sides. It became clear that using fixed supports on the longitudinal edges has minimum influence on the amount of generated stress and the amount of displacement compared to pinned supports.

Therefore, I decided to explore the potentials of using four supports in this section and the following sections of this chapter to have a clear vision about the behaviour of thin glass. The third variant is shown in figure 7.3.1, where the generated stress and the amount of displacement is examined and studied.

The third possible boundary condition is supported with the same method as variant 1, as explained in section 7.1. In addition pinned supports are added along the short sides of the panel. Line C represent a hinges support, where translation in the X, Z directions is prevented. In the opposite direction of Line C, Line D is modelled to represent a roller bearing support, that prevents translation in the Z- axis. Both supporters are situated 50 mm from the edges, to allow rotation of the edges and at the same time to protect it from damage.

The maximum displacement in this case is measured in the middle with a value of 55.9 mm (fig. 7.3.2). Unlike the two sided pinned supports, the short edges in four-sided boundary conditions did not bend due to the applied supports. This causes an asymmetrical bending behaviour (Chart (7.3.1)), where the maximum displacement tends to occur nearby support line A, which has freedom of movement towards the Y-axis allowing rotation around the X-axis.

By looking at the displacement behaviour of the four edges of that panel, it is found that they move towards the Z-axis as a consequence of allowing them to rotate around the X-axis. The maximum value of that displacement is located nearby support line A where it can reach 12.3 mm of displacement towards the Z-axis.

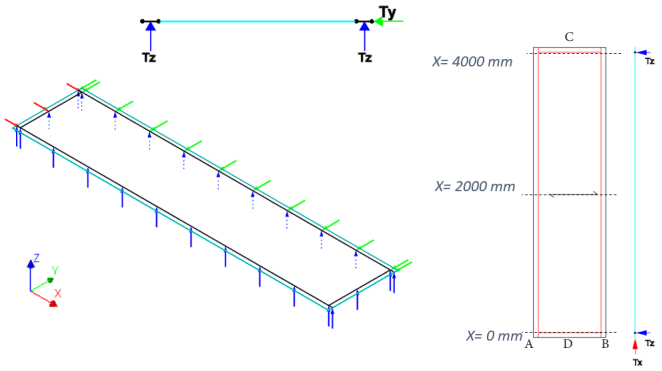


Figure 7.3.1: Four-sided pinned supports configuration.

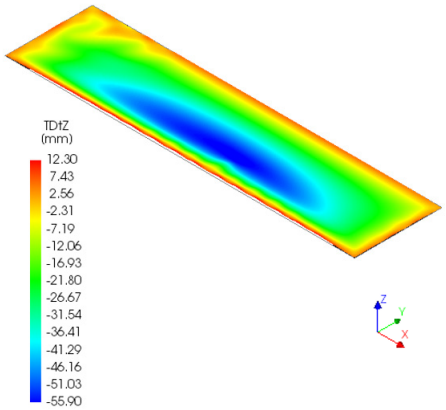


Figure 7.3.2: The displacement of single layer thin glass panel according to four-sided pinned supports.

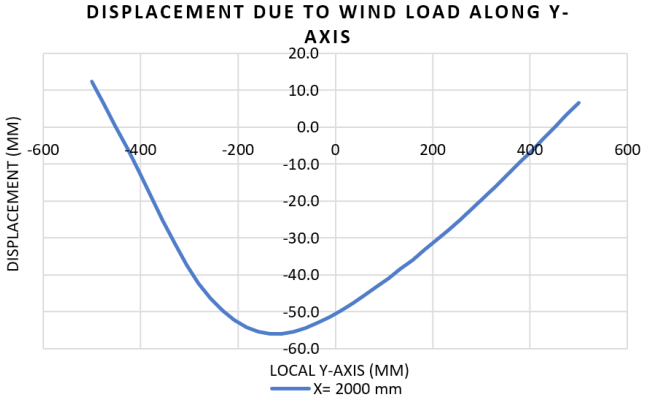


Chart 7.3.1: The displacement due to wind load 1 kN/m² of single layer thin glass panel according to four-sided pinned supports.

Considering the behaviour of principal stresses of pinned supports on four sides, thin glass seems to become unstable. The results show an irregular pattern of stress contour (fig. 7.3.3). It was expected that the short supported areas would not be affected by moment forces. In addition, the moment force would be at its highest in the middle of the panel, like the results of principal stress by variant 2. Chart 7.3.2 gives an overview of the generated principal stresses, where 59.4 N/mm2 is measured. Despite my expectations, it is understandable that the panel of variant 3 does not bend like variant 2, because the resistance of the supported short areas. These areas prevent support line A to move towards the Y-direction, which explains the increased principal stress close to support line A.

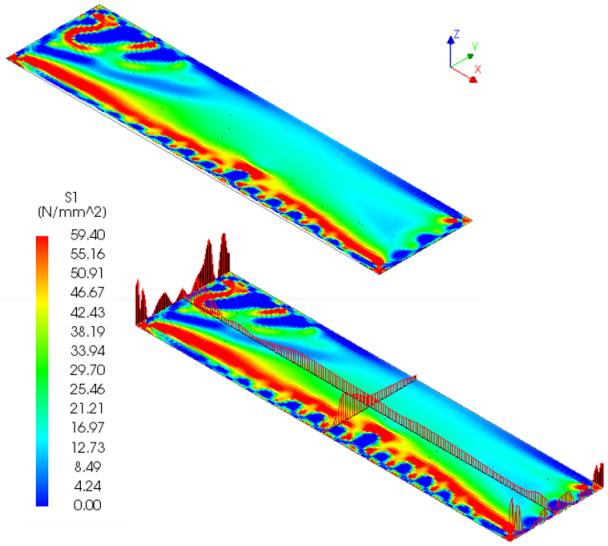


Figure 7.3.3: Principal stress distribution on the top layer due to wind load 1kN/m² of single layer thin glass panel four-sided pinned supports.

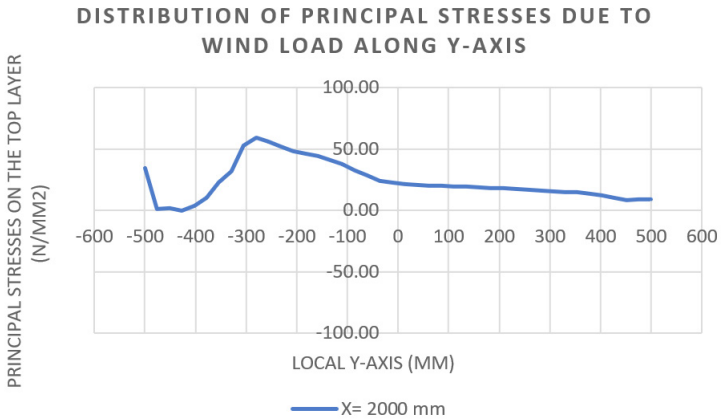


Chart 7.3.2: Principal stress distribution on the top layer due to wind load 1kN/m² of single layer thin glass panel according to four-sided pinned supports.

## 7.4 Four-sided fixed supported single thin glass layer

The fourth variant is provided with fixed boundary conditions on four edges of the panel. This method of supporting thin glass avoids displacement on the short edges unlike variant 2 and it offers protection for the edges. Moreover, these boundary conditions prevent the supported areas for rotation and transitions, as is illustrated in figure 7.4.1. It shows the influence and performance of fix supports on a single layer thin glass panel regarding the displacement and the generated principal stresses.

Figure 7.4.2 shows the results of displacement as a consequence of applying an evenly distributed wind load of 1 Kn/m2. As expected the supported areas prevent displacements at the edges, which is illustrated as a red area in figure 7.4.2. The dark blue area represents the maximum displacement of 7.1 mm. That is 0.2 mm less deflection than variant 2. Compared to the three previous variants, this variant of support gives the most suitable boundary conditions to get minimal displacement.

Chart 7.4.1 illustrates the displacement of the middle of the thin glass panel. It is obvious that the glass panel has a symmetrical parabolic graph where the highest displacement is settled as 7.1 mm and the supported areas remain at their initial state.

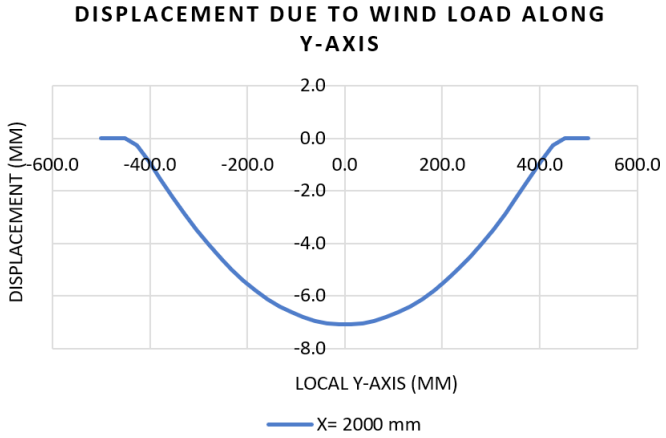


Chart 7.4.1: The displacement due to wind load 1 kN/m² of single layer thin glass panel according to four-sided fixed supports.

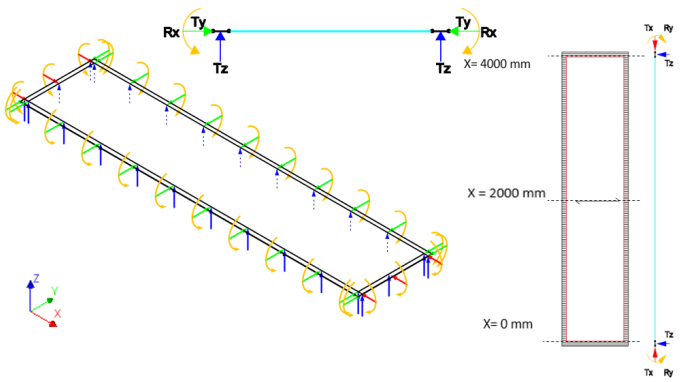


Figure 7.4.1: Four-sided fixed supports configuration.

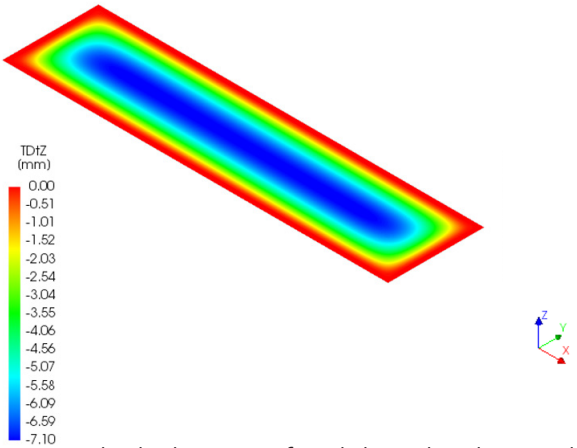


Figure 7.4.2: The displacement of single layer thin glass panel according to four-sided fixed supports.

By exploring the influence of adding fix supports to the short edges, it has shown significant effects on generating principal stresses on thin glass panels. Chart 7.4.2 describes the magnitude of the principal stresses along the middle section of the panel. The highest value is situated close to the short and longitudinal edges with a value of 48.90 N/mm2. The additional generated stresses by the short edges are identical to the principal stresses on the longitudinal edges.

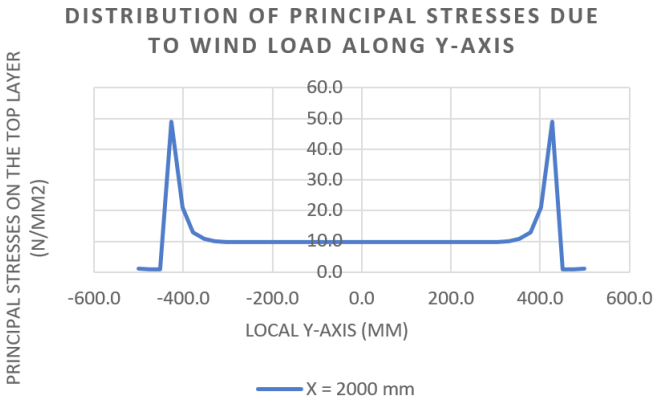


Chart 7.4.2: Principal stress distribution on the top layer due to wind load 1kN/m² of single layer thin glass panel according to four-sided fixed supports.

Figure 7.4.3 gives an accurate indication of the principal stresses over the entire panel, where the principle stresses reach 48.90 N/mm² by the supported areas. In addition, the panel reaches 10 N/mm2 over a large part of the surface.

This variant of supporting single thin glass panel with fixed boundary conditions along four edges provide thin glass with high potentials to be used as second façade skin, because of its ability to resist wind pressure of 1 kN/m2 by a deflection of 7.1 mm without to break and maximum principal stresses of 48.9 N/mm² that occupy around 8% of the total panel surface.

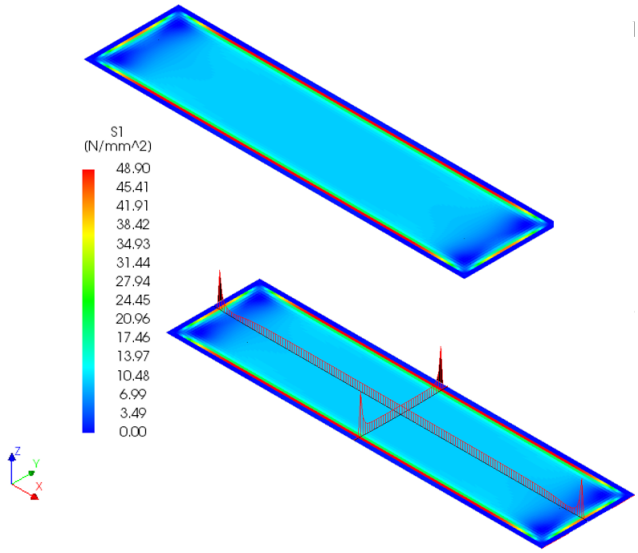


Figure 7.4.3: Principal stress distribution on the top layer due to wind load 1kN/m² of single layer thin glass panel four-sided fixed supports.

## 7.5 Four-sided fixed and pinned supported single thin glass layer

Other possible boundary conditions for thin glass are illustrated in figure 7.5.1, where the longitudinal edges are supported with fix boundary conditions and the short edges with pinned boundary conditions. As mentioned before, the supported areas are placed 50 mm from the edges of the panel. In addition, as a consequence of freedom of movement, the short edges are moving towards the Z-direction with 2.34 mm, the longitudinal edges remain at their initial state as expected from fixed boundary conditions(fig. 7.5.2). Moreover, chart 7.5.1 shows that the maximum displacement of this variant is equal to variant 2 with a value of 7.3 mm.

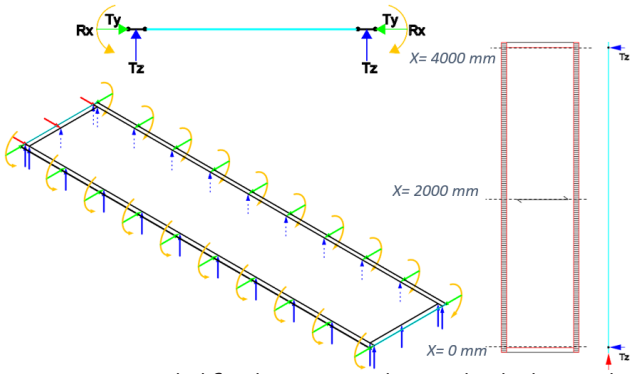


Figure 7.5.1: Two-sided fixed supports at longitudinal edges and Two sided pinned supports at short edges configuration.

After analyzing the generated principal stresses of this alternative, it becomes clear that the influence of fixed boundary conditions provide thin glass with 49.2 N/mm2 of principal stresses nearby the supported area (chart 7.5.2). That is 0.3 N/mm2 higher than the obtained principal stresses of the comparable variants 2 and 4. Furthermore, figure 7.5.3 shows that the short edges ensure no moment force as expected, due to the pinned supports. Since principal stresses are derived from the moment, it is evident that no principal stresses are generated around the supported short edges.

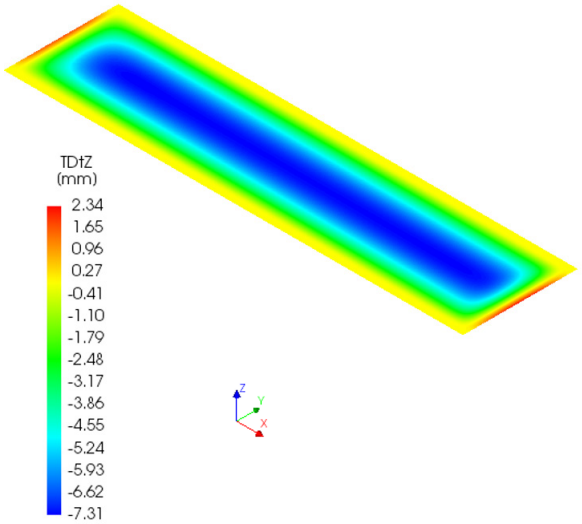


Figure 7.5.2: The displacement of single layer thin glass panel according to four-sided fixed and pinned supports.

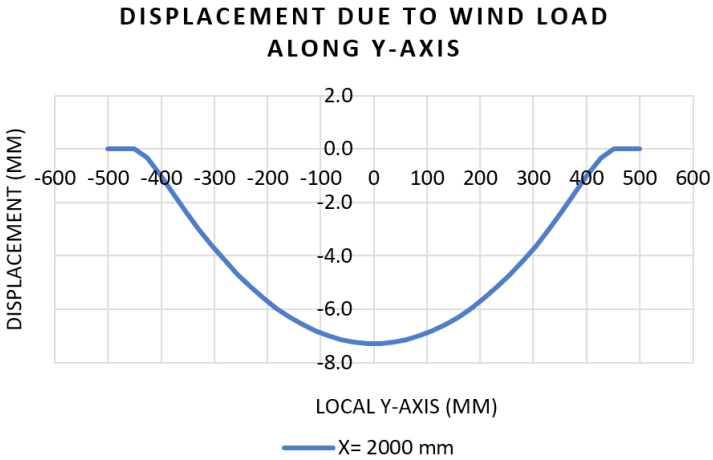


Chart 7.5.1: The displacement due to wind load 1 kN/m² of single layer thin glass panel according to four-sided fixed and pinned supports.

Figure 7.5.3: Principal stress distribution on the top layer due to wind load 1kN/m² of single layer thin glass panel four-sided fixed and pinned supports.

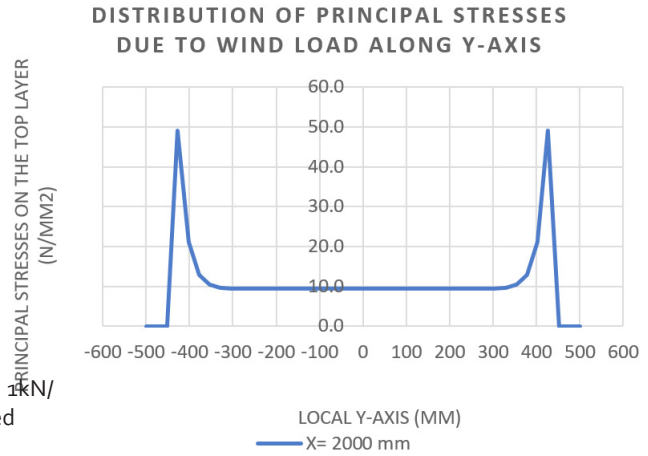


Chart 7.5.2: Principal stress distribution on the top layer due to wind load 1kN/m² of single layer thin glass panel according to four-sided fixed and pinned supports.

## 7.6 **Four-sided pinned and fixed supported single thin glass layer**

The last variant of boundary conditions is illustrated in figure 7.6.1. It consists of pinned supports around the longitudinal edges and fix supports around the short edges. The results of the magnitude of displacement is visible in figure 7.6.2. It describes the performance of a single layer of thin glass under a wind load of 1 kN/m2. Chart 7.6.1 shows that the maximum displacement in the middle cross-section of the panel is equal to 32.80 mm. It's remarkable that the displacement tends to bend more towards support line A, where only vertical reaction force is applied. That is because the lack of the horizontal reaction force gives line A the freedom to move in the horizontal direction.

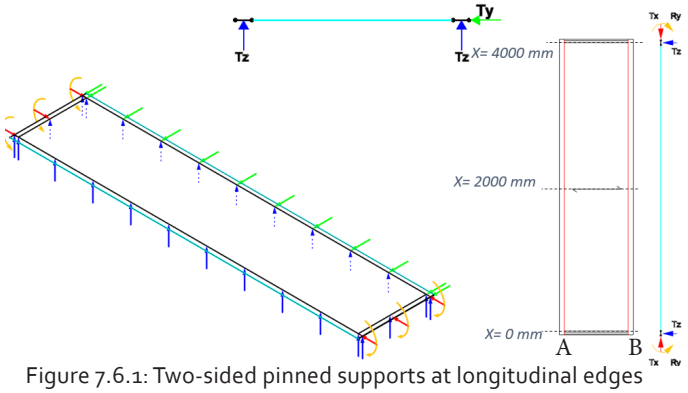


Figure 7.6.1: Two-sided pinned supports at longitudinal edges and Two-sided fixed supports at short edges configuration.

Figure 7.6.3 shows the contour of the generated principal stresses of thin glass. The major principal stresses are measured at the edges with a value of 92.2 kN/m2, which is the highest obtained value among the four supported edges alternatives. Graph 7.6.2 shows an asymmetrical pattern of the principle stresses by an increase of principal stresses towards the support line B. In general, this variant will cause irregular distribution of the principal stresses on the thin glass panel. That makes this type of boundary condition for thin glass unsuitable for façade application.

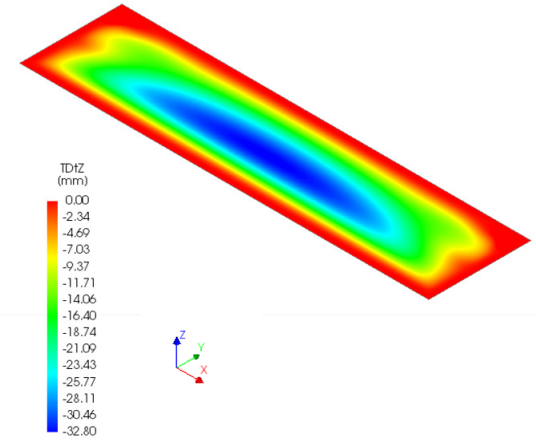


Figure 7.6.2: The displacement of single layer thin glass panel according to four-sided pinned and fixed supports.

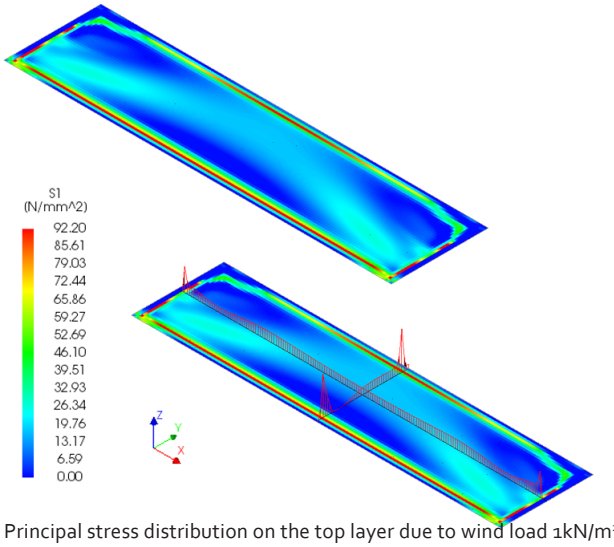


Figure 7.6.3: Principal stress distribution on the top layer due to wind load 1kN/m² of single layer thin glass panel four-sided pinned and fixed supports.

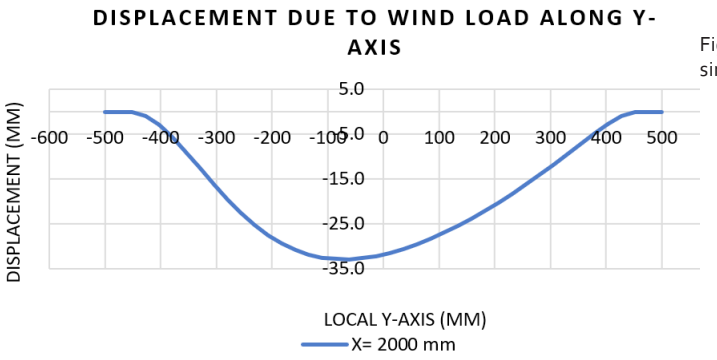


Chart 7.6.1: The displacement due to wind load 1 kN/m² of single layer thin glass panel according to four-sided pinned and fixed supports.

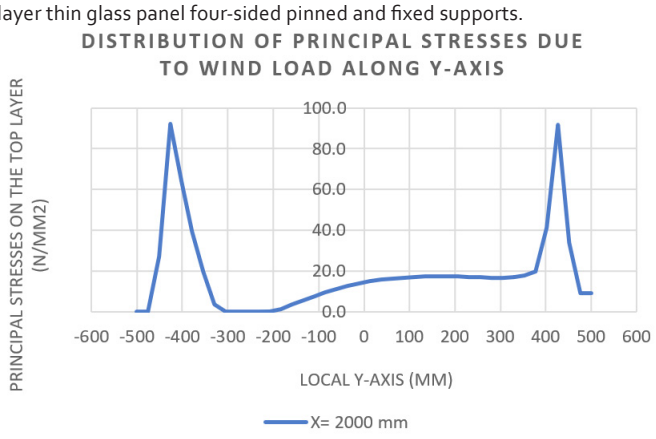


Chart 7.6.2: Principal stress distribution on the top layer due to wind load 1kN/m² of single layer thin glass panel according to four-sided pinned and fixed supports.

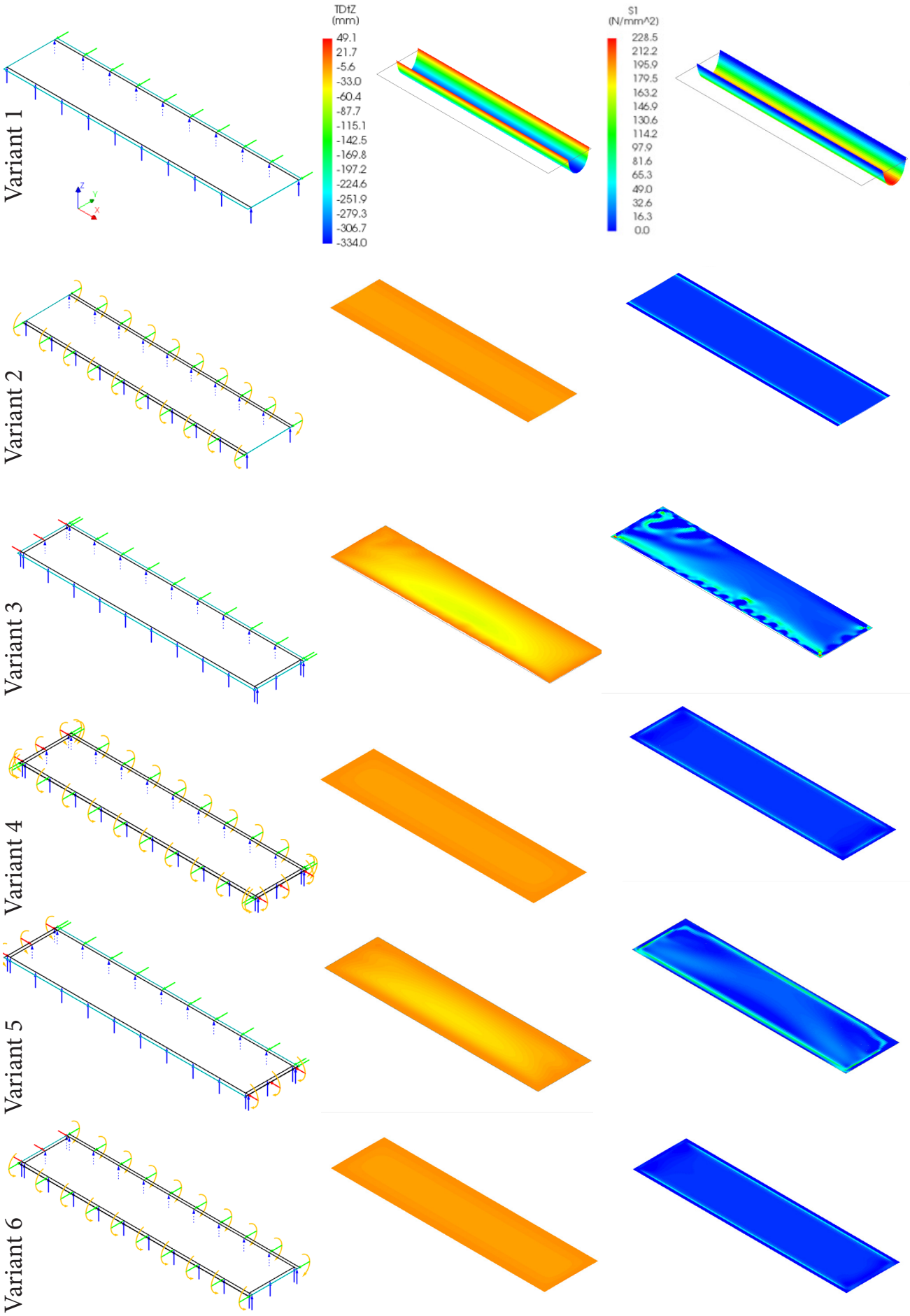
Variant 1
TDtZ
(mm)
49.1
21.7
-5.6
-33.0
-60.4
-87.7
-115.1
-142.5
-169.8
-197.2
-224.6
-251.9
-279.3
-306.7
-334.0
S1
(N/mm^2)
228.5
212.2
195.9
179.5
163.2
146.9
130.6
114.2
97.9
81.6
65.3
49.0
32.6
16.3
0.0
Variant 2
Variant 3
Variant 4
Variant 5
Variant 6

## 7.7 Conclusion

The aim of this chapter is to apply suitable boundary conditions on a thin glass, in order to locate and to define the stress concentrations and the displacement caused by bending in case of applying evenly distributed wind pressure of 1kN/m2.

Therefore, a sub question is formulated as:

*What are the possible boundary conditions for a single thin glass panel? And what are the influences of these boundary conditions on thin glass, in terms of displacement and stresses?*

To be able to give an answer to this question six variants of boundary conditions are investigated on a single layer of thin glass panel with 1 mm thickness. The chosen dimension for this panel is 4000 mm by 1000 mm. These dimensions are suitable for façade applications for office buildings, since the height of an office room is considered 4 meters.

Variant 1 is supported along the two longitudinal edges by using pinned supports. The results of maximum displacement due to the applied wind pressure is 334.0 mm. Moreover, this thin glass panel has identical and symmetrical bending shape, since the displacements on the top, in the middle and at the bottom are similar. Moreover, support A has a considerable translation of 456.5 mm towards the Y-axis. Support A represent a vertical reaction force, where the edge is free to move in the horizontal direction. The generated principal stresses by this variant is 228.5 N/mm2 by the areas where the maximum displacement has been reached.

Variant 2 is the second possible boundary conditions for a single layer of thin glass panel where fixed supports are used along the longitudinal edges, which prevent rotation. This variant differs from variant 1, in terms of generated principal stresses and displacement.

Regarding the obtained results, the first observation was that the magnitude of the displacement is much lower than with pinned support.

The maximum displacement in this case is 7.3 mm, which means 98% of the maximum displacement by pinned is reduced due to replacing pinned supports by fix supports. Even this variant provides an identical and symmetrical displacement across the entire panel. Considering the generated principal stresses of this variant, it is concluded that fixed supports generates stresses along the supported edges, where 48.90 N/mm2 is obtained. This maximum principal stress covers only 6 % of the surface of single thin glass layer. Moreover, it is only 21% of the total generated principal stress by pinned supports.

Variants 3 to 6 are four sided supported due to the curiosity whether this type of boundary conditions would have influence on the displacement and principal stresses of single thin glass panel.

Variant 3 is supported with the same boundary conditions as variant 2 with adding pinned supports along the short edges of the panel. The maximum displacement in this case is measured in the middle with a value of 55.9 mm. This variant has an asymmetrical bending behaviour where the maximum displacement tends to occur nearby support A, which has freedom of movement towards the Y-axis. The principal stresses of this variant appear to be irregular, where the maximum value is established by 59.4 N/mm2.

Variant 4 has fixed boundary conditions on the four edges of the panel. In addition, like all four supported variants, this variant offer protection for the edges. The maximum displacement of this variant is defined by 7.1 mm in the middle of the single layer thin glass panel. That is a 0.2 mm less deflection compared to variant 2. Compared to the three previous variants is this variant of boundary condition the most suitable to get minimal displacement.

Moreover, it provides the panel with a symmetrical displacement, where the supported areas remain at their initial state. Also, the generated principal stress of this variant is studied where a value of 48.90 N/mm2 is obtained.

These stresses are mainly located close to the short edges and the longitudinal edges. This variant of supporting single thin glass panel with fixed boundary conditions along four edges provide thin glass with high potentials to be used as second façade skin, because of its ability to resist wind pressure of 1 kN/m2 by a deflection of 7.1 mm without to break and maximum principal stresses of 48.9 N/mm2 that occupy around 8% of the total panel surface.

Variant 5 is supporting thin glass with fix supports along the longitudinal edges and pinned supports along the short edges. The short edges are moving towards the Z-direction with 2.34 mm whether the longitudinal edges remain at their initial state as expected from fixed boundary conditions. The maximum displacement of this variant is equal to variant 2 wat a value of 7.3 mm. The generated principal stress on thin glass is 49.2 N/mm2. That is 0.3 N/mm2 higher than the obtained principal stresses of the comparable variants 2 and 4.

Variant 6 consist of pinned supports around the longitudinal edges and fix supports around the short edges. The maximum displacement is in the middle of the panel, which is equal to 32.8 mm. This variant has an unsymmetrical bending behaviour. More over the generated principal stress of this variant is 92.2 kN/m2 , which is the highest obtained value among the four supported edges alternatives. This variant has an irregular distribution of the principal stresses along the thin glass panel. That makes this variant unsuitable for façade applications.

# 8

# Cold Bending Single Layer Thin Glass

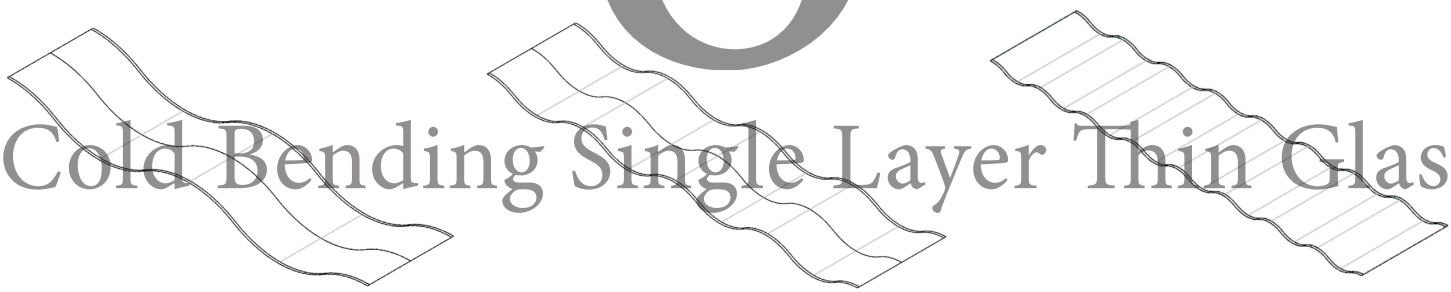

## 8.1 Introduction

In this chapter the ability of bending thin glass by cold bending condition will be explored. As mentioned in chapter 3, the mechanical properties and production process of chemically strengthened thin glass make it possible to cold bend glass to a certain radius without breaking it. The purpose of this part of the research is to explore the displacement and the generated tensile stresses by adapting curvature radius. This helps to understand the mechanical behaviour and the consequences of possible design choices. Therefore, in this chapter the following sub question will be answered:

*How does cold bending influence the tensile stress generation on thin glass? What is the influence on its load bearing capacity compared to a flat panel?*

Three FE models were made in FEA Diana in order to investigate the results. Each model represents a single layer of thin glass with a required amplitude. These amplitudes are derived from the neutral line that cuts the intersection curve in half. This intersection curve is generated between circles with a specific radius (fig. 8.1.1). The radii of the circles are 1000 mm, 500 mm, 250 mm respectively. It is necessary to gain more understanding on the relation between curvature radius, amplitude and generated tensile stress.

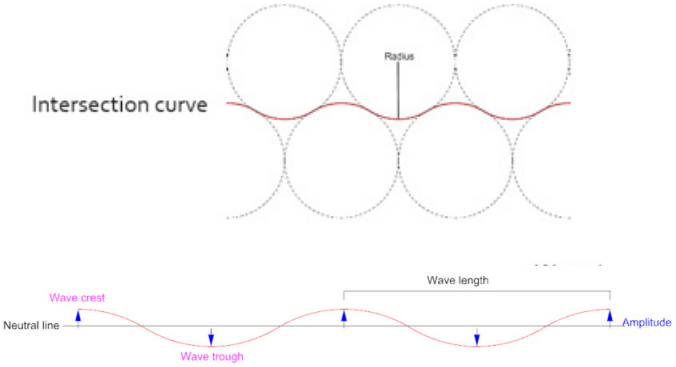


Figure 8.1.1: Principles of the generated sinus shape.

The boundary conditions for these single layers are determined by using fixed supports along the longitudinal edges. As proven by chapter 7, using fixed supports provides thin glass with the least stresses and displacement.

## 8.2 Single layer thin glass with amplitude of 134 mm

The first possible curved shape that is studied is derived from circles with a radius of 1000 mm. The amplitudes describe the distance from the neutral line to the wave crest or to the wave trough. That would mean that the amplitude is established as 134 mm, which provides the panel with three wave crests and two wave troughs (fig. 8.1.3). These amplitudes are modelled in Diana as a prescribed deformation along the supported areas to simulate cold bending along the edges.

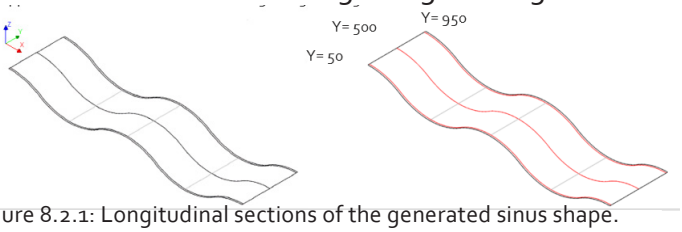


Figure 8.2.1: Longitudinal sections of the generated sinus shape.

To identity the magnitude of the desired amplitude and the tensile stresses caused by cold bending, there longitudinal sections are made. These cross-sections are situated in Y= 500 mm, Y= 50 mm and Y= 950 mm (fig. 8.2.2). The latest two sections are positioned along the supported areas, while Y=500 mm represents the middle of the curved panel. The aim was to check if only bending the edges of the panel is sufficient to create a curved single glass layer with an identical curvature across the entire panel.

By analysing the outcome of bending the glass panel, it is concluded that by forcing the edges to move vertically with 134 mm and -134 mm an ideal curvature was created (fig. 8.2.3). Chart 8.2.1 shows that all cross-sections overlap, which means that the panel has succeeded to have a fully curved panel with the required amplitudes. The distance between wave crest and wave trough is measured as 1000 mm with a wave length of 2000 mm.

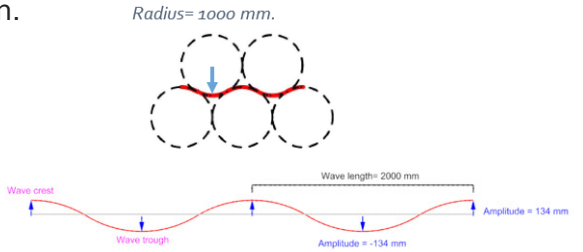


Figure 8.2.2: Principles of the generated sinus shape.

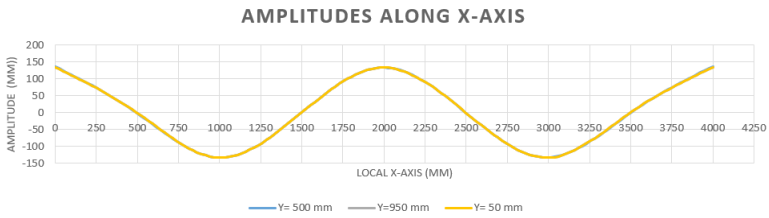


Chart 8.2.1: Amplitudes of the three longitudinal sections of the generated sinus shape by cold bending single thin glass layer.

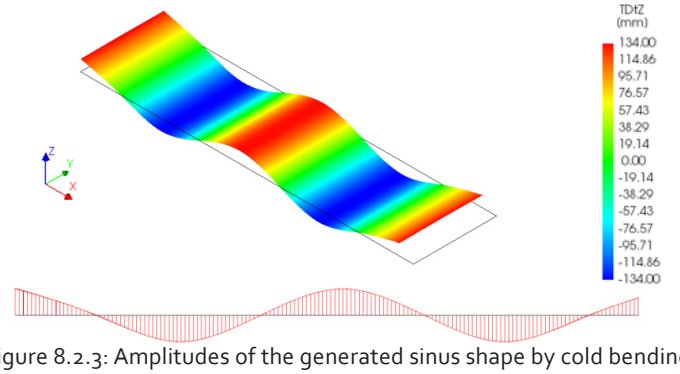


Figure 8.2.3: Amplitudes of the generated sinus shape by cold bending single thin glass layer.

The generated stresses by bending on the top layer of thin glass emphasis tensile stresses (red contour) and compressive stresses (blue contour) (fig. 8.2.4). The major tensile stresses are generally located on the wave crest at the supported area with a value of 76 N/mm². In the middle of the panel the tensile stresses are around 16 N/mm2 lower (chart 8.2.3). Because of the fixed supports, the stresses are more concentrated in the supported area, unlike the unsupported short edges where no stresses are generated.

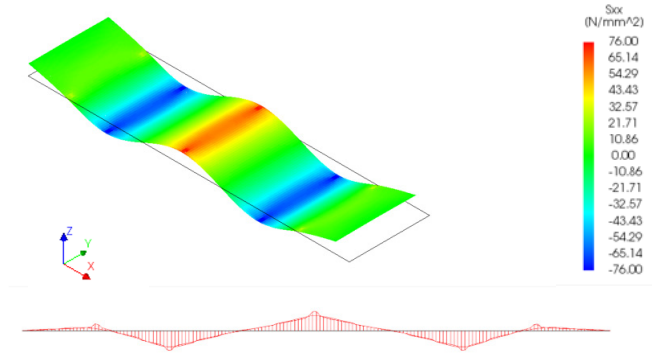


Figure 8.2.4: Initial bending stresses on the top layer of single thin glass layer.

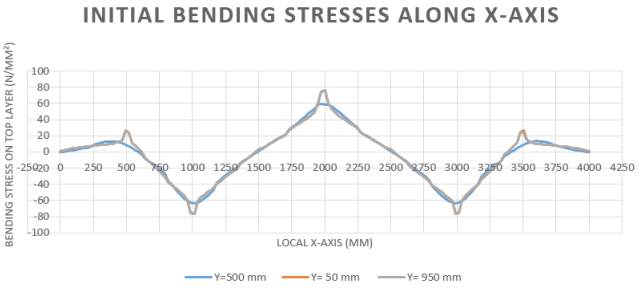


Chart 8.2.3: Initial bending stresses of the three longtindual sections on the top layer of single thin glass layer.

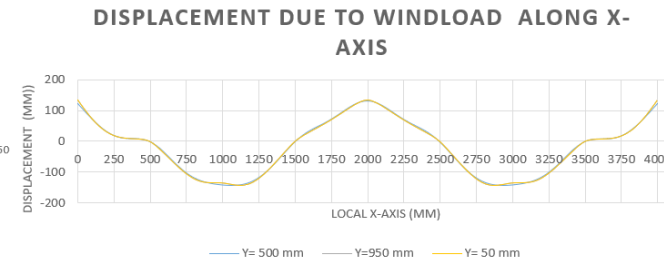


Chart 8.2.4: Displacement of the three longitudinal sections of the generated sinus shape of single thin glass layer due to wind load 1 kN/m².

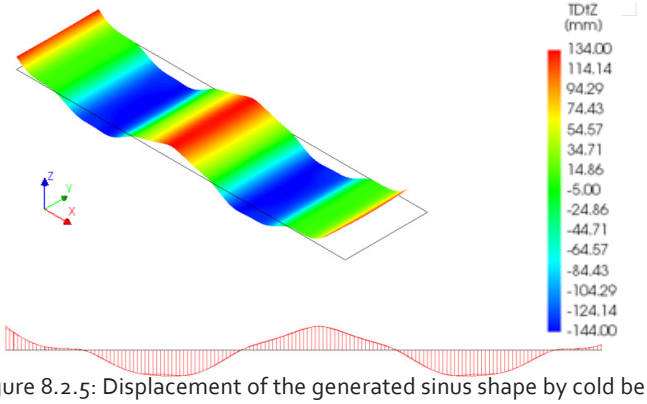


Figure 8.2.5: Displacement of the generated sinus shape by cold bending single thin glass layer due to wind load 1 kN/m².

When a wind load of 1 kN/m2 is generated, the curved panel starts to deform (fig. 8.2.5). This displacement is mainly occurring between the wave crests and the wave troughs. The maximum deformation is measured at local x = 250 mm; 3750 mm by 51 mm ( chart 8.2.4 ).

In addition, the tensile stresses increase with 187 N/mm2 at the supported edges, while in the middle they increase by 40 N/mm² ( fig. 8.2.6). In addition, the bending stresses have an unstable pattern, because of the added stresses that influence the negative compressive stresses to be positive and to turn them into tensile stresses (chart 8.2.5).

Figure 8.2.6: Increased bending stresses on the top layer of single thin glass layer.

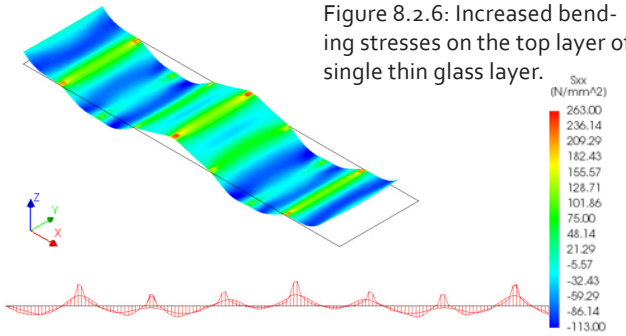


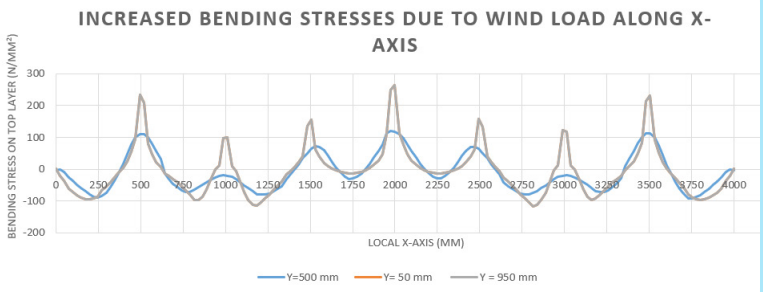


Chart 8.2.5: Increased bending stresses of the three longtindual sections on the top layer of single thin glass layer.

## 8.3 Single layer thin glass with amplitude of 67 mm

In this section the second possible alternative for cold bending thin glass will be explored. The curved shape is derived from the intersection between circles with a radius of 500 mm (fig. 8.3.1). The obtained amplitude of this curved shape is 67 mm. The distance between wave crest and wave through is established as 500 mm with a wave length of 1000 mm. These amplitudes are used to simulate the cold bending curvature along the longitudinal edges in FEA Diana.

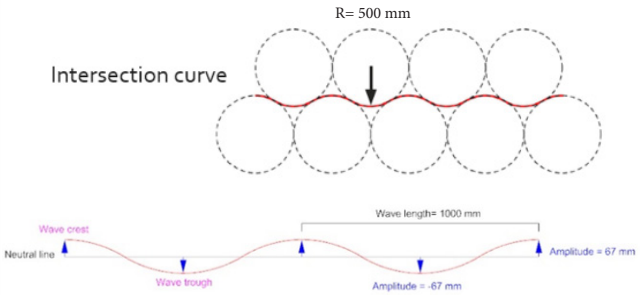


Figure 8.3.1: Principles of generated sinus shape.

The first phase was to investigate the influence of applying the mentioned amplitudes on thin glass, in terms of approaching the ideal curvature. To assay the desired magnitude of the amplitudes, three longitudinal sections were made. These sections represent the curvatures of the edges (Y=50 mm; Y=950) and the middle of the panel (500 mm) (fig. 8.3.2).

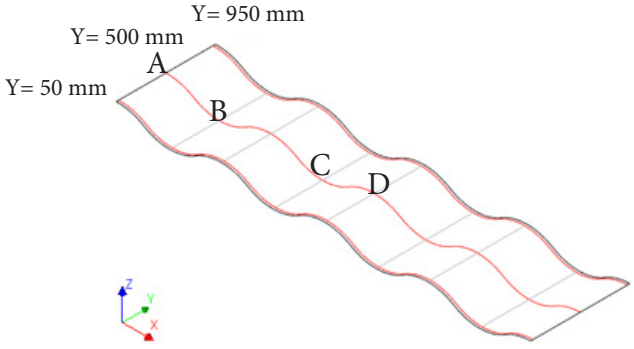


Figure 8.3.2: Longtindual sectionsof generated sinus shape.

Charts 8.3.1 to 8.3.3 describes the magnitude of the amplitudes of the three created sections. The given results show that by cold bending thin glass by the edges to the mentioned amplitudes the rest of the panel is forced to pursue the same curvature as the edges, except for the area around the short edges. Furthermore, the created curved shape consists of five wave crests and four wave troughs.

It is necessary to mention that although the end parts (X= 0 mm and X= 4000 mm) of the middle section panel are 6 mm higher than the desired 67 mm amplitude, the middle section deviates from the curvature of the longitudinal edges at node B (local axis X=250 mm) with 6 mm (chart 8.2.2). Between node C and node D the middle section (Y=500) has almost identical pattern to the ideal curavture of the longitudinal sections (Y= 50 mm and Y= 950 mm) with 1 mm difference (chart 8.3.3).

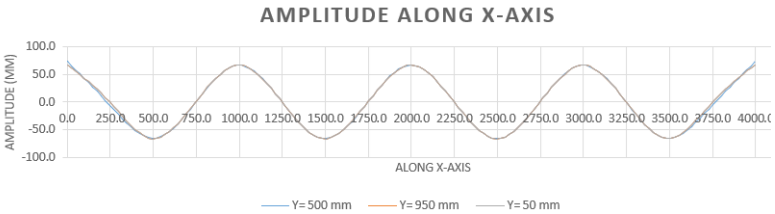


Chart 8.3.1: Amplitudes of the three longitudinal sections of the generated sinus shape by cold bending single thin glass layer.

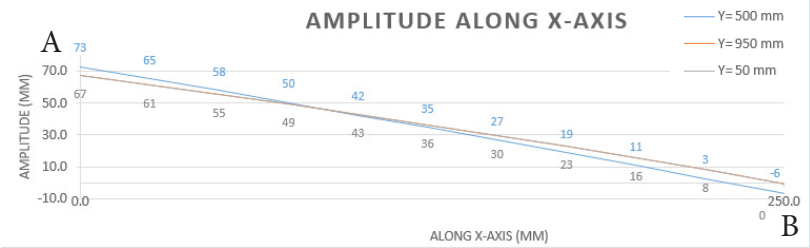


Chart 8.3.2: Amplitudes of the three longitudinal sections of the generated sinus shape by cold bending single thin glass layer between Node A and Node B.

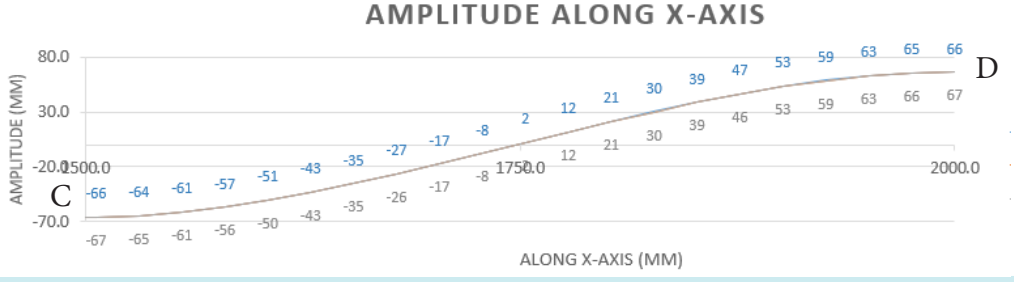


Chart 8.3.3: Amplitudes of the three longitudinal sections of the generated sinus shape by cold bending single thin glass layer between Node C and Node D.

By implementing an evenly distributed wind load of 1 N/mm² on the curved panel the following results were discovered. Figure 8.3.3 shows the contours of the obtained displacements compared to its initial curved state (fig. 8.3.5). The major displacement is measured in the middle of the short edges(Node A) with 13 mm regarding its curved state (chart 8.3.2 ). Moreover, the part between the wave crests and wave troughs are affected in the middle by the applied wind load. This causes a displacement of 6 mm compared to its initial curved state (chart 8.3.5).

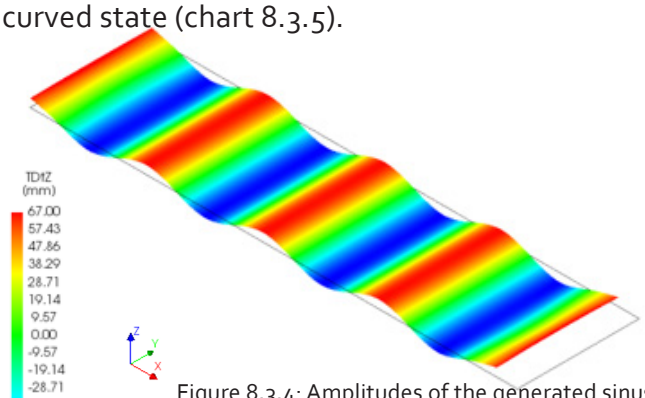


Figure 8.3.4: Amplitudes of the generated sinus shape by cold bending single thin glass layer.

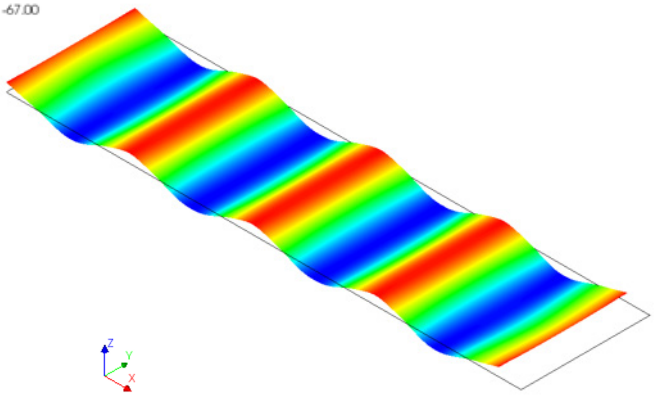

Figure 8.3.5: Displacement of the generated sinus shape by cold bending single thin glass layer due to wind load 1 kN/m².

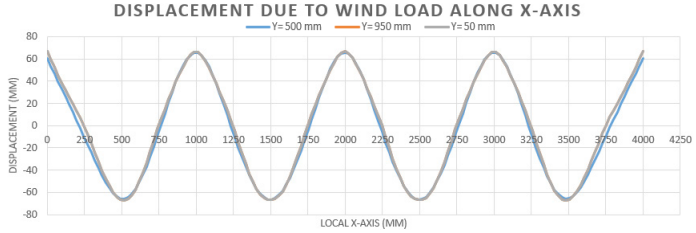


Chart 8.3.4: Displacement of the three longitudinal sections of the generated sinus shape of single thin glass layer due to wind load 1 kN/m².

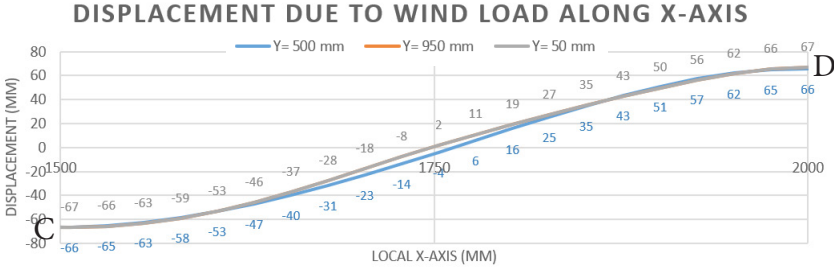


Chart 8.3.3: Displacement of the three longitudinal sections of the generated sinus shape of single thin glass layer due to wind load 1 kN/m² between Node C and Node D.

Figure 8.3.6 illustrates the generated tensile stresses and compressive stresses caused by wind load on the top layer of the curved thin glass panel. The generated tensile stresses by cold bending thin glass panel are the highest by the longitudinal supporters, where the tensile stresses reach a value of 161.80 N/mm². That value decreases with 50 kN/m2 in the middle of the panel, which results in 111 N/mm². This describes the influence of fix boundary conditions, which is explained in chapter 7. At the same time, the part between Node C and Node D appears to be the lowest affected part by bending thin glass( chart 8.3.7) . According to chart 8.3.6 the part around the short edges do not gain stresses, which means it does not bend and remains flat. That part is less stiff than the rest of the panel.

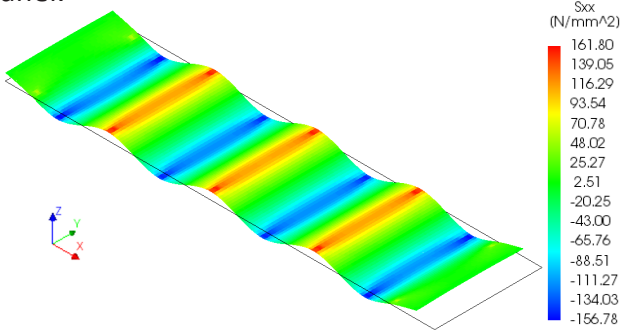


Figure 8.3.6: Initial bending stresses on the top layer of single thin glass layer.

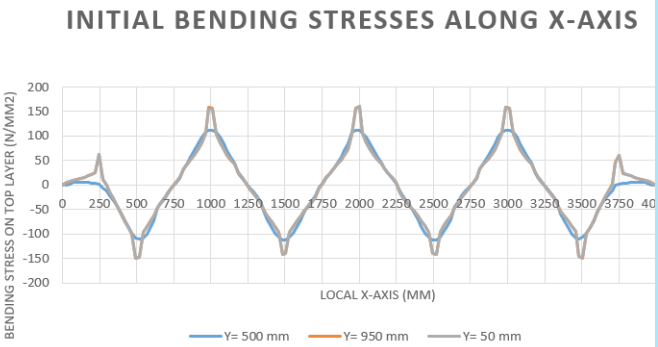


Chart 8.2.6: Initial bending stresses of the three longtindual sections on the top layer of single thin glass layer.

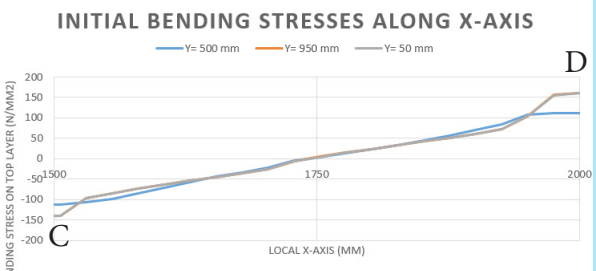


Chart 8.2.7: Initial bending stresses of the three longtindual sections on the top layer of single thin glass layer between Node C and D.

In addition, figure 8.2.7 shows that the tensile stresses of the supported longitudinal edges (Y=50 mm, Y =950 mm) increase due to wind pressure by 81 N/mm² compared to its initial tensile stressess (fig. 8.3.6). However the middle of the panel increases with 18.6 N/mm². In general, this alternative shows a considerable different between the generated tensile stresses along the edges and the tensile stresses in the middle of the panel in chart 8.3.7. That should be optimized to get equal tensile stresses across the entire panel, which cause an evenly stiffness (chart 8.3.6).

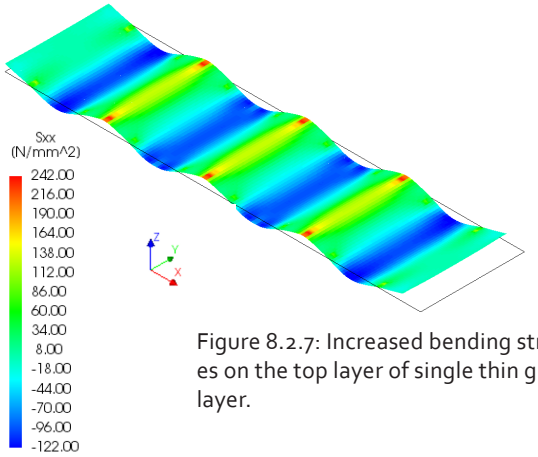


Figure 8.2.7: Increased bending stresses on the top layer of single thin glass layer.

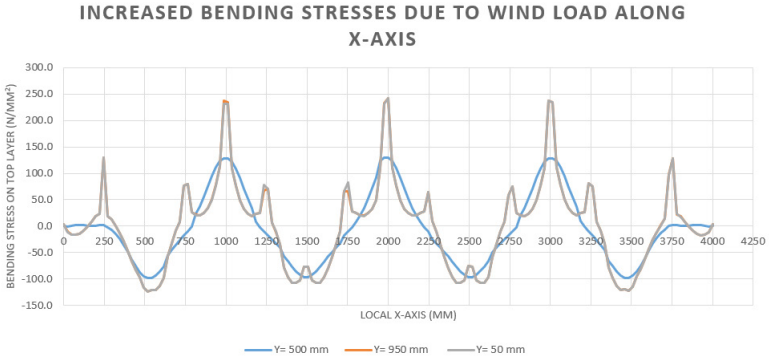


Chart 8.2.6: Increased bending stresses of the three longtindual sections on the top layer of single thin glass layer.

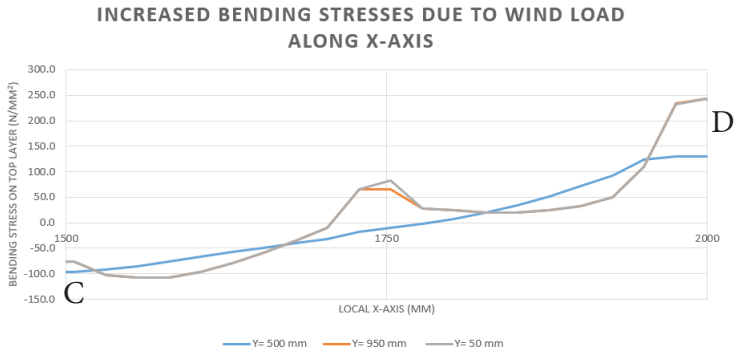


Chart 8.2.7: Increased bending stresses of the three longtindual sections on the top layer of single thin glass layer betweem node C and node D.

## 8.4 Single layer thin glass with amplitude of 33.5 mm

By analysing the bending of the third alternative it generates nine wave crests and eight wave troughs. The first observation was that the amplitudes of wave crests and wave troughs along the supported edges are equal to 33.5 mm, except by the short unsupported edges. Although, the amplitude of wave crest between the supported edges start to decrease in the middle section of the panel. A deviation of 2 mm is identified in the middle toward the z-axis between the wave crests and the wave troughs (chart 8.4.1). In addition, it is noticeable that the middle of the unsupported short edges tends to not follow the amplitudes of the supported longitudinal edges (fig. 8.4.3 & 8.4.4). It only reaches an amplitude of 24.84 mm, which can explain the differences between the amplitudes of the curved supported edges and the amplitudes in the middle across the entire panel.

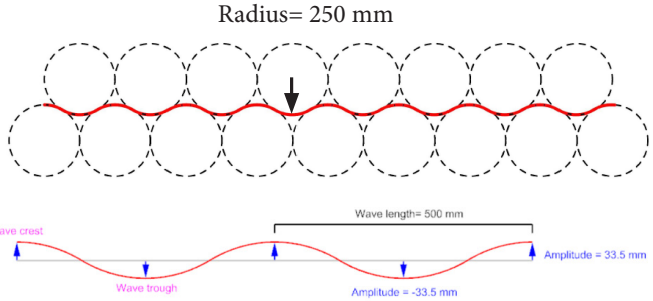


Figure 8.4.1: Principles of generated sinus shape.

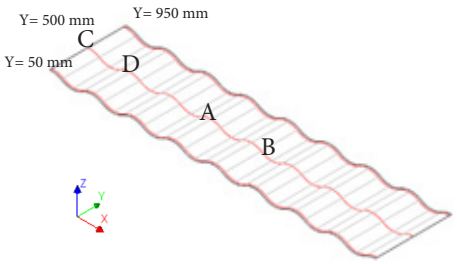


Figure 8.4.2: Longtindual sectionsof generated sinus shape.

Despite the irregular amplitudes of the short edges, this curved single layer might have potential for façade application (i.e. second façade skin) if it can resist the wind load. Therefore, a wind load of 1 Kn/ m² is applied to test the displacement of this curved single glass. As a results, the area most affected by wind load is in the middle of the unsupported short edges,which decreases by 4.11 mm from its initial state. (chart 8.4.2).The obtained amplitude is established there at a value of 24.84 mm.

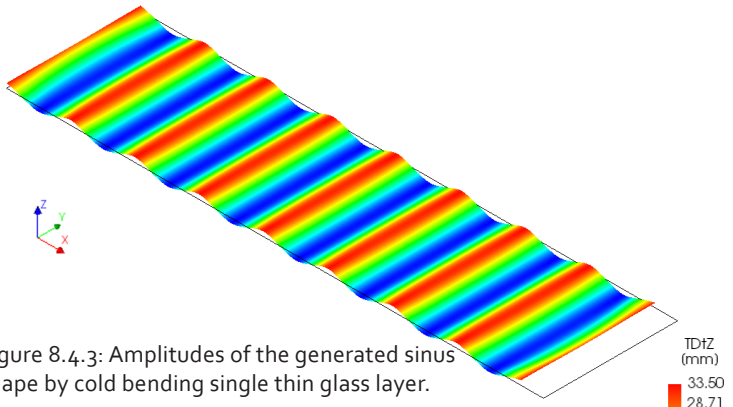


Figure 8.4.3: Amplitudes of the generated sinus shape by cold bending single thin glass layer.

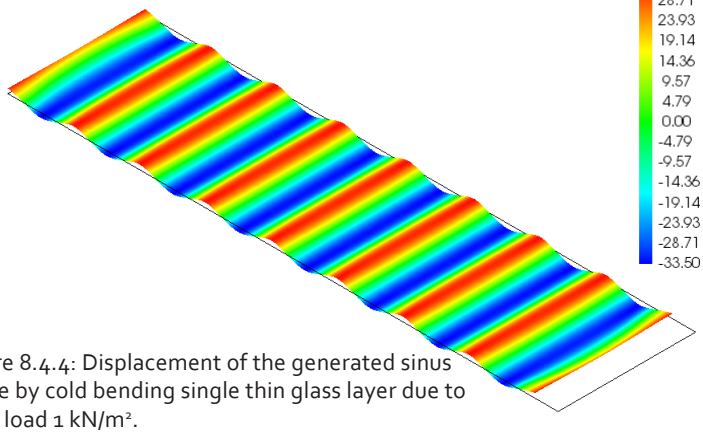

Figure 8.4.4: Displacement of the generated sinus shape by cold bending single thin glass layer due to wind load 1 kN/m².

However, between the wave crests and wave troughs the maximum displacement due to wind load is 0.91 mm. The supported areas are not affected by the wind load and remain in their initial state. (chart 8.4.1).

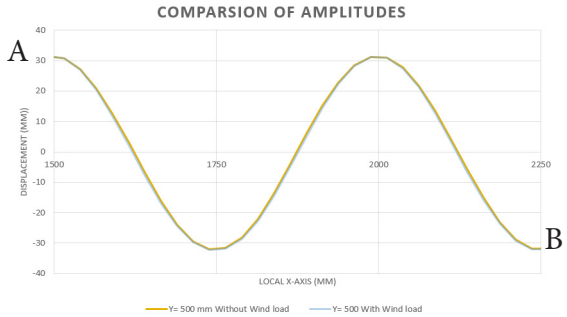


Chart 8.4.1: Comparison of displacement of Y= 500 mm the generated sinus shape of single thin glass layer due to wind load 1 kN/m², between node A and B.

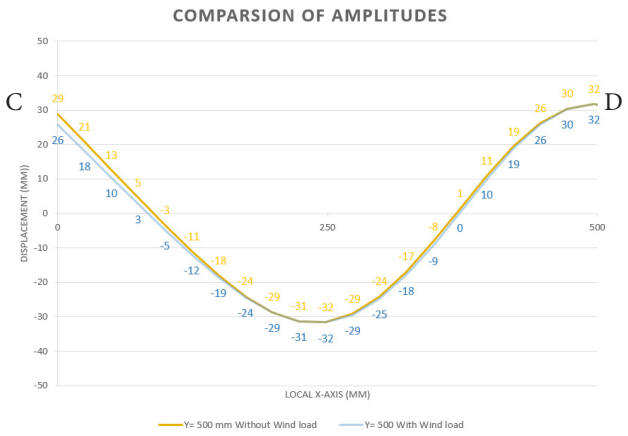


Chart 8.4.2: Comparison of displacement of Y= 500 mm the generated sinus shape of single thin glass layer due to wind load 1 kN/m², between node C and D.

Figure 8.4.5 illustrates the generated tensile and compressive stresses while bending thin glass to the desired shape. The first observation is that the major tensile and compressive stresses are measured at the supported longitudinal edges, like the previous alternatives. The maximum tensile stresses and compressive stresses due to cold bending are located at the edge supporting lines (Y=50 mm and Y=950 mm) and are equal to 375.15 N/mm² and -293.4 N/mm². While in the middle section of the panel, the tensile stresses are equal to 200 N/mm² and the compressive stresses are -200 N/mm². That means that the supported longitudinal edges have 175.15 N/mm² more than the maximum tensile stresses in the middle. In addition, the short edges appear to have the lowest tensile stresses, because of the lack of bending around that area (charts 8.4.3 and 8.4.4). .

Figure 8.4.5: Initial bending stresses on the top layer of single thin glass layer.

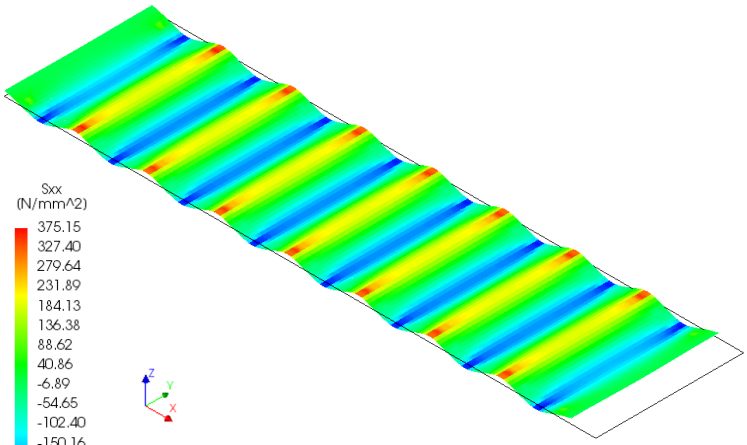


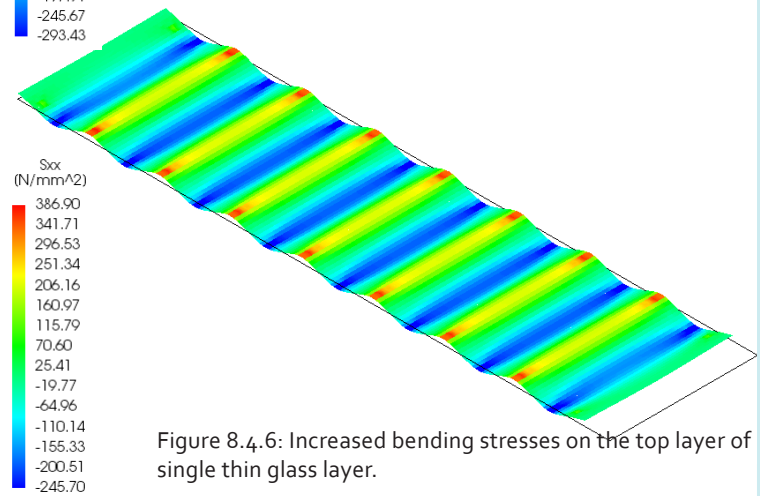


Figure 8.4.6: Increased bending stresses on the top layer of single thin glass layer.

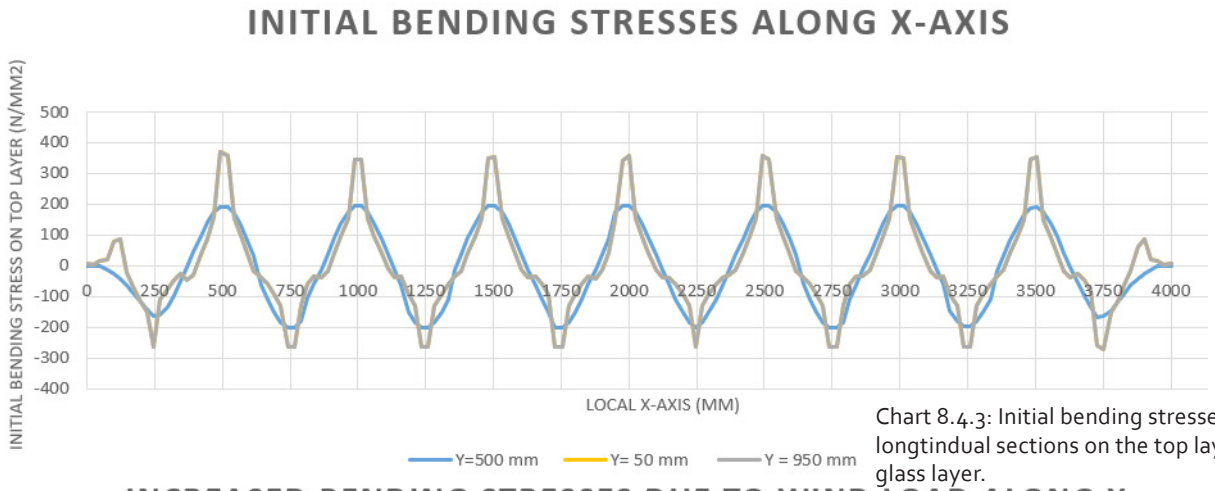


Chart 8.4.3: Initial bending stresses of the three longtindual sections on the top layer of single thin glass layer.

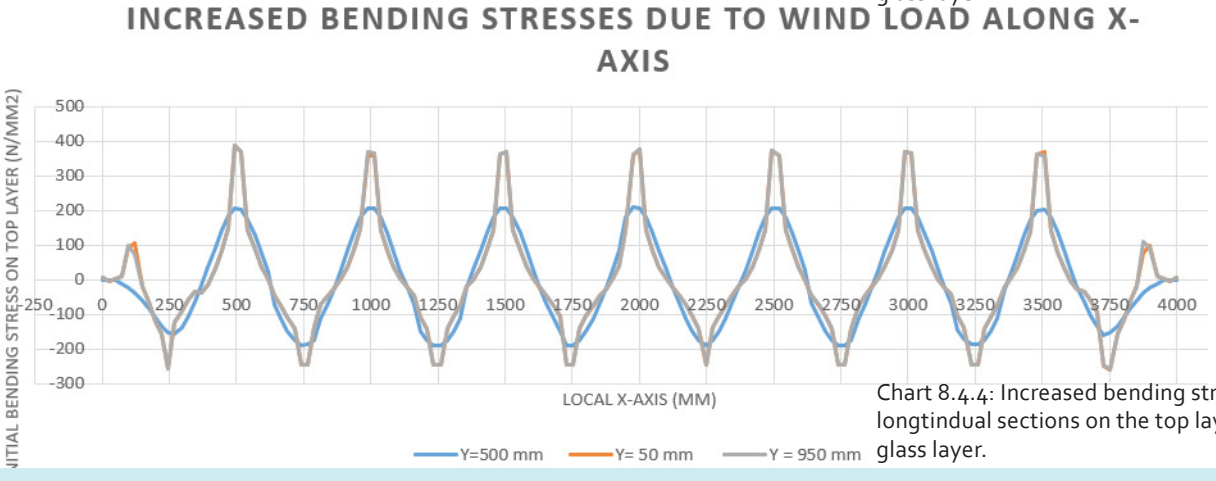


Chart 8.4.4: Increased bending stresses of the three longtindual sections on the top layer of single thin glass layer.

## 8.5 Conclusion

Chapter 8 describes the ability of bending a single layer thin glass by cold bending. The mechanical properties and production process of chemically strengthened thin glass make it possible to cold bend glass to a certain radius without breaking it.

The purpose of this chapter is to identify the displacement and the generated stresses of the thin glass by adapting the curvature radius. There fore the following sub question is established:

*How does cold bending influence the tensile stress generation on thin glass? What is the influence on its load bearing capacity compared to a flat panel?*

In order to give an answer to this question three sinus curved single layers of thin glass are investigated according to certain radius and amplitude. The amplitudes are 134, 67 and 33.5 respectively. The single layers of thin glass are supported along the longitudinal edges with fixed supports. As it is proven in chapter 7 that fix supports provides thin glass with the least stresses and displacement.

The first possible curved shape has an amplitude of 134, to create a sinus shape with three wave crests and two wave troughs. This amplitude is applied along the longitudinal edges to create the desired shape.

To identify the magnitude of the desired amplitude and the tensile stresses caused by cold bending, there longitudinal sections were made, in the middle of the panel (Y= 500 mm) and the supported edges (Y=50 mm, Y= 950 mm). The amplitudes of this sinus shape are fully achieved by cold bending. The generated tensile stresses by cold bending is measured on the top layer of thin glass. The major tensile stresses are mainly located at the supported edges with a value of 76 N/mm2. Although the middle section reaches around 50 N/mm2 of tensile stress, which is 16 N/mm2 lower compared to the tensile stresses at the supported edges.

When a wind pressure of 1 kN/m2 is applied, the curved panel starts to deform. The maximum displacement is measured between the wave crests and the wave troughs with a value of 51 mm. Moreover, the generated tensile stresses due to wind load pressure is increased compared to the tensile stresses of the curved shape (caused by cold bending) with 187 N/mm2. Also, the middle section of the panel increases in terms of tensile stress with 40 N/mm2.

The second shape is created with amplitudes of 67 mm. In this case the curved panel appear to have identical amplitudes across the entire panel, except for the area around the unsupported short edges. This sinus shape includes five waves crests and four wave troughs. The middle section of the unsupported short edges is 6 mm higher than the desired amplitude of 67 mm. Moreover, the middle section deviates from the ideal curvature of the longitudinal edges with 6 mm difference. Although between node C and D the middle section appears to have an identical pattern to the ideal curvature of the longitudinal edges, with only 1 mm of deviation. The major displacement due to wind load is measured at node A with a value of 13 mm regarding to its initial curved shape.

The obtained tensile stresses due to cold bending is 161.8 N/mm along the supported edges, while in the middle is 111 kN/mm2. Both sections are affected by wind pressure, in terms of increased tensile stresses. The generated tensile stresses in the middle are increased with 18.6 kN/mm2, while at the supported edges the tensile stresses increased by 81 N/mm2. These considerable differences between the generated tensile in the middle of the panel and the generated tensile stresses at the supported edges creates an unequal stiffness across the entire panel.

The last sinus shape that has been studied consist of nine wave crests and eight wave troughs. The desired amplitudes of this shape is 33.5 mm and -33.5 mm. The first observation by the obtained curved shape is that the amplitudes of wave crests and wave troughs at the supported edges are equal to the desired amplitude. Except for the middle section of the short edges, where it tends to deviate from the ideal curvature. The amplitude of the middle section of the short edges decreases by 4.11 mm from its initial state to reach an amplitude of 24.84 mm due to wind pressure. The less affected area by wind pressure, in terms of displacement is between wave crests and wave through. The maximum measured displacement is that area is 0.91 mm. In addition, like the previous variants in this chapter, the major tensile stresses are located by the supported edges with a value of 375.15 N/mm2. This value increase by 11.75 N/mm2 of tensile stress due to wind pressure.

In general, curved thin glass panels are stiffer than flat panels, due to the generated stresses by cold bending that allows the panel to resist wind pressure of 1kN/m2, in terms of displacement and the added tensile stresses by wind pressure. In short, by creating more curves in a single layer of thin glass, the glass becomes stiffer. Therefore, I strongly suggest continuing with last sinus shape to create a sandwich structure.

# 9 Curved Thin Glass Supported by GFRP Profiles

## 9.1 Inroduction

After exploring and analysing different curved shapes of single layer thin glass in chapter 8, it is decided to continue with the last mentioned curved shape. This curved shape comprises multiple amplitudes of 33.5 mm. In this chapter the potentials of adding GFRP profiles combined with a suitable adhesive layer to a single layer curved thin glass will be analysed. This is necessary to improve the bending behaviour of the entire panel. GFRP profiles will take place underneath the wave crests and wave troughs, create multiple span length of 250 mm for thin glass along the X-axis (fig. 9.1.1). As mentioned in section 4.3, where the advantage of using GFRP elements in the building industries include its high corrosion resistance, low moisture absorptions and high tensile stresses resistance. Moreover, GFRP is relatively lighter than the common reinforcements as steel.

In the previous chapters, namely chapters 7 and 8 the span length for thin glass was settled by 1000 mm along with the Y-axis. By implementing GFRP profiles as supporters for thin glass, the span length has changed to the X-axis, to achieve a smaller span length of 250 mm. In addition, the length of GFRP is established as 1000 mm, where it is pinned supported by aluminium profiles. The aluminium profiles are calculated according to the obtained reaction forces in appendix 4. Moreover, these aluminium profiles are positioned 50 mm from the edges, to create a span length of 900 mm for the GFRP profiles. Furthermore, the cantilevers of 50 mm are not included by the calculation (fig. 9.1.2).

To examined if the chosen dimensions GFRP profiles meets the required conditions, hand calculations for an individual GFRP profile are made according to the rules of thumbs. That is necessary to get an estimation of the possible displacement and the generated stresses under wind load of 1 kN/m2.

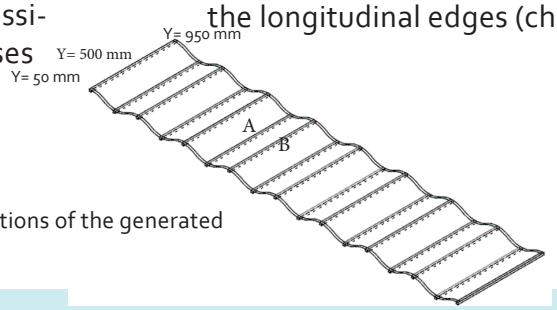


Figure 9.1.1: Longitudinal sections of the generated sinus shape.

The outcome of the maximum displacement is established by 1.64 mm, which is 46% of the maximum allowed displacement for this GFRP profile. In addition, the generated stress is in the middle with a value of 9.72 N/mm2. That is only 8% of the maximum stresses that this GFRP profile can permit.

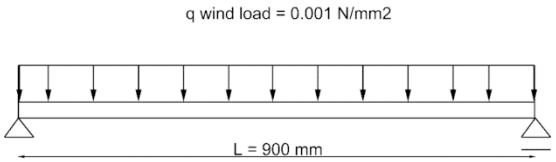


Figure 9.1.2: Hand calculation pultruded GFRP profile .

## 9.2 Curved single layer thin glass supported by GFRP profiles

A single layer flat panel is created with 17 GFRP supports to be simulated in the FEA DIANA. The distance between the GFRP profiles is 250 mm, which is equal to the mentioned span length. First the panel was bent according to vertical movement towards the z-axis, to create a sinus shape with the desired amplitudes. Theses prescribed amplitudes take place by the end parts of the each GFRP support, which prevents the GFRP profiles to rotate.

By running the calculation to measure the obtained amplitudes the figure 9.2.1 below appears. It is obvious that the amplitudes of the short edges have improved by reaching the desired amplitude of 33.5 mm, compared to variant 3 in chapter 8. Even de amplitudes of the middle of the panel are almost equal to the amplitude of the supported longitudinal edges, with 0.3 mm difference (chart 9.2.1).

Between node A and node B of section middle and the sections of the longitudinal edges, the middle section is inflated with 1.6 mm towards the z-axis compared to the section of the longitudinal edges (chart 9.2.2).

Figure 9.2.1: Amplitudes of the generated sinus shape by cold bending single thin glass layer supported vy GFRP profiles.

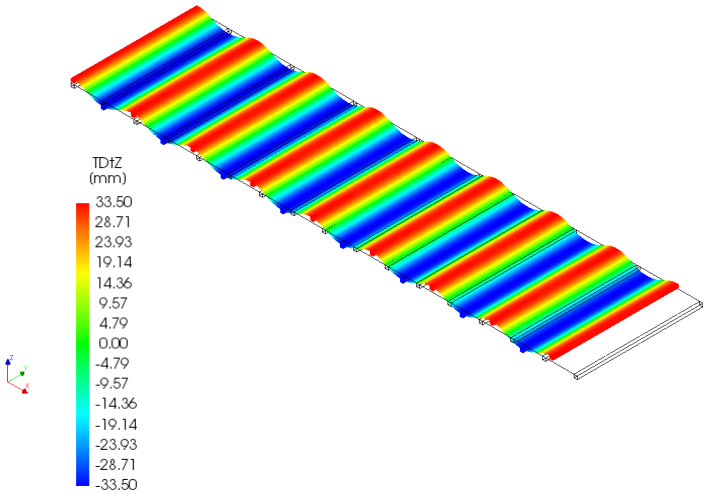


Figure 9.2.2: Displacement of the generated sinus shape by cold bending single thin glass layer due to wind load 1 kN/m².

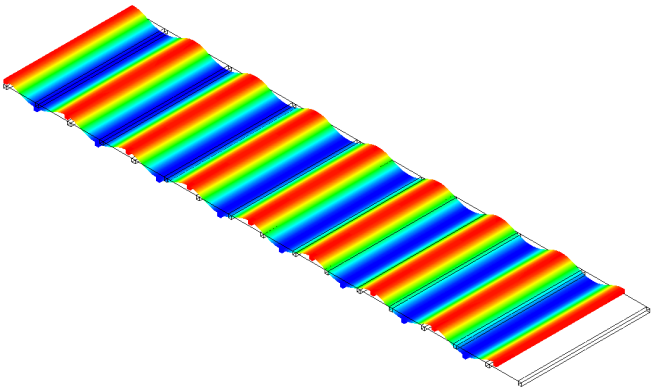

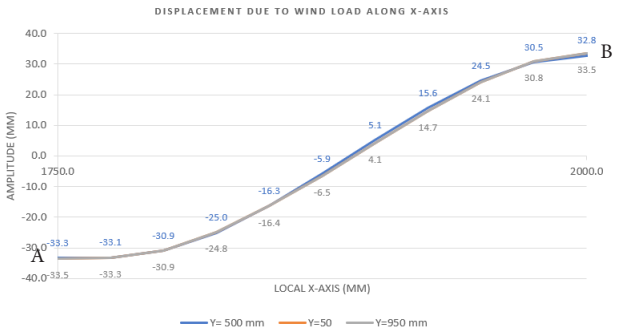


Chart 9.2.3: Displacement of the three longitudinal sections of the generated sinus shape of single thin glass layer supported by GFRP due to wind load 1 kN/m².

After analysing the obtained results of bending thin glass with GFRP supports, it was necessary to check if this created panel is able to resist wind load pressure of 1 kN/m2. The results is given chart 9.2.3, where a section between 1750 mm and 2000 mm is illustrated. The longitudinal edges have an equal pattern. Both wave crest and wave trough are not affected by the applied wind load pressure, in terms of displacement. Only the middle section, which is represented by the blue curve in chart 9.2.3, is with 0.6 mm of displacement compared to its initial curved state. While the displacement at the same point by variant 3 was 0.91 mm. Thus, using GFRP supports have advantage to reduce the displacement of thin glass.

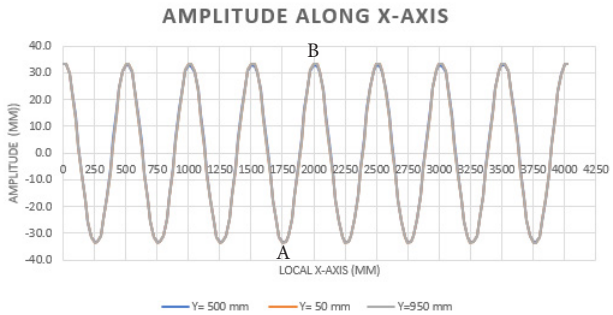


Chart 9.2.1: Amplitudes of the three longitudinal sections of the generated sinus shape by cold bending single thin glass layer supported by GFRP profiles.

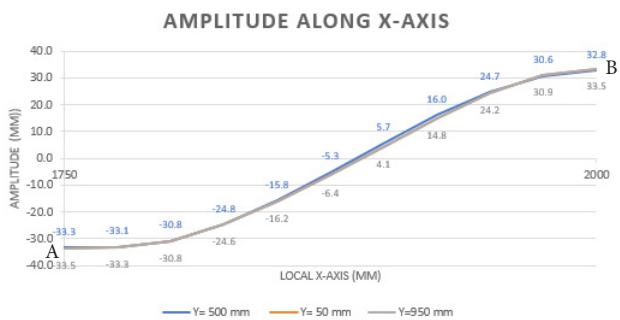


Chart 9.2.2: Amplitudes of the three longitudinal sections of the generated sinus shape of single thin glass layer supported by GFRP.

Figure 9.2.3 shows the obtained tensile stresses and compressive stresses on the top layer regarding to cold bent thin glass supported by GFRP profiles. The first remarkable observation that the generated stresses are almost equal concentrated along the Y-axis and close to the GFRP supports, instead of only by the longitudinal edges like the variants mentioned in chapter 8. Moreover, the specific areas of thin glass that have been supported by GFRP profiles have no stresses, which mean that these areas remain flat. During the simulation adhesives layers were not included to simulate the connection between GFRP profiles and thin glass.

In order to improve that, different adhesives sorts will be added to the simulation. Two adhesives sorts will be simulated according to their mechanical properties (section 5.5).

The major obtained tensile stresses are still located at the longitudinal edges with 324.20 N/mm². While this value decreases in the middle section of the panel with 48.1 N/mm² to obtain a total tensile stress of 276.1 in the middle. That tensile stress is generated in each wave crest of the panel (Charts 9.2.4 &8.2.5. .

It is necessary to check the behaviour of this structure under wind load, in terms of generating tensile stresses. Figure 9.2.4 illustrated the obtained results, where the major tensile stresses are increased by 10.9 N/mm2 at the longitudinal edges compared to its initial curved state. While the tensile stresses in the middle slightly increased by 6.5 N/mm2, to achieve a value of 282.6 N/mm2. In general, the created shape shows enough stiffness to handle the external load. The differences between the tensile stresses generated at the edges and in the middle, is 52.5 N/mm2 (charts 9.2.6 & 9.2.7) .

Chart 9.2.4: Initial bending stresses of the three longtindual sections on the top layer of single thin glass layer.

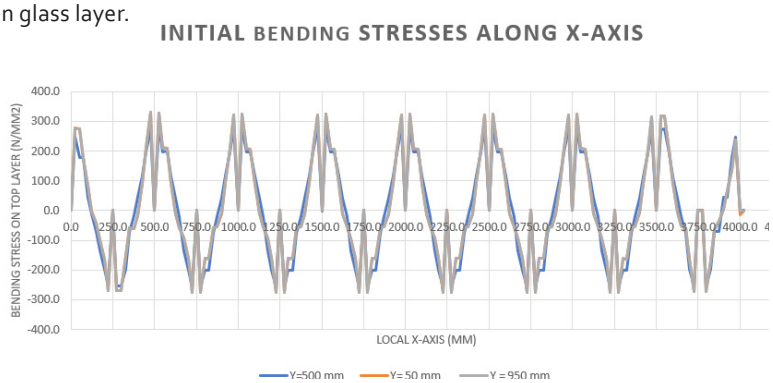


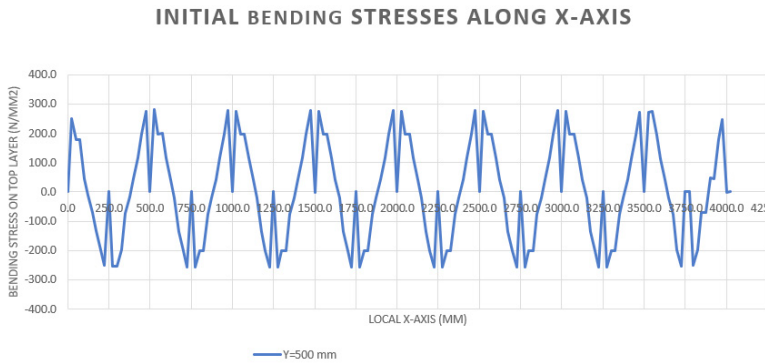


Chart 9.2.5: Initial bending stresses of the middle section (Y=500 mm) on the top layer of single thin glass layer.

Chart 9.2.6: Increased bending stresses of the three longtindual sections on the top layer of single thin glass layer supported by due to wind load 1kN/m².

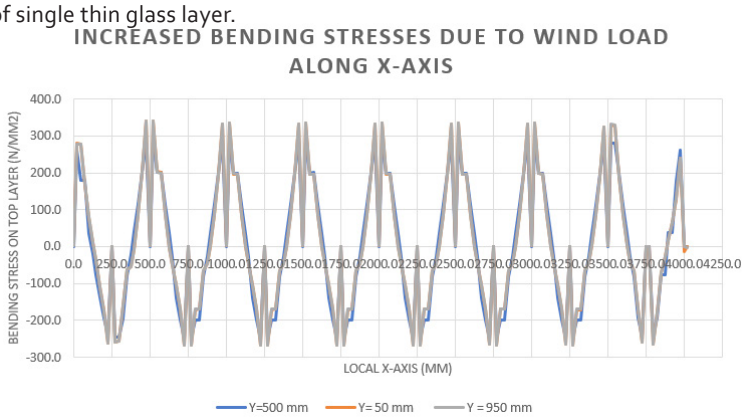


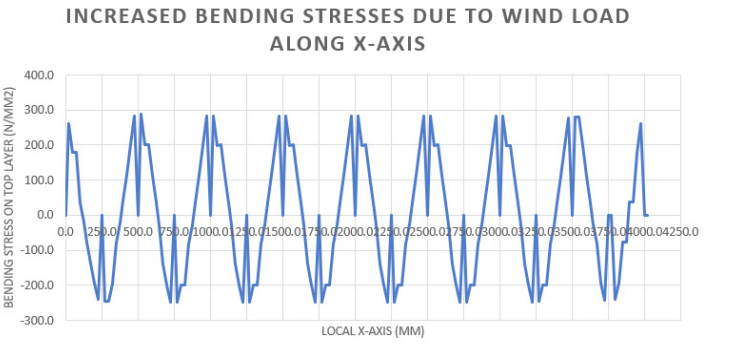


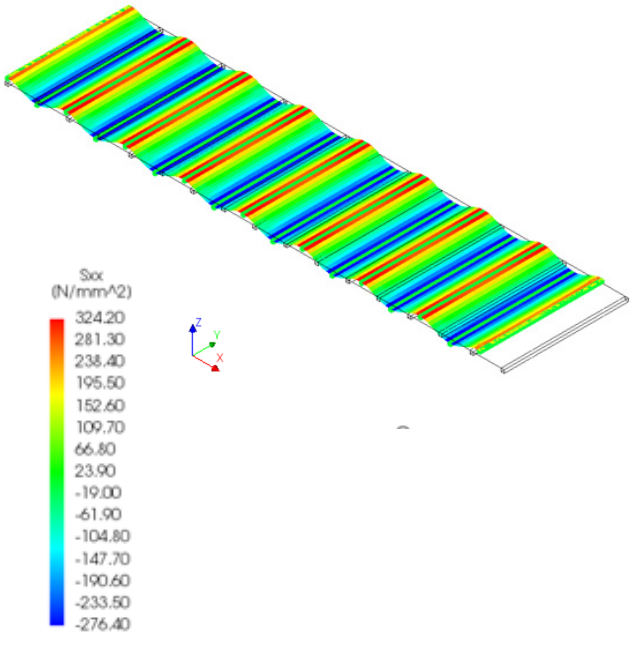


Figure 9.2.3: Initial bending stresses on the top layer of single thin glass layer supported by GFRP profiles.

Chart 9.2.7: Increased bending stresses of the middle section (Y=500 mm) on the top layer of single thin glass layer supported by due to wind load 1kN/m².

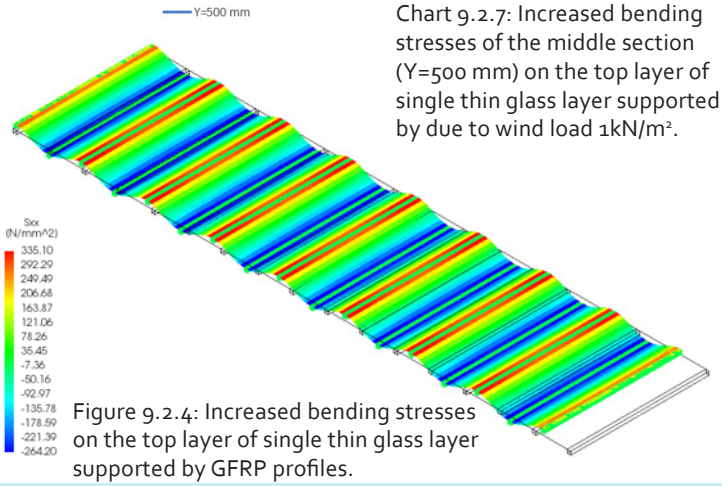


Figure 9.2.4: Increased bending stresses on the top layer of single thin glass layer supported by GFRP profiles.

## 9.3 Sandwich structure of two layers of thin glass and GFRP profiles.

As mentioned in section 6.2, a sandwich panel consists of three main layers: two surface layers, which called facing and a core layer (fig. 9.3.1). The two surface layers are represented by two sheets of thin glass of each 1 mm thick. In general, sandwich structures ensure high loadbearing capacity. This sandwich structure is created and simulated in FEA DIANA to get accurate values of both displacement and tensile stresses.

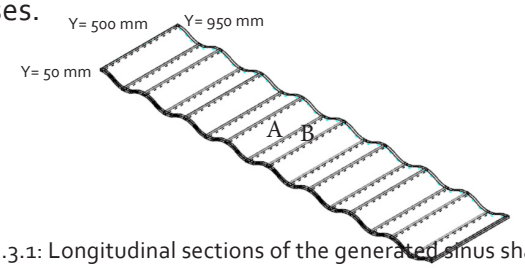


Figure 9.3.1: Longitudinal sections of the generated sinus shape of the sandwich structures .

First the condition of the curved sandwich panel is analysed. The curved sandwich panel is obtained by cold bending of flat sandwich panel. Subsequently, the influence of wind pressure on the outer layer of the created curved sandwich structure is studied. Figure 9.3.3 shows the results of cold bending the mentioned sandwich structure, in terms of amplitudes.

The figure shows a sandwich structure with an ideal curvature with smooth transition of the contour colours. The desired amplitudes of this sinus shape is achieved on the longitudinal edges with respectively 33.5 mm, -33.5 mm (fig. 9.3.2 & chart 9.3.1). The middle section of the panel is 0.3 lower than the desired amplitude, like the previous panel in section 9.2. Between nodes A and B is the middle section is 0.8 mm higher than the ideal curvature of the longitudinal edges (chart 9.3.2). In addition, it is an improvement compared to the curved shape of the previous variant in section 9.2, where the difference is 1.6 mm.

To examine the influence of the wind pressure on the created sandwich panel, an evenly distributed wind pressure of 1 kN/m2 is simulated on the outer layer of the sandwich structure in FEA Diana. Figure 9.3.3 shows the contour colours between 33.5 mm and -33.5 mm. This curved shape appears to have the same contour pattern as before applying wind pressure. Chart 9.3.4 represents a comparison of the middle section (Node A and B) of the panel before as after applying wind pressure, where the exact values of the amplitudes are represented.

Chart 9.3.2: Amplitudes of two longitudinal sections of the generated sinus shape by cold bending sandwich structure between node A and node B.

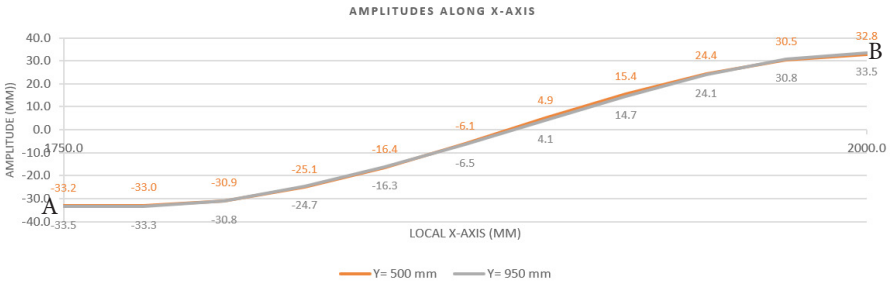


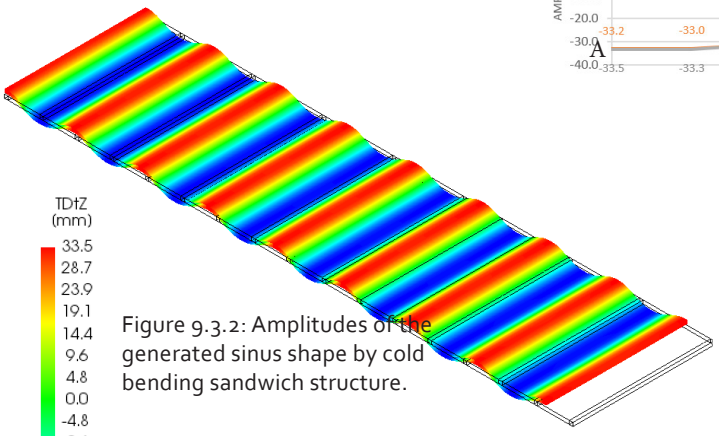


Figure 9.3.2: Amplitudes of the generated sinus shape by cold bending sandwich structure.

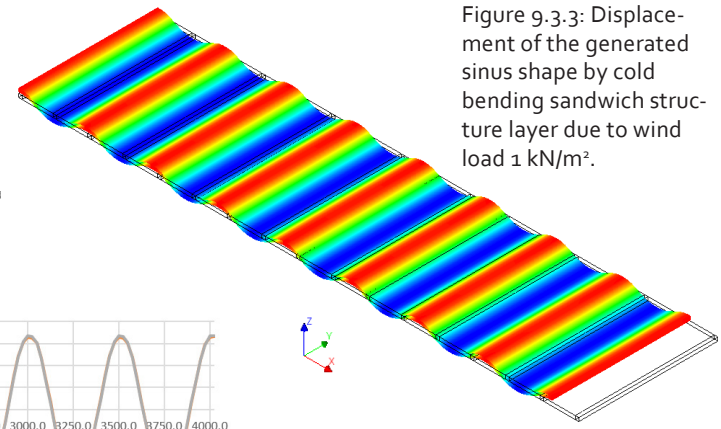

Figure 9.3.3: Displacement of the generated sinus shape by cold bending sandwich structure layer due to wind load 1 kN/m².

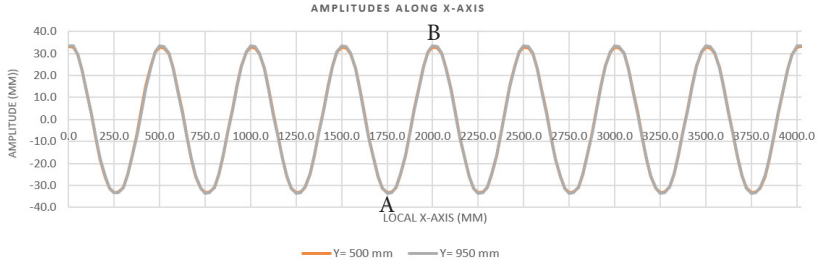


Chart 9.3.1: Amplitudes of two longitudinal sections of the generated sinus shape by cold bending sandwich structure.

It is remarkable that this chart has similar pattern as before applying wind pressure. That means no displacement took place by exposing this sandwich structure to the mentioned wind pressure, due to its extreme stiffness (charts 9.3.3 and 9.3.4).

Despite the slightly differences of the middle section to the ideal curvature, the sandwich structure has in general improved in achieving a more stable sinus shape compared to the pervious variant.

To test if the stiffness also has improved figure 9.3.4 shows the influence of bending this sandwich structure on the tensile stresses and the compressive stresses on the top layer of the outer thin glass sheet.

The major tensile stress that is obtained, is at small area near by the longitudinal edges where it reaches 415.66 N/mm2. The longitudinal section taken in the middle of the panel is represented in Chart 9.3.5. This chart shows major tensile stresses of 281.1 N/mm2 and major compressive stresses of -249.5 N/mm2 on the top layer of the outer thin glass layer. That means that the tensile stresses slightly increased by 5 N/mm2 compared to the previous variant. Even the tensile stresses along the longitudinal edges has increased compared to the previous variant 9.2, which create more stiffer structure. In other words, the greater the tensile stresses the stiffer the panel will be. That will make this sandwich structure more able to resist wind pressure and reduce displacement.

Chart 9.3.3: Comparison of amplitudes of Y= 500 mm the generated sinus shape of the sandwich structure before and after applying wind load 1 kN/m².

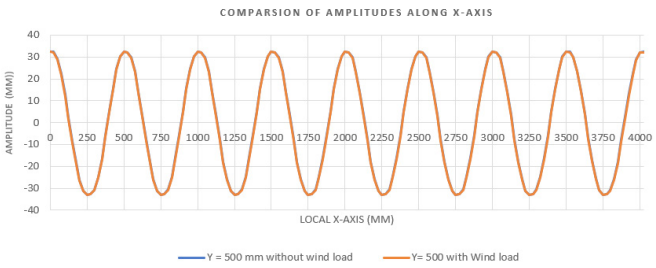


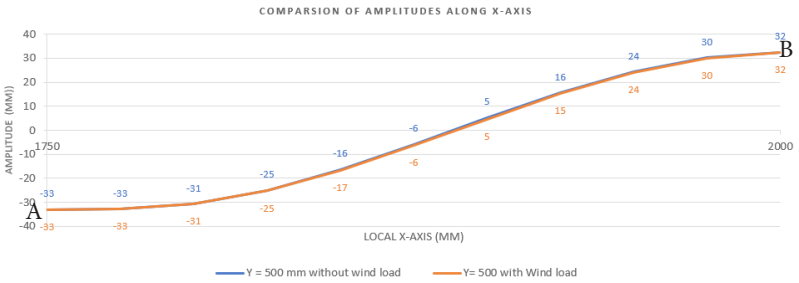


Chart 9.3.4: Comparison of amplitudes of Y= 500 mm the generated sinus shape of the sandwich structure before and after applying wind load 1 kN/m², between node A and B.

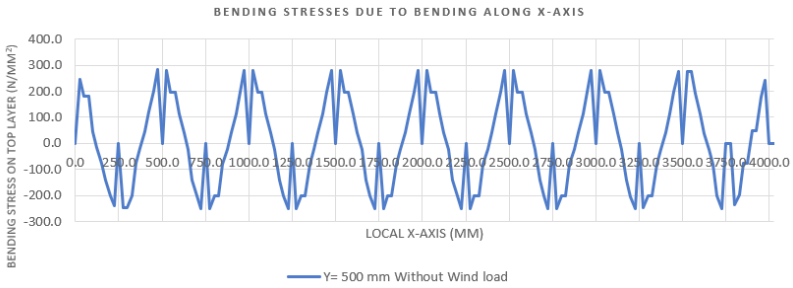


Chart 9.3.5: Initial bending stresses of the middle section (Y=500 mm) on the top layer of sandwich structure.

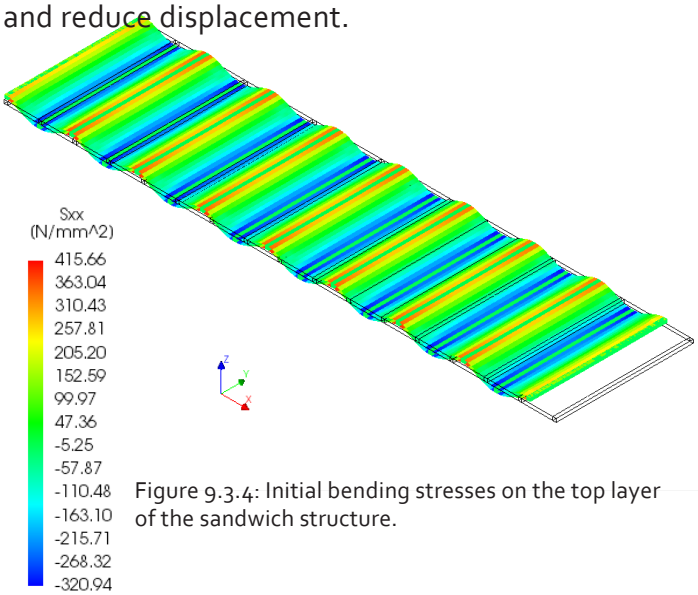


Figure 9.3.4: Initial bending stresses on the top layer of the sandwich structure.

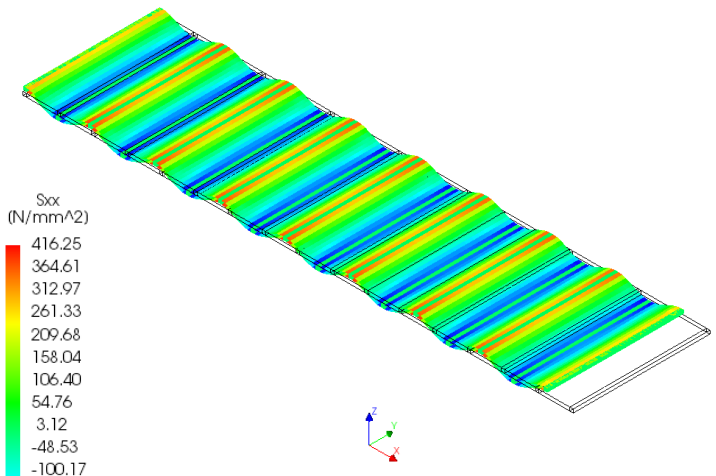


Figure 9.3.5: Increased bending stresses on the top layer of the sandwich structure.

The generated tensile stresses due to wind pressure has slightly increased by 0.59 N/mm² at the longitudinal edges of both layers of thin glass sheets (fig. 9.3.5). The middle section is represented in chart 9.3.6 were the values of the tensile stress are visible. The obtained results are almost identical to the results of the generated tensile stresses that is caused by bending the sandwich structure.

Chart 9.2.7 shows a comparison between the tensile stresses before and after applying wind load. The chart is zoomed in to have a closer look if there is actual increasing of tensile stress caused wind load.

This section is taken between node A (y=500 mm ; x= 1750 mm) , and node B (y= 500 mm; x= 2000 mm). There is a clearly defined pattern to the graph, and this can be taken to mean that the tensile stresses have increased by a value of 8.3 N/mm2 close to the supported area by GFRP profile, where the tensile stress drops back to 0 N/mm².Thus, the major generated tensile stresses are 280.1 in the middle section of the outer layer of the sandwich structure.

Chart 9.3.6: Increased bending stresses of the middle section (Y=500 mm) on the top layer of sandwich structure due to wind load 1kN/m².

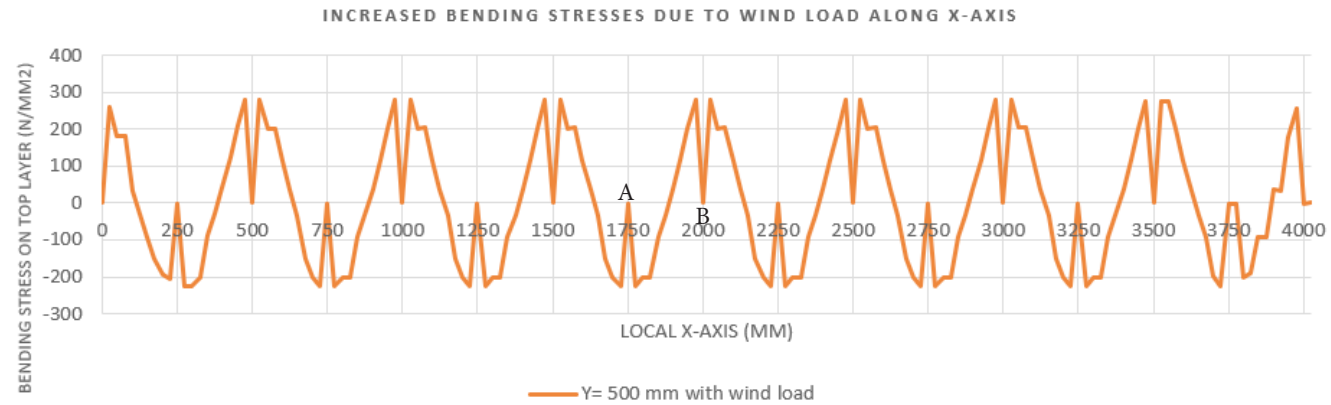


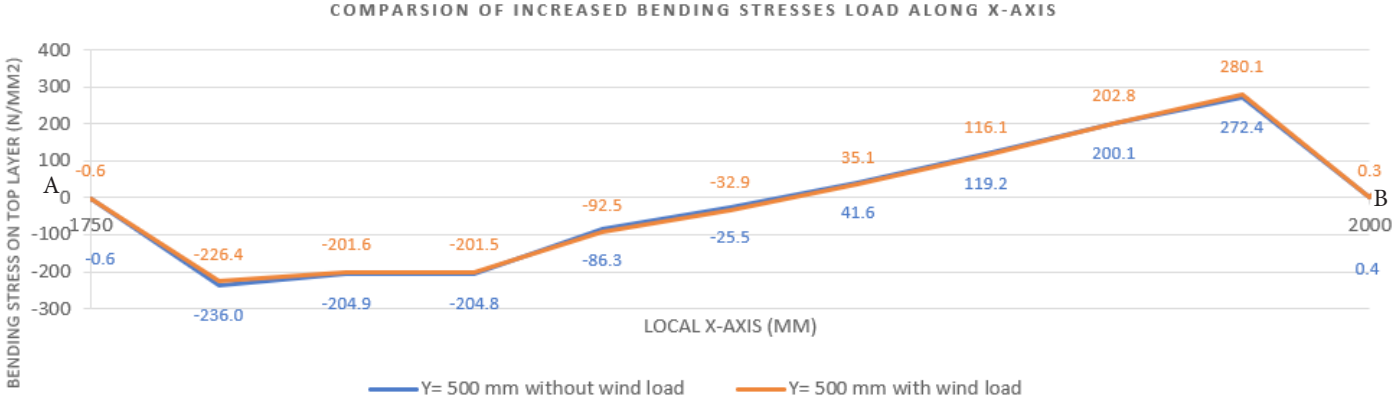


Chart 9.2.7: Increased bending stresses of the middle section (Y=500 mm) on the top layer of sandwich structure due to wind load 1kN/m² between node A and node B.

## 9.4 Numerical analysis Adhesives

After studying the mechanical and physical properties of several adhesives in chapter 5, this section is created. In order to verify their influence on thin glass and their stiffness, by simulating two commonly used adhesives for (thin)glass bonding in FEA Diana, using the mechanical properties in table 5.5.1. The chosen adhesives are Epoxy and Polyurethane, because of their relatively higher strength and stiffness compared to silicone adhesives. Moreover, silicone adhesives require a thickness of at least 6 mm to be able to use it for structural applications. Because of the limit of the cavity width to obtain a desirable thermal performance only 1 mm of thickness is required for adhesive. Therefore, silicone adhesive is excluded from the simulation.

These adhesives are compared according to three factors, namely their influence on the tensile stress on the thin glass (before and after wind load), the generated shear stress in the adhesive by bending the sandwich structure and their ability of elongation. Finally, a conclusion will be drawn based on the analysis of the obtained results to give an answer to the following sub question:

*Which adhesive layer is suitable in order to connect curved thin glass to GFRP profiles, to create a sandwich structure?*

To simulate these adhesives in FEA Diana the following mechanical properties are required. The Young's modulus, the Shear strength . The Young's modulus describes the stiffness of the adhesive and emphasize the relationship between the stress and the stain (fig. 9.4.2), while the shear strength defines the strength of the adhesive when it fails in shear. In other words, the ability of the adhesive to resist forces which cause the internal structure to slide against itself (fig. 9.4.1). Moreover, elongation is a crucial property of adhesive because it defines the stretch distance of an adhesive before it breaks (fig.9.4.3 ).

As mentioned in chapter 5, epoxies are stiffer than polyurethane due to its high Young's modulus, which is around 196 times higher than polyurethane. That reflects the lower elongation of epoxies compared to polyurethane. In addition, the shear strength of epoxy is around 4 times higher than polyurethane. The exact values of these mechanical properties are obtained from the table given in chapter 5.

A fragment of the total sandwich panel is design in FEA diana in order to simulate the behaviour of the adhesives between the GFRP profiles and thin glass. The influence of the chosen adhesives on the height of the amplitude is illustrated in figure 9.4.4. There are no differences found between epoxy and polyurethane in terms of reaching the desired amplitude of 33.5 mm by bending the sandwich structure. Even in the middle of the structure appears to be stable when a wind pressure 1 kN/m2 is applied on the sandwich structure, without affecting the height of amplitude in both adhesives.

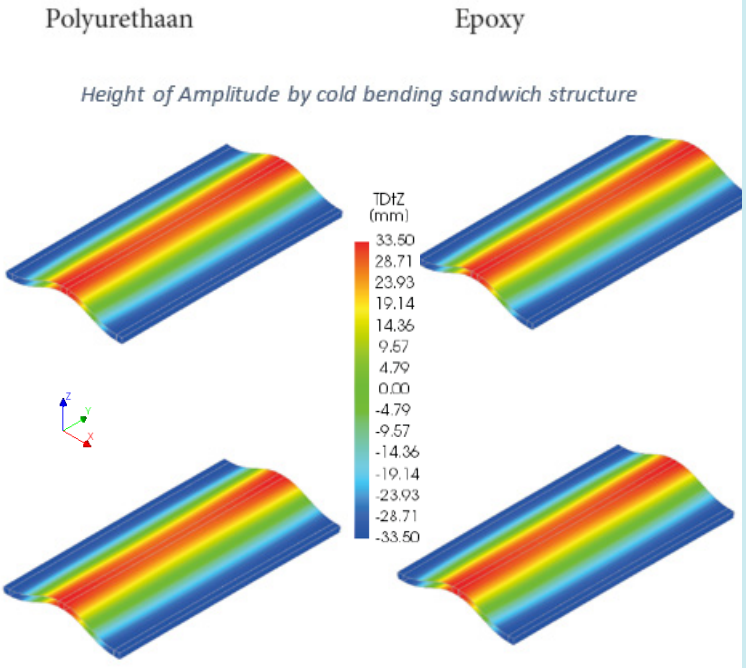


Figure 9.4.4: Comparison of the height of amplitude according to epoxy and polyurethane adhesives.

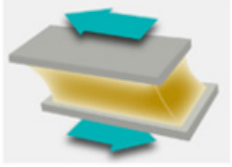

Figure 9.4.1: Shear strength of adhesive layer (Masterbond).

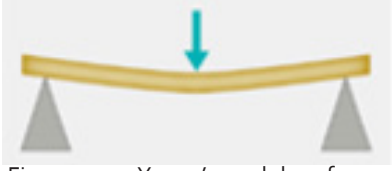

Figure 9.4.2: Young's modulus of adhesive layer (Masterbond).

Figure 9.4.3: Elongation of adhesive layer (Masterbond).

Another important aspect for using adhesives to create a sandwich structure made of two thin glass panels as facings and GFRP profiles as core layer is its influence on the generated stresses on thin glass. Figure 9.4.5 verify this influence by the contours pattern between 333.03 N/mm2 represent tensile stresses) and -333.03 N/mm2 (represent compressive stresses) of the top layer of the outer pane of the sandwich structure.

It is obvious that polyurethane adhesive causing lower tensile stresses on thin glass compared to epoxy adhesives. In both cases bending and wind load pressure are the colours of the contour in the middle part of the created fragment by polyurethane adhesive lighter compared to epoxy adhesive. The main reason behind these results is the high stiffness and shear strength of epoxy compared to polyurethane adhesive, which increase the bonding between GFRP profiles and thin glass.

The obtained shear stress on the two adhesives by bending the sandwich structure is illustrated in figure 9.4.6. From the studies about the mechanical properties of these adhesive the shear strength a significant property to investigate. The obtained shear stress by the end parts of epoxy adhesive layers is higher than polyurethane, which confirm its high shear strength compared to polyurethane. It is remarkable that the shear stresses did not increase by applying wind load pressure of 1 kN/m2, which refers to the lack of displacement.

The middle adhesives are simulated to prevent movement in the X-ditection, in order to measure the effect of shear on the adhesive layers of the edges. The upper adhesive layers of the edges define the shear stress towards the middle by bending the sandwich structure. The lower adhesive layer are always in the opposite direction of the top adhesive layers, which represent the shear behaviour of the adhesive (fig. 9.4.6).

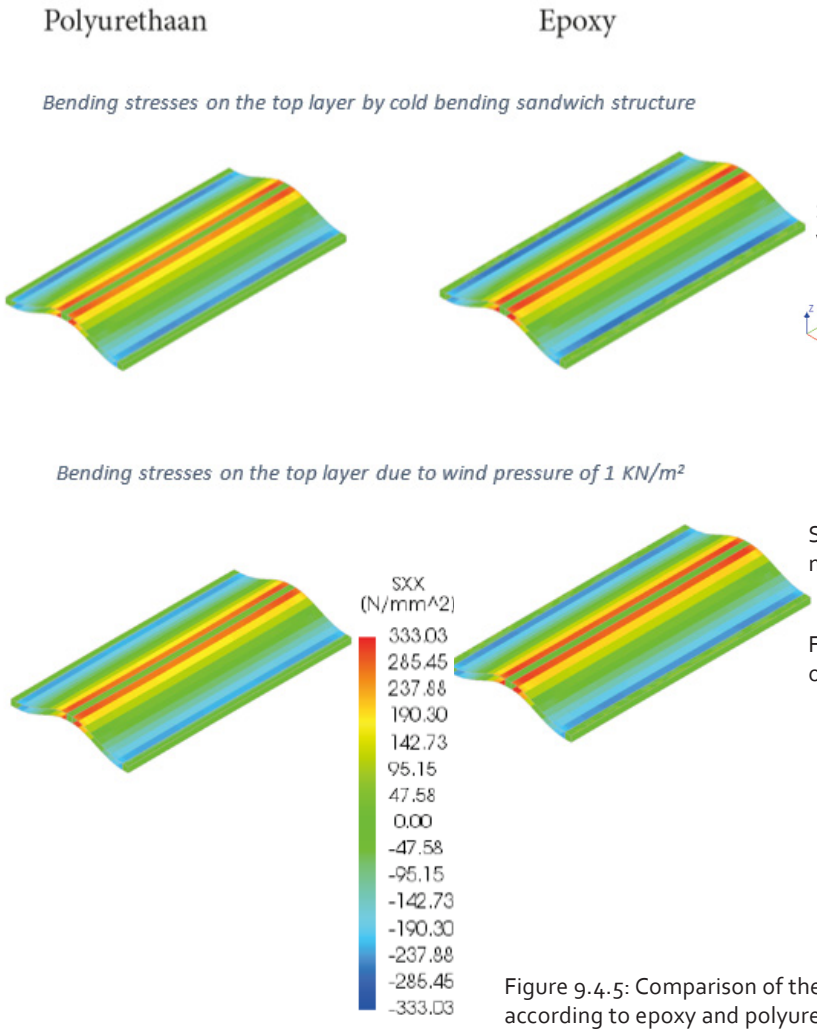


Figure 9.4.5: Comparison of the generated bending stresses according to epoxy and polyurethane adhesives.

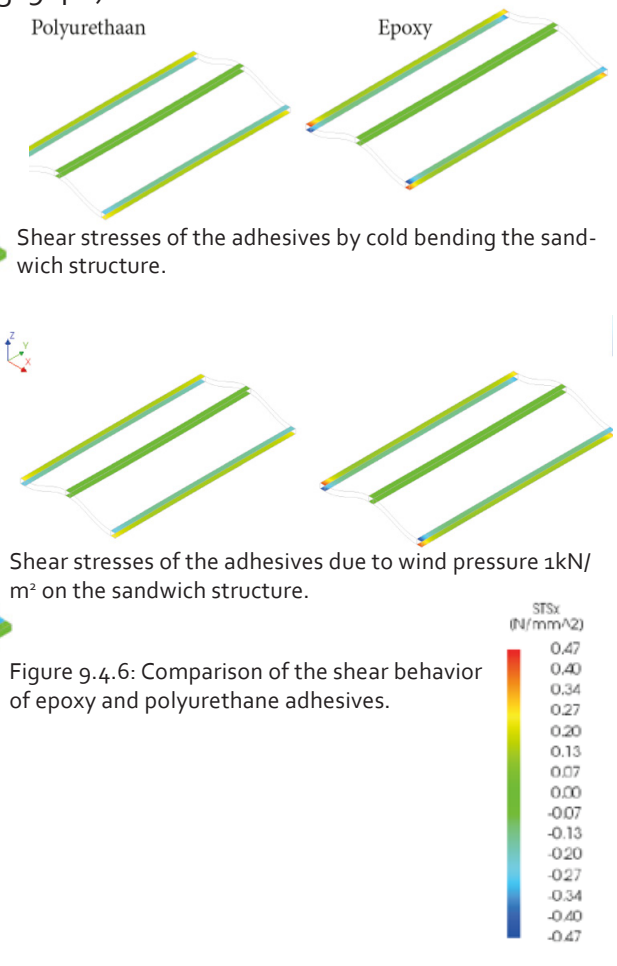


Shear stresses of the adhesives by cold bending the sandwich structure.

Shear stresses of the adhesives due to wind pressure 1kN/m² on the sandwich structure.

Figure 9.4.6: Comparison of the shear behavior of epoxy and polyurethane adhesives.

In addition, the position of the GFRP profiles between the thin glass facings defines the magnitude of these specific stresses. The GFRP profiles are positioned between the curvatures of the thin glass panels, to prevent rotation of the profile during cold bending of the sandwich structure. These profiles are only allowed to translate in the vertical direction without to rotate. Because rotation of the GFRP profiles will increase the shear stress on the adhesive layers that connect the thin glass panels and de GFRP profiles. That procedure requires high precision during the assembling of the sandwich panel to avoid unnecessary shear stress on the adhesive layers.

By looking to the results of elongation of the adhesives, it is concluded that the elongation of epoxy adhesive layers did not affected by either cold bending and applying wind pressure, since epoxies have the lowest ability to allow elongation compared to the mentioned adhesives in chapter 5.

That is slightly different by polyurethane, where it is more flexible than epoxy adhesive. The results show that elongation of approximately 0.05 mm is achieved by the ends of the adhesive layers (fig. 9.4.7). That is mainly because of the connected GFRP profiles are not rotated, which prevents elongation of the adhesive layers between the thin glass panels and the GFRP profiles. Even here no differences are found between the elongation of curved sandwich structure and when wind pressure of 1 kN/m2 is applied, due to the lack of displacement.

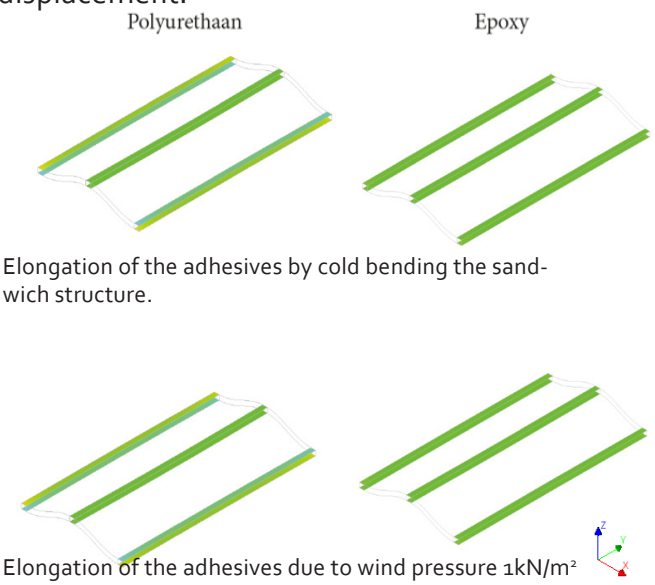


Elongation of the adhesives by cold bending the sandwich structure.

Elongation of the adhesives due to wind pressure 1kN/m² on the sandwich structure.

Figure 9.4.7: Comparison of elongations of epoxy and polyurethane adhesives.

## 9.5 Conclusion

Section 9.4 describes a comparison between Epoxy and polyurethane adhesives. These adhesives are compared according to three aspects: their influence on the generated tensile stress in thin glass, the generated shear stress in the adhesives and their ability of elongation. These are significant aspects to investigate in order to answer the following sub question:

*Which adhesive layer is suitable in order to connect curved thin glass to GFRP profiles, to create a sandwich structure?*

In order to answer this question a fragment of the chosen sandwich structure is design in FEA Diana to simulate the adhesives.

Epoxy adhesives are stiffer compared to polyurethane adhesives. A disadvantage of epoxies compared to polyurethane is that epoxy adhesives have much lower elongation. That cause more stiff bonding between the GFRP profiles and thin glass layer. That is directly related to more generation of stresses on thin glass, in terms of bending the sandwich structure. As opposed, polyurethane adhesives are mainly used to resist dynamic loads. Polyurethane adhesive has lower shear stress, according to the obtained results of the generated shear stress in these adhesives. All of this points to the fact that polyurethane is preferred to be used for the chosen sandwich structure compared to epoxy adhesive.

# 10

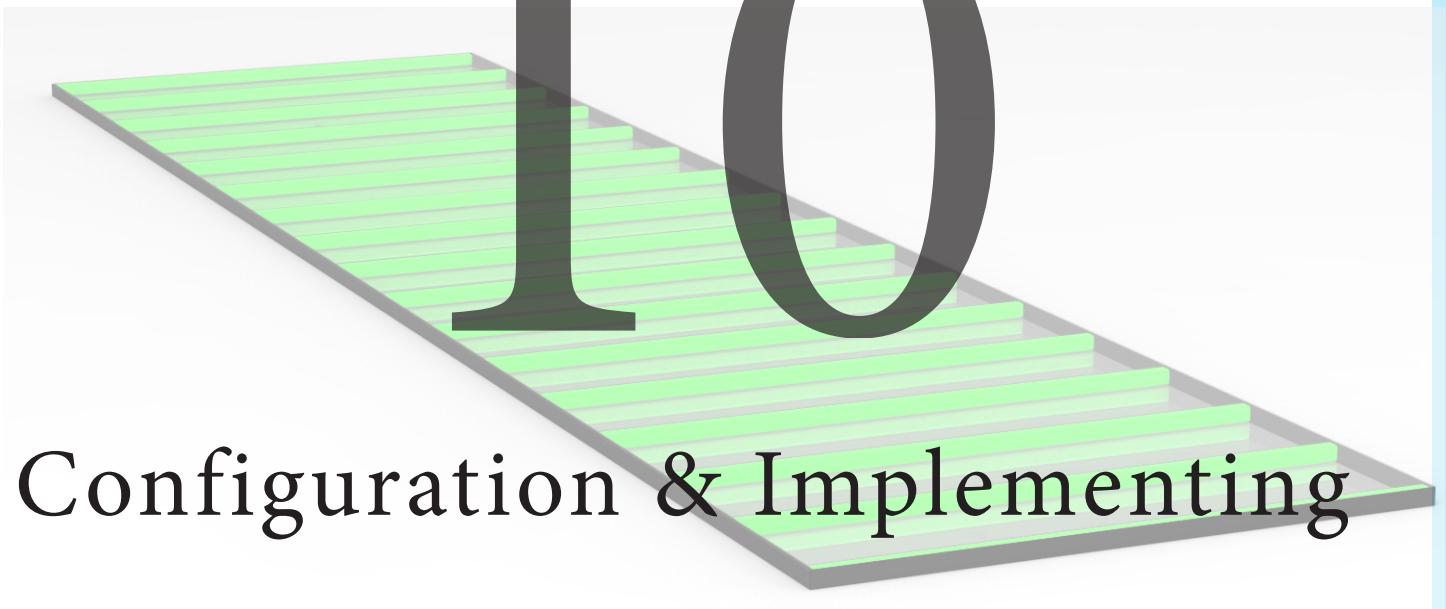

# Configuration & Implementing

## 10.1 Introduction

This chapter reviews the configuration elements that are necessary to assemble a façade panel out of a chosen sandwich structure as described in chapter 9 for curtain wall systems. The materials used for the final design will be explained to gain more understanding of the advantages and disadvantages of these configuration elements. Subsequently, an assembly sequence of these materials will be articulated. Finally, a conclusion will be drawn to answer the sub question:

*Which configuration elements are needed for a curved façade panel?*

## 10.2 Curtain wall

A curtain wall forms the skin of a building but also acts as a building envelope component (Morris, 2013). The primary function of a curtain wall is separating the outdoor environment from the indoor environment. The name "curtain wall" is originally derived from the way panels hang, like a curtain, to the primary structures of the building. In addition, a curtain wall is light weight compared to other cladding materials such as precast and masonry. Moreover, a curtain wall has no load bearing capacity regarding vertical loads. That means it does not support vertical structural loads except for its own weight.

The process regarding the production of a curtain wall includes the following elements: fabrication, assembly, glazing and installation. Fabrication entails all mechanical operations such as cutting, drilling, milling and punching (Morris, 2013). These procedures are mainly applied to the aluminium extruded frames. The main function of assembly is to fasten the aluminium framing members together to create a frame support for the glazing infill. In addition, sealants are significant to ensure the frame is sealed against air and water.

Moreover, glazing implicates attaching the infill to the area between aluminium frames. The infill involves an insulated glass unit; however, it can be replaced by aluminium, granite or stainless steel panels. To conclude the process, the installation of the curtain walls on the construction site are performed.

In general, there are two types of curtain wall systems in terms of attaching panels to the primary constructions of the building. These types are stick built systems and unitized systems (fig. 10.2.1). Stick built system are based on fabricating the components in a factory and shipping them as individual pieces to the construction site. These components are installed and glazed on the construction site. The disadvantage of stick built system compared to unitized system is the labour cost. The on site installation process of stick built system is generally more expensive than unitized system. That is because of the more additional time is required to enclose the building and the related higher on site labour cost relative to a factory. The main disadvantage of stick built is that the installation is performed outdoors where it is exposed to the weather conditions which can affect the durability of the sealant and hence the essential need to enclose the building (Morris, 2013).

In contrast to a stick built system, a unitized curtain wall is fabricated and assembled in the factory where controlled environments ensure the durability of the panels. Subsequently, the panels are transported to the construction site for installation. Moreover, with unitized systems the time that is required to enclose the building is dramatically reduced due to assembly of the panels in the factory. The installation of a unitized system includes attaching the prefab panels to the main construction of the building.

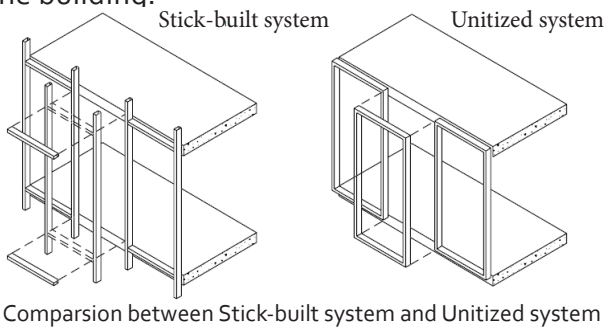


Figure 10.2.1: Comparsion between Stick-built system and Unitized system (Watts, 2001).

In addition, the prefab panels are placed side by side where the aluminium frames are interlocked by incorporated gaskets in a male-female method. That ensures a joint that is both water and air tight.

Due to the complexity of assembling curved sandwich panels, the necessity for a controlled environment is required. That leads to greater precision during the assembly of the components to create a curved sandwich panel that is both water and air tight. Hence, given the shorter installation time and reduced labour costs, it is preferable to use unitized systems for assembling the panels as part of the primary construction of the building.

## 10.3 Curved sandwich panel

The desired curved sandwich panel consists of a transparent sandwich structure and a prefab curved aluminium sandwich panel for the spandrel infill in which both are supported by the aluminium extrusion frames. The transparent sandwich structure consists of two facings layers represented by thin glass panes and 17 GFRP profiles that represent the core layer. Polyurethane adhesive is mainly responsible for connecting the core layer to the facings. The spandrel infills are mainly used to increase the thermal performance and to hide the slab edge and the ceiling cavity. In addition, commonly used infills for spandrel are painted or are anodized aluminium panels filled with insulation material. Rock wool is selected to fill the cavity between the anodized aluminium panels to increase the thermal performance of the prefab curved aluminium sandwich panel (fig. 10.3.1). In addition, rock wool insulation material ensures fire resistance.

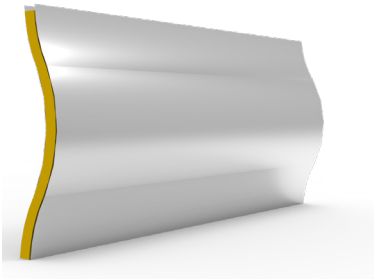

Figure 10.3.1: Prefab curved aluminium sandwich panel filled with rock wool insulation.

Glass is a significant component for curtain wall systems that can aesthetically accentuate the architectural value of a building. In addition, it provides visibility to the exterior space and allows daylight to enter the interior space.

A transparent sandwich structure is defined as a glazing assembly of two thin glass panes which are connected by GFRP profiles. This structure consists of four glass surfaces. These surfaces are numbered 1 to 4 from the exterior to the interior. Glass surfaces 2 and 3 face each other in the cavity where a low emissivity coating is applied on surface 2.

The purpose of using low-e coating is that it focuses the reflection and absorption of long-wave lengths (> 780nm) otherwise known as infrared radiation without affecting the amount of visible light that enters the space (Laufs, 2013). In general, it reduces the solar gain entering the space and therefore the cooling costs during the summer season. Furthermore, it reflects the indoor heat flow which reduces heating during the winter season.

In order to assemble a transparent sandwich unit containing two thin glass panes and 17 GFRP profiles, the following sequence should be followed:

1. First, a super foam spacer should be attached to the surface edges of the number 1 thin glass pane which represents surface 3 of the sandwich structure.

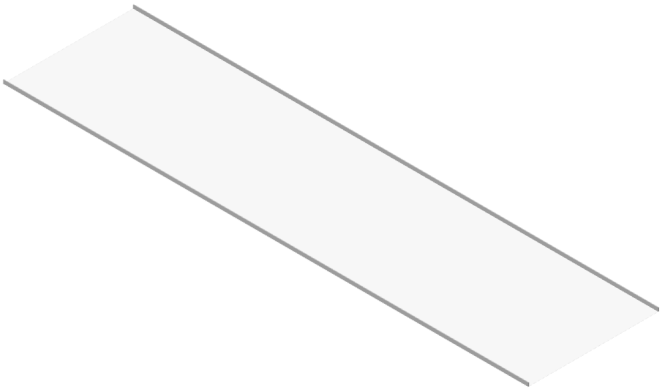

2. Next, polyurethane adhesive is added to surface 3. The areas where the adhesive should be applied are predetermined by the labours to avoid misplacing of this adhesive. In addition, these areas represent the regions where the bottom layers of the GFRP profiles will be glued to. The distance between the GFRP profiles is 250 mm. Moreover, there should be 1 mm of space between the GFRP profiles and the super foam spacers. This is necessary due to the thermal expansion of the GFRP profiles.

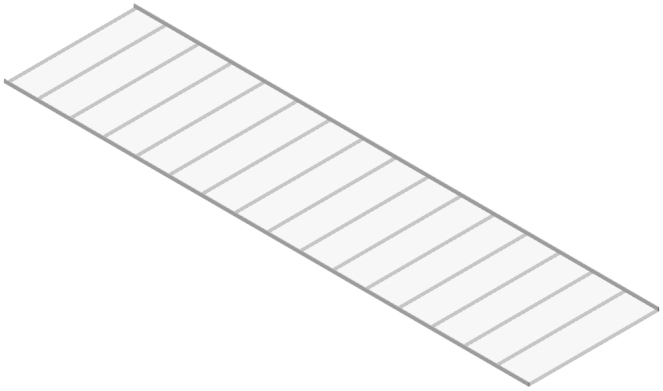

3. Placement of the GFRP profiles on the PU adhesives comes next. This action has to be fast in order to create a proper bonding between the profiles and the thin glass pane before the adhesive cures.

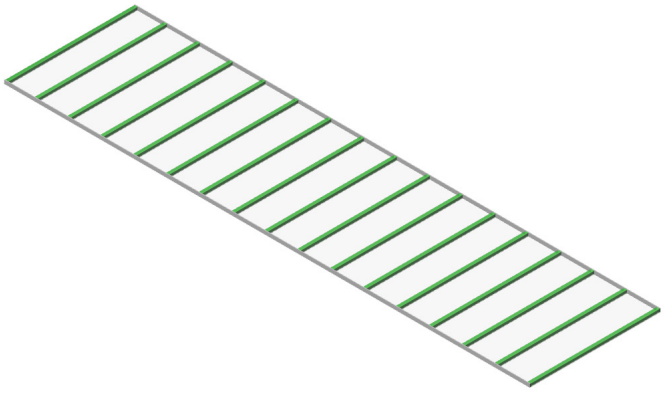

4. A similar approach of step 2 should be applied to surface 2 of the outer thin glass pane (number 2 thin glass panel) where the pane is glued to the top layers of the GFRP profiles.

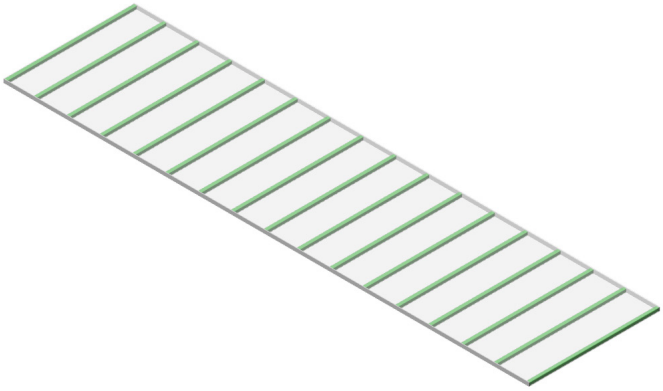

5. The sandwich structure is then sealed by silicone to create a closed structure panel.

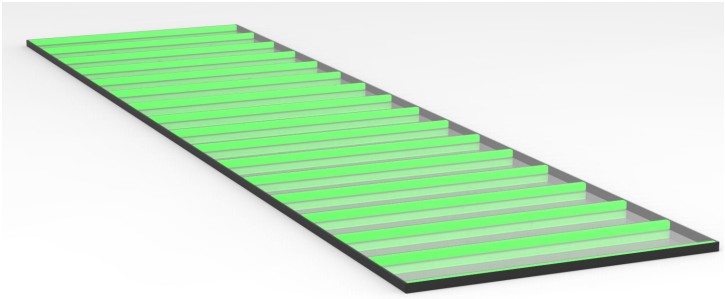

Filling the cavity with argon gas to improve the thermal performance of the sandwich panel completes the process. The argon gas flows through the voids between the GFRP profiles and the super foam spacer to ensure a completely insulated sandwich panel.

Aluminium framing is used in different system depths for vertical and horizontal profiles. The vertical profile is defined as mullion and for horizontal profiles as transom (McFarquhar, 2013). One of the important architectural advantages of using aluminium frames is that the profiles can be easily extruded to develop curve shapes with high accuracy promoting a clean finish. In addition, coatings can be applied for protection against environmental and chemical factors. In general, aluminium framing is light compared to the more commonly used steel framing that is used in several curtain wall systems.

Because aluminium frames are extrusions than contain different alloys, limits for stresses and deflection must be established. The aluminium framing alloy that is used for the final design is 6061-T6, due to its high yield strength (Appendix 5). In addition, aluminium alloy 6061-T6 is comparable to the yield strength of steel (McFarquhar, 2013). To estimate the feasibility of using this type of aluminium frame, a hand calculation is made according to the documented reaction forces in appendix 6. According to the results, these aluminium frames reach only 13 % of their ultimate tensile strength.

The advantages given above prove that aluminium frames are generally beneficial for weight and stiffness. In addition, curved profiles can be readily manufactured with high precision which enable the desired curved shape. Therefore, in this thesis, the mentioned aluminium frames are chosen to support the curved sandwich structure.

To attach the infills (the transparent sandwich panel and insulated aluminium panel) to the aluminium frames, a capped system is used. A capped system physically locks the infills to the aluminium frame by means of aluminium cap profiles (McFarquhar, 2013). In addition, these profiles can be manufactured in a curved shape due to the aluminium extruding process.

This technique is illustrated in figure 10.3.2 where the transparent sandwich structure is pushed by the aluminium caps and is combined with rubber gaskets to the aluminium mullions so as to create the desired curved shape of the sandwich structure. Subsequently, the cap is mounted to the mullions by bolts on the wave crest and wave troughs. That prevents a spring back effect of the sandwich panel and keeps the sandwich structure in a curved state. After that the horizontal caps are interlocked with the aluminium transoms to complete the assembly process of the curved transparent sandwich panel. From an architectural perspective, the transparent sandwich structure seems to have a picture frame of anodized aluminium around it.

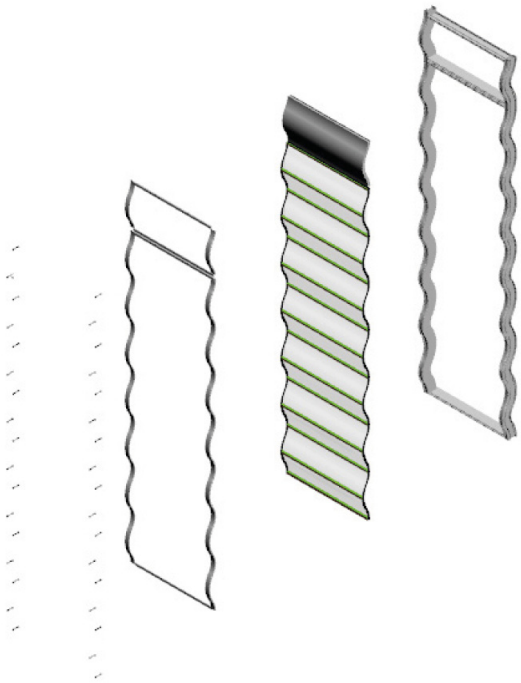

Figure 10.2.1: Configuration transparent sandwich panel.

## 10.4 Flexible spacer

Another significant feature of the transparent sandwich panel is the edge spacer. Edge spacers generally contain desiccant that absorbs moisture and prevents condensation. The common edge spacer for insulated glass unite (IGU) is made of aluminium filled with desiccant grains. To ensure long-term durability at the edges and desirable thermal performance for curved sandwich applications of unite, a flexible foam edge spacer is selected. Flexible foam edge spacers are preferred due to their bendable quality. In addition, flexible spacers are responsible for keeping the cavity in a consistent curved state that results from cold bending.

Given the above reasoning, this thesis strongly suggests a specific flexible foam edge spacer that is called "Super Spacer Premium" (Appendix 7). This super foam spacer is an extruded thermoset polymer structural silicone foam spacer combined with desiccants. Figure 10.4.1 shows which materials the super spacer is constructed from. Moreover, no metals are included in this foam edge spacer, which increases the thermal efficiency of the curved sandwich panel.

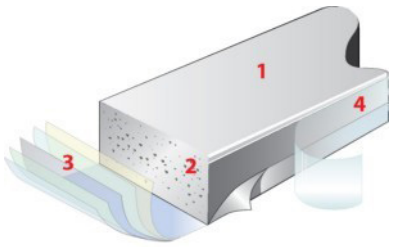


1. Smooth, matte fininsh guarated against blistering an bubbling.
2. Thermoset foam matrix.
3. Proprietary mulit-layer vapor barrier.
4. Acrylic structural adhesive.

Figure 10.4.1: Configuration of super spacer premium (Hartung-Glass, Edgetech).

In general, a super foam spacer blocks transfer of heat and is characterized by one of the lowest thermal conductive spacer available at the moment (Hartung-Glass, Edgetech).Moreover, a super foam spacer is 950 times more heat flow resistant in comparison to a typical aluminium spacer. That leads to a reduction of both condensation and opportunities for fungi growth related to heat. Furthermore, resistance to heat flow is directly linked to lower energy costs.

Super foam spacers have shown outstanding performance in the widely used durability test "The P-1 chamber" (Hartung-Glass, Edgetech). The results include resistance of 60 °C temperatures and 95-100% humidity. Due to its low thermal conductivity, less differences between the surface temperatures of the curved sandwich panel occur.

In addition, super foam spacers are more efficient compared to conventional aluminium spacers in terms of noise reduction.

## 10.5 Thermal performance

To produce a curved sandwich panel with low thermal conductivity or U-value, it is necessary to use insulating materials that reduce both cooling and heating demands and hence a reduction of carbon dioxide emissions of a building (Pfundstein et al. 2008). Materials with low insulted properties (or with a high U-value) lead to heat loss during the winter (heating required) and heat gains during the summer (cooling required). The extent of thermal conductivity is expressed in λ with W/m²K.

The density of the cavity infill materials is the key to determine the insulating performance of these materials. For instance, cavity infill materials with low density provide higher insulating performance than materials with high densities. That is because materials with low density contain a high porosity where a large number of voids lowers thermal conductivity (Laufs, 2013).

In general, argon cavity infill reduces convective heat loss compared to air cavity infill due to its lower density. Krypton is slightly better in terms of thermal performance compared to argon because it is a bit denser. The main advantage of argon is its cost quality ratio compared to krypton as argon is cheaper than krypton and it is the most affordable cavity infill with sufficient thermal performance. In addition, the insulating performance of the cavity filled with argon gas improves by adding Low-e coating.

The thermal performance of the sandwich structure depends on two factors, namely the cavity width and the cavity infill. Table (10.5.1) shows the relationship between the cavity width and the cavity infills and their U-values. These values are obtained by an online U-value calculator which is supported by the AGC company. Cavity infills play a significant role in determining the total thermal resistance of the sandwich panel. There are three commonly used cavity infills: air, argon and krypton for conventional insulated glass unite and they are selected here to study their thermal performance in three different cavity widths respectively: 12 mm, 20 mm and 25 mm.

It is important to mention that these values are based on insulated glass unite of Planibel Clearlite - glass where the thickness of these glass panels are predetermined by 4 mm. The cavity width and cavity infill are variable parameters. The given results are estimated but still offer sufficient insight. The obtained U-values do not include Low-e coating.

| *Cavity infill* | *Air (100%)* | *Argon (90%) air(10%)* | *Krypton (90%) air(10%)* |
|---|---|---|---|
| *Cavity width* | | | |
| *12 mm* | **2.9** | **2.7** | **2.6** |
| *20 mm* | **2.7** | **2.6** | **2.6** |
| *25 mm* | **2.8** | **2.6** | **2.6** |

Table 10.5.1: U-value W/m2K of different cavity infill in various cavity thicknesses. (Glass configurator- AGC Glass Europe).

The width of the cavity is related to the height of GFRP profiles, which is calculated by the formula: 1/40 * span length (Appendix 4 ). Therefore, the U-value of cavity width of 25 mm is determined according to the mentioned cavity infill gasses. The given U-value for argon and krypton is almost identical whereas air is higher. In other words, the insulating performance of argon and krypton is better than air cavity infill. Despite the similarity of thermal performance of krypton and argon, argon is preferred as a cavity infill for the sandwich panel given its lower cost.

To improve the insulating performance of a sandwich panel, a low emissivity coating is implemented on surface 2 of the outer thin glass pane (number 2 thin glass panel). Appendix 8 representing the total U-value based on a hand calculation for a cavity width of 24 mm. This predicts the insulating performance of this cavity width as well as to allow comparison with values obtained by the AGC's thermal performance calculator. It is required in order to identify the following aspects so as to calculate the thermal conductivity of the curved sandwich panel:

- The transition resistance from the indoor air to inner glass surface: Ri ( 0.13 m2K/W);
- Thermal resistance of thin glass (for the outer panel and the inner panel) : Rglass (m2K/W);
- Thermal resistance of the cavity, which is based on the gas infill): Rcavity (m2K/W);
- The transition resistance from outer glass surface to outdoor air: Re ( 0.04 m2K/W).

The U-value given by the AGC's thermal performance calculator is 1.5 W/m2K while the U-value obtained by the hand calculation is 1.1 W/m2K. By comparing the calculated U-value with the U-value of AGC's calculator for the same cavity width and cavity infill, a difference of 0.4 W/m2K is determined. This difference can be related to the differences in glass thicknesses between Planibel Clearlite glass (4 mm) and thin glass (1 mm) combined with the tolerance of the hand calculation. Because each panel of Planibel Clearlite glass is 4 times thicker than the chosen thickness of thin glass, an increase in the thermal conductivity of the thin glass naturally occurs.

The actual cavity width is determined by the height of the GFRP profiles (25 mm) combined with the thickness of the polyurethane adhesives (2x 1 mm) to achieve a total cavity width of 27 mm. Appendix 9 shows the obtained U-value of a 27 mm cavity width calculated by the AGC thermal performance calculator. The thermal conductivity of these configurations are identical to the one with the 24 mm cavity infill with a U-value of 1.5 W/m2K. This U-value is considered as the indicator of the thermal conductivity of the final design of the sandwich panel.

## 10.6 Conclusion

There are two types of curtain wall systems in terms of attaching panels to the primary constructions of the building, namely stick built systems and unitized systems. Stick built system are based on fabricating the components in a factory and shipping them as individual pieces to the construction site. The disadvantage of stick-built system compared to unitized system is that its more expensive due to the more labour cost. In addition, another disadvantage of stick-built system is that the installation is performed outdoors where it is exposed to the weather conditions which can affect the durability of the sealant and hence the essential need to enclose the building.
A unitized curtain wall is fabricated and assembled in the factory where controlled environments ensure the durability of the panels. The installation of a unitized system includes attaching the prefab panels to the main construction of the building.
Given the shorter installation time and reduced labour costs, it is preferable to use unitized systems for assembling the panels as part of the primary construction of the building.

The transparent sandwich structure consists of two facings layers represented by thin glass panes and 17 GFRP profiles that represent the core layer. Polyurethane adhesive is mainly responsible for connecting the core layer to the facings. In addition, commonly used infills for spandrel are painted or are anodized aluminium panels filled with insulation material. Rock wool is selected to fill the cavity between the anodized aluminium panels to increase the thermal performance of the prefab curved aluminium sandwich panel.

The aluminium framing alloy that is used for the final design is 6061-T6 due to its high yield strength.
Aluminium frames have many advantages and are generally beneficial for weight and stiff ness, therefore, in this thesis the mentioned aluminium frames are chosen to support the curved sandwich structure. To attach the infills (the transparent sandwich panel and insulated aluminium panel) to the aluminium frames, a capped system is used.
A capped system physically locks the infills to the aluminium frame by means of aluminium cap profiles.

Edge spacers generally contain desiccant that absorbs moisture and prevents condensation. In this thesis I strongly suggest a specific flexible foam edge spacer that is called "Super Spacer Premium". No metals are included in this foam edge spacer, which increases the thermal efficiency of the curved sandwich panel. Moreover, a super foam spacer is 950 times more heat flow resistant in comparison to a typical aluminium spacer which means lower energy costs.

In order to o produce a curved sandwich panel with low thermal conductivity or U-value, it is necessary to use insulating materials that reduce both cooling and heating demands and hence a reduction of carbon dioxide emissions of a building. Cavity infills play a significant role in determining the total thermal resistance of the sandwich panel. There are three commonly used cavity infills: air, argon and krypton. Despite the similarity of thermal performance of krypton and argon, argon is preferred as a cavity infill for
the sandwich panel given its lower cost.

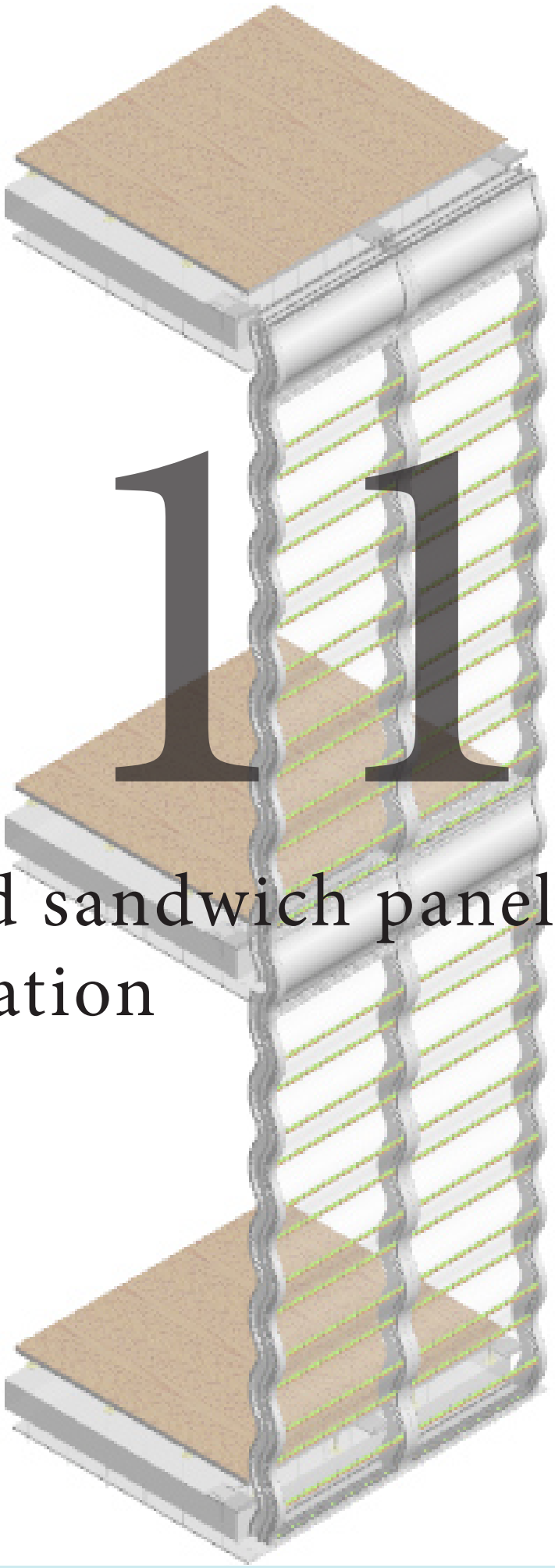

# 11

# Curved sandwich panel to Facade Installation

## 11.1 Introduction

In this chapter potential panel to façade configuration will be investigated and applied within the chosen case study.

## 11.2 Case study

The case study is an international secondary school along the Bentincklaan in Rotterdam. Rotterdam International Secondary School (RISS) is the name of the school, where it carries the name of the largest haven city in Europa. RISS has an excellent location to been seen by many train travellers, since it is established in 2003. RISS is designed by architect Jan weeda and built directly along the train railway. In addition, it is located on a distance of approximately 1 km from the central station of Rotterdam.

Figure 11.2.1: Case study: RISS (Pictures taken by author of this thesis).

The municipality of Rotterdam strived for publishing and representing the international education to the city of Rotterdam through this building, since the demand for an international education in Rotterdam increased. This building forms a composition of opaque and transparency by using façade elements as brick and glass (fig. 11.2.3).

The design is based on dividing the activities in the school by introvert space (classrooms) and extrovert space (school restaurant, staircase and theatre). The introvert space is directly linked to the brick façade while the extrovert space is represented by curtain wall façade. In 2003, a high level of sustainable measures was integrated into the building. This resulted in a nomination as one of the most sustainable buildings of the municipality of Rotterdam.

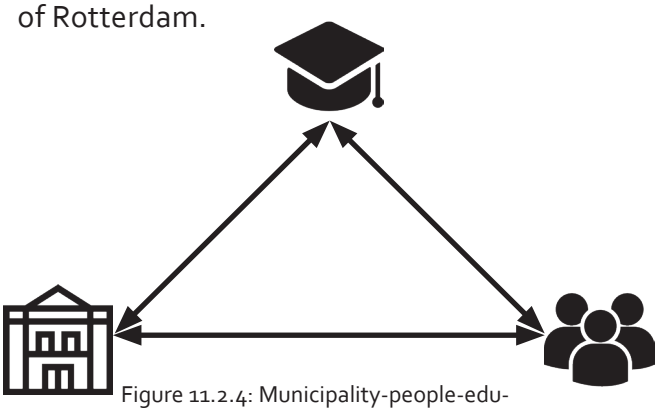

Figure 11.2.4: Municipality-people-education relationship. (Illustrations made by author of this thesis).

In order to accomplish the aim of the municipality of Rotterdam this building needs to be an eye catcher for the public by means of innovative building cladding. Therefore, substitution of the current use curtain wall by curved panel will stimulate the publishing of this building and improve its architectural value.

Figure 11.2.2: View from interior (school restaurant) to exterior (train rail ways) (Pictures taken by author of this thesis).

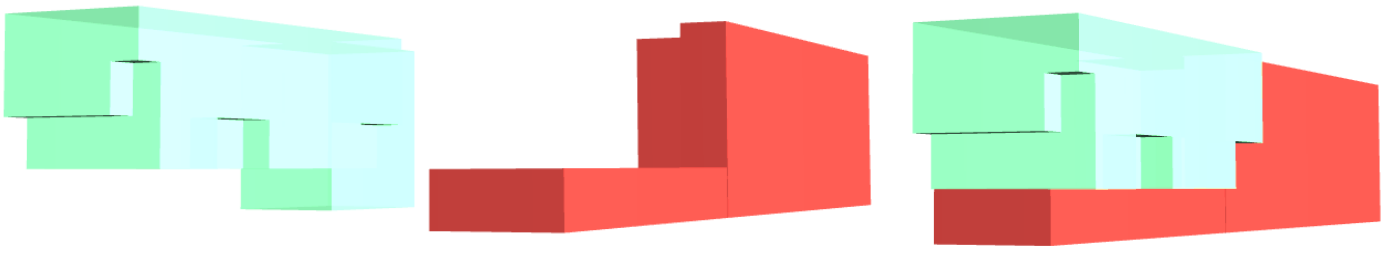

Figure 11.2.3: Composition of opaque and transparent facade cladding. (Illustrations made by author of this thesis).

## 11.3 Curved sandwich panel to facade configuration

A possible assembling method for unitized curtain wall system is attaching the prefab curved sandwich panel to the floor slab by means of mounting anchors. These anchors have a hook shape and are integrated to the mullions of the curved prefab sandwich panel. With these anchors the prefab element can be hanged on the galvanized steel brackets, which are attached to the floor. These brackets are mounted by T-bots to in the floor slab integrated anchor channel. This assembling method ensures three-dimensional adjustability (appendix 10).

When the curved prefab element is suspended to the bracket by the mounting anchors, a space is created between the floor edge and the prefab sandwich panel. This space is filled with insulating material to mainly prevent fire and sound transfer. Therefore, Rock wool is chosen to fulfil these requirements. In addition rock wool increase thermal performance between the floor slab and the curved prefab sandwich panel. Subsequently a fire-resistant aluminium plate is applied underneath the rock wool insulation to seal the construction. Silicone gaskets are crucial elements in assembling a water and air tight curtain wall façade as mentioned in section 10.2.

Finally, raised floor system and suspended ceiling are applied to achieve a rapid and easy assembling. This will be an advantage in case of replacing a damaged curved sandwich panel where an easily and rapid dissembling of the floor and ceiling system is required. Both of the raised floor and suspended ceiling are sealed by a 3M double sided tape.

The curved sandwich panel to façade configuration for unitized system is illustrated in figures 1 to 4 according to assembly construction sequence.

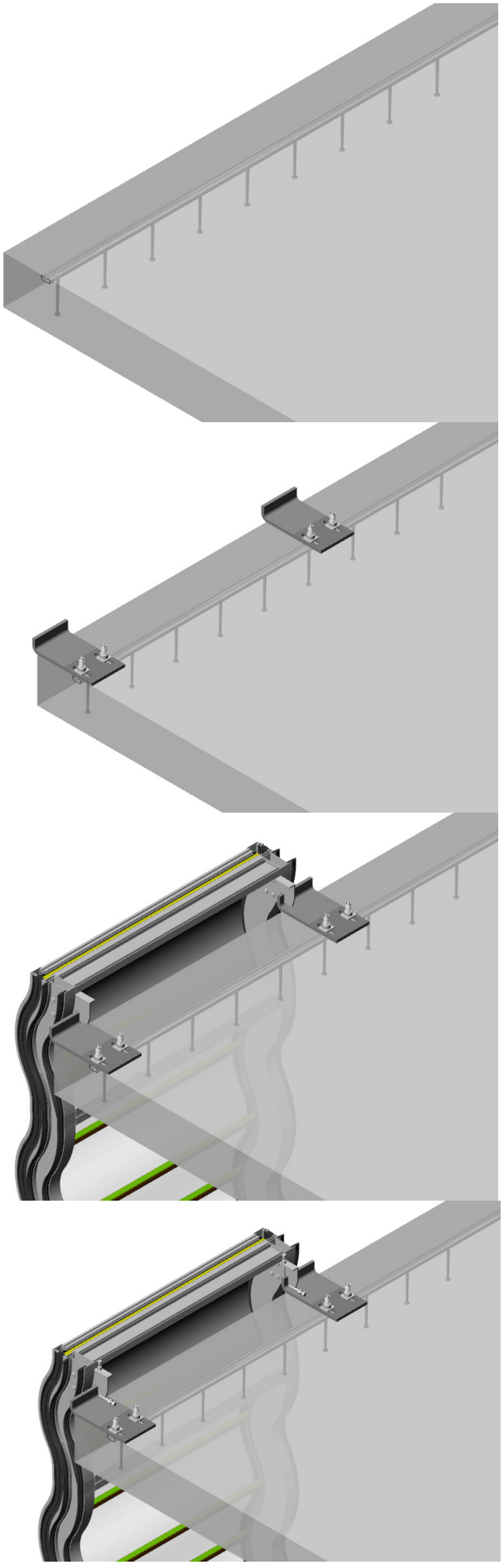

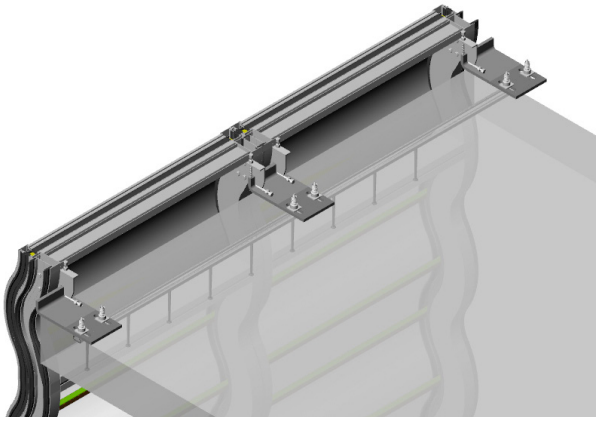

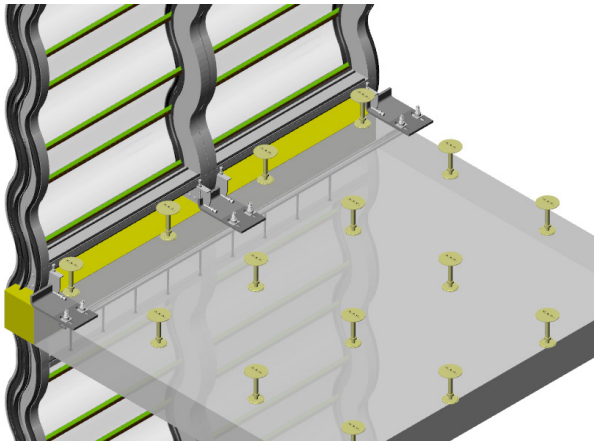

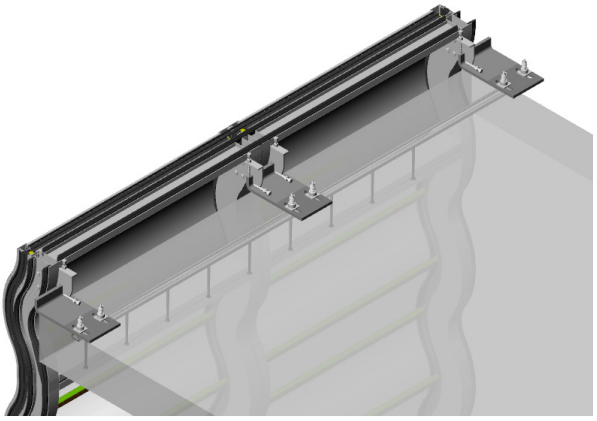

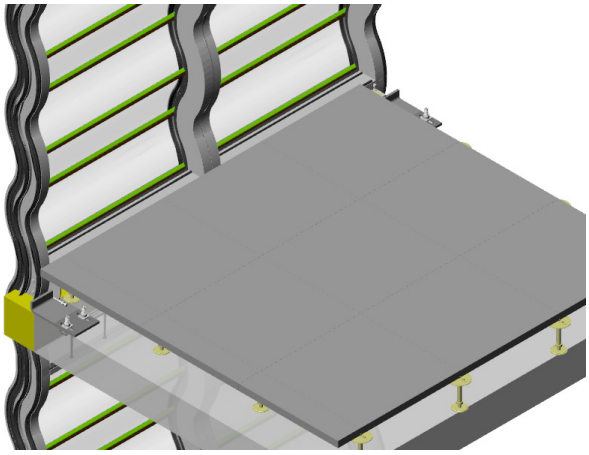

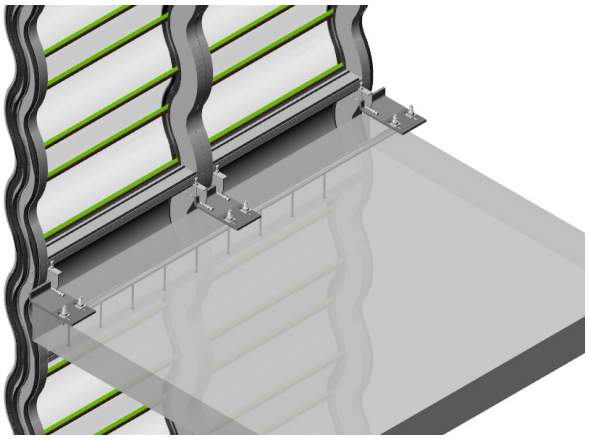

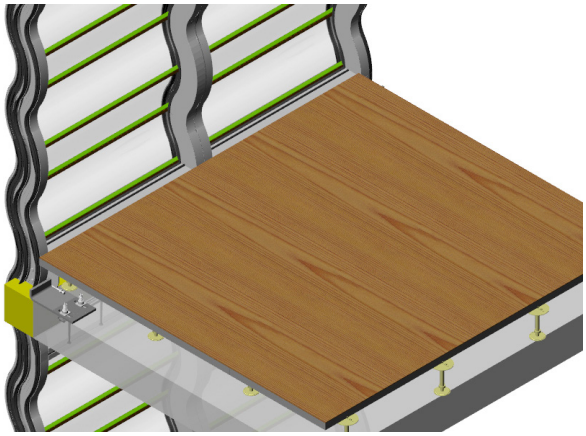

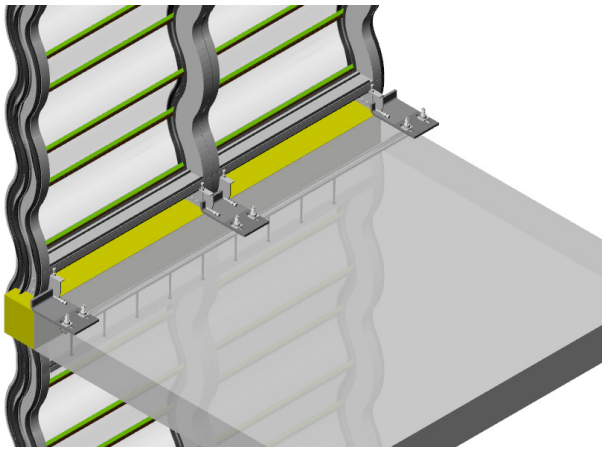

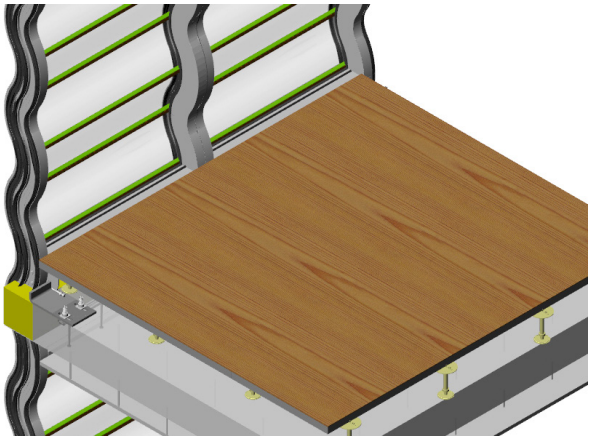

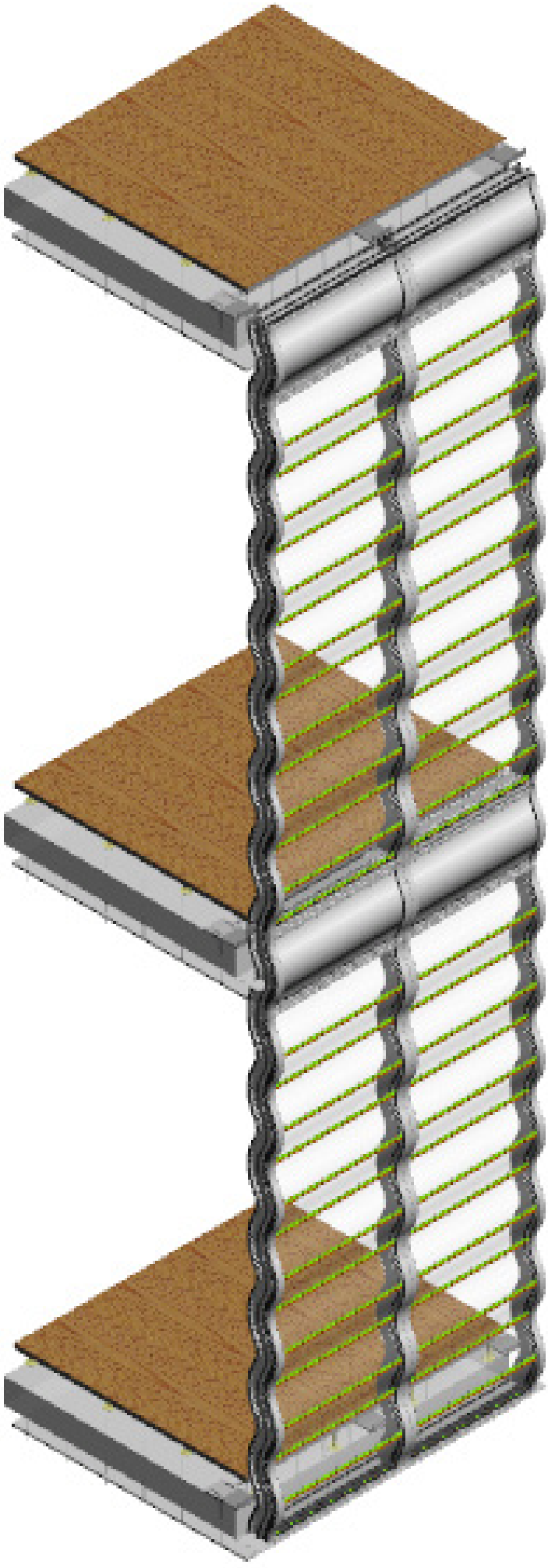

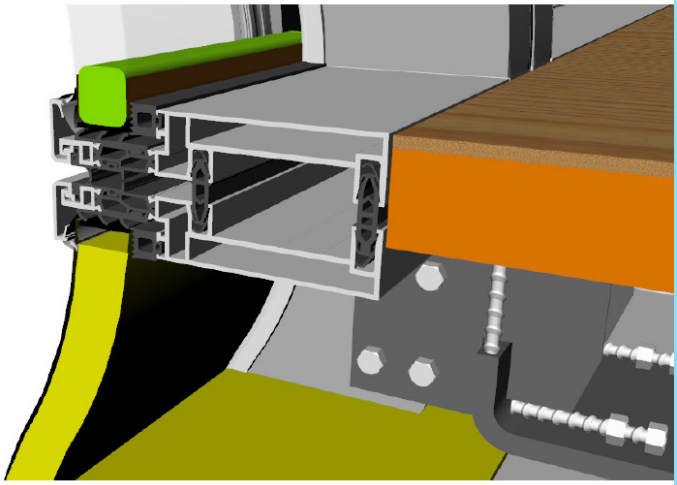

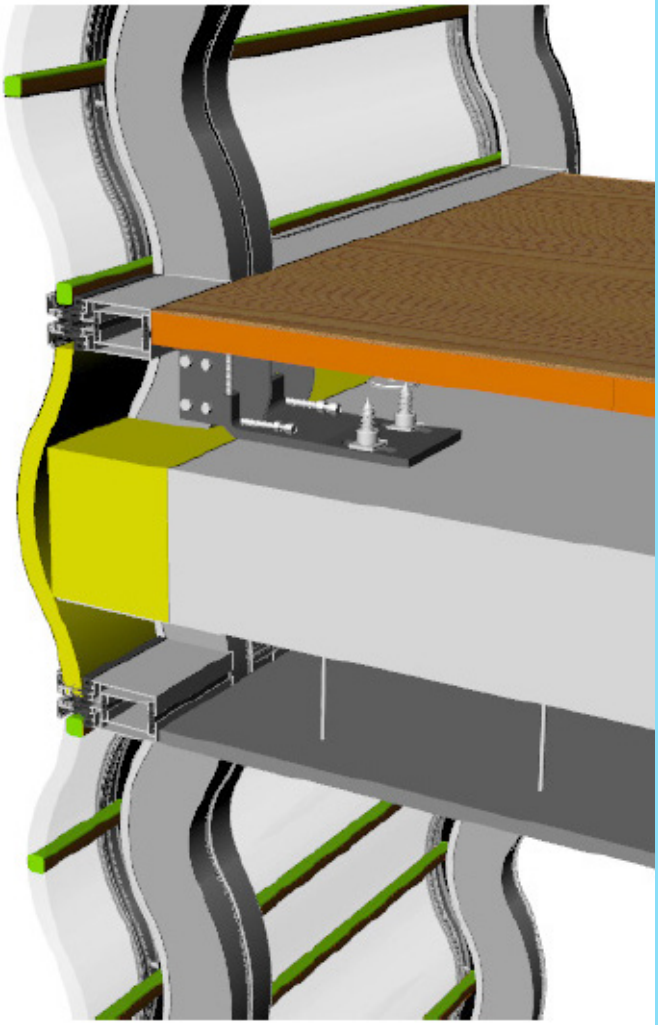

1: 40 Front view & longtindual and cross-section

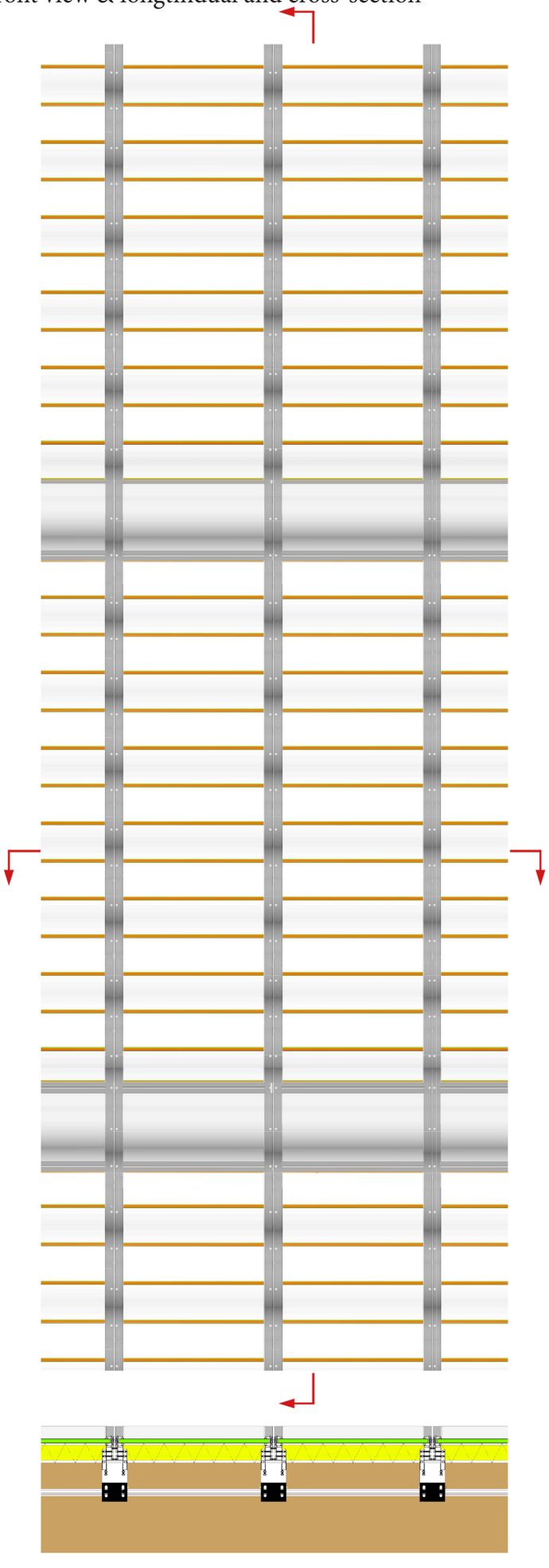

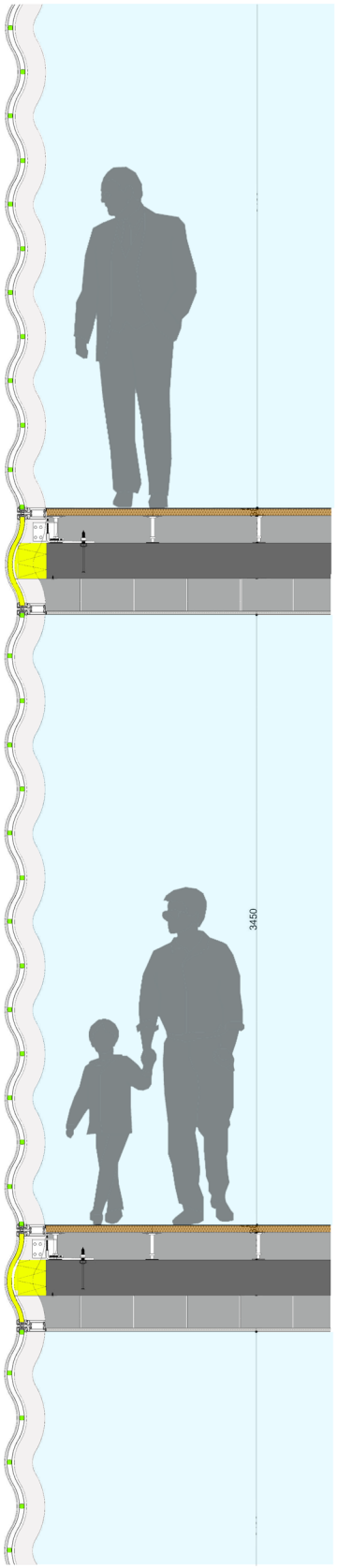

## 11.4 Sun light reflection

Glass is considered as a reflective material, where sun rays can be reflected through a curtain wall to a create a focal point on the street. The reflection of sun rays has significant influence on the adjacent street, where pedestrians experience a high level of concentrated heat from the reflected sun rays. In addition, objects will be melted and damaged due to that reflection. A good example is the "Walkie Talkie" skyscraper in London where a car partially melted by the sun reflection ( Figure). In addition, sun reflection creates glare on the façade, which blocks the appearance of the curtain wall facade ().

Figure 11.4.1: Damages caused by reflection of Walki Talki curtain wall facade .

The law of reflection is simple: the angle of incident is equal to the angle of reflection (fig 11.4.2). The shape of the façade is significant for the angle of the sun light reflection. Therefore, measuring the reflection of the sun light is important for curtain wall to avoid the accidents of the Walki Talki building. Especially in the chosen case study, where the train rails are exposed to the reflected sun rays.

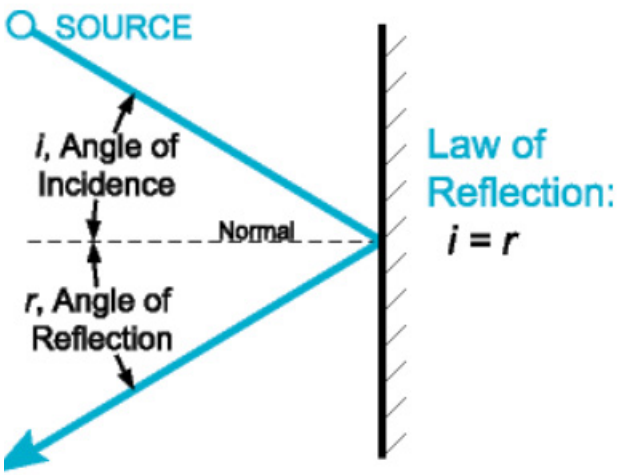


Figure 11.4.2: Reflection law.

The reflection angle on the curved façade is illustrated in figure 11.4.3 during the summer and winter seasons. The angle of reflection is determined by the angle of inclination of the sun and the normal line. During the summer season is the sun has an angle of inclination of 61.5 degrees while in the winter is much lower where it reaches 14.5 degrees. The normal line is perpendicular to the surface of the façade. The curved shape of the façade ensures diffuse sun reflection, that avoid concentrated focal point.

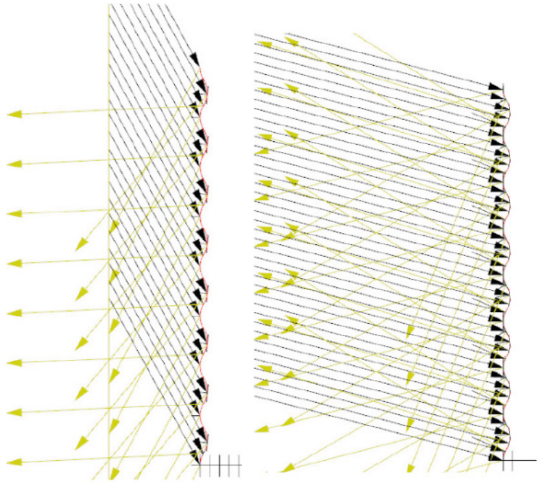

Figure 11.4.3: Sun rays reflections during summer and winter seasons by curved sandwich facade .

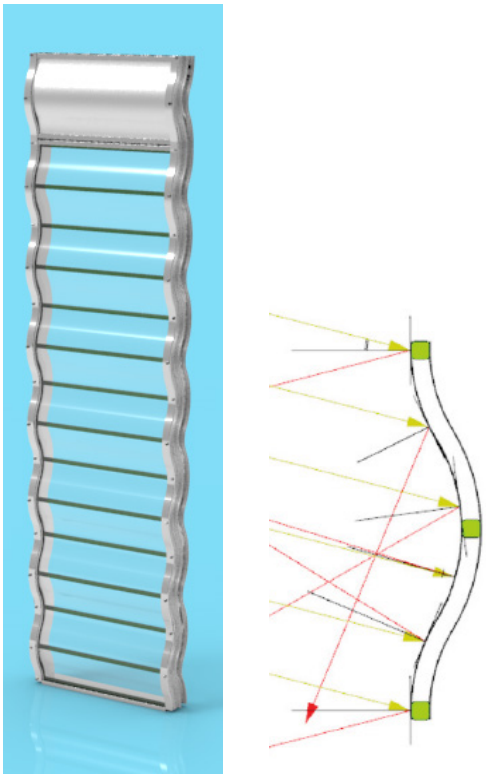

Figure 11.4.4: Glare and sun rays reflection of The curved sandwich panel made out of Thin glass and GFRP profiles.

## 11.5 Sun shading

Curtain wall is the most exposed façade types to the solar radiation, that creates an inflow of heat into the interior space of a building. To be able to control the amount of sun radiation that enters the interior space through a transparent façade and avoiding the risk of overheating, sun shading system is required. Common examples of operable sun shading unites are louvers, shutters, overhangs and exterior venetian blinds.

The design of sun shading devices can be expensive and complex, where accurately shape of sun shades require specific computer calculations and purposes. Although, designing a sun protection can be made manually with little knowledge about the mechanics of sun positions and sun path diagrams.

The created sandwich panel provides sun protection, due to the integrated GFRP profiles. These profiles are considered as opaque materials that blocks sun radiation to enter the building. More over, they create a shadow pattern on the interior floor, which change constantly according to the sun position (figure 11.4.5). At the same time, the space between the GFRP profiles is more than sufficient to have a clear visibility to the exterior space, especially when it is compared with the Twin wall GFRP panels (section 6.4).

Figure 11.4.5: Shadow pattern caused by curved cladding.

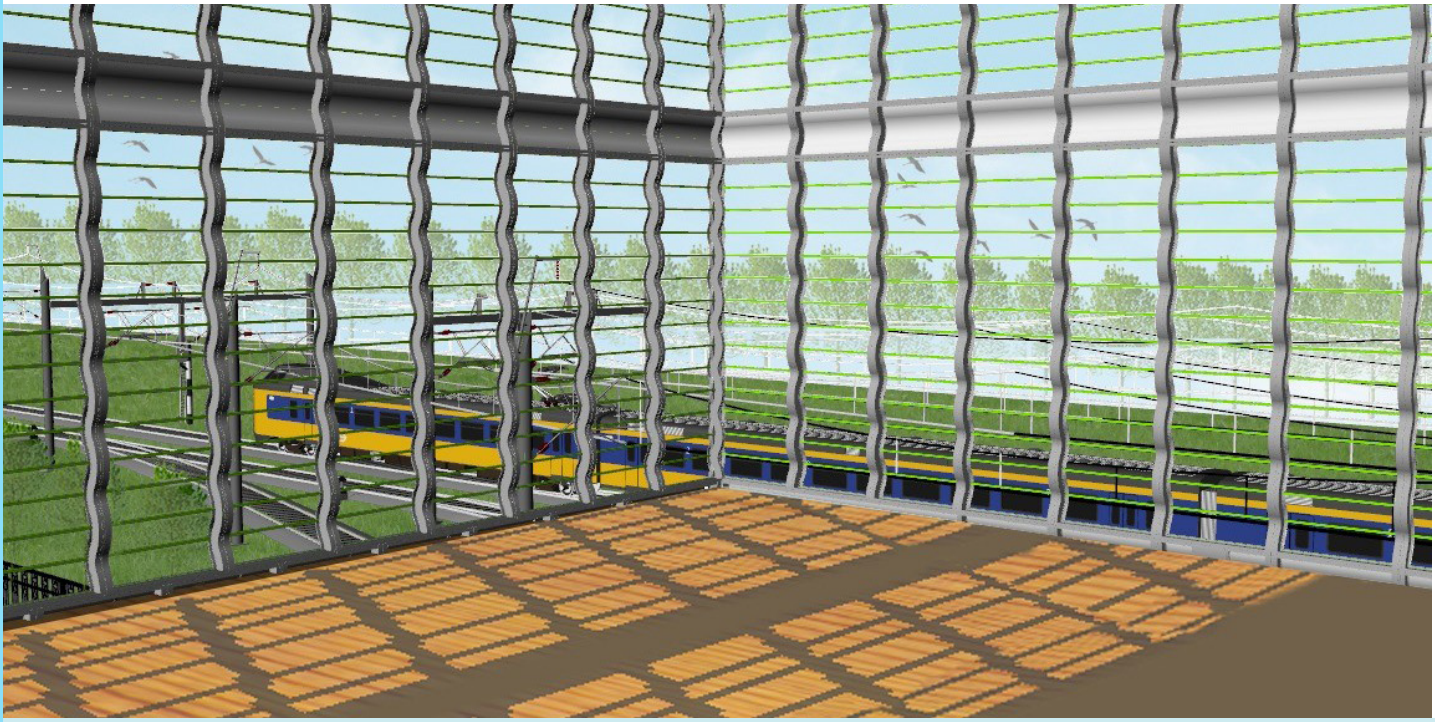

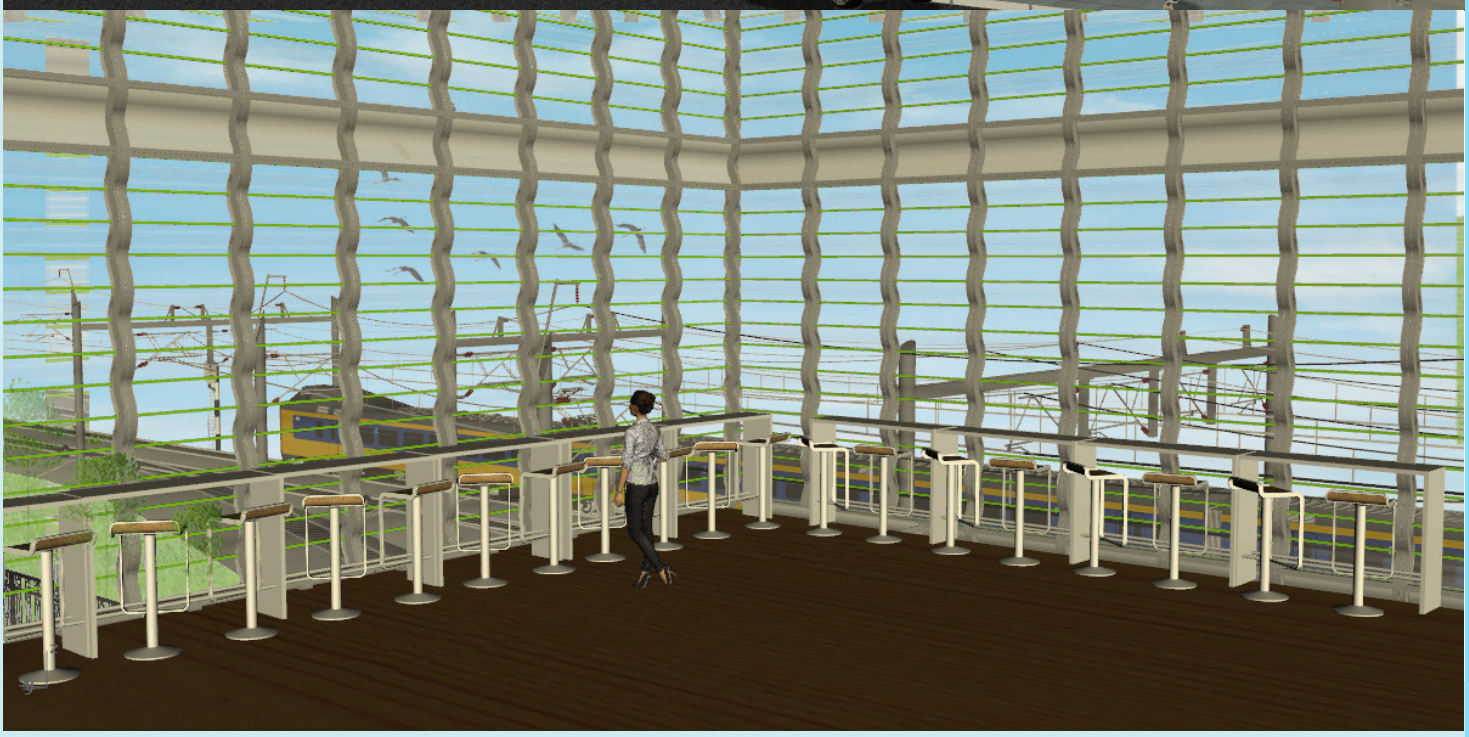

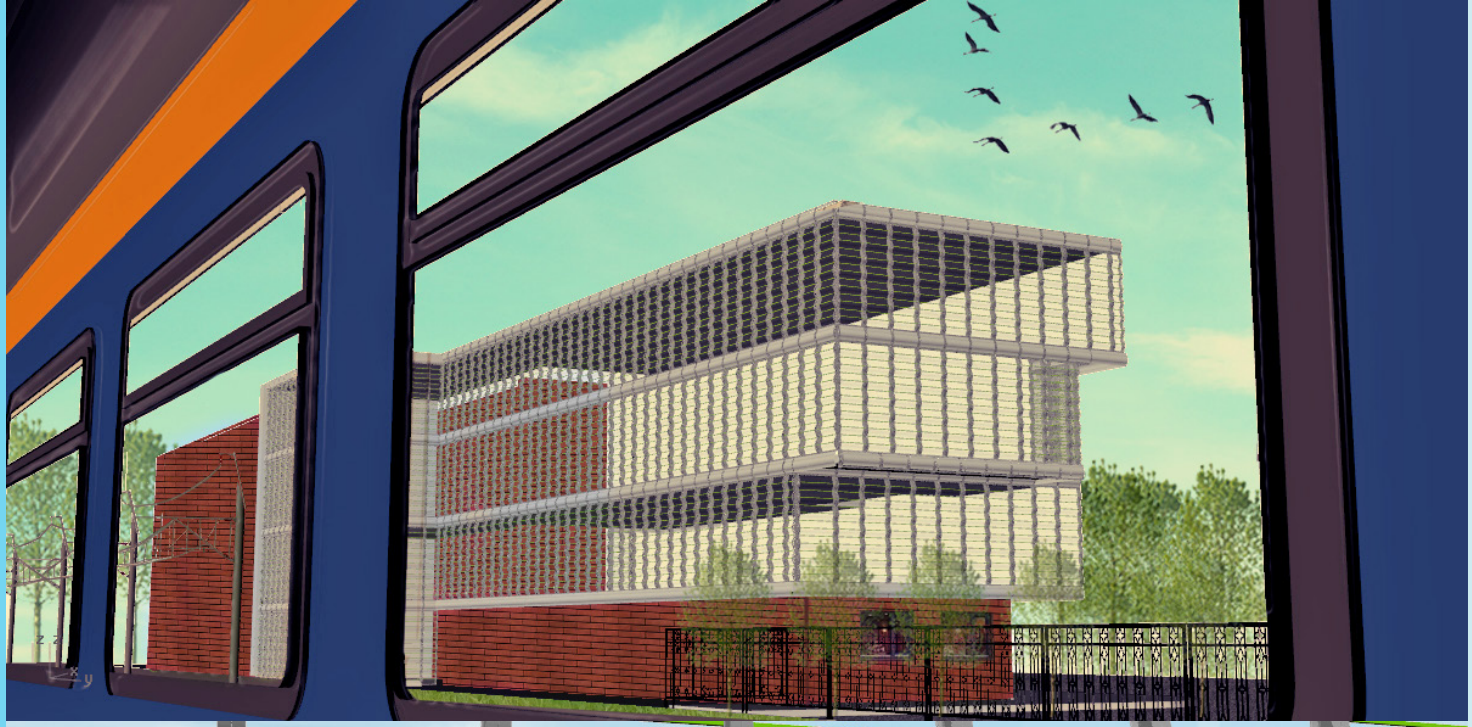

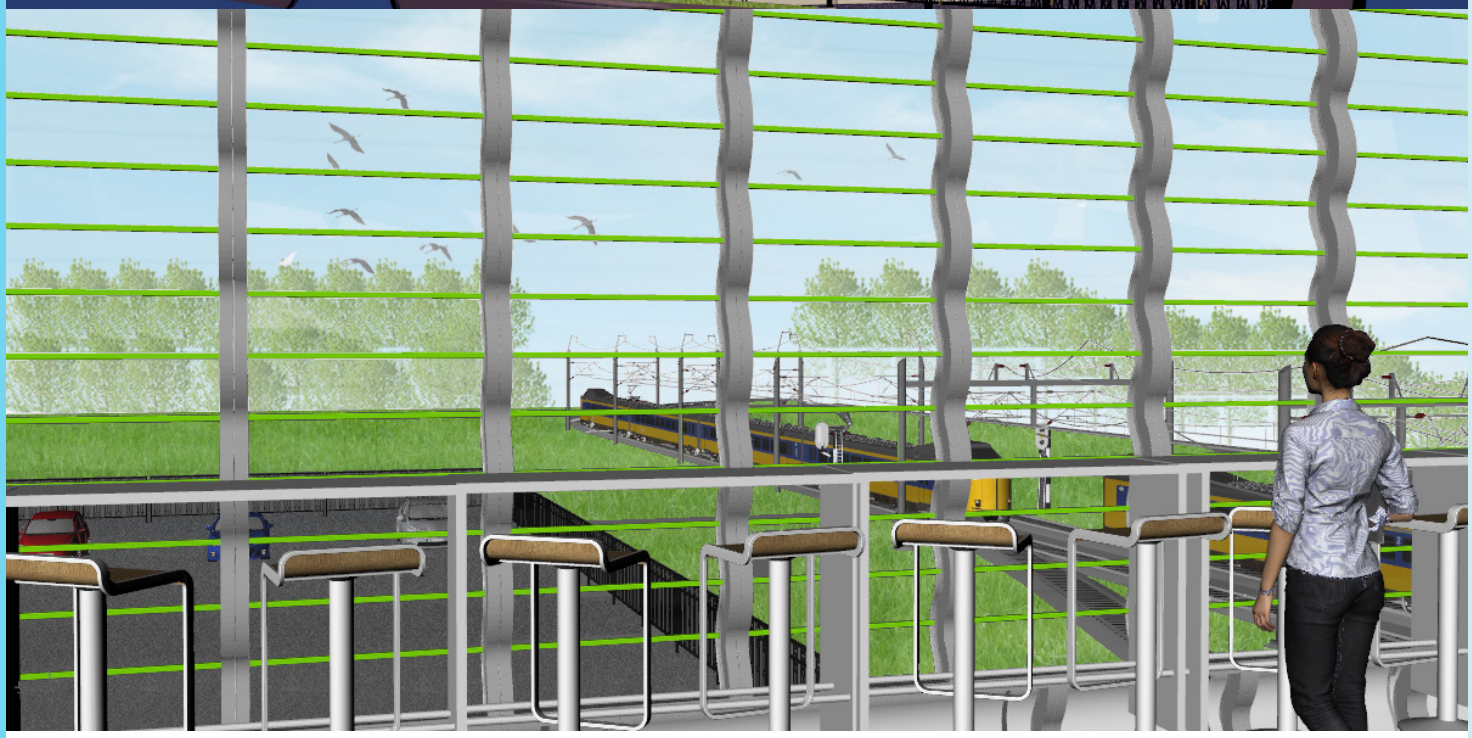

# 12

# Details

1: 5 longitudinal section

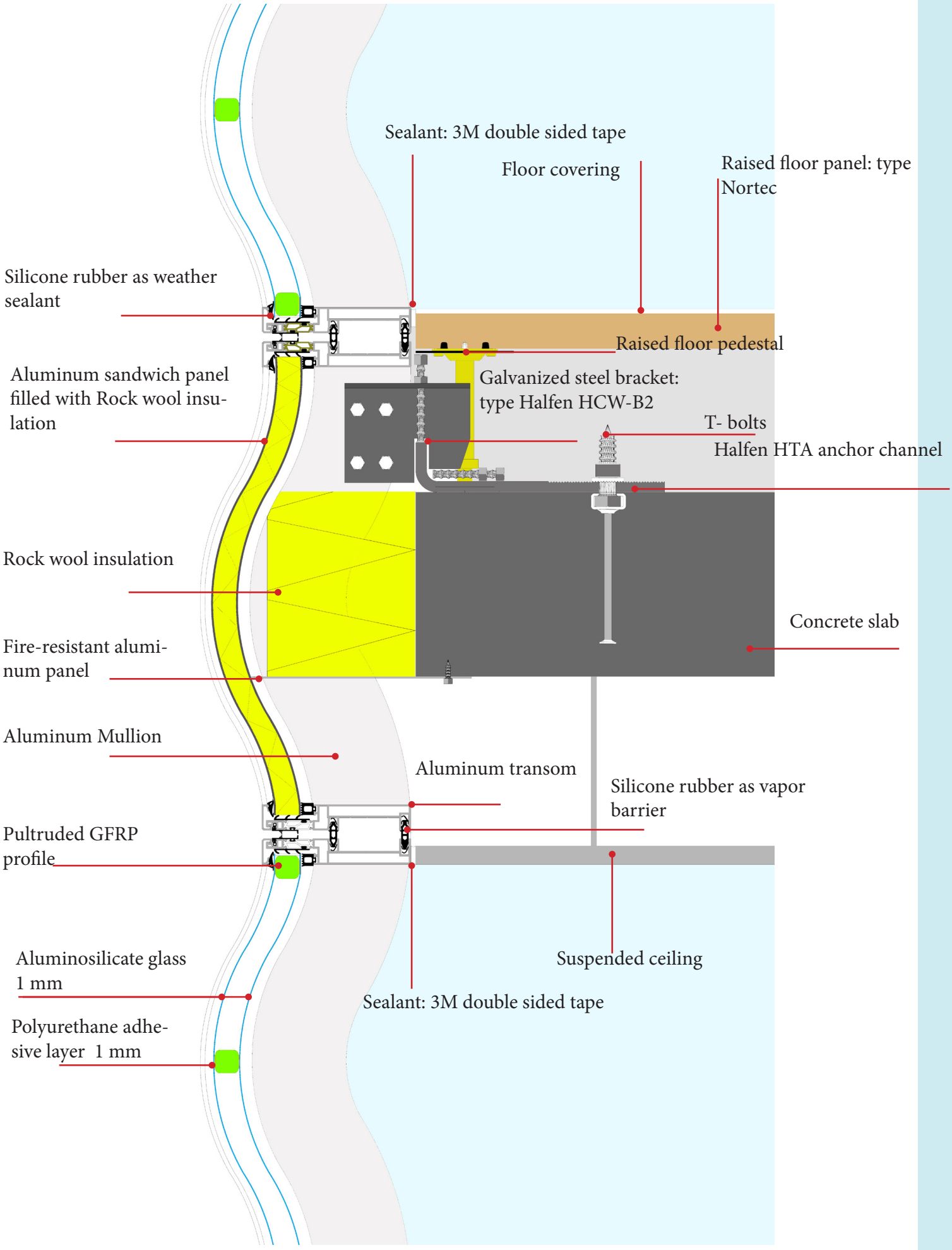

1: 10 Cross-section

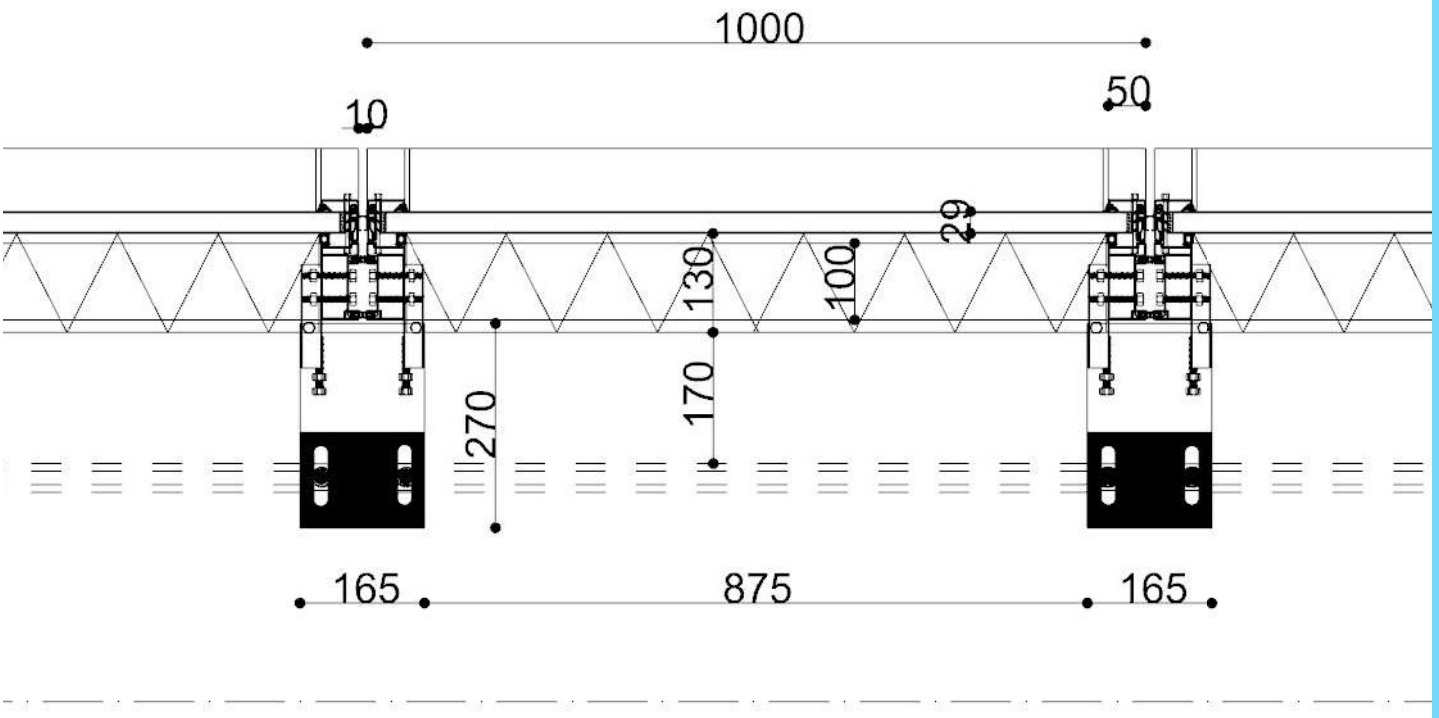

1: 2 longitudinal section

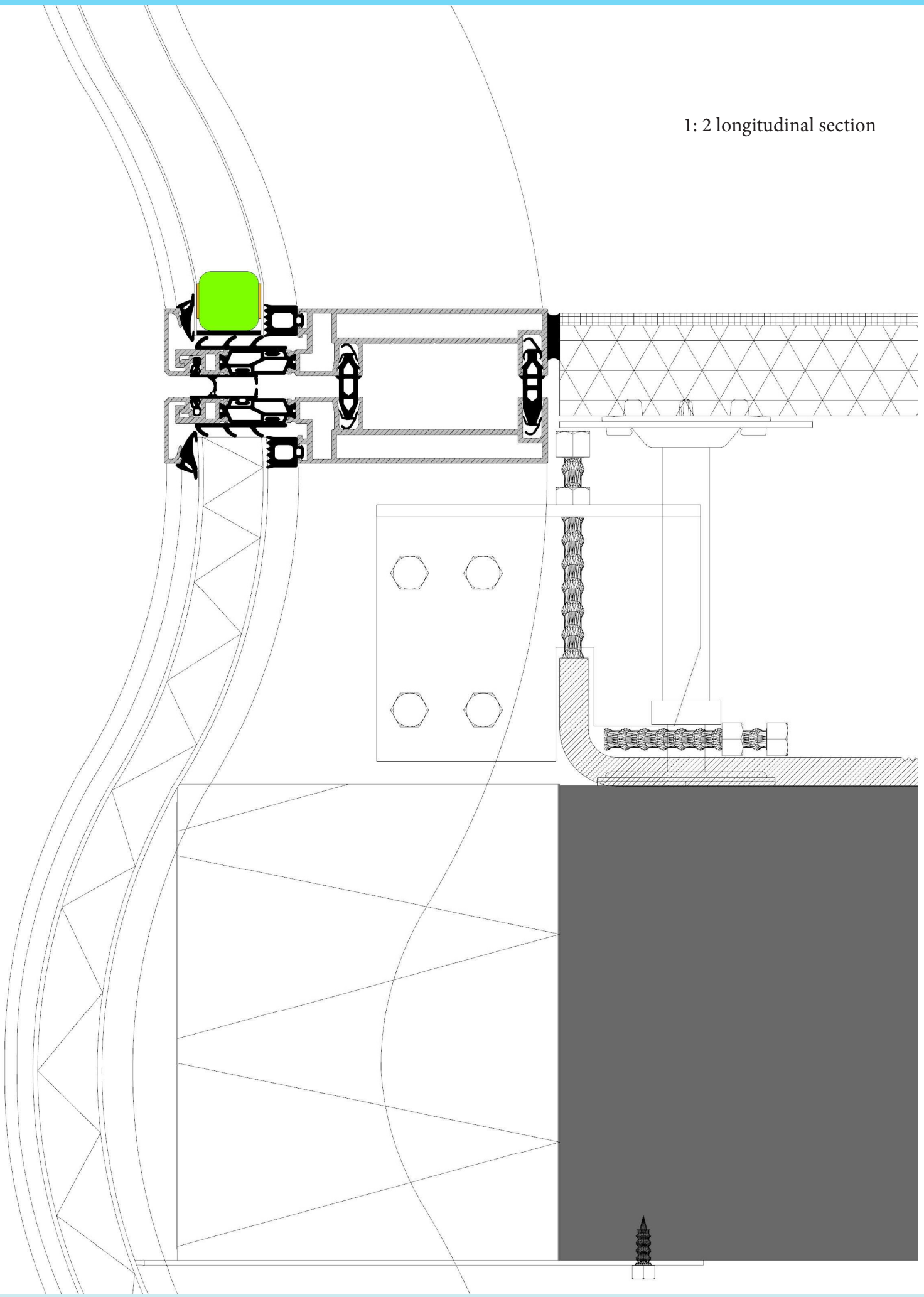

1: 1 longitudinal section

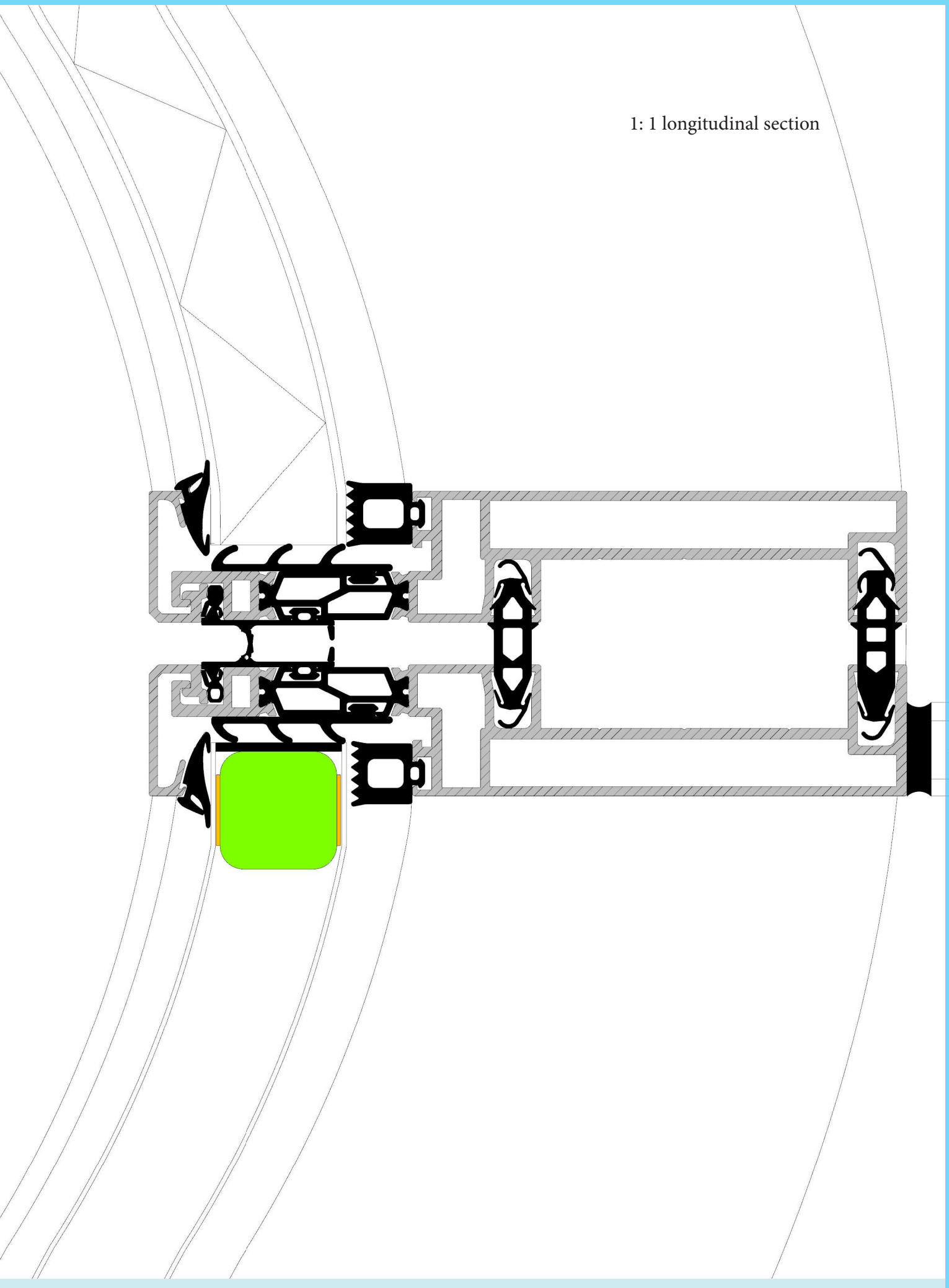

1: 2 Cross-section

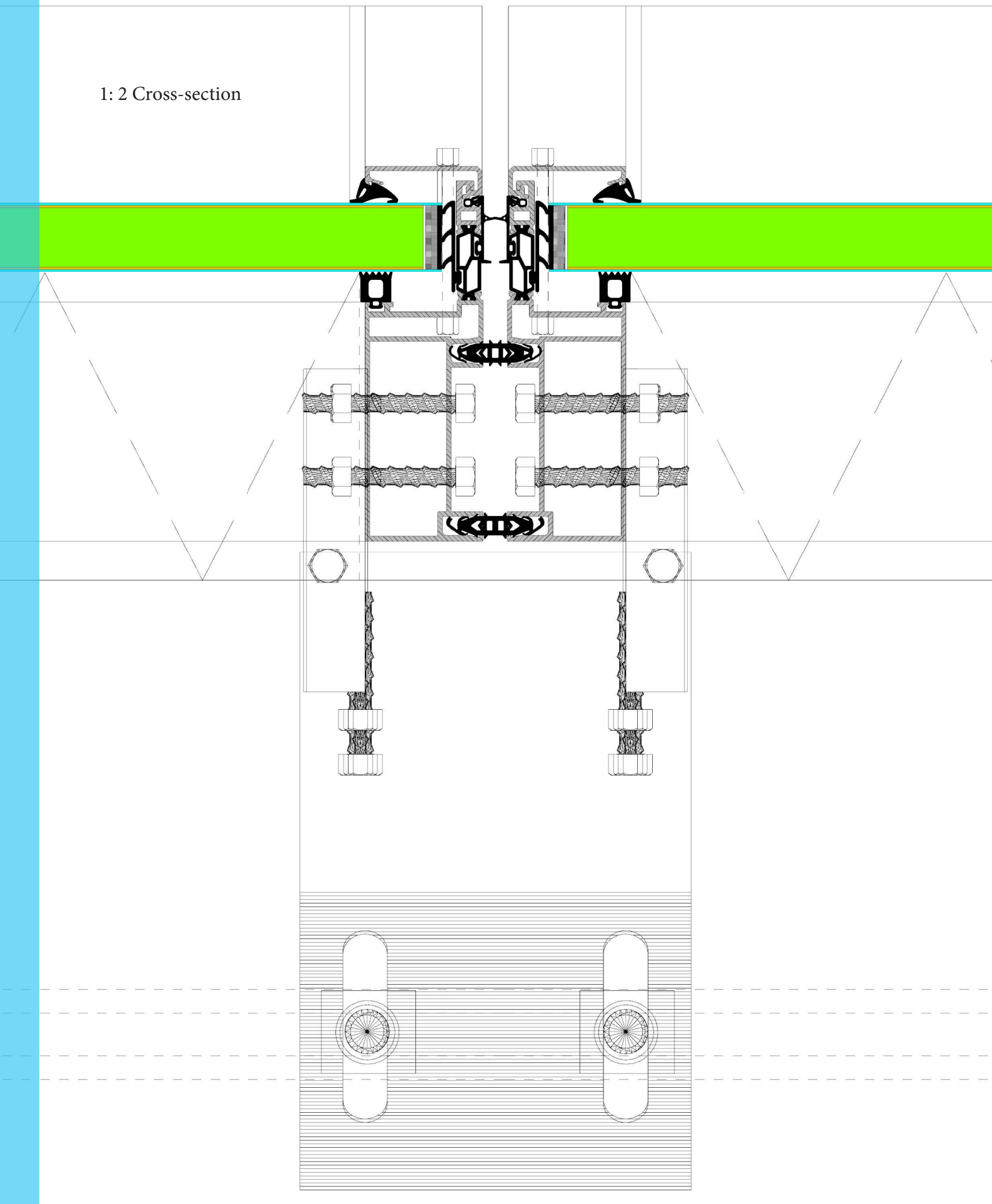

1: 1 Cross-section

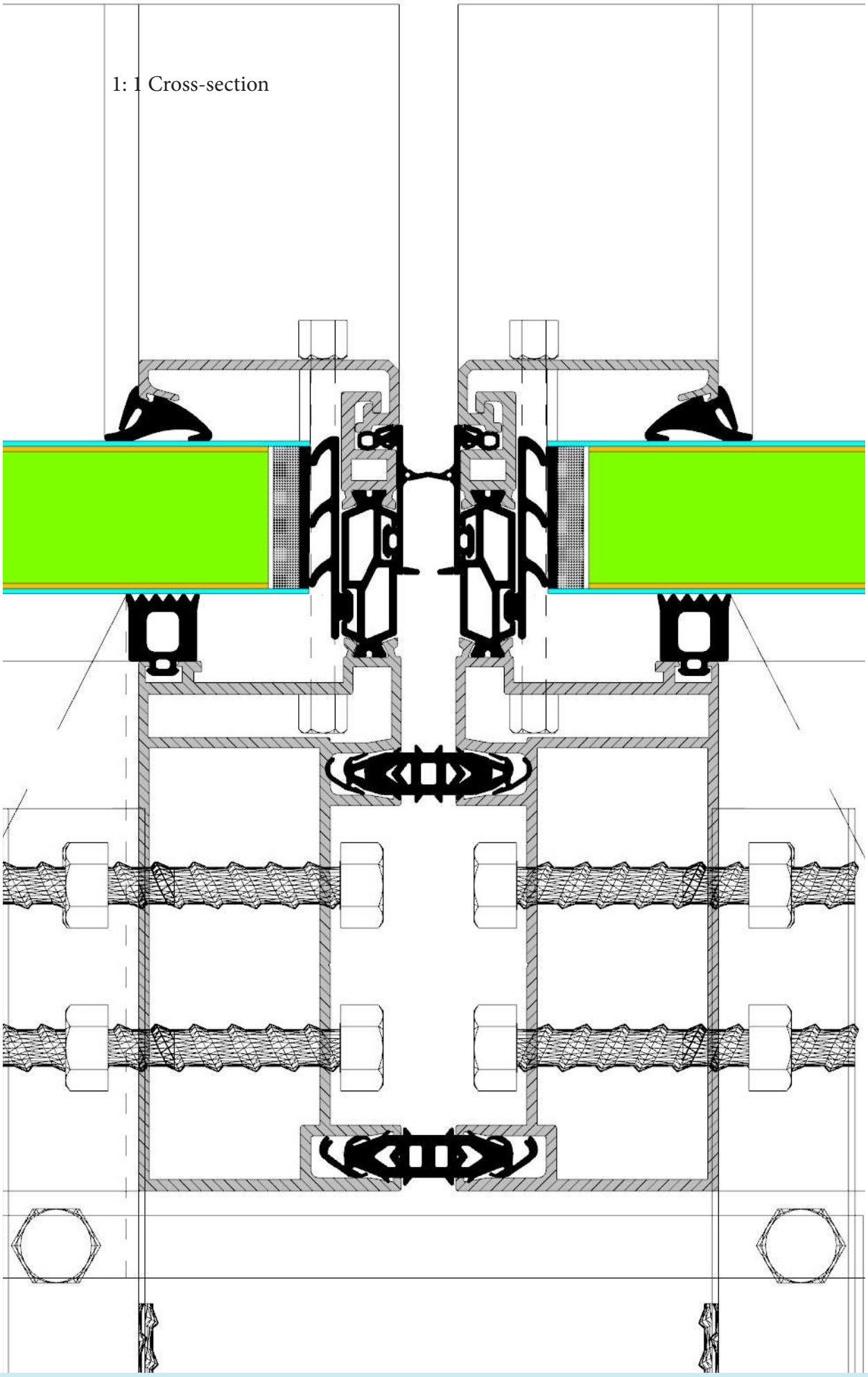

# 13

# Reflection

This chapter is created to evaluate the process of this thesis and my personal experience regarding to planning.

This thesis is based on a study of combining two relatively new materials to the built environment. This was an extraordinary challenge with multiple obstacles that delayed the process of achieving the aim of this research.

The two main obstacles in my point of view were the lack of trusted literatures about these materials and using FEM simulation to verify the assumptions regarding to thin glass.

The strategy of the desired process was difficult to follow in the first place, but with more accurate schedule and planning strategy combined with daily studies about the materials I succeeded to continue.

Also, I strongly believe that working with a FEM software increase the knowledge of a student regarding to structural design.

In general, this thesis gives a clear overview of using these materials in the built environment and I believe that it will help increasing the knowledge about these materials and how to implement them in the built environment.

# References

## Literatures:


AGC. **AGC Develops World's Thinnest Sheet Float Glass at Just 0.1 mm**. Press release. May, 2011.

ALBUS, J. ROBANUS, S. **Glass in Architecture- Future developments**. Detail magazine - english edition. March - April. 2015.

CORNING MUSEUM OF GLASS. **The long road to success: fusion drawn glass**. October 2011. Available at: http://www.cmog.org/article/long-roadsuccess-fusion-draw-glass. Retrieved in 7 May 2016.

GY, R. **Ion exchange for glass strengthening**. Materials Science and Engineering: Page 159-165. November 2007.

WELLER, B. et al. **Glass in Building**. DETAIL Practice. Book. 2009.

SCHITTICH, C. et al. **Glass construction manual**. Birkhauser Architecture, 2007.

LU, Z. OVEREND, M. **Cold Bent Glass**. University of Cambridge.

Bradt, R.C. Evans, A.G. Hasselman, D.P.H. Lange, F.F. **Fracture Mechanics of Ceramics**. Page 88-9. February 2003.

Bouyne, E. Gaume, O. **Glass Technol**. Page 300–302. 2002.

HUNDEVAD, J. **Super lightweight glass structures (a study)**. GlassCon Global. Page 324-325. 2014.

MURATA, T. YANASE,T. MIWA,S. YAMAZAKI, H. **Ultra thin glass roll for flexible AMOLED display**. Nippon Electric Glass Co. Japan.

HARTMAN D.R., GREENWOOD M.E., MILLER D.M. **High Strength Glass Fibers**. Owens-Corning, 1998.

CAMPBELL, F. C. **Structural composite materials**. ASM international. 2010.

BAGHERPOUR, S. **Fibre Reinforced Polyester Composites**. Islamic Azad University. Iran. 2012.

WURM, Jan. **Glass structures: design and construction of self-supporting skin**s. Walter de Gruyter. 2007.

Mostert, P. **Filament Winding Composite Forming in Architecture (a study)**. 2015

Albus, J. Robanus, J. **Glas in der Architektur**: Neue Entwicklungen. 2014. Available at: http://www.detail. de/artikel/glas-in-der-architektur-neue-entwicklungen-1-12954/. Retrieved in 8 May 2016.

Schneider, J. **Then glasses- A future envelope?**. TU Darmstadt.

The Pultrusion process- **How Pultrusions are manufactured.** Available at: http://www.libertypultrusions. com/pultrusion-process/. Retrieved in 5 June 2016.

The Vacuum infusion process. Available at: http://www.composites.ugent.be/home_made_composites/ organizing_your_composite_workshop.html. Retrieved in 5 June 2016.

Bels, J. Callewaert, D. Van Hulle, A. **Bouwen met glas en adhesieven**: praktische gids voor ontwerper en uitvoerder. ISBN 978 90 382 1902 8 . Universiteit Gent, Laboratorium voor Modelonderzoek. Gent.

Von Karman, Th., Stock, P., **British Patent** 235,884 (1924).

Prove Kluit, P.W.C. **The Development of In-Situ Foamed Sandwich Panels**. ISBN: 90 407 1493 2. Delft University Press. 1997.

Knippers, J. Cremers, J. Glabler, M. Lienhard, J. **Construction manual for polymers and membranes.** ISBN: 978 3 0346 0733 9. Institut fur internationale Architektur-Dokumentation GmbH & Co. KG, Munich. 2011.

Telow, K. **Translucent Cellular Polycarbonate Delivers Deign Versatility**. EXTECH/Exterior Technologies, Inc. Augustus 2012.

Herwijnen, F. van, (2008). **Warm en koud gebogen glas**.

Morris, F.A. **Curtain wall systems**. *Definition of curtain wall*. pp. 3-7. 2013.

Laufs, W. , Verboon, E. **Curtain wall systems**. *Innovative Façade Design and Products*. pp. 157-167. 2013.

McFarquhar, D.G. **Curtain wall systems.** *Materials and configurations*. Pp. 17-24. 2013.

Pfundstein, M. Rudolphi, A. Spitzner, H. ; Gellert, R. **Detail Practice**. *Insulating Materials*. Basel, Boston, Berin. 2004.

## Figures & Tables:

**Chapter 1:**

Figure 2.1.1 : Louter, P.C. **Adhesively bonded reinforced glass beams**. Faculty of Architecture. Delft University of Technology. TU Delft.

Image 1 **Chapter 3:**
http://var.glassonline.com/uploads/publications/section_news/201609/20160902061133_schott.jpg

Table 3.2.1 CES Edupack 2016. **Alumino silicate – 1720**. 2015.

Figure 3.3.1: Neugebauer, J. **A Movable Canopy.** 2015

Figure 3.3.2: HUNDEVAD, J. **Super lightweight glass structures (a study)**. GlassCon Global. Page 324-325. 2014.

Figure 3.4.1: WURM, Jan. **Glass structures: design and construction of self-supporting skin**s. Walter de Gruyter. 2007.

Figure 3.4.2: HUNDEVAD, J. **Super lightweight glass structures (a study)**. GlassCon Global. Page 324-325. 2014.

Figure 3.6.1: MURATA, T. YANASE,T. MIWA,S. YAMAZAKI, H. **Ultra thin glass roll for flexible AMOLED display**. Nippon Electric Glass Co. Japan.

Image **Chapter 4:**
http://www.dynasylan.com/product/dynasylan/ImageGallery/Glasfaser%20Detail.jpg?RenditionID=31

Table 4.2.1: HARTMAN D.R., GREENWOOD M.E., MILLER D.M. **High Strength Glass Fibers**. Owens-Corning, 1998.

Table 4.2.2: CAMPBELL, F. C. **Structural composite materials**. ASM international. 2010.

Chart 4.3.1 & Chart 4.3.2 : BAGHERPOUR, S. **Fibre Reinforced Polyester Composites**. Islamic Azad University. Iran. 2012.

Figure 4.1.1: Pultrusion process: - **How Pultrusions are manufactured.** Available at: http://www.libertypultrusions. com/pultrusion-process/. Retrieved in 5 June 2016.

Figure 4.1.2: The Vacuum infusion process. Available at: http://www.composites.ugent.be/home_made_composites/organizing_your_composite_workshop.html. Retrieved in 5 June 2016.

Image **Chapter 5**: https://www.antala.uk/wp-content/uploads/2017/09/permabond-glass-bonding.png

Figure 5.1.1: Goss, B**. Practical Guide to Adhesive Bonding of Small Engineering Plastic and Rubber Parts.** Smithers Rapra Technology.2010.

Figure 5.3.1: Bels, J. Callewaert, D. Van Hulle, A. **Bouwen met glas en adhesieven**: praktische gids voor ontwerper en uitvoerder. ISBN 978 90 382 1902 8 . Universiteit Gent, Laboratorium voor Modelonderzoek. Gent.

Figure 5.3.1: Bels, J. Callewaert, D. Van Hulle, A. **Bouwen met glas en adhesieven**: praktische gids voor ontwerper en uitvoerder. ISBN 978 90 382 1902 8 . Universiteit Gent, Laboratorium voor Modelonderzoek. Gent.

Table 5.5.1: Matweb. Material Property Data. Available at: http://www.matweb.com/. . Retrieved in 7 June 2016.

**Image Chapter 6 :**
https://www.plasticsportal.net/wa/plasticsEU~bg_BG/function/conversions:/publish/common/images/news_images/2011/11_423_large.jpg?doc_lang=en_GB'

Figures 6.2.1 & 6.2.2 : Fradelou, G**. Research on the development on a glass fiber reinforced polyester (GRP) façade with integrated operable GRP window frames a study**. TU Delft University. 2013.

Figures 6.2.3 - 6.3.1.1: Knippers, J. Cremers, J. Glabler, M. Lienhard, J. **Construction manual for polymers and membranes.** ISBN: 978 3 0346 0733 9. Institut fur internationale Architektur- Dokumentation GmbH & Co. KG, Munich. 2011.

Figure 6.3.1.3: Telow, K. **Translucent Cellular Polycarbonate Delivers Deign Versatility**. EXTECH/Exterior Technologies, Inc. Augustus 2012.

Figure 6.3.1.3: Polycarbonate Police shield and light transmission. Available at: http://www.iplasticsupply.com/) (http://www.archdaily.com/9218/hq-13-parisian-subway-line-atelier-phileas/. Retrieved in 5 June 2017.

Figure 6.3.1.5: Available at: www. Rodeca.de/?L=1 . Retrieved in 5 June 2017.

Tables 6.3.1.1 - 6.3.1.2: Telow, K. **Translucent Cellular Polycarbonate Delivers Deign Versatility**. EXTECH/Exterior Technologies, Inc. Augustus 2012.

Figures 6.3.2.1 – 6.3.2.8: Knippers, J. Cremers, J. Glabler, M. Lienhard, J. **Construction manual for polymers and membranes.** ISBN: 978 3 0346 0733 9. Institut fur internationale Architektur- Dokumentation GmbH & Co. KG, Munich. 2011.

**Chapter 10:**

Figure 10.2.1: Watts,A. **Modern construction handbook.** 2001.

Figure 10.4.1 : Hartung glass industries. **HGI super spacer Brochure**. Edgetech. www. Hartung-glass.com. Retrieved in 23 August 2017.

Table: 10.5.1: AGC Glass Europe**. Glass configurator**. https://www.yourglass.com/configurator/nl/nl/toolbox/configurator/main.html. Retrieved in 19 september 2017.

**Chapter 11:**

Figure : 11.4.1 Mailonline, No more Walkie Scorchie! London skyscraper which melted cars by reflecting sunlight is fitted with shading. http://www.dailymail.co.uk/news/article-2786723/London-skyscraper-Walkie-Talkie-melted-cars-reflecting-sunlight-fitted-shading.html. Retrieved 20 November 2017.

Figure: 11.4.2: Ryer, A. **Light Measurement Handbook**. *How Light Behaves: Reflection*. 2000. http://www.dfisica.ubi.pt/~hgil/Fotometria/HandBook/ch03.html. Retrieved 01 November 2017.

**Chapter 9:**

Figures 9.4.1 – 9.4.3 : MasterBond : Adhesives | Sealants| Coatings. Available at: https:// www.masterbond.com/properties/high-shear-strength-adhesives . Retrieved 12.12.2017.

Appendix 1

# Leoflex Alumino-Silicate Glass

AGC

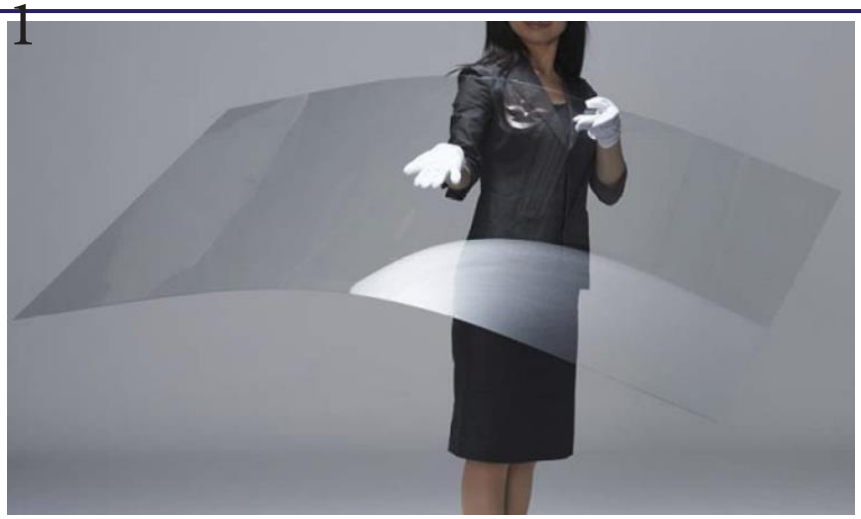

## Transmittance (Leoflex 0.85t, Solite 3.2t)

AGC

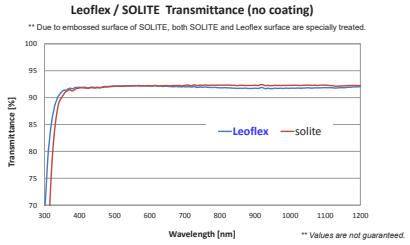


Leoflex shows the same transmittance as SOLITE.

AGC confidential

## Chemical vs Thermal Tempering

AGC

(Thermal tempering : Conventional technique for PV module glass)

| | Thermally tempered | Leoflex (Chemically tempered) | Leoflex features |
|---|---|---|---|
| Minimum thickness limit | 3.2 mmt | 0.55mmt | Light weight |
| Mechanical strength (Compressive Marginal stress) | 80 MPa | 260 MPa | Resistance to bending |
| Ion concentration at glass surface | $Na^+$ rich ($Na_2O$ >10 wt.%) | less $Na^+$ ($Na_2O$ < 3 wt.%) $K^+$ rich | Chemically stable |

** Values are not guaranteed.

<Image of thermally tempered glass>

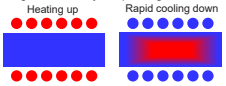


Rapid cooling glass after heating up beyond its softening point creates compressive stress at glass surface. There is no ion exchange at glass surface.

AGC confidential

## Surface Compressive Stress Strength

AGC

Breaking stress are compared by Ring on Ring measurement method

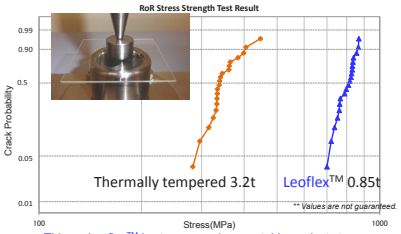


Thinner Leoflex™ is stronger and more stable against stress compared to thermally tempered glass.
Appropriate module design is required because Leoflex is flexible.

AGC confidential

## Chemical Stability against Weathering

AGC

Leoflex seldom whitened after accelerated weathering test.

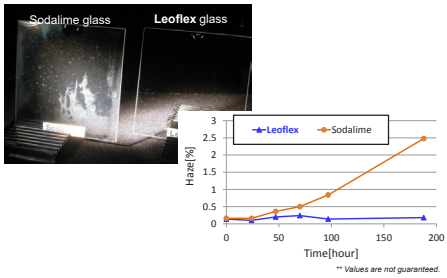


AGC confidential

## Scratch Resistance

AGC

Scratch mark is made by scratching intensity tester HEIDON.

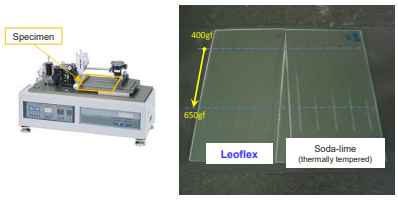


** Values are not guaranteed.

AGC confidential

## Leoflex Features

AGC

- Lightweight
- Impact resistant
- Scratch resistant
- Flexible
- Chemically stable
- Weather resistant
- Optically Clear

- Million of m2 already sold for electronics, solar, building & industrial
- Glass currently produced and processed in Asia
- Working on having local supply chain in US and EU (2016-17)

AGC confidential

## Properties comparison (Summary)

AGC

| | Leoflex (0.85mm) | Thermally tempered (3.2mm) |
|---|---|---|
| **MECHANICAL CHARACTERISTICS** | | |
| Strength / Marginal stress 短期許容応力 (MPa) | 260 | 80 |
| Young modulus ヤング率 (GPa) | 74 | 70 |
| Poisson ratio ポアッソン比 | 0.23 | 0.2 |
| Density 密度 (g/cm³) | 2.48 | 2.5 |
| Vickers Hardness ビッカース硬度 | 673 | 527 |
| **OPTICAL CHARACTERISTICS** | | |
| Energy Transmission 日射透過率 (%) | 91.6 | 91.1 |
| **THERMAL CHARACTERISTICS** | | |
| Expansion coefficient 線膨張係数 ($10^{-6}$ 1/K) | 9.8 | 9 |
| Strain point 歪点 (℃) | 556 | 500 |

** Values are not guaranteed.

AGC confidential

## Key Properties

AGC

- Alumino-silicate glass
- Thicknesses:
  - 0.55 to 1.3 mmt
- Can be chemically strengthened (CS)
  - DOL 15 – 40 um
  - Compressive Stress – 550 to 850 MPa +
- Large sheet size
  - Up to 2070mm X 1650mm
- Bendable after chemical strengthening
  - Between 100mm and 300mm bending radius

AGC confidential

# Specialty Glass Materials
# Products & Specifications 11/15

## Corning® Gorilla® Glass

Is an environmentally friendly alkali-aluminosilcate thin sheet glass. Its superior composition allows a deeper layer of chemical strengthening than is possible with most other chemically strengthened glasses, making it durable and damage resistant.

## Benefits:

- Glass designed for a high degree of chemical strengthening
  - High compression
  - Deep compression layer
- High retained strength after use
- High resistance to scratch damage
- Pristine surface quality


## Applications:

- Ideal protective cover for electronic displays in:
  - Handheld devices and instrumentation
  - Laptops and tablet computer screens
  - Mobile devices including smart phones
- Touchscreen devices
- Optical components
- High strength glass articles

## Dimensions:

- Available thicknesses 0.55 mm - 2.0 mm
- Non-standard sizes may also be available upon request
- Available in Gen 5 - 49.21 x 35.43" (1250 x 900mm) sheets

## Viscosity:

| | |
|---|---|
| Softening Point (107.6 poises) | 852˚C |
| Annealing Point (1013.2poises) | 613˚C |
| Strain Point (1014.7 poises) | 563˚C |

## Properties:

| | |
|---|---|
| Density 2 | .44 g/cm$^3$ |
| Young.s Modulus | 71.7 GPa |
| Poisson.s Ratio | 0.21 |
| Shear Modulus | 29.7 GPa |
| Vickers Hardness (200 g load) | |
| Un-strengthened | 625 kgf/mm$^2$ |
| Strengthened | 674 kgf/mm$^2$ |
| Fracture Toughness | 0.7 MPa m0.5 |
| Coefficient of Expansion (0 ˚C - 300 ˚C) | 84.5 x 10-7/˚C |

## Chemical Strengthening:

| | |
|---|---|
| Compressive Stress | Capable ≥800 MPa |
| Depth of Layer | Capable ≥40µm |

## Optical:

- Refractive Index (633nm)

| | |
|---|---|
| Core Glass | 1.5094 |
| Compression layer | 1.5116 |

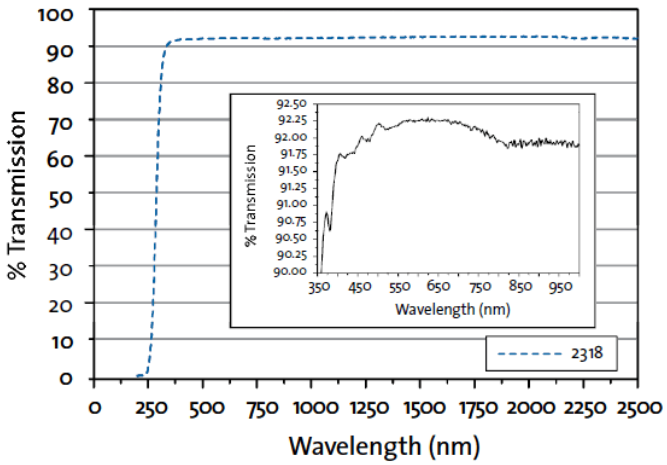


## Chemical Durability:

Durability is measured via weight loss per surface area after immersion. Values are highly dependent upon actual testing conditions. Data is reported for Code 2318 glass. Unless otherwise noted, concentrations refer to weight percent.

| Reagent | Time | Temperature (C) | Weight Loss (mg/cm2) |
|---|---|---|---|
| HCl - 5% | 24 hrs | 95 | 0.04 |
| NH4F:HF - 10% | 20 min | 20 | 3.14 |
| HF - 10% | 20 min | 20 | 11.96 |
| NaOH - 5% | 6 hrs | 95 | 1.10 |

## Corning Gorilla Glass *(cont.)*

### Electrical: Characteristics:

| Frequency (MHz) | Dielectric Constant | Loss Tangent |
|---|---|---|
| 54 | 7.38 | 0.013 |
| 490 | 7.26 | 0.013 |
| 912 | 7.30 | 0.014 |
| 1977 | 7.22 | 0.015 |
| 2986 | 7.19 | 0.016 |

### Has Greater Damage Resistance:

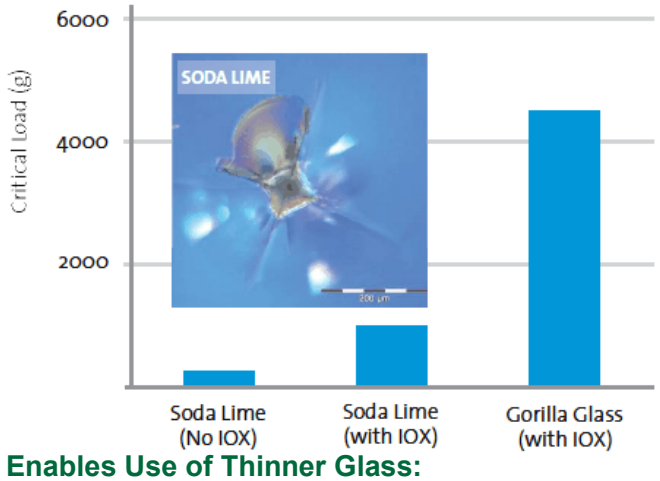


### Enables Use of Thinner Glass:

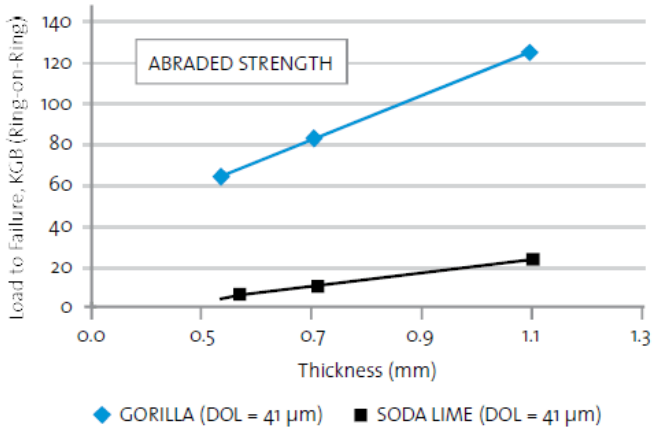


Devices benefit from a greater retained strength.

### Has Greater Design Strength:

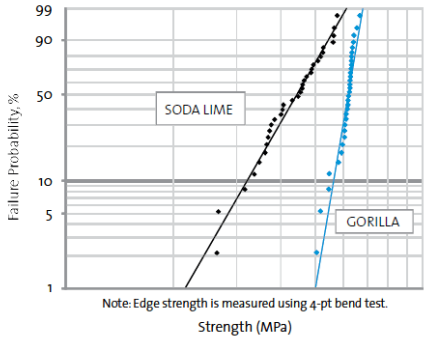


Corning Gorilla Glass exhibits tighter strength distribution.

### Greater Retained Strength:

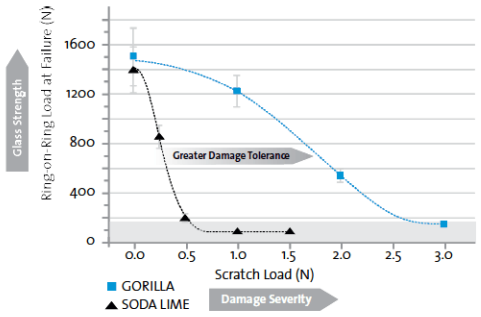


There is less strength degradation after scratching.

### Scratches are Less Visible:

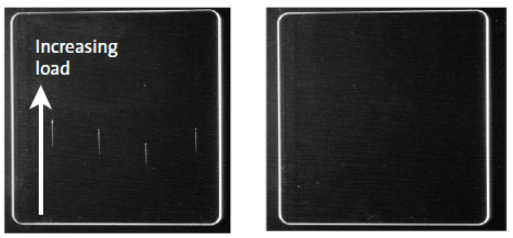


***Ion-Exchanged Soda Lime Silicate***
*8 mm scratches made with load ramped from 20 g to 100 g*

***Ion-Exchanged Corning Gorilla Glass***
*Scratches on Corning Gorilla Glass are visible only under a microscope*

***Corning Gorilla Glass suppresses damage zone and lateral cracking that make scratches less visible.***

# Specialty Glass Materials
# Products & Specifications 11/15

## SCHOTT Xensation™

SCHOTT Xensation™ is a high-quality alumino-silicate glass with outstanding resistance to breakage and scratches for all cover and touch applications, including capacitive, resistive, optical, and acoustic touch technologies.

## Key-Benefits of Xensation™ Cover:

- SCHOTT's unique micro-float manufacturing process gives the Xensation™ Cover alumino-silicate glass its excellent sheet quality.
- Impressively high and very stable Compressive Stress (CS) and Depth of Layer (DoL), ensure that Xensation™ Cover offers outstanding strength.

## Thermal Properties:

| | |
|---|---|
| Thermal Conductivity $\lambda$ (25 °C) | 0.96 W/(m•K) |
| Specific Heat Capacity $C_p$ (20 °C; 100 °C) | 0.84 KJ/(Kg•K) |
| Coefficient of Mean Linear Thermal Expansion $\alpha$ (20 °C; 300 °C) | $8.8 \cdot 10^{-6}\ K^{-1}$* |
| Transformation Point Tg | 615 °C* |
| Annealing Point ($10^{13}$ dPas) | 635 °C |
| Softening Point ($10^{7.6}$ dPas) | 880 °C |
| Working Point ($10^{4}$ dPas) | 1265 °C |

*cooled according to DIN

## Chemical Properties:
## Optical Properties:

| | | |
|---|---|---|
| Hydrolytic Resistance | DIN ISO 719 | Class HGB 1 |
| Acid Resistance | DIN 12116 | Class S 4 |
| Alkali Resistance | DIN ISO 695 | Class A 1 |

| Refractive Index at | 588 nm ($n_d$) | 633 nm | 780 nm |
|---|---|---|---|
| Core Glass | 1.508 | 1.506 | 1.502 |
| Compression Layer $KNO_3$ pure | 1.516 | 1.514 | 1.510 |
| Transmittance τ (Glass Thickness 0.7mm) | | | |
| 840 nm | | | > 91.5 % |
| 560 nm | | | > 91.5 % |
| 380 nm | | | > 90 % |
| Photoelastic Constant | | | 29.2 nm/cm/MPa |

## Sheet Dimensions:

- Sheet Size: 475 x 575mm (18.7 x 22.64")
  1150 x 950mm (45.27 x 37.4")
- Thickness Range: 0.55 to 2mm stocked other requirements available on request

## Electrical Properties:

| Frequency MHz | Dielectric Constant ε′ | Loss Tangent tanδ |
|---|---|---|
| 1 | 7.74 | 0.011 |
| 54 | 7.49 | 0.008 |
| 480 | 7.40 | 0.009 |
| 825 | 7.38 | 0.010 |
| 912 | 7.38 | 0.010 |
| 1977 | 7.35 | 0.012 |
| 2170 | 7.35 | 0.012 |
| 2986 | 7.34 | 0.012 |
| Electric Volume Resistivity $\rho_D$ for A.C. at 50Hz | | |
| ν = 250 °C | | $1.5 \cdot 10^{6}\ \Omega \cdot cm$ |
| ν = 350 °C | | $8.9 \cdot 10^{4}\ \Omega \cdot cm$ |

*These values are no guaranteed data - for customer orientation only.

## Mechanical Properties:

| | |
|---|---|
| Density | 2.477 g/cm³* |
| Young's Modulus E | 74 kN/mm² |
| Poisson's Ratio | 0.215 |
| Shear Modulus | 30 kN/mm² |
| Knoop Hardness HK 0.1/20 | |
| Non-strengthened | 534 |
| Strengthened | 639 |
| Vickers Hardness HV 0.2/20 | |
| Non-strengthened | 617 |
| Strengthened | 681 |

*cooled according to DIN

## Chemical Strengthening:

| | |
|---|---|
| Compressive Stress | capable > 900 MPa |
| Depth of Layer | capable > 50 µm |
| 4-Point Bending Strength | cap. > 800 MPa |

# Appendix 2

| q wind load N/mm2 | Length mm | Elastic modulus | I (1/12*w*h^3) mm4 |
|---|---|---|---|
| 0.001 | 900 | 74000 | 333 |

| W (1/6 *w*h^2) mm3 | Max.Bending moment (1/8)q*l^2 (N/mm) | h mm | w mm | Y | f |
|---|---|---|---|---|---|
| 667 | 45562.5 | 1 | 4000 | 1 | 450 |

| Max. bending stress M/W N/mm2 | max. deformation (5*q*l^4)/(384*E*I) mm |
|---|---|
| 68.34375 | 155.8514569 |

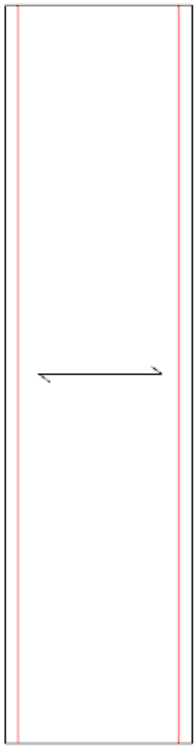

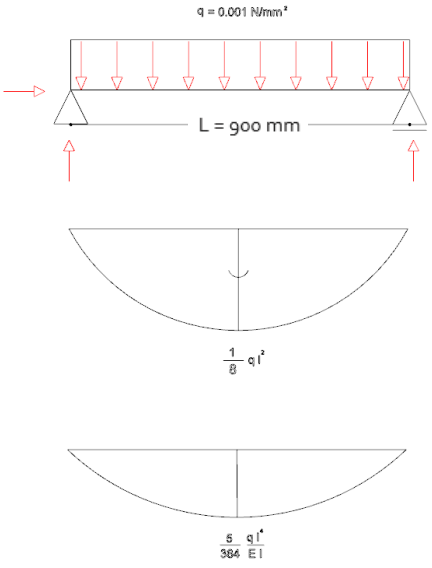

# Appendix 3

| q wind load N/mm2 | Length mm | Elastic modulus | I (1/12*b*h^3) mm4 |
|---|---|---|---|
| 0.001 | 900 | 74000 | 333 |

| W (1/6 *w*h^2) mm3 | **R:** Max.Bending moment (1/12) q*l^2 (N/mm) | **M:** Max.Bending moment (1/24) q*l^2 (N/mm) | h mm | w mm |
|---|---|---|---|---|
| 667 | 30375 | 15187.5 | 1 | 4000 |

| Y | f |
|---|---|
| 1 | 450 |

| M: Max. bending stress M/W N/mm2 | max. deformation (1*q*l^4)/(384*E*I) mm |
|---|---|
| 22.78125 | 31.17029139 |

| E: Max. bending stress M/W N/mm2 |
|---|
| 45.5625 |

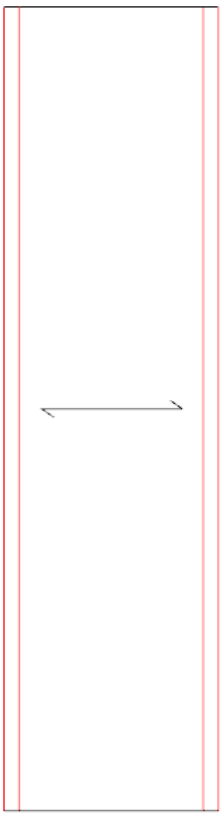

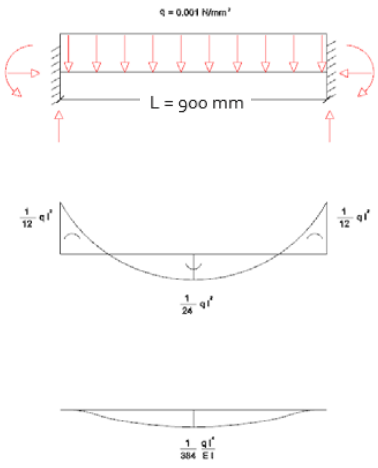

# Appendix 4

**GFRP hand calculation**

$q_{windload}$= 0.001 N/mm²

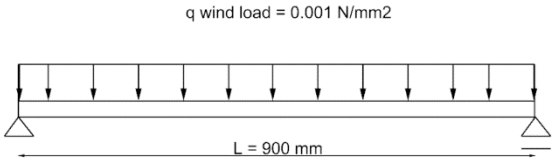


Span length= 900 mm

Estimated height of GFRP = 1/40* span length =1/40* 900 = 22.5 mm; Here I will use a height of 25 mm to improve thermal performance of the cavity.

Yield strength laminated GFRP = 125 N/mm²

Elastic modulus= 40000 N/mm²

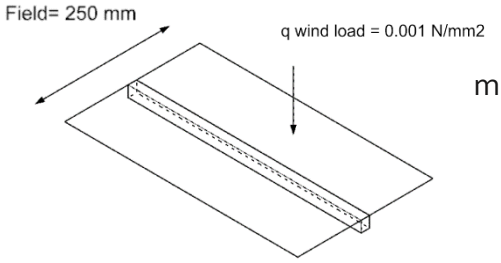


Moment of inertia ($I_x$) = $\frac{1}{12}$ * w * h³ = $\frac{1}{12}$ * 25 * 25³ = 32552 mm⁴

Section modulus ($W_x$)= $\frac{1}{6}$ * w * h² = $\frac{1}{6}$ * 25 * 25² = 2604 mm³

Safety factor for permanent load= 1

Field= 250 mm

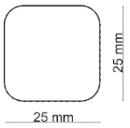


**Ultimate limit state (ULS)**

Maximum bending moment ($M_B$)= $\frac{1}{8}$ * q * L²

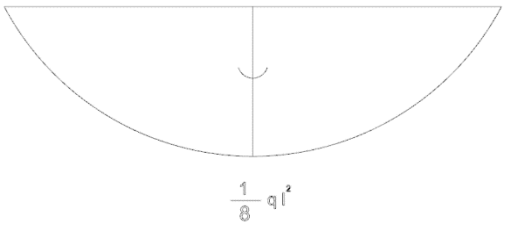


q= $q_{windload}$ * f * Y = 0.001*250*1 = 0.25 N/mm

Max. Bending moment ($M_B$)= $\frac{1}{8}$ * 0.25* 900² = 25312.5 N.mm

Max. Bending stress $\sigma_{max;B}$ = $\frac{M}{W}$ = $\frac{25312.5}{2604}$ = 9.72 N/mm² < 125 N/mm²

Unity check= $\frac{\sigma}{f}$ = $\frac{9.72}{125}$ = 0.08 < 1 → Suffice

**Serviceability limit state (SLS)**

Request for $u_{end}$ = 0.004 * L = 0.004*900= 3.6 mm;

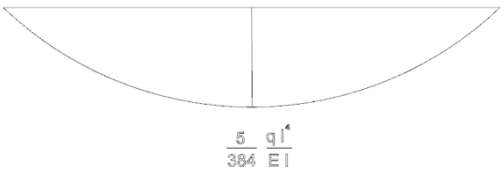


$U_{end}$ = $\frac{5 * q * l^4}{384 * E * Ix}$ = $\frac{5 * 0.25 * 900^4}{384 * 40000 * 32552}$ =1.64 mm < 3.6 mm

Unity check= $\frac{1.64}{3.6}$ = 0.46 < 1 → Suffice.

# Appendix 5

## Alloy 6005A

### 6005A Extruded Mechanical and Physical Property Limits[1]

| Alloy | Standard Tempers | Wall Thickness[2] (min.) | | Tensile Strength ksi (MPa) | | Elongation[3] % (min.) | Typical Thermal Conductivity, @77°F, BTU-in./ft.²hr.°F (W/m-K@25°C) | Typical Electrical Conductivity, @68°F, % IACS |
|---|---|---|---|---|---|---|---|---|
| | | inches | mm | Ultimate (min. ) | Yield - 0.2% offset (min.) | | | |
| 6005A | -T1 | up thru 0.249 | up thru 6.30 | 25.0 (170) | 14.5 (100) | 15 | 1220 (176) | 47 |
| | -T5 | up thru 0.249 | up thru 6.30 | 38.0 (260) | 31.0 (215) | 7 | 1340 (193) | 50 |
| | | .250 - 0.999 | 6.30 - 25.00 | 38.0 (260) | 31.0 (215) | 9 | 1340 (193) | 50 |
| | -T61 | up thru 0.249 | up thru 6.30 | 38.0 (260) | 35.0 (240) | 8 | 1310 (188) | 49 |
| | | 0.250 - 1.000 | 6.30 - 25.00 | 38.0 (260) | 35.0 (240) | 10 | 1310 (188) | 49 |
| | Open profiles (Per EN755-2 Spec) | | | | | | | |
| | -T6 | up thru .197 | up thru 5.00 | 39.2 (270) | 32.6 (225) | 8 | NA | NA |
| | | .198 - .394 | 5.00 - 10.00 | 37.7 (260) | 31.2 (215) | 8 | | |
| | | .395 - .984 | 10.00 - 25.00 | 36.3 (250) | 29.0 (200) | 8 | | |
| | Hollow profiles (Per EN755-2 Spec) | | | | | | | |
| | -T6 | up thru .197 | up thru 5.00 | 37.0 (255) | 31.2 (215) | 8 | NA | NA |
| | | .198 - .591 | 5.00 - 15.00 | 36.3 (250) | 29.0 (200) | 8 | | |
| 6061 | -T6 | up thru .249 | up thru 6.30 | 38.0 (260) | 35.0 (240) | 8 | 1160 (167) | 43 |
| | | .250 & above | | 38.0 (260) | 35.0 (240) | 10 | | |
| 6005 | -T5 | up thru .124 | up thru 3.20 | 38.0 (260) | 35.0 (240) | 8 | 1310 (188) | 50 |
| | | .125 - 1.000 | 3.20 - 25.00 | 38.0 (260) | 35.0 (240) | 10 | | |

1. Minimum property levels unless shown as a range or indicated as a maximum (max.)
2. The thickness of the cross section from which the tension test specimen is taken determines the applicable mechanical properties.
3. For materials of such dimensions that a standard test specimen cannot be taken, or for shapes thinner than .062", the test for elongation is not required. Elongation percent is minimum in 2" or 4 times specimen diameter.

* Mechanical property values for 6005A -T1, -T5, -T61 tempers per Aluminum Association. Values for 6005A-T6 temper per EN755-2 specification, elongation represents 'A' value.

### Comparative Characteristics of Related Alloys/Tempers[1]

| Alloy | Temper | Formability | Machinability | General Corrosion Resistance | Weldability | Brazeability | Anodizing Response |
|---|---|---|---|---|---|---|---|
| | | D C B A | D C B A | D C B A | D C B A | D C B A | D C B A |
| 6005A | -T1 | ■■■■ | ■■■■ | ■■■■ | ■■■■ | ■■■■ | ■■■■ |
| | -T5 | ■■■■ | ■■■■ | ■■■■ | ■■■■ | ■■■■ | ■■■■ |
| | -T6 | ■■■■ | ■■■■ | ■■■■ | ■■■■ | ■■■■ | ■■■■ |
| | -T61 | ■■■■ | ■■■■ | ■■■■ | ■■■■ | ■■■■ | ■■■■ |
| 6061 | -T6 | ■■■■ | ■■■■ | ■■■■ | ■■■■ | ■■■■ | ■■■■ |
| 6005 | -T5 | ■■■■ | ■■■■ | ■■■■ | ■■■■ | ■■■■ | ■■■■ |
| 6063 | -T6 | ■■■■ | ■■■■ | ■■■■ | ■■■■ | ■■■■ | ■■■■ |

1. Rating: A = Excellent B = Good C = Fair D = Poor

**SAPA EXTRUSION NORTH AMERICA**
6250 North River Road, Suite 5000 ▪ Rosemont, IL 60018
Phone: 877-710-Sapa (877-710-7272)
E-mail: NorthAmerica.Sales@sapagroup.com
**www.sapagroup.com**


Revision 2017/01 (03/2017)

# Appendix 6

**Frame calculation**

Sandwich panel under wind load pressure:

- Node coördinaties → X= 2010 mm, Y= 50 mm, Z = -25 mm
- $F_{\text{reaction force}}$ = 1111.73 N;
- a = ½ x span length
- Span length = 900 mm
- Section Modulus ($W_x$) = ?
- Moment= ?
- Maximum bending stress σ = ?

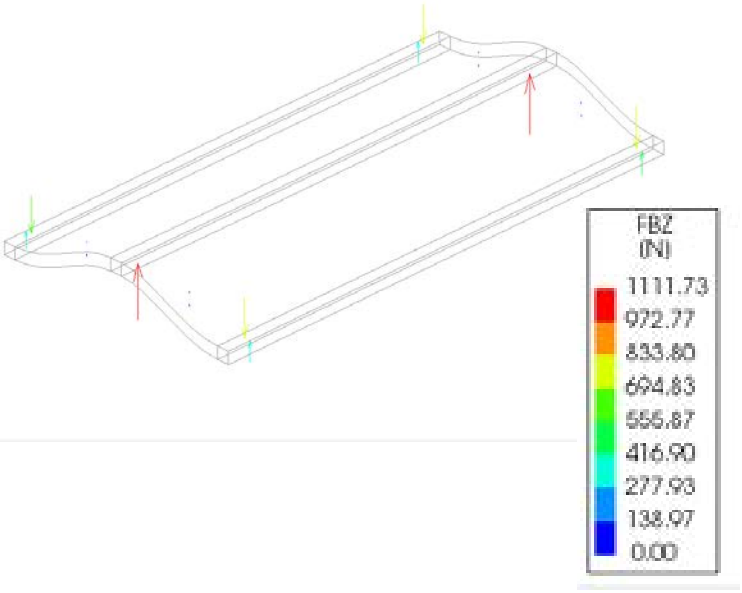


$W_x = wh^3 - \frac{(w-2t)(h-2t)^3}{6h}$ = 50 x100³ - $\frac{(50-2x2)(100-2t)^3}{6 \times 100}$ = 15504 mm³

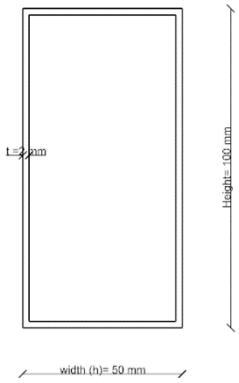


ΣM= F x a = 1111.73 x 450= 500278.5 Nmm

$\sigma = \frac{M}{W} = \frac{500278.5}{15504}$ = 32.6 N/mm² < 117 N/mm²

Unity Check = $\frac{32.6}{117}$ = 0.3 < 1 → Suffice.

# Appendix 7

## Super Spacer Selection Chart
### for Architectural Structural and Captured Glazing Units

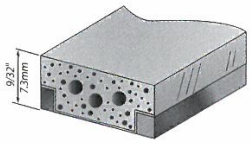


**TRISEAL™**

| | |
|---|---|
| Available sizes: | 0.323" (8.2mm) to 0.874" (22.2mm) airspace |
| Standard Color: | Black, Grey and Aluminum Grey |
| Optional Colors: | Are Available (Minimum Order Required) |
| Custom Options: | As defined by Specifier (Minimum Order Required) |

### for Architectural Captured Glazing Units

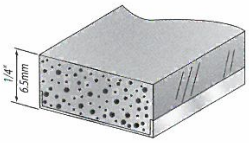


**PREMIUM PLUS** **(Recommended for IG greater than 65 sq. ft.)**

| | |
|---|---|
| Available sizes: | 0.125" (3.2mm) to 0.787" (20.0mm) airspace |
| Standard Colors: | Black, Grey and Aluminum Grey |
| Optional Colors: | Are Available (Minimum Order Required) |
| Custom Options: | As defined by Specifier (Minimum Order Required) |

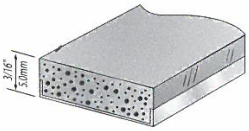


**PREMIUM**

| | |
|---|---|
| Available sizes: | 0.188" (4.8mm) to 0.787" (20.0mm) airspace |
| Standard Colors: | Black, Grey and Aluminum Grey |
| Optional Colors: | Are Available (Minimum Order Required) |
| Custom Options: | As defined by Specifier (Minimum Order Required) |

### COMPARISON OF SUPER SPACER PRODUCT PERFORMANCE

| | Aluminum Spacer | Stainless | TriSeal™ | Premium/Premium Plus |
|---|---|---|---|---|
| Glass Surface Temperature | Poor | Good | Excellent | Excellent |
| Thermal Performance | Poor | Good | Excellent | Excellent |
| Condensation Resistance | Poor | Good | Excellent | Excellent |
| Edge Seal Integrity | Good | Very Good | Excellent | Excellent |
| Dew Point Drop | Good | Good | Excellent | Excellent |
| Sound Absorption | Good | Good | Excellent | Excellent |
| Sealant Stress Reduction | Good | Very Good | Excellent | Excellent |
| Compression Set | Good | Good | Excellent | Excellent |
| UV Resistance | Excellent | Excellent | Excellent | Excellent |
| Desiccant Capacity | Excellent | Excellent | Excellent | Excellent* |
| Structural Strength | Excellent | Excellent | Excellent | Excellent |
| Volatile Out-Gassing | Pass | Pass | Pass | Pass |
| Triple Glaze | Yes | Yes | Yes | Yes |
| Wind Loading | Very Good | Very Good | Excellent | Excellent |
| Captured Glazing | Yes | Yes | Yes | Yes |
| Structural Glazing | Yes | Yes | Yes | No |
| Compatible with Performance Coatings | Yes | Yes | Yes | Yes |
| Standard Colors | Varies | Varies | Three | Three |
| Optional Colors | Available | Available | Available | Available |
| Custom Colors | Available | Available | Available | Available |

# Appendix 8

Rtotal= ra + r glass+ rcavity + r glass + ri

$R_{glass} = \frac{d}{\lambda} = \frac{0.001}{1} = 0.001\ m^2\ K / W$

$\lambda = 1\ W/mK$

$thickness = 0.001\ m$

$\alpha_{a=23}\ W/(m2.K)$

$\alpha_{i=8}\ W/(m2.K)$

$r_a = \frac{1}{\alpha} = \frac{1}{23} = 0.04\ m^2\ K / W$

$r_i = \frac{1}{\alpha} = \frac{1}{8} = 0.13\ m^2\ K / W$

| SPOUW-BREEDTE | K-GLAS Lucht | K-GLAS Argon | LOW-E Lucht | LOW-E Argon | CLEARLITE Lucht | SUPERLITE Argon | ASTRALITE N Lucht | STARLITE N Argon | STARLITE N Krypton | ENERGY Lucht | ENERGY Argon | ENERGY Krypton |
|---|---|---|---|---|---|---|---|---|---|---|---|---|
| 9 mm | 2,3 | 1,9 | 2,1 | 1,7 | 2,1 | 1,7 | 2,0 | 1,6 | 1,2 | 1,9 | 1,6 | 1,1 |
| 12 mm | 2,0 | 1,7 | 1,8 | 1,5 | 1,8 | 1,5 | 1,7 | 1,3 | 1,1 | 1,6 | 1,3 | 1,1 |
| 15 mm | 1,8 | 1,6 | 1,6 | 1,3 | 1,6 | 1,3 | 1,5 | 1,2 | 1,2 | 1,4 | 1,1 | 1,1 |
| 20 mm | 1,8 | 1,6 | 1,6 | 1,4 | 1,6 | 1,4 | 1,5 | 1,2 | 1,2 | 1,4 | 1,2 | 1,1 |
| 24 mm | 1,9 | 1,7 | 1,6 | 1,4 | 1,6 | 1,4 | 1,4 | 1,1 | 1,2 | 1,4 | 1,2 | 1,1 |
| LTA-waarde | 76 % | 76 % | 79 % | 79 % | 79 % | 79 % | 79 % | 79 % | 79 % | 71 % | 71 % | 71 % |
| ZTA-waarde | 62 % | 62 % | 67 % | 67 % | 67 % | 67 % | 64 % | 64 % | 64% | 39 % | 39 % | 39 % |

source: http://www.bouwonline.nl/4/resourcefile/01/03/69/page1.html

$U_{cavity\ filled\ with\ argon,\ low\ e} = 1.4\ W/(m2.K) \Rightarrow R_{cavity} = \frac{1}{1.4} = 0.7\ m^2\ K / W$

Thus,

$R_{total} = r_a + r_{glass} + r_{cavity} + r_{glass} + r_i$ ;

$R_{total} = 0.04 + 0.001 + 0.7 + 0.001 + 0.13 = 0.9\ m^2\ K / W$

$U_{total} = \frac{1}{0.9} = \mathbf{1.1}\ W/(m2.K)$

Low emissivity =0.14

AGC Your Glass

$propertyEntry.value 28-10-2017

Your composition:

Thermobel: 4 mm Planibel Clearlite - 24 mm Argon 90% - 4 mm Planibel Low-e G fasT pos.3

Personal notes:

| LIGHT | |
|---|---|
| Transmission | 75 |
| Reflection | 17 |

| ENERGY | |
|---|---|
| Solar factor | 76 |
| Reflection | 16 |

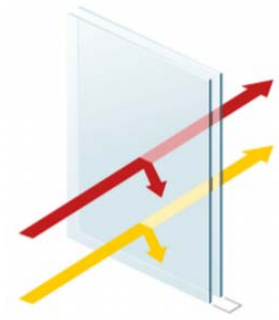

| THERMAL PROPERTIES (EN 673) | EN 673 |
|---|---|
| Ug-Value - W/(m².K) | 1.5 |

| LIGHT PROPERTIES (EN 410) | EN 410 |
|---|---|
| Light Transmission - τv (%) | 75 |
| Light Reflection - ρv (%) | 17 |
| Internal light reflection - ρvi (%) | 16 |
| Colour Rendering - RD65 - Ra (%) | 99 |

| ENERGY PROPERTIES | EN 410 | ISO 9050 |
|---|---|---|
| Solar factor - g (%) | 76 | 74 |
| Energy Reflection - ρe (%) | 16 | 17 |
| Direct Energy Transmission - τe (%) | 66 | 63 |
| Solar abs. Glass 1 - αe (%) | 6 | 7 |
| Solar abs. Glass 2 - αe (%) | 12 | 13 |
| Total Energy absorption - αe (%) | 18 | 20 |
| Shading coefficient - SC | 0.87 | 0.85 |
| UV Transmission - UV (%) | 43 | |
| Selectivity | 0.99 | 1.01 |

| OTHER PROPERTIES | |
|---|---|
| Resistance to fire - EN 13501-2 | NPD |
| Reaction to fire - EN 13501-1 | NPD |
| Bullet Resistance - EN 1063 | NPD |
| Burglar Resistance - EN 356 | NPD |
| Pendulum body impact resistance - EN 12600 | NPD / NPD |

| ACOUSTIC PROPERTIES | |
|---|---|
| Direct airborne sound insulation(Rw (C;Ctr) - ESTIMATED) - dB | 32 (-1; -4)(2) |

# Appendix 9

AGC Your Glass $propertyEntry.value 28-10-2017

**Your composition:**

Thermobel: 4 mm Planibel Clearlite - 27 mm Argon 90% - 4 mm Planibel Low-e G fasT pos.3

Personal notes:

| LIGHT | |
|---|---|
| Transmission | 75 |
| Reflection | 17 |

| ENERGY | |
|---|---|
| Solar factor | 76 |
| Reflection | 16 |

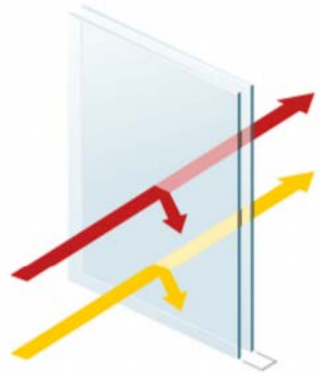

| THERMAL PROPERTIES (EN 673) | EN 673 |
|---|---|
| Ug-Value - W/(m².K) | 1.5 |

| LIGHT PROPERTIES (EN 410) | EN 410 |
|---|---|
| Light Transmission - τv (%) | 75 |
| Light Reflection - ρv (%) | 17 |
| Internal light reflection - ρvi (%) | 16 |
| Colour Rendering - RD65 - Ra (%) | 99 |

| ENERGY PROPERTIES | EN 410 | ISO 9050 |
|---|---|---|
| Solar factor - g (%) | 76 | 74 |
| Energy Reflection - ρe (%) | 16 | 17 |
| Direct Energy Transmission - τe (%) | 66 | 63 |
| Solar abs. Glass 1 - αe (%) | 6 | 7 |
| Solar abs. Glass 2 - αe (%) | 12 | 13 |
| Total Energy absorption - αe (%) | 18 | 20 |
| Shading coefficient - SC | 0.87 | 0.85 |
| UV Transmission - UV (%) | 43 | |
| Selectivity | 0.99 | 1.01 |

| OTHER PROPERTIES | |
|---|---|
| Resistance to fire - EN 13501-2 | NPD |
| Reaction to fire - EN 13501-1 | NPD |
| Bullet Resistance - EN 1063 | NPD |
| Burglar Resistance - EN 356 | NPD |
| Pendulum body impact resistance - EN 12600 | NPD / NPD |

| ACOUSTIC PROPERTIES | |
|---|---|
| Direct airborne sound insulation(Rw (C;Ctr) - ESTIMATED) - dB | 32 (-1; -4)[2] |

# Appendix 10

## HALFEN CURTAIN WALL SUPPORT SYSTEMS

### Top of Slab Brackets Type HCW-B1

**Support bracket for horizontal and vertical loads**

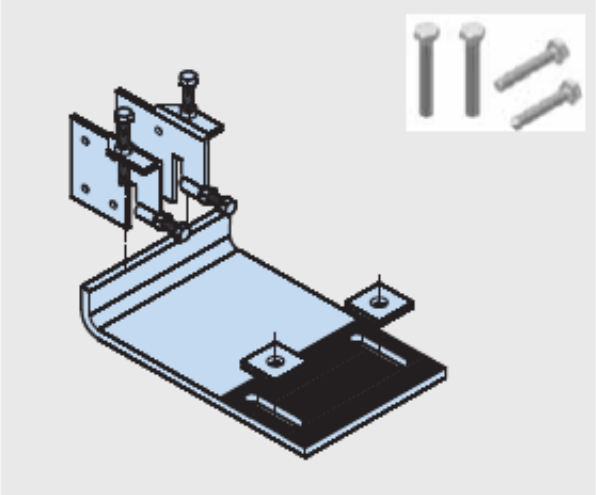

HALFEN Brackets type HCW-B1 for top of slab installation are available in two load ranges and three sizes. The brackets are made of S355 grade quality galvanized steel. Three dimensional adjustability is ensured when used in combination with HALFEN HTA Anchor Channels. The lateral connecting plates are connected to the façade posts using M8 (5/16") screws (order separately).

Typical assembly

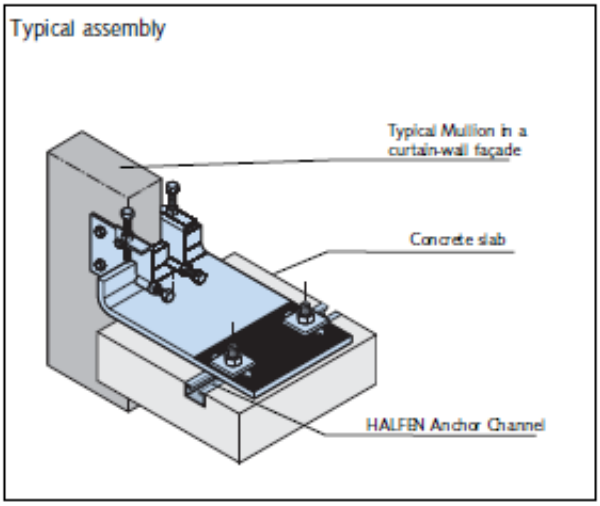


Use HALFEN T-Bolts M16 (5/8") grade 8.8 (order separately) to connect the base bracket to the HALFEN Anchor Channel. Depending on the façade type, the connection between the connecting plate and the base bracket can be designed to allow lateral expansion or as a fixed point.

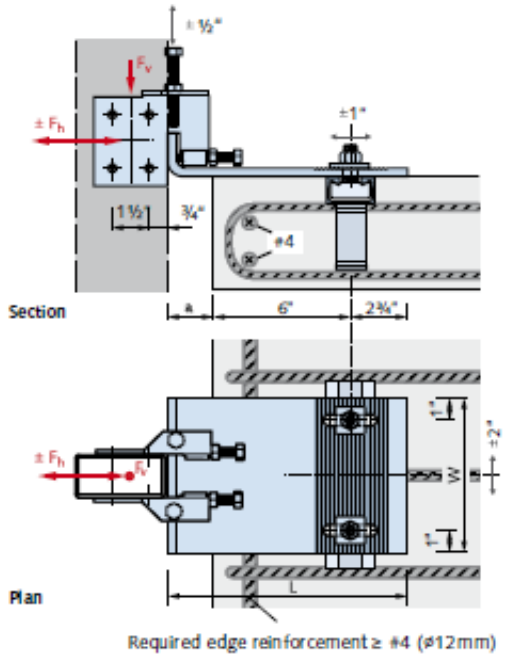


Required edge reinforcement ≥ #4 (ø12mm)

**Dimensioning / Type selection**

**Design load ranges**

| Load range | | dead load | | wind load | |
|---|---|---|---|---|---|
| | | $F_{v\,allow.}$ | $F_{v,d}$ | $F_{h\,allow.}$ | $F_{h,d}$ |
| 4/12 | [lbs] | 660 | 900 | ±1,800 | ±2,700 |
| | [kN] | 2.95 | 4.0 | ± 8.0 | ±12 |
| 7/20 | [lbs] | 1,160 | 1570 | ±2,990 | ±4,500 |
| | [kN] | 5.15 | 7.0 | ± 13.3 | ±20 |

$F_{v,d}$, $F_{h,d}$: design loads with a partial safety factor $\gamma_F$ = 1.35 for dead loads and $\gamma_F$ = 1.5 for wind loads.

$F_{v,d} = F_{v\,allow.} \times 1.35$

$F_{h,d} = F_{h\,allow.} \times 1.50$

**Type selection**

| Load range | a [inch] | Item name HCW-B1-... | L [inch] | W [inch] | HALFEN Anchor Channel ① | Recommended HALFEN T-bolt 8.8 |
|---|---|---|---|---|---|---|
| 4/12 | 2" | ...-4/12-50 | 10¾" | 6" | HTA 40/22 250mm (10") 2 Anchors | HS 40/22 M16×60 (⅝"×2⅜") |
| | 3" | ...-4/12-75 | 11¾" | 6" | | |
| | 4" | ...-4/12-100 | 12¾" | 6" | | |
| 7/20 | 2" | ...-7/20-50 | 10¾" | 7" | HTA 50/30 300mm (12") 3 Anchors | HS 50/30 M16×60 (⅝"×2⅜") |
| | 3" | ...-7/20-75 | 11¾" | 7" | | |
| | 4" | ...-7/20-100 | 12¾" | 8" | | |

① Recommended HALFEN Anchor Channel exploiting the full load capacity of the bracket.